

Some pages of this thesis may have been removed for copyright restrictions.

If you have discovered material in AURA which is unlawful e.g. breaches copyright, (either yours or that of a third party) or any other law, including but not limited to those relating to patent, trademark, confidentiality, data protection, obscenity, defamation, libel, then please read our [Takedown Policy](#) and [contact the service](#) immediately

**A multimodal investigation of dynamic face
perception using functional magnetic resonance
imaging and magnetoencephalography**

Elaine Foley

Doctor of Philosophy

Aston University

November 2012

This copy of the thesis has been supplied on condition that anyone who consults it is understood to recognise that its copyright rests with its author and that no quotation from the thesis and no information derived from it may be published without proper acknowledgement.

A multimodal investigation of dynamic face perception using functional magnetic resonance imaging and magnetoencephalography

Elaine Foley
Aston University
Doctor of Philosophy
November 2012

Motion is an important aspect of face perception that has been largely neglected to date. Many of the established findings are based on studies that use static facial images, which do not reflect the unique temporal dynamics available from seeing a moving face. In the present thesis a set of naturalistic dynamic facial emotional expressions was purposely created and used to investigate the neural structures involved in the perception of dynamic facial expressions of emotion, with both functional Magnetic Resonance Imaging (fMRI) and Magnetoencephalography (MEG). Through fMRI and connectivity analysis, a dynamic face perception network was identified, which is demonstrated to extend the distributed neural system for face perception (Haxby et al.,2000). Measures of effective connectivity between these regions revealed that dynamic facial stimuli were associated with specific increases in connectivity between early visual regions, such as inferior occipital gyri and superior temporal sulci, along with coupling between superior temporal sulci and amygdalae, as well as with inferior frontal gyri. MEG and Synthetic Aperture Magnetometry (SAM) were used to examine the spatiotemporal profile of neurophysiological activity within this dynamic face perception network. SAM analysis revealed a number of regions showing differential activation to dynamic versus static faces in the distributed face network, characterised by decreases in cortical oscillatory power in the beta band, which were spatially coincident with those regions that were previously identified with fMRI. These findings support the presence of a distributed network of cortical regions that mediate the perception of dynamic facial expressions, with the fMRI data providing information on the spatial co-ordinates paralleled by the MEG data, which indicate the temporal dynamics within this network. This integrated multimodal approach offers both excellent spatial and temporal resolution, thereby providing an opportunity to explore dynamic brain activity and connectivity during face processing.

Keywords: Face perception, functional magnetic resonance imaging, magnetoencephalography.

Acknowledgements

I would like to thank my supervisor Carl Senior, and my associate supervisor Gina Rippon, for their help and advice throughout the course of my studies. I have really enjoyed the time that I have spent working on this project and gaining experience in this field. I am also extremely grateful to Jade Thai for her invaluable assistance with fMRI, and her endless support and encouragement over the years. I also owe particular thanks to Jessica Gilbert for all her help with MEG, her valuable feedback on a draft of this thesis, and her continued friendship. Finally, I would like to thank my family for their unwavering support and encouragement throughout.

Data reported in this thesis has been published in the *Journal of Cognitive Neuroscience* (Foley et al., 2012), and has been presented at a number of different conferences (see appendix section for full details). I am grateful to all of those who have offered helpful suggestions and comments on my research.

Contents

1	A review of face perception research: from a specialised module to a distributed network	26
1.1	Overview	26
1.2	Early face perception research	26
1.2.1	Neuropsychological studies	27
1.2.2	Behavioural studies	28
1.2.2.1	Dynamic information	29
1.2.3	The functional model for face recognition	31
1.3	Neuroimaging and neurophysiological studies of face perception	32
1.3.1	A specialised face perception module?	33
1.3.2	The distributed neural system for face perception	35
1.3.3	Anatomical location and relative timing of evoked potentials	37
1.3.4	Facial expressions of emotion	40
1.3.4.1	Temporal processing of facial expressions	42
1.3.5	A model of emotion recognition from faces	44
1.3.6	Ecological validity of facial expression stimuli	46
1.3.7	Biological motion perception	48
1.3.8	Dynamic face perception	52
1.4	An integrative approach to face perception research	53
1.4.1	Connectivity analysis	54
1.5	A brief overview of applied methods	58
1.5.1	Basic principles of fMRI and the BOLD signal	58
1.5.2	fMRI data analysis	60
1.5.3	Advantages and limitations of fMRI	62
1.5.4	Basic principles of MEG	62
1.5.5	MEG source localisation	63
1.5.6	Group level analysis of MEG data	65
1.5.7	Advantages and limitations of MEG	66
1.6	Multimodal integration	66
1.7	Objectives	68
2	The neural substrates of dynamic face perception	70
2.1	Introduction	70
2.1.1	Overview	70
2.1.2	Neuroimaging studies of dynamic face perception	70

2.1.3	Objectives and hypotheses	74
2.2	Methods	75
2.2.1	Stimuli	75
2.2.2	fMRI participants	78
2.2.3	Experimental design and imaging paradigm	78
2.2.4	Imaging protocol	79
2.2.5	Image analysis	80
2.2.5.1	Subtractive analysis	80
2.2.5.2	Regions of interest analysis	81
2.3	Results	82
2.3.1	Dynamic versus static facial expressions	82
2.3.2	Dynamic facial expressions of emotion versus dynamic speech displays	84
2.3.3	Regions of interest analysis	85
2.4	Discussion	88
2.4.1	The common neural substrates of dynamic face perception	88
2.4.2	Distinct neural substrates associated with the perception of different dynamic facial expressions	92
2.4.3	Summary	95
3	Connectivity analysis of the dynamic face perception network	96
3.1	Introduction	96
3.1.1	Overview	96
3.1.2	Functional connectivity within the distributed face perception network	97
3.1.3	Effective connectivity analysis of the face perception network	98
3.1.4	Objectives and hypotheses	101
3.2	Methods	102
3.2.1	fMRI participants	102
3.2.2	Experimental design and imaging paradigm	103
3.2.3	Imaging protocol	104
3.2.4	Image analysis	104
3.2.4.1	Connectivity analysis	105
3.3	Results	106
3.3.1	Psychophysiological interaction results	106
3.3.1.1	Inferior occipital gyri	107
3.3.1.2	Superior temporal sulci	109
3.3.1.3	Amygdalae	110
3.3.1.4	Inferior frontal gyri	112
3.3.2	Physiophysiological interaction results	113
3.4	Discussion	124
3.4.1	Dynamic versus static faces	124
3.4.2	Dynamic facial expressions of anger	126

3.4.3	Dynamic facial expressions of happiness	128
3.4.4	Dynamic speech versus static speech facial displays	129
3.4.5	Physiophysiological interactions	130
3.4.6	Summary	132
4	The time-course of cortical oscillatory responses to dynamic faces	134
4.1	Introduction	134
4.1.1	Overview	134
4.1.2	Timecourse and oscillatory responses to dynamic faces	135
4.1.3	Objectives and hypotheses	137
4.2	Methods	138
4.2.1	MEG participants	138
4.2.2	Experimental design and imaging paradigm	138
4.2.3	Data analysis	140
4.3	Results	141
4.3.1	Source analysis results	141
4.3.2	Time frequency results	142
4.3.2.1	Inferior occipital gyri	142
4.3.2.2	Middle temporal gyri	145
4.3.2.3	Superior temporal sulci	148
4.4	Discussion	148
4.4.1	Temporal progression within the dynamic face perception network .	150
4.4.2	Summary	154
5	The timecourse and oscillatory responses to facial displays of emotion	155
5.1	Introduction	155
5.1.1	Overview	155
5.1.2	Emotional face perception	156
5.1.3	Frequency characteristics of emotional face processing	157
5.1.4	Objectives and hypotheses	160
5.2	Methods	162
5.2.1	MEG participants	162
5.2.2	Experimental design and imaging paradigm	162
5.2.3	Data analysis	163
5.3	Results	165
5.3.1	Dynamic facial expressions of anger	165
5.3.1.1	Source analysis results	165
5.3.1.2	Time frequency results	167
5.3.2	Dynamic facial expressions of happiness	183
5.3.2.1	Source analysis results	183
5.3.2.2	Time frequency results	185
5.3.3	Dynamic speech versus static speech facial displays	206
5.3.3.1	Source analysis results	206

5.3.3.2	Time frequency results	208
5.4	Discussion	223
5.4.1	Occipito-temporal responses to dynamic facial expressions of emotion	223
5.4.2	Prefrontal and insular cortex responses to dynamic facial expressions of emotion	228
5.4.3	Summary	232
6	Discussion	233
6.1	Introduction	233
6.2	Key findings	234
6.2.1	Key findings from fMRI	234
6.2.2	Key findings from MEG	238
6.2.3	Integration of fMRI and MEG data	241
6.2.3.1	A neural network for processing dynamic faces in time, space and frequency	242
6.2.3.2	Differential activation of the dynamic face perception network	245
6.3	Methodological considerations and limitations	249
6.4	Future directions	250
6.5	Conclusion	252

List of Figures

Figure 1.2.1	The functional model of face recognition adapted from Bruce and Young (1986), shows two distinct pathways for identity and facial expression processing.	31
Figure 1.3.1	The distributed human neural system for face perception, adapted from Haxby et al. (2000). This model shows a core system in occipito-temporal cortex where visual analysis of faces takes place. Changeable and invariant aspects of faces are processed in two distinct pathways in the core system. The extended system incorporates additional brain regions for further face processing.	36
Figure 1.3.2	The neural system for recognising emotion from facial expressions, adapted from Adolphs (2002).	47
Figure 2.2.1	Behavioural face rating data showing: (A) % correct for each of the different dynamic and static facial affect stimuli (B) Mean intensity ratings for each of the different dynamic and static facial affect stimuli. Black bars indicate the dynamic stimulus condition and white bars denote the static stimulus condition, error bars indicate standard error of mean (S.E.M).	77
Figure 2.2.2	Group motion capture data (n=4) shows the mean amount of motion for each of the different facial affects. Error bars indicate standard error of mean (S.E.M).	78
Figure 2.2.3	fMRI experimental design shows 24 s on-block where 8 stimuli were presented for 3 s within each block of the same condition. This alternated with a 24 s block of no visual stimulation (fixation cross). Participants (N=14) performed a 1-back memory task on the individual identity within each block, making all responses via the lumina response pad.	79
Figure 2.3.1	The dynamic face perception network. Results of whole brain group analysis (N=14) for the dynamic versus static condition projected onto the surface of an inflated standard brain, showing both lateral and ventral views. Bilateral activation is clearly shown on both left (L) and right (R) hemispheres in; (1) middle occipital gyri (2) middle temporal gyri (3) superior temporal sulci (4) inferior frontal gyri (5) and middle frontal gyri. Colour bar denotes T-statistic and images are thresholded at $p < .05$ corrected for multiple comparisons.	84

Figure 2.3.2	Results of whole brain group analysis (N=14) for the dynamic angry versus static angry condition projected onto the surface of an inflated standard brain, showing both lateral and ventral views (L=Left; R=Right). Activation is shown bilaterally in middle occipital gyri, middle temporal gyri, superior temporal sulci, as well as the right insula and right amygdala. Colour bar denotes T-statistic and images are thresholded at $p < .05$ corrected for multiple comparisons.	85
Figure 2.3.3	Results of whole brain group analysis (N=14) for the dynamic happy versus static happy condition projected onto the surface of an inflated standard brain, showing both lateral and ventral views (L=Left; R=Right). Activation is shown in left middle occipital gyrus, left fusiform gyrus, right middle temporal gyrus and bilateral superior temporal sulci. Colour bar denotes T-statistic and images are thresholded at $p < .05$ corrected for multiple comparisons.	86
Figure 2.3.4	Results of whole brain group analysis (N=14) for the dynamic speech versus static speech condition projected onto the surface of an inflated standard brain, showing both lateral and ventral views (L=Left; R=Right). Activation is shown bilaterally in middle occipital gyri, middle temporal gyri, superior temporal sulci and middle frontal gyri, and in right precentral gyrus and left inferior frontal gyrus. Colour bar denotes T-statistic and images are thresholded at $p < .05$ corrected for multiple comparisons.	86
Figure 2.3.5	Regions of interest analysis shows mean percent signal change in left (L) and right (R) inferior occipital gyri (IOG), superior temporal sulci (STS), amygdalae (AMG) and inferior frontal gyri (IFG). White bars indicate the dynamic stimulus condition and black bars denote the static stimulus condition, error bars indicate standard error of mean.	88
Figure 3.2.1	fMRI experimental design shows 24 s on-block where 8 stimuli were presented for 3 s within each block of the same condition. This alternated with a 24 s block of no visual stimulation (fixation cross). Participants (N=14) performed a 1-back memory task on the individual identity within each block, making all responses via the lumina response pad.	103
Figure 3.3.1	Effective connectivity of the four main seed voxels in the dynamic face perception network: (a) Inferior occipital gyri; (b) Superior temporal sulci; (c) Amygdalae; (d) Inferior frontal gyri. Results are thresholded at $p < .001$ for the dynamic versus static contrast for all 14 participants. L=Left; R=Right.	108

Figure 3.3.2	Connectivity maps for (a) Dynamic angry versus static angry expressions; (b) Dynamic happy versus static happy facial expressions; (c) Dynamic speech versus static speech facial displays. Red sections indicate the seed voxels in the PPI analysis shown separately for left and right hemispheres.	114
Figure 4.2.1	MEG experimental design: 120 dynamic and 120 static images were presented for 2.5 s in a random sequence, alternating with a 2.5 s fixation cross. Participants (N=14) performed a 1-back memory task and responded via button press as to whether the identity of the current image matched the previous image.	139
Figure 4.3.1	Group SAM image (N=14) shows decreases in beta power (12-30 Hz) within 5 different time windows 0-500; 500-1000; 1000-1500; 1500-2000; and 2000-2500 ms post stimulus onset. Shows progression of activation within the face perception network over time. Activation is shown in bilateral IOG, MTG, STS, and IFG. Blue-purple-white colour scale represents a decrease in signal power ($p < .05$).	144
Figure 4.3.2	Group time frequency findings in: (a) Left inferior occipital gyrus (N=12) shows an early decrease in low frequency power. Left: Dynamic faces compared to baseline shows sustained power decrease within 200 ms of stimulus onset between 10-30 Hz. Middle: Static faces compared to baseline shows slight power increase at 80 ms followed by power decrease between 10-25 Hz. Right: Direct comparison of dynamic and static faces shows early power decrease within first 200 ms between 10-30 Hz; (b) Right inferior occipital gyrus (N=12) shows an early decrease in low frequency power. Left: Dynamic faces compared to baseline shows sustained power decrease within 200 ms of stimulus onset between 10-30 Hz. Middle: Static faces compared to baseline shows slight power increase at 80 ms followed by power decrease between 10-20 Hz. Right: Direct comparison of dynamic and static faces shows early power decrease within 200 ms between 5-30 Hz.	146

Figure 4.3.3	Group time frequency findings in: (a) Left middle temporal gyrus (N= 8). Left: Dynamic faces compared to baseline shows sustained power decrease from 200 ms between 20–30 Hz and sustained power decrease from 500 ms between 10-15 Hz. Middle: Static faces compared to baseline shows power decrease from 400 ms between 20-30 Hz. Right: Direct comparison of dynamic and static faces shows power decrease around 200 ms between 12-25 Hz and power decrease from 800-1500 ms between 10-25 Hz; (b) Right middle temporal gyrus (N= 8). Left: Dynamic faces compared to baseline shows sustained power decrease from 500 ms between 10–30 Hz. Middle: Static faces compared to baseline shows power decrease from 400-800 ms between 10-30 Hz and a later decrease from 1600 ms between 8-25 Hz. Right: Direct comparison of dynamic and static faces shows power increase from 400-800 ms between 10-20 Hz, and a power decrease from 900 ms between 12-30 Hz.	147
Figure 4.3.4	Group time frequency findings in: (a) Left superior temporal sulcus (N=8). Left: Dynamic faces compared to baseline shows sustained power decrease from 400-2000 ms around 12 Hz. Middle: Static faces compared to baseline shows power decrease from 200-600 ms between 10-30 Hz, and decreases in low frequency power 3-8 Hz from onset to 1000 ms. Right: Direct comparison of dynamic and static faces shows power increase around 500 ms followed by a sustained power decrease from 800 ms onwards between 10-30 Hz; (b) Right superior temporal sulcus (N=9). Left: Dynamic faces compared to baseline shows power decrease (20-60 Hz) between 200-1600 ms, and a sustained decrease in low frequency power (5-13 Hz) from 1000 ms onwards. Middle: Static faces compared to baseline shows slight power decrease between 20-30 Hz at 200 ms and 600 ms. Right: Direct comparison of dynamic and static faces shows a sustained decrease in power from 800 ms onwards between 8-30 Hz.	149
Figure 5.2.1	MEG experimental design: 120 dynamic and 120 static images were presented for 2.5 s in a random sequence, alternating with a 2.5 s fixation cross. Participants (N=14) performed a 1-back memory task and responded via button press as to whether the identity of the current image matched the previous image.	163
Figure 5.3.1	Group time frequency findings in left inferior occipital gyrus (N=12), shows early differences between dynamic angry and static angry expressions around 200 ms. This is due to a larger decrease in power for dynamic angry expressions between 8-35 Hz within 0-200 ms. Top left: Dynamic angry faces versus baseline fixation; Top right: Static angry faces versus baseline fixation; Bottom left: Dynamic versus static angry faces.	168

Figure 5.3.2	Group time frequency findings in right superior temporal sulcus (N=11), shows early differences between dynamic angry and static angry expressions within 200 ms. This is due to a larger decrease in power for dynamic angry expressions between 8-30 Hz within 0-200 ms. Top left: Dynamic angry faces versus baseline fixation; Top right: Static angry faces versus baseline fixation; Bottom left: Dynamic versus static angry faces.	169
Figure 5.3.3	Group time frequency findings in left middle occipital gyrus (N=10), shows greater power for dynamic angry relative to static angry expressions from 400-600 ms, between 10-22 Hz. This is due to a greater peak decrease in power (8-28 Hz) for static angry expressions around 400 ms. Top left: Dynamic angry faces versus baseline fixation; Top right: Static angry faces versus baseline fixation; Bottom left: Dynamic versus static angry faces.	170
Figure 5.3.4	Group time frequency findings in right middle temporal gyrus (N=12), shows greater power for dynamic angry relative to static angry expressions from 400-600 ms, between 10-40 Hz. This is due to a greater peak decrease in power (10-40 Hz) for static angry expressions around 400 ms. Top left: Dynamic angry faces versus baseline fixation; Top right: Static angry faces versus baseline fixation; Bottom left: Dynamic versus static angry faces.	171
Figure 5.3.5	Group time frequency findings in left inferior occipital gyrus (N=11), shows significantly less power for dynamic angry relative to static angry expressions from 800-1000 ms, between 10-30 Hz. This is due to a greater and more sustained peak decrease in power for dynamic angry expressions around 800 ms. Top left: Dynamic angry faces versus baseline fixation; Top right: Static angry faces versus baseline fixation; Bottom left: Dynamic versus static angry faces.	172
Figure 5.3.6	Group time frequency findings in right inferior occipital gyrus (N=10), shows significantly less power for dynamic angry relative to static angry expressions from 800-1000 ms, between 5-30 Hz. This is due to a greater and more sustained peak decrease in power for dynamic angry expressions around 800 ms. Top left: Dynamic angry faces versus baseline fixation; Top right: Static angry faces versus baseline fixation; Bottom left: Dynamic versus static angry faces.	174
Figure 5.3.7	Group time frequency findings in left middle frontal gyrus (N=8), shows significantly less power for dynamic angry relative to static angry expressions from 1800-2000 ms, between 10-25 Hz. This is due to a greater peak decrease in power for dynamic angry expressions around 1800 ms. Top left: Dynamic angry faces versus baseline fixation; Top right: Static angry faces versus baseline fixation; Bottom left: Dynamic versus static angry faces.	175

Figure 5.3.8	Group time frequency findings in right superior frontal gyrus (N=8), shows significantly less power for dynamic angry relative to static angry expressions from 1800-2000 ms between 10-30 Hz. This is due to a greater decrease in power for dynamic angry expressions from 1400 ms onwards. Top left: Dynamic angry faces versus baseline fixation; Top right: Static angry faces versus baseline fixation; Bottom left: Dynamic versus static angry faces.	176
Figure 5.3.9	Group time frequency findings in left inferior frontal gyrus (N=12), shows significantly greater power (2-6 Hz) for dynamic angry relative to dynamic speech displays from 200-1000 ms between. This is due to a greater increase in low frequency power (2-6 Hz) for dynamic angry expressions from 200 ms onwards. Top left: Dynamic angry faces versus baseline fixation; Top right: Dynamic speech faces versus baseline fixation; Bottom left: Dynamic angry versus dynamic speech displays.	177
Figure 5.3.10	Group time frequency findings in right inferior frontal gyrus (N=11), shows significantly greater power (2-8 Hz) for dynamic angry relative to dynamic speech displays from 0-800 ms. This is due to a greater increase in power (2-8 Hz) for dynamic angry expressions from 0-800 ms. Top left: Dynamic angry faces versus baseline fixation; Top right: Dynamic speech faces versus baseline fixation; Bottom left: Dynamic angry versus dynamic speech displays.	178
Figure 5.3.11	Group time frequency findings in right superior temporal sulcus (N=12), shows significantly less power (8-30 Hz) for dynamic angry relative to dynamic speech displays from 0-1000 ms. This is due to a greater decrease in power (8-30 Hz) for dynamic angry expressions between 0-800 ms. Top left: Dynamic angry faces versus baseline fixation; Top right: Dynamic speech faces versus baseline fixation; Bottom left: Dynamic angry versus dynamic speech displays.	179
Figure 5.3.12	Group time frequency findings in left inferior occipital gyrus (N=13), shows significantly less power (8-30 Hz) for dynamic angry relative to dynamic speech displays from 800-1200 ms. This is due to a greater decrease in power (8-30 Hz) for dynamic angry expressions between 800-1200 ms. Top left: Dynamic angry faces versus baseline fixation; Top right: Dynamic speech faces versus baseline fixation; Bottom left: Dynamic angry versus dynamic speech displays.	180

Figure 5.3.13	Group time frequency findings in right inferior occipital gyrus (N=14), shows significantly less power (10-30 Hz) for dynamic angry relative to dynamic speech displays from 800-1400 ms. This is due to a greater decrease in power (10-30 Hz) for dynamic angry expressions between 800-1400 ms. Top left: Dynamic angry faces versus baseline fixation; Top right: Dynamic speech faces versus baseline fixation; Bottom left: Dynamic angry versus dynamic speech displays.	181
Figure 5.3.14	Group time frequency findings in right insula (N=8) shows significantly greater power (3-20 Hz) for dynamic angry relative to dynamic speech displays from 400-1600 ms between. This is due to a greater increase in low frequency power (3-12 Hz) for dynamic angry expressions around 800 ms. Top left: Dynamic angry faces versus baseline fixation; Top right: Dynamic speech faces versus baseline fixation; Bottom left: Dynamic angry versus dynamic speech displays.	182
Figure 5.3.15	Group time frequency findings in right inferior frontal gyrus (N=10), shows early differences between dynamic happy and static happy expressions around 200 ms between 5-30 Hz. This is due to an increase in power (3-6 Hz) for dynamic happy faces and a decrease in power for static happy expressions (10-45 Hz) within 0-200 ms. Top left: Dynamic happy faces versus baseline fixation; Top right: Static happy faces versus baseline fixation; Bottom left: Dynamic versus static happy faces.	186
Figure 5.3.16	Group time frequency findings in left inferior occipital gyrus (N=12), shows early differences between dynamic happy and static happy expressions around 200 ms between 8-30 Hz. This is due to a greater decrease in power (8-30 Hz) for dynamic happy faces within 0-200 ms. Top left: Dynamic happy faces versus baseline fixation; Top right: Static happy faces versus baseline fixation; Bottom left: Dynamic versus static happy faces.	187
Figure 5.3.17	Group time frequency findings in right inferior occipital gyrus (N=12), shows early differences between dynamic happy and static happy expressions around 200 ms between 8-30 Hz. This is due to a greater decrease in power (8-30 Hz) for dynamic happy faces within 0-200 ms. Top left: Dynamic happy faces versus baseline fixation; Top right: Static happy faces versus baseline fixation; Bottom left: Dynamic versus static happy faces.	188

Figure 5.3.18	Group time frequency findings in right middle occipital gyrus (N=9), shows greater power for dynamic happy relative to static happy expressions within 200-400 ms between 8-30 Hz. This is due to a greater peak decrease in power (8-30 Hz) for static happy faces within 200-400 ms. Top left: Dynamic happy faces versus baseline fixation; Top right: Static happy faces versus baseline fixation; Bottom left: Dynamic versus static happy faces.	189
Figure 5.3.19	Group time frequency findings in left fusiform gyrus (N=11), shows greater power for dynamic happy relative to static happy expressions within 400-600 ms between 12-40 Hz. This is due to a greater peak decrease in power (8-28 Hz) for static happy faces around 500 ms. Top left: Dynamic happy faces versus baseline fixation; Top right: Static happy faces versus baseline fixation; Bottom left: Dynamic versus static happy faces.	190
Figure 5.3.20	Group time frequency findings in right fusiform gyrus (N=10), shows greater power for dynamic happy relative to static happy expressions within 400-600 ms between 8-25 Hz. This is due to a greater peak decrease in power (8-30 Hz) for static happy faces around 500 ms. Top left: Dynamic happy faces versus baseline fixation; Top right: Static happy faces versus baseline fixation; Bottom left: Dynamic versus static happy faces.	191
Figure 5.3.21	Group time frequency findings in left inferior frontal gyrus (N=9), shows decreased power for dynamic happy relative to static happy expressions within 400-600 ms between 2-22 Hz. This is due to an increase in low frequency power (2-10 Hz) and a decrease in power (15-22 Hz) for dynamic happy faces around 400 ms. Top left: Dynamic happy faces versus baseline fixation; Top right: Static happy faces versus baseline fixation; Bottom left: Dynamic versus static happy faces.	193
Figure 5.3.22	Group time frequency findings in left postcentral gyrus (N=8), shows greater power for dynamic happy relative to static happy expressions within 400-600 ms between 5-50 Hz. This is due to a greater decrease in power (15-60 Hz) for static happy faces around 500 ms. Top left: Dynamic happy faces versus baseline fixation; Top right: Static happy faces versus baseline fixation; Bottom left: Dynamic versus static happy faces.	194
Figure 5.3.23	Group time frequency findings in left postcentral gyrus (N=9), shows greater power for dynamic happy relative to static happy expressions within 600-800 ms between 10-40 Hz. This is due to a greater decrease in power (10-40 Hz) for static happy faces around 600 ms. Top left: Dynamic happy faces versus baseline fixation; Top right: Static happy faces versus baseline fixation; Bottom left: Dynamic versus static happy faces.	195

Figure 5.3.24	Group time frequency findings in left middle occipital gyrus (N=11), shows decreased power for dynamic happy relative to static happy expressions within 800-1000 ms between 12-35 Hz. This is due to a greater peak decrease in power (12-35 Hz) for dynamic happy faces from 800 ms onwards. Top left: Dynamic happy faces versus baseline fixation; Top right: Static happy faces versus baseline fixation; Bottom left: Dynamic versus static happy faces.	196
Figure 5.3.25	Group time frequency findings in left middle temporal gyrus (N=10), shows decreased power for dynamic happy relative to static happy expressions within 1000-1200 ms between 8-35 Hz. This is due to a greater decrease in power (10-40 Hz) for dynamic happy faces from 800 ms onwards. Top left: Dynamic happy faces versus baseline fixation; Top right: Static happy faces versus baseline fixation; Bottom left: Dynamic versus static happy faces.	197
Figure 5.3.26	Group time frequency findings in right superior temporal sulcus (N=11), shows decreased power for dynamic happy relative to static happy expressions within 1000-1200 ms between 5-35 Hz. This is due to a greater and more sustained decrease in power (8-40 Hz) for dynamic happy faces from 800 ms onwards. Top left: Dynamic happy faces versus baseline fixation; Top right: Static happy faces versus baseline fixation; Bottom left: Dynamic versus static happy faces.	199
Figure 5.3.27	Group time frequency findings in right fusiform gyrus (N=12), shows decreased power for dynamic happy relative to static happy expressions within 1200-1400 ms between 2-40 Hz. This is due to a greater and more sustained decrease in power (10-30 Hz) for dynamic happy faces from 1000 ms onwards. Top left: Dynamic happy faces versus baseline fixation; Top right: Static happy faces versus baseline fixation; Bottom left: Dynamic versus static happy faces.	200
Figure 5.3.28	Group time frequency findings in left superior temporal sulcus (N=8), shows decreased power for dynamic happy relative to static happy expressions within 2000-2200 ms between 8-35 Hz. This is due to a decrease in power (5-60 Hz) for dynamic happy faces around 2000 ms. Top left: Dynamic happy faces versus baseline fixation; Top right: Static happy faces versus baseline fixation; Bottom left: Dynamic versus static happy faces.	201

Figure 5.3.29	Group time frequency findings in left inferior frontal gyrus (N=8), shows significantly greater power (2-6 Hz) for dynamic happy relative to dynamic speech facial displays between 0-800 ms. This is due to a greater increase in low frequency power (2-6 Hz) for dynamic happy faces within 200 ms of stimulus onset. Top left: Dynamic happy faces versus baseline fixation; Top right: Dynamic speech faces versus baseline fixation; Bottom left: Dynamic happy versus dynamic speech faces.	202
Figure 5.3.30	Group time frequency findings in right inferior frontal gyrus (N=9), shows significantly greater power (2-6 Hz) for dynamic happy relative to dynamic speech facial displays between 0-500 ms. This is due to a greater increase in low frequency power (2-6 Hz) for dynamic happy faces within 200 ms of stimulus onset. Top left: Dynamic happy faces versus baseline fixation; Top right: Dynamic speech faces versus baseline fixation; Bottom left: Dynamic happy versus dynamic speech faces.	203
Figure 5.3.31	Group time frequency findings in left middle occipital gyrus (N=12), shows significantly less power (8-22 Hz) for dynamic happy relative to dynamic speech facial displays between 200-800 ms. This is due to a greater decrease in power (8-22 Hz) for dynamic happy faces around 200 ms. Top left: Dynamic happy faces versus baseline fixation; Top right: Dynamic speech faces versus baseline fixation; Bottom left: Dynamic happy versus dynamic speech faces.	204
Figure 5.3.32	Group time frequency findings in left fusiform gyrus (N=12), shows significantly less power (6-20 Hz) for dynamic happy relative to dynamic speech facial displays between 900-1600 ms. This is due to a greater decrease in power (6-20 Hz) for dynamic happy faces from 900-1600 ms. Top left: Dynamic happy faces versus baseline fixation; Top right: Dynamic speech faces versus baseline fixation; Bottom left: Dynamic happy versus dynamic speech faces.	205
Figure 5.3.33	Group time frequency findings in left inferior frontal gyrus (N=8), shows early differences between dynamic speech and static speech displays around 200 ms, between 5-40 Hz. This is due to an increase in low frequency power (3-10 Hz) for dynamic speech faces and a decrease in power for static speech faces (20-40 Hz) within 0-200 ms. Top left: Dynamic speech faces versus baseline fixation; Top right: Static speech faces versus baseline fixation; Bottom left: Dynamic versus static speech faces.	209

Figure 5.3.34	Group time frequency findings in right inferior frontal gyrus (N=10), shows early differences between dynamic speech and static speech displays around 200 ms, between 5-60 Hz. This is due to an increase in low frequency power for dynamic speech faces (3-10 Hz) and a decrease in high frequency power for static speech faces (20-60 Hz) within 0-200 ms. Top left: Dynamic speech faces versus baseline fixation; Top right: Static speech faces versus baseline fixation; Bottom left: Dynamic versus static speech faces.	210
Figure 5.3.35	Group time frequency findings in left inferior occipital gyrus (N=12), shows early differences between dynamic speech and static speech displays around 200 ms, between 5-22 Hz. This is due to an early decrease in power (5-20 Hz) for dynamic speech faces within 0-200 ms. Top left: Dynamic speech faces versus baseline fixation; Top right: Static speech faces versus baseline fixation; Bottom left: Dynamic versus static speech faces.	211
Figure 5.3.36	Group time frequency findings in right inferior occipital gyrus (N=12), shows early differences between dynamic speech and static speech displays around 200 ms between 5-22 Hz. This is due to an early decrease in power (5-20 Hz) for dynamic speech faces within 0-200 ms. Top left: Dynamic speech faces versus baseline fixation; Top right: Static speech faces versus baseline fixation; Bottom left: Dynamic versus static speech faces.	212
Figure 5.3.37	Group time frequency findings in right superior temporal sulcus (N=9), shows significantly less power for dynamic speech relative to static speech displays within 800-1000 ms, between 10-40 Hz. This is due to a sustained decrease in power (5-30 Hz) for dynamic speech faces from 500 ms onwards. Top left: Dynamic speech faces versus baseline fixation; Top right: Static speech faces versus baseline fixation; Bottom left: Dynamic versus static speech faces.	213
Figure 5.3.38	Group time frequency findings in left postcentral gyrus (N=9), shows significantly greater power for dynamic speech relative to static speech displays within 1000-1200 ms, between 8-35 Hz. This is due to an increase in power (12-30 Hz) for dynamic speech faces and a decrease in power (10-20 Hz) for static speech faces within 1000-1200 ms. Top left: Dynamic speech faces versus baseline fixation; Top right: Static speech faces versus baseline fixation; Bottom left: Dynamic versus static speech faces.	214

Figure 5.3.39	Group time frequency findings in left middle occipital gyrus (N=10), shows significantly less power for dynamic speech relative to static speech displays within 1000-1200 ms, between 5-30 Hz. This is due to a sustained decrease in power (5-20 Hz) for dynamic speech faces from 800 ms onwards. Top left: Dynamic speech faces versus baseline fixation; Top right: Static speech faces versus baseline fixation; Bottom left: Dynamic versus static speech faces.	215
Figure 5.3.40	Group time frequency findings in left inferior frontal gyrus (N=8), shows significantly less power for dynamic speech relative to static speech displays within 1000-1200 ms, between 8-40 Hz. This is due to a decrease in power (8-50 Hz) for dynamic speech faces and an increase in power (10-40 Hz) for static speech faces around 1200 ms. Top left: Dynamic speech faces versus baseline fixation; Top right: Static speech faces versus baseline fixation; Bottom left: Dynamic versus static speech faces.	216
Figure 5.3.41	Group time frequency findings in left middle temporal gyrus (N=10), shows significantly less power for dynamic speech relative to static speech displays within 1200-1400 ms, between 5-20 Hz. This is due to a sustained decrease in power (5-30 Hz) for dynamic speech faces from 800 ms onwards. Top left: Dynamic speech faces versus baseline fixation; Top right: Static speech faces versus baseline fixation; Bottom left: Dynamic versus static speech faces.	217
Figure 5.3.42	Group time frequency findings in left middle frontal gyrus (N=9), shows significantly less power for dynamic speech relative to static speech displays within 1200-1400 ms, between 3-30 Hz. This is due to an increase in power (3-30 Hz) for static speech faces around 1200 ms. Top left: Dynamic speech faces versus baseline fixation; Top right: Static speech faces versus baseline fixation; Bottom left: Dynamic versus static speech faces.	218
Figure 5.3.43	Group time frequency findings in left inferior occipital gyrus (N=11), shows significantly less power for dynamic speech relative to static speech displays within 1800-2000 ms, between 1-30 Hz. This is due to a greater sustained decrease in power (8-30 Hz) for dynamic speech faces from 800 ms onwards and an increase in low frequency power (2-8 Hz) for static speech faces. Top left: Dynamic speech faces versus baseline fixation; Top right: Static speech faces versus baseline fixation; Bottom left: Dynamic versus static speech faces.	219

Figure 5.3.44	Group time frequency findings in right middle temporal gyrus (N=10), shows significantly less power for dynamic speech relative to static speech displays within 1800-2000 ms, between 5-30 Hz. This is due to a sustained decrease in power (5-30 Hz) for dynamic speech faces from 500 ms onwards. Top left: Dynamic speech faces versus baseline fixation; Top right: Static speech faces versus baseline fixation; Bottom left: Dynamic versus static speech faces.	220
Figure 5.3.45	Group time frequency findings in right superior temporal sulcus (N=9), shows significantly less power for dynamic speech relative to static speech displays within 2000-2200 ms, between 5-40 Hz. This is due to a more sustained decrease in power (5-40 Hz) for dynamic speech faces from 1800 ms onwards. Top left: Dynamic speech faces versus baseline fixation; Top right: Static speech faces versus baseline fixation; Bottom left: Dynamic versus static speech faces.	221
Figure 5.3.46	Group time frequency findings in right inferior occipital gyrus (N=12), shows significantly less power for dynamic speech relative to static speech displays within 2200-2400 ms, between 5-30 Hz. This is due to a more sustained decrease in power (5-30 Hz) for dynamic speech faces from 1800 ms onwards. Top left: Dynamic speech faces versus baseline fixation; Top right: Static speech faces versus baseline fixation; Bottom left: Dynamic versus static speech faces.	222
Figure 6.2.1	fMRI and MEG integration: (A) fMRI whole brain group results (N=14) for the dynamic versus static condition displayed on lateral and ventral views. Shows bilateral activation in MOG, MTG and extending along STS to frontal regions of the cortex, IFG and MFG, in both left (L) and right (R) hemispheres. Red-orange-yellow colour scale depicts increasing BOLD amplitude ($p < 0.05$). (B) Group SAM image (N=14) shows decrease in beta band power (12-30 Hz) for the contrast of dynamic versus static faces, between 1000-1500 ms post stimulus onset in bilateral IOG, MTG, STS and IFG, on lateral and ventral views. Blue-purple-white colour scale represents a decrease in signal power ($p < 0.05$).	243

List of Tables

Table 2.1	Brain regions showing significant activations in response to all dynamic compared to all static expressions. Coordinates indicate local maxima in Talairach space. L = Left; R = Right. Multiple peaks within a cluster are shown on subsequent lines.	82
Table 2.2	Brain regions showing significant activations in response to dynamic angry compared to static angry expressions. Coordinates indicate local maxima in Talairach space. L = Left; R = Right. Multiple peaks within a cluster are shown on subsequent lines.	83
Table 2.3	Brain regions showing significant activations in response to dynamic happy compared to static happy expressions. Coordinates indicate local maxima in Talairach space. L = Left; R = Right. Multiple peaks within a cluster are shown on subsequent lines.	83
Table 2.4	Brain regions showing significant activations in response to dynamic speech compared to static speech expressions. Coordinates indicate local maxima in Talairach space. L = Left; R = Right. Multiple peaks within a cluster are shown on subsequent lines.	83
Table 2.5	Brain regions showing significant activations in response to dynamic angry compared to dynamic speech facial displays. Coordinates indicate local maxima in Talairach space. L = Left; R = Right. Multiple peaks within a cluster are shown on subsequent lines.	85
Table 2.6	Brain regions showing significant activations in response to dynamic happy compared to dynamic speech facial displays. Coordinates indicate local maxima in Talairach space. L = Left; R = Right. Multiple peaks within a cluster are shown on subsequent lines.	87
Table 2.7	Location of regions of interest within the face perception network. Coordinates are presented in Talairach space. L = Left; R = Right. N indicates the number of subjects who showed significant activation in each region. Standard error of the means are indicated in parentheses.	89

Table 3.1	Brain regions showing effective connectivity with left IOG under condition of (A) All dynamic compared to all static expressions; (B) Dynamic angry compared to static angry expressions; (C) Dynamic happy compared to static happy expressions; (D) Dynamic speech compared to static speech expressions; (E) Dynamic angry compared to dynamic speech displays; (F) Dynamic happy compared to dynamic speech displays. Coordinates indicate local maxima in Talairach space. L = Left; R = Right. Multiple peaks within a cluster are shown on subsequent lines.	115
Table 3.2	Brain regions showing effective connectivity with right IOG under condition of (A) All dynamic compared to all static expressions; (B) Dynamic angry compared to static angry expressions; (C) Dynamic happy compared to static happy expressions; (D) Dynamic speech compared to static speech expressions; (E) Dynamic angry compared to dynamic speech displays; (F) Dynamic happy compared to dynamic speech displays. Coordinates indicate local maxima in Talairach space. L = Left; R = Right. Multiple peaks within a cluster are shown on subsequent lines.	116
Table 3.3	Brain regions showing effective connectivity with left STS under condition of (A) All dynamic compared to all static expressions; (B) Dynamic angry compared to static angry expressions; (C) Dynamic happy compared to static happy expressions; (D) Dynamic speech compared to static speech expressions; (E) Dynamic angry compared to dynamic speech displays; (F) Dynamic happy compared to dynamic speech displays. Coordinates indicate local maxima in Talairach space. L = Left; R = Right. Multiple peaks within a cluster are shown on subsequent lines.	117
Table 3.4	Brain regions showing effective connectivity with right STS under condition of (A) All dynamic compared to all static expressions; (B) Dynamic angry compared to static angry expressions; (C) Dynamic happy compared to static happy expressions; (D) Dynamic speech compared to static speech expressions; (E) Dynamic angry compared to dynamic speech displays; (F) Dynamic happy compared to dynamic speech displays. Coordinates indicate local maxima in Talairach space. L = Left; R = Right. Multiple peaks within a cluster are shown on subsequent lines.	118
Table 3.5	Brain regions showing effective connectivity with the left amygdala under condition of (A) All dynamic compared to all static expressions; (B) Dynamic angry compared to static angry expressions; (C) Dynamic happy compared to static happy expressions; (D) Dynamic speech compared to static speech expressions; (E) Dynamic angry compared to dynamic speech displays; (F) Dynamic happy compared to dynamic speech displays. Coordinates indicate local maxima in Talairach space. L = Left; R = Right. Multiple peaks within a cluster are shown on subsequent lines.	119

Table 3.6	Brain regions showing effective connectivity with the right amygdala under condition of (A) All dynamic compared to all static expressions; (B) Dynamic angry compared to static angry expressions; (C) Dynamic happy compared to static happy expressions; (D) Dynamic speech compared to static speech expressions; (E) Dynamic angry compared to dynamic speech displays; (F) Dynamic happy compared to dynamic speech displays Coordinates indicate local maxima in Talairach space. L = Left; R = Right. Multiple peaks within a cluster are shown on subsequent lines.	120
Table 3.7	Brain regions showing effective connectivity with the region in left inferior frontal gyrus under condition of (A) All dynamic compared to all static expressions; (B) Dynamic angry compared to static angry expressions; (C) Dynamic happy compared to static happy expressions; (D) Dynamic speech compared to static speech expressions; (E) Dynamic angry compared to dynamic speech displays; (F) Dynamic happy compared to dynamic speech displays Coordinates indicate local maxima in Talairach space. L = Left; R = Right. Multiple peaks within a cluster are shown on subsequent lines.	121
Table 3.8	Brain regions showing effective connectivity with the region in right inferior frontal gyrus under condition of (A) All dynamic compared to all static expressions; (B) Dynamic angry compared to static angry expressions; (C) Dynamic happy compared to static happy expressions; (D) Dynamic speech compared to static speech expressions; (E) Dynamic angry compared to dynamic speech displays; (F) Dynamic happy compared to dynamic speech displays Coordinates indicate local maxima in Talairach space. L = Left; R = Right. Multiple peaks within a cluster are shown on subsequent lines.	122
Table 3.9	Physiophysiological interaction results in the left hemisphere.	123
Table 3.10	Physiophysiological interaction results in the right hemisphere.	123
Table 4.1	Brain regions showing decreases in beta power (12-30Hz) in response to all dynamic compared to static faces within the following time windows (A) 0 to 500 ms (B) 500 to 1000 ms (C) 1000 to 1500 ms (D) 1500 to 2000 ms (E) 2000 to 2500 ms. Co-ordinates indicate local maxima in Talairach space. L = Left; R = Right. Clusters are significant at $p < .05$	143
Table 4.2	Mean stereotactic co-ordinates for the virtual electrodes in Talairach space. N = number of participants showing a significant peak in a particular region.	143
Table 5.1	Brain regions showing significant differences in oscillatory power in response to dynamic angry versus static angry facial expressions within the following time windows: (A) 0-200 ms (B) 400-600 ms (C) 800-1000 ms (D) 1800-2000 ms. Co-ordinates indicate local maxima in Talairach space. Clusters are significant at $p < .05$. N = number of participants showing a peak in that region. L= Left, R = Right.	166

Table 5.2	Brain regions showing significant differences in oscillatory power in response to dynamic angry facial expressions versus dynamic speech facial displays within the following time windows: (A) 200-400 ms (B) 600-800 ms (C) 800-1000 ms. Co-ordinates indicate local maxima in Talairach space. Clusters are significant at $p < .05$. N = number of participants showing a peak in that region. L= Left, R = Right.	167
Table 5.3	Brain regions showing significant differences in oscillatory power in response to dynamic happy versus static happy facial expressions within the following time windows: (A) 0-200 ms (B) 200-400 ms (C) 400-600 ms (D) 600-800 ms (E) 800-1000 ms (F) 1000-1200 ms (G) 1200-1400 ms (H) 2000-2200 ms. Co-ordinates indicate local maxima in Talairach space. Clusters are significant at $p < .05$. N = number of participants showing a peak in that region. L= Left; R = Right.	184
Table 5.4	Brain regions showing significant differences in oscillatory power in response to dynamic happy facial expressions versus dynamic speech facial displays within the following time windows: (A) 0-200 ms (B) 200-400 ms (C) 1000-1200 ms. Co-ordinates indicate local maxima in Talairach space. Clusters are significant at $p < .05$. N = number of participants showing a peak in that region. L= Left, R = Right.	185
Table 5.5	Brain regions showing significant differences in oscillatory power in response to dynamic speech versus static speech facial displays within the following time windows: (A) 0-200 ms (B) 800-1000 ms (C) 1000-1200 ms (D) 1200-1400 ms (E) 1800-2000 ms (F) 2000-2200 ms and (G) 2200-2400 ms. Co-ordinates indicate local maxima in Talairach space. Clusters are significant at $p < .05$. N = number of participants showing a peak in that region. L = Left; R = Right.	207

List of Abbreviations

AMG	amygdala
BA	brodmann area
BOLD	blood oxygen level dependent
DCM	dynamic causal modelling
DTI	diffusion tensor imaging
ERP	event related potential
FFA	fusiform face area
FG	fusiform gyrus
fMRI	functional magnetic resonance imaging
IFG	inferior frontal gyrus
IOG	inferior occipital gyrus
LiG	lingual gyrus
MEG	magnetoencephalography
MFG	middle frontal gyrus
MOG	middle occipital gyrus
MTG	middle temporal gyrus
OFA	occipital face area
POCG	postcentral gyrus
PPI	psychophysiological interaction
PRCG	precentral gyrus
PYPI	physiophysiological interaction
ROI	regions of interest
SAM	synthetic aperture magnetometry
SnPM	statistical non-parametric mapping
SPM	statistical parametric mapping
STS	superior temporal sulcus

Chapter 1

A review of face perception research: from a specialised module to a distributed network

1.1 Overview

In this chapter, face perception literature relevant to the present thesis will be reviewed. To begin, a review of the early face perception literature will be provided, starting from the early studies and models developed in cognitive psychology, and proceeding to neuroimaging studies, which focused on functional specialisation within the cortex. More recent neural models of face perception and emotion recognition will then be described, and the important factor of motion in face processing will be discussed. Neuroimaging studies of biological motion and dynamic face perception will then be presented. This will be followed by a discussion of network theories on functional integration and distributed networks in face perception. Then a brief overview of the neuroimaging methods used in the present thesis will be provided, followed by a discussion of multimodal integration. Finally the overall objectives and goals of the present thesis will be outlined.

1.2 Early face perception research

The human face not only acts as a means of identification but also serves to provide insights into emotional states and intentions through facial expressions, interpretation

of speech through lip reading, and information about personality, attractiveness, age and gender. The sheer complexity of this information suggests that face perception is an advanced cognitive ability. Consequently, face perception has emerged as a major research area spanning many different disciplines including, psychology, cognitive neuroscience, computer science and neuroimaging, among others (Tovée, 1998), which highlights the broad focus of current face perception research.

However, before the advent of neuroimaging techniques the primary methods of face perception research were neuropsychological observations of single cases and behavioural investigations using various photographs of faces, where the derivation of identity was the most popular topic for research (Bruce and Young, 1986). Yet, despite this relatively narrow focus of early face perception research on identity processing, researchers did recognise that faces constitute a unique visual stimulus and evidence from neuropsychological studies suggested that the brain may possess systems that are specifically important for processing faces (Young et al., 2008). These early cognitive behavioural and neuropsychological face perception studies will be discussed in the following sections.

1.2.1 Neuropsychological studies

Initial evidence to show that the brain may process faces differently from other objects came from neuropsychological studies of patients with prosopagnosia (Damasio et al., 1982). Prosopagnosic patients are described as having normal visual abilities but impaired face recognition abilities, usually following ventral occipital or temporal lobe lesions. In the literature a distinction has been made between ‘apperceptive’ and ‘associative’ prosopagnosia (Damasio et al., 1990). Patients with ‘apperceptive’ prosopagnosia are unable to perceive faces due to an impairment in visual perception, which is generally associated with damage to the right visual association cortices within the occipital and parietal regions. Conversely, patients with ‘associative’ prosopagnosia appear to be able to perceive faces correctly, but are unable to recognise familiar faces. This is generally due to bilateral damage within inferior occipital and temporal visual cortices. Furthermore, Moscovitch et al. (1997) have reported a patient with object agnosia but intact face recognition abilities. This is an important double dissociation between face and object recognition, as it suggests that the two abilities are functionally distinct and anatomically

separable.

There are also cases of prosopagnosia, where patients can interpret facial expressions correctly but are unable to correctly identify familiar faces (Humphreys et al., 1993). This dissociation lends support to the theory that the processing of facial expression and identity proceed independently in different neural regions (see subsection 1.3.2). However, caution must be taken when interpreting such data because brain damage can affect large and diffuse areas making it difficult to localise function to specific regions. Furthermore, some researchers claim that prosopagnosia may constitute more than a face disorder, as many prosopagnosic patients also show signs of impaired object recognition (Gauthier et al., 1999). Hence, it has been suggested that studies of prosopagnosic patients may not have used adequate controls and patients may in fact be impaired at category judgements of visually similar objects (Gauthier et al., 1999).

1.2.2 Behavioural studies

Much of the early behavioural face perception research focused on face recognition, however this topic is only briefly mentioned here as it is outside the scope of this thesis to review the face recognition literature (for review see Bruce and Young, 1986). Researchers have investigated the factors affecting face recognition abilities by manipulating various conditions such as viewing angle, changes in appearance and changes in expression (Bruce and Young, 1986). In general, the main finding from these studies was that recognition of unfamiliar faces was affected by changes in facial expression and viewing angle, whereas recognition of familiar faces was largely unaffected by these different viewing conditions. Furthermore, changing facial expression did not appear to affect identity judgements and vice versa. It was therefore suggested that different processes are involved in the recognition of familiar and unfamiliar faces, and that facial identity and expression are processed independently. These findings were later incorporated into the influential cognitive face perception model of Bruce and Young (1986) (see subsection 1.2.3).

While the majority of behavioural face perception research at that time was concerned with face recognition, the processing of facial expressions did receive some attention. Notably, research by Ekman and colleagues on the universals of emotion, which was inspired by Darwin (1872)'s seminal work, investigated the perception and categorisation of fa-

cial expressions (Ekman and Friesen, 1971). In 1872 Charles Darwin described in detail how humans and animals express facial emotions, and claimed that facial expressions are innate and universal throughout all cultures and races.

A century later, the work by Ekman and colleagues (Ekman and Friesen, 1971; Izard, 1971; Ekman, 1992) appeared to confirm Darwin's observations. In a series of studies, category judgements of facial expressions were examined by showing static photographs of various facial expressions to observers from different cultures (e.g. USA, Brazil, Chile, Japan). They found that some facial expressions, including anger, happiness, fear, disgust, surprise and sadness, were recognised universally across cultures. It is now generally accepted that these represent the six basic emotion categories (Ekman et al., 1987). However this interpretation has received criticism, particularly from Russell (1994) who argues that the studies lack ecological validity (see subsection 1.3.6 for further discussion of ecological validity). For a recent review and alternative interpretation of Darwin's theory see Barrett (2011).

1.2.2.1 Dynamic information

An important aspect of face perception that has generally been neglected is the dynamic nature of the human face. The majority of studies have used static facial images such as line drawings or photographs to explore face perception, but human faces are not static entities. Human faces can move in a variety of ways for numerous reasons, and it is therefore unlikely that this inherent dynamic information is redundant. Traditionally facial motion has been described as being a form of either rigid or non-rigid motion. Rigid facial motion is usually used to describe the rotations and translations of the entire head, such as nodding or turning the head. In contrast, non-rigid facial motion refers to internal motion of the facial features such as lip movements or eyebrow motion. In general, naturally occurring facial motion contains both rigid and non-rigid motion and there is converging evidence suggesting that both types of motion play an important role in face perception (O'Toole et al., 2002).

One of the first formal studies on dynamic face perception was conducted by Bassili in 1978 using the point light experimental technique. This technique involves the creation of animation sequences by using a number of dots to represent the main joints of the

body or face and creating realistic movement patterns of these joints. Static sequences are viewed as a meaningless group of dots but when animated give the impression of a human form. Bassili (1978) found that subjects were better able to distinguish faces from non-face objects, and to correctly identify different emotions, in the moving condition compared to the static condition.

Bruce and Valentine (1988) later replicated these results using the same technique. They found a significant improvement in identity judgements and recognition of expression for moving dot displays and concluded that motion provides information in situations where the static cues are impoverished, by contributing to perception of the 3D structure of the face. However, it must be noted that point-light displays are highly impoverished stimuli as the spatial information about facial structure is absent (Hill and Johnston, 2001). Nevertheless these studies demonstrate the value of motion cues in emotion classification in the absence of other information, but it is difficult to generalise to the perception of faces in the real world.

Recently, Hill and Johnston (2001) found that facial motion can convey information about gender. While research by Pike et al. (1997) and Christie and Bruce (1998), among others, revealed that facial motion can contribute to identity judgements. Furthermore, Ekman and Friesen (1982) discovered differences in the timing of false and genuine smiles, suggesting that temporal information can be used to assess the emotional valence of a dynamic expression.

Similarly, Wehrle et al. (2000) found that dynamic emotional expressions facilitate emotional processing, and propose that this may be due to additional information encoded in facial action patterns, which is not present in static stimuli. A contention supported by Kamachi et al. (2001) who found that judgements of facial affect were influenced by changing the velocity of a moving expressing face, which implies that the dynamic display of facial expressions provides unique temporal information about the expressions which is not available in static displays. Thus, in order to understand human face perception abilities in naturalistic contexts the role of motion should be considered, because human faces are dynamic objects and are always perceived as moving in their natural social ecology (Knight and Johnston, 1997).

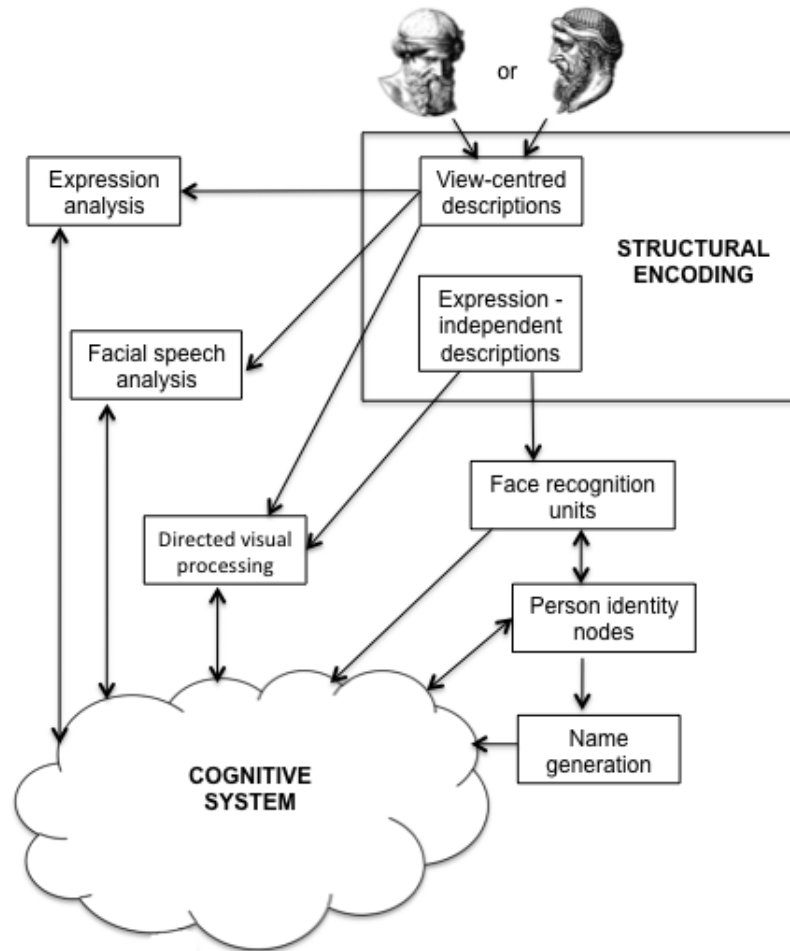


Figure 1.2.1: The functional model of face recognition adapted from Bruce and Young (1986), shows two distinct pathways for identity and facial expression processing.

1.2.3 The functional model for face recognition

By merging the findings from behavioural and neuropsychological studies, and casting them in a unified framework, Bruce and Young (1986) developed an influential theoretical model of face recognition, which has dominated the psychological literature for over twenty years. This model gives a modular account of the face processing system, which is described in terms of processing pathways and specific modules involved in face recognition. The first level of analysis is the structural encoding stage where visual analysis of the face is performed. Facial expression and identity information are processed independently at this stage, and diverge into different processing pathways (see Figure 1.2.1). The facial expression 'route' contains specialised modules for expression analysis and facial speech analysis, whereas modules for face recognition, person identity and name generation are in the recognition pathway. There is then an all encompassing cognitive system, which is required to combine information from the different modules (see Figure 1.2.1).

This model can be used to explain certain neuropsychological phenomenon, for example, aperceptive prosopagnosia can be explained by deficits in the structural encoding stage, whereas associative prosopagnosia could be due to damage to the face recognition or person identity nodes (Henson et al., 2003). Furthermore, prosopagnosic patients who can interpret facial expressions correctly but are unable to correctly identify familiar faces, support the division between facial expression and identity processing (Humphreys et al., 1993). The notion of functional independence between identity and expression processing is also supported by behavioural evidence showing that the recognition of facial expressions are not affected by the familiarity of a face and vice versa (Young et al., 1986). However, Schweinberger and Soukup (1998) found that expression judgements were modulated by identity and familiarity, suggesting that there may be some interaction between expression and identity processing. The independence between identity and expression processing is still a current source of investigation in face perception research and will be discussed in more detail in subsection 1.3.2 and subsection 2.1.2.

The main benefit of the Bruce and Young model is that it provided a unified framework from which testable hypotheses could be derived. However, the model is primarily concerned with the functional components within the face perception system and does not provide a neural description of these areas. The model is also dated now as it implies that the brain is organised in independent modules, which work serially and independently, resembling the computer analogy that was prevalent at the time. But this view is no longer presentable (Grossberg, 2000).

1.3 Neuroimaging and neurophysiological studies of face perception

In recent years, face perception research has benefited from the application of neuroimaging and neurophysiological techniques, which have been used to examine neural activation patterns in response to numerous face processing tasks (see section 1.5 for a discussion of these methods). In keeping with the traditional modular view in face perception research, many of these studies aimed at determining whether a specific area or module exists in the human brain that is selectively involved in face processing (Kanwisher et al., 1997).

However, recent results have uncovered a broad neural network of regions involved in the processing of faces (Haxby et al., 2000; Ishai, 2008). The findings from these studies will be reviewed in the following sections and a recent neural model of face processing proposed by Haxby and colleagues will be discussed.

1.3.1 A specialised face perception module?

In addition to evidence from neuropsychological studies of patients with prosopagnosia (see subsection 1.2.1), single unit recording studies in non-human primates are also believed to provide further evidence for a specialised face perception system. These studies revealed selective face-responsive neurons in inferior temporal cortex, where faces are represented by the combined activity of groups of neurons forming unique patterns of activation, a population code, for every face (Young and Yamane, 1992). However, cells in inferotemporal cortex have also been shown to respond to other objects such as hands (Gauthier et al., 1999). Nonetheless, a recent study by Tsao et al. (2006) claims to have found a region in the macaque temporal lobe that consists completely of face-selective cells. They used functional magnetic resonance imaging (fMRI) to localise the face selective region in two macaques to guide the single-cell recording and report 97% of cells in this region responded selectively to faces. They therefore claim that these results provide evidence for a specialised face perception region. Although this is not so obvious given that they found many cells that responded significantly to non-face objects such as orange lines, and the small sample of only two monkeys.

Evidence from human electrophysiological studies also suggests that face processing may be unique, and activates specialised neural areas in ventral occipito-temporal cortex within 200 ms of stimulus presentation (Allison et al., 1999). Electroencephalography (EEG) and magnetoencephalography (MEG) studies have identified the N170 and M170 response components respectively, which are selectively responsive to faces, occurring at approximately 170 ms post stimulus presentation (see chapter 4 for more detailed discussion). The N/M170 response is generally twice as large for faces compared to other control objects (Bentin et al., 1996; Liu et al., 2002). A similar response has also been measured intracranially known as the N200 response. However, there is much debate as to whether such activation is uniquely specific to faces, or whether it represents more general effects

of expertise that are not exclusive to face processing (for recent discussions see Rossion et al., 2003; Xu et al., 2005).

Numerous fMRI studies, have identified a region in the fusiform gyrus that is consistently activated when subjects view faces compared with other objects such as letters, animals and human body parts (Kanwisher et al., 1997). Some researchers believe that these results reflect activity of a specialised module for face perception and consequently termed it the 'fusiform face area' (FFA). This area appears to correspond with the region that has been damaged in prosopagnosic patients, and the region implicated in electrophysiological studies (Kanwisher et al., 1997; Kanwisher, 2000). Thus providing support for a specialised anatomically discrete face processing area in both temporal and spatial domains.

However, this view has been challenged, particularly by Gauthier et al. (1999), who proposed that this region is not specialised to faces but to visual expertise. This is based on findings from studies where FFA exhibited increased activation for (highly familiar) objects of expertise including 'Greebles' (complex three dimensional similar shapes), birds and cars. Hence, Gauthier et al. (1999) argue that activation in the so-called fusiform face area may reflect processing of highly similar objects rather than faces per se. There is still ongoing debate as to whether this particular region in the fusiform gyrus is domain or process specific (for recent reviews see Xu et al., 2005; Kanwisher and Yovel, 2006).

An alternative view was presented by Ishai and colleagues (1999), where they proposed that the representations of different categories of objects including faces are distributed within ventral temporal cortex based on their features. In a series of studies they report similar patterns of response to faces and other objects in bilateral regions of ventral occipital cortex. They found that objects with similar shape and features were clustered together, creating a consistent topographical arrangement and activation pattern. Haxby et al. (2001) therefore propose that faces and objects are represented within a widely distributed and overlapping network of regions in ventral temporal cortex. This is contrary to the notion of a highly specialised neural area for face perception or a face specific module. Rather, in this view, the fusiform gyrus forms part of a larger extended network, which is involved in the representation of all objects.

1.3.2 The distributed neural system for face perception

Based on the broad activation of cortical areas in response to faces Haxby and colleagues (2000) proposed a distributed neural system for face processing, which is compatible with the Bruce and Young (1986) framework (see subsection 1.2.3). Like the Bruce and Young (1986) model, the distributed face perception model distinguishes between the representation of the invariant versus the changeable aspects of faces. This model is hierarchical, consisting of a core system and an extended system (see Figure 1.3.1). The core system comprises three bilateral regions in occipito-temporal cortex. Within this core system, the initial perception of facial features occurs in the inferior occipital gyri (IOG). It is suggested that from here there are two functionally and neurologically distinct pathways, based on the idea that facial structure is more important for identification purposes, while changeable aspects are necessary to facilitate social communication. Thus the perception of identity, the invariant aspect of a face, occurs in the lateral fusiform gyri (FG), whereas the superior temporal sulci (STS) are involved in the processing and representation of the changeable facial features.

The extended system incorporates additional brain regions that are recruited to process and assess the importance of information drawn from the face. For example, the amygdala, insula and limbic system are recruited to process emotional content, whereas the intraparietal sulcus is involved in processing spatially directed attention such as eye gaze. Additionally, auditory cortex is engaged in processing speech-related mouth movements, and personal identity and biographical information are accessed via anterior temporal regions. This model therefore takes into account the two main aspects of face processing, which are, the representation of the invariant aspects of a face to facilitate recognition, and the interpretation of the changeable aspects of a face to facilitate social interaction and communication. However, this model does not account for the importance of dynamic information in social communication.

This limitation was addressed by O'Toole et al. (2002), where they amended Haxby et al.'s (2000) model to incorporate findings from studies on moving faces (see subsection 1.2.2.1). They propose that when a face is encountered its static structure is processed by the ventral stream and the dorsal stream processes facial motion. In the dorsal stream facial motion such as dynamic characteristics gained from facial speech, expressions and head/face

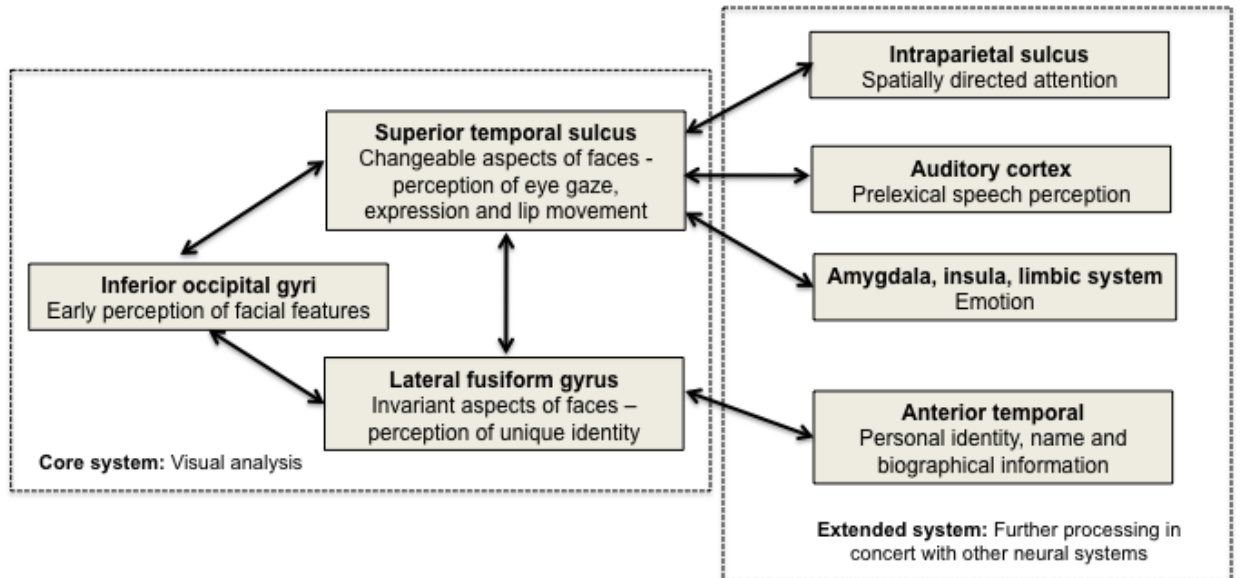


Figure 1.3.1: The distributed human neural system for face perception, adapted from Haxby et al. (2000). This model shows a core system in occipito-temporal cortex where visual analysis of faces takes place. Changeable and invariant aspects of faces are processed in two distinct pathways in the core system. The extended system incorporates additional brain regions for further face processing.

movements are processed in the middle temporal visual area (MT) before projecting to STS. Contrary to Haxby’s model, this suggests that the STS plays a role in facial identification when identification can be gleaned from dynamic facial signatures, this is known as the supplemental information hypothesis. Furthermore O’Toole et al. (2002) suggest that dorsal and ventral streams may communicate via middle temporal visual area MT thus facilitating recognition through structure-from-motion, which is known as the representation enhancement hypothesis. Taken together these models provide a sound framework to study various face-related processing and activity. However in order to develop a better understanding of human face perception the degree of separation and interactions between the different regions within the distributed neural system needs to be examined.

Recently the degree of separation between the fusiform gyrus, which is involved in processing facial identity, and the superior temporal sulcus involved in facial expression analysis has been examined. Evidence to support the existence of independent visual pathways for identity and expression processing comes from neuropsychological and behavioural studies (as previously discussed in section 1.2), as well as from neurophysiological and neuroimaging research. Neurophysiological studies in non-human primates have reported cells responsive to facial identity in inferior temporal cortex, while cells in STS

show selectivity towards facial expressions, viewing angle, and gaze direction (Hasselmo et al., 1989; Perrett et al., 1992). Additionally, findings from neuroimaging studies have revealed increased activation in the fusiform gyrus to facial identity, whereas facial expressions elicited increased activation in the STS (Haxby et al., 2000).

However, in a recent review, Calder and Young (2005) argue that the evidence appears to support partial separation between the coding of facial identity and expression, rather than independent processing pathways. For example, Perrett et al. (1985) found cells in the STS that are sensitive to both facial expression and identity. In addition, recent fMRI studies have reported increased activation in the fusiform gyrus to both facial identity and expression (Vuilleumier et al., 2001). Calder and Young (2005) therefore propose an alternative approach based on computational modelling studies using principal component analysis, where the relative separation of facial identity and expression processes evolves from a common integrated representational system, rather than a complete bifurcation of the visual processing pathways (see chapter 2 for further discussion).

While Haxby et al.'s (2000) model provides an excellent framework, it is primarily concerned with the spatial localisation of the neural structures involved in face perception but does not address the related temporal processing. Hence, Adolphs (2002b) later extended Haxby et al.'s (2000) model to include temporal information (see subsection 1.3.5). Nevertheless, Haxby et al.'s (2000) model highlights the importance of facial expression in social interaction, and has paved the way from merely studying face recognition processes, to the investigation of more broader aspects of face and emotion perception. This will be discussed in the proceeding section.

1.3.3 Anatomical location and relative timing of evoked potentials

Numerous electrophysiological studies using various techniques have investigated the time-course of face processing and have shown a relatively consistent pattern of results. It has been shown that just as information about faces is spatially distributed across cortical sites, faces are also processed at various temporal scales (Vuilleumier and Pourtois, 2007). In a series of studies Allison et al. (1999) recorded intracranial event-related potentials (ERPs) from a group of patients with epilepsy and reported face responsive activity at

200 ms (termed the N200 response), recorded over ventral occipito-temporal cortex and middle temporal gyrus. This response was greater for faces compared to other objects and was found consistently across three different studies.

ERP scalp recording studies in healthy control populations have reliably reported a similar negative evoked potential, recorded over posterior scalp electrodes, at approximately 170 ms (N170) in response to faces. This response is larger for faces than all other object categories tested (Bentin et al., 1996; Itier and Taylor, 2004). An earlier positive response has also been recorded at approximately 100 ms (P100) over occipital scalp electrodes, which is responsive to face stimuli (Itier and Taylor, 2002, 2004). It has been proposed that the P100 response reflects the coarse processing of faces, while the N170 response represents more detailed structural encoding processes where a perceptual representation of the face is extracted (Itier et al., 2006). In support of this a recent study by Nakashima et al. (2008) did indeed find that the P100 was responsive to low spatial frequency information, reflecting coarse face-selective processing, whereas the N170 showed a greater response to high spatial frequency information and thus was related to the encoding of the detailed feature information of faces.

A similar face sensitive response has also been found with MEG, at approximately 170 ms (M170) on posterior-lateral sensors (Watanabe et al., 1999; Liu et al., 2000). Furthermore, an earlier response occurring between 90 and 140 ms (M100) over occipital sites has also been reported which shows some face sensitivity (Liu et al., 2002). Liu et al. (2002) investigated the different temporal responses to face stimuli using MEG and found that the M100 response is involved in processing local face parts, whereas the M170 response reflects processing of more global face configuration. They therefore propose that the M100 and the M170 reflect two different stages of face perception. The M100 reflects the first stage whereby a stimulus is categorised as a face based on the low level features such as face parts, and in the second stage the M170 facilitates identification and is based on more broad configural information processing of the face.

However, because electrophysiological methods have poor spatial resolution it is difficult to accurately localise these evoked responses. A number of studies have tried to resolve this issue by using source analysis techniques and found that the M170/N170 was localised to the fusiform gyrus for both the M170 (Liu et al., 2000) and N170 (Itier and Taylor,

2002). However, there is still some debate over this (Itier and Taylor, 2004). For example, Horowitz et al. (2004) used fMRI and EEG to investigate the sources of the N170 and found significant correlations between the fMRI signal and N170 amplitudes for faces in bilateral fusiform gyrus as well as the superior temporal gyrus.

Furthermore, Itier et al. (2006) used MEG and an event-related SAM beamformer to determine the sources of the M170 and M100. They found a bilateral occipital source centred around the lingual gyrus and cuneus for the M100 component, whereas source analyses of the M170 component revealed two different sources, which the authors term the M170A and M170B. The M170A was situated in occipital extrastriate areas while the M170B was located in the fusiform gyrus. They later suggest that there are in fact three distinct components that form part of the N170/M170 response. These include a lateral temporal source in the posterior STS (N170), a fusiform gyrus source (M170B), and a more medial inferior occipital source (M170A). Notably, these three sources are consistent with the ‘core system’ in Haxby et al.’s model.

More recently, Sato et al. (2008) used fMRI and MEG with a 3D spatial filter to investigate the temporal pattern of activation in the STS compared with that of the fusiform gyrus in response to eye gaze. They found increased activation in the STS in response to averted versus straight gazes, between 150–200 ms, which peaked at 170 ms post stimulus onset. In contrast, the fusiform gyrus did not show a selective response to gaze aversion at 170 ms but did respond to faces in general. They conclude that the STS is involved in gaze processing at around 170 ms but the fusiform gyrus is not, which again is consistent with the model of Haxby et al. (2000).

To summarise, the findings from these electrophysiological studies converge on a network of brain regions that are known to contribute to face perception and have provided additional information on the temporal processing of information in these regions. An early evoked response has been identified in early visual regions such as lingual and inferior occipital gyri at approximately 100 ms post stimulus onset, followed by later evoked responses in STS and fusiform gyrus at approximately 170 ms. However, as with much of the face perception literature to date, the studies described so far have used static images of faces, which lack important temporal information (see subsection 1.2.2.1). These static facial stimuli represent impoverished displays lacking natural facial motion,

therefore they do not allow a complete description of the temporal structure of face specific neural activities to be made. Dynamic stimuli would offer a more suitable means of examining the neural basis of realistic natural face perception.

1.3.4 Facial expressions of emotion

Haxby et al. (2000) highlighted the importance of facial expressions in social interactions, as they can carry information about emotional state, intention, or focus of attention, among others. Consequently the recognition of emotional facial expressions draws not only on brain areas involved in visual processing of the structural aspects of the face, but also recruits brain areas involved in processing the emotional information (Haxby et al., 2000). Emotions can be perceived via different modalities such as the face and voice, and different cues such as facial cues and bodily gestures. Yet the face appears to be one of the most important cues for perceiving an emotional state. Thus, many studies focus exclusively on the perception of facial expressions, whereby facial expressions of emotion have been used as a means of investigating the neural substrates of emotion perception (e.g. Vuilleumier et al., 2001; Adolphs, 2002b). This section will provide an overview of the current research on the recognition and perception of facial expressions and the associated underlying functional and cognitive processes within the brain.

As previously described, evidence from neuropsychological patients suggests that different neural regions are involved in processing different types of face-related information (i.e. in prosopagnosia). Similarly, findings from clinical studies of patients with lesions or certain neurological disorders have revealed selective impairment of specific facial expressions, generally fear and disgust (Calder et al., 2001). For example, numerous human lesion studies have reported impaired recognition of fearful facial expressions following amygdala damage (e.g. Adolphs et al., 1994; Young et al., 1995; Calder et al., 1996; Sprengelmeyer et al., 1999). While a patient with lesions in the left insula and basal ganglia, was unable to selectively recognise facial expressions of disgust. Additionally, patients with Huntington's disease display a selective deficit in the recognition of facial expressions of disgust, which is believed to be due to basal ganglia degeneration (Sprengelmeyer et al., 1997).

Consistent with these clinical observations, neuroimaging studies reliably report amygdala

activation to fearful facial expressions (e.g. Breiter et al., 1996; Morris et al., 1996; Phillips et al., 1997; Whalen et al., 1998; Vuilleumier et al., 2001), whereas facial expressions of disgust elicited activation in the insula and basal ganglia but not the amygdala (Phillips et al., 1997). Based on this converging clinical and neuroimaging evidence showing a double dissociation between fear and disgust processing, it is claimed that dissociable neural subsystems for fear and disgust have been established (Calder et al., 2001). Consequently, it has been suggested that different facial expressions of emotion are processed by dissociable neural subsystems, which is again consistent with a modular approach to face processing. However, while convincing results appear to exist for the expressions of fear and disgust, there is little consistent empirical evidence for specialised neural representations of the other basic emotion categories of anger, happiness, surprise and sadness. This is principally due to lack of neuropsychological evidence that demonstrates specific impairments in recognising these emotions (Winston et al., 2003).

Furthermore, the role of the amygdala in the selective recognition of fear is debatable. Human lesion studies have shown that bilateral amygdala damage can cause impaired recognition of multiple facial expressions of emotion including anger, disgust and sadness, as well as fear (Adolphs et al., 1999; Schmolck and Squire, 2001). Similarly, functional imaging studies have reported amygdala activation for angry, happy and neutral facial expressions in addition to fearful faces. Based on a meta-analysis of fifty-five neuroimaging studies, Phan et al. (2004) found amygdala activation in many different emotional contexts and thus propose that the amygdala responds to the salience of emotional stimuli rather than to specific emotion categories. Similarly, Fusar-Poli et al. (2009) conducted a meta-analysis of emotional face perception studies, and found amygdala activation to neutral faces among others. They therefore propose that the amygdala plays a role in vigilance or in processing the saliency of emotional stimuli.

Equally, recent evidence suggests that the insula may not necessarily be selectively responsive to facial expressions of disgust (Phan et al., 2004). In their meta-analysis Phan et al. (2004) found increased insular activation in response to other emotions besides disgust, particularly aversive or threat-related emotions such as fear. Likewise, Fusar-Poli et al. (2009) found insular activation during the processing of both disgusted and angry facial stimuli. Hence it has been suggested that the insula may play a more general role in

mediating responses to aversive or distressing stimuli, rather than specifically responding to the emotion of disgust only. Due to its extensive connections with primary sensory areas the insular cortex is now believed to play an important role in emotion processing and pain perception (Nagai et al., 2007), as it forms part of the interoceptive system that links external and internal information (Gobbini and Haxby, 2007).

1.3.4.1 Temporal processing of facial expressions

The important aspect of the speed with which facial expressions of emotions are processed has only recently been investigated neurophysiologically (Eimer and Holmes, 2007). Electrophysiological studies of emotional face perception have demonstrated emotion effects arising at both early and late latencies (Vuilleumier and Pourtois, 2007). Many of these studies have focused on the face selective N170 or M170 by using EEG or MEG to examine the effect of emotion on this face-selective component.

A number of studies have reported some emotional modulations on the amplitude and latency of the N170 (Vuilleumier and Pourtois, 2007). For example, Batty and Taylor (2003) investigated event related potential (ERP) responses to the six basic facial expressions of emotion (angry, happy, fear, disgust, surprise and sadness) and neutral faces, using an implicit emotional perception task. They found that the latency of the N170 evoked by negative facial expressions, specifically, fear, disgust and sadness was later than the N170 evoked by neutral and positive emotions of happiness and surprise. In addition, the amplitude of the N170 evoked by fearful faces was larger than that evoked by all other expressions.

On the other hand, some researchers have found that the N170 component is not affected by emotional facial expressions (Krolak-Salmon et al., 2001; Münte et al., 1998). For example, Eimer et al. (2003) compared the ERP responses elicited by the six basic facial expressions of emotion (angry, happy, fear, disgust, surprise and sadness) and neutral faces to assess whether ERP waveforms were modulated by different emotional facial expressions. Stimuli were presented as face pairs to the left and right of fixation and participants had to respond as to whether the face pair was emotional or neutral. They found that emotional faces elicited a greater positivity in the ERP waveform at 180 ms post stimulus onset compared to neutral faces. However, they did not find any

differences in terms of magnitude and duration of the N170 across the different emotions. Furthermore they found that scalp topographies were statistically indistinguishable across the different emotions. Factors such as stimulus repetition, the number of faces and/or facial expressions used, as well as the type of paradigm, may have contributed to these conflicting results between different studies.

Some studies have also reported an influence of emotional expression on very early brain responses even prior to the N170 at approximately 100 ms (Pizzagalli et al., 1999; Eger et al., 2003). For example, Batty and Taylor (2003) reported emotion effects occurring during this earlier time-window, affecting the amplitude of the visual P1 component over posterior cortex, which showed an increased amplitude to emotional faces relative to neutral. Eimer and Holmes (2002) report a similar effect arising around the same latency (~120 ms) from fronto-central ERP components, showing greater amplitudes to fearful relative to neutral facial expressions. Similarly, Esslen et al. (2004) report an early emotional effect during a face perception and emotion generation task.

In a recent MEG study, Liu and Ioannides (2010) examined the spatio-temporal profile of responses to happy, fearful and neutral facial expressions during a facial affect recognition task. They found very early differential responses starting well before 100 ms (M1), and the specific pattern and timing depended on where faces appeared in the visual field. For centrally presented faces, the emotions were separated quickly, within 100 ms post-stimulus, first in the right STS (35–48 ms; happy faces distinguished from fearful), followed by the right amygdala (57–64 ms; happy from neutral) and prefrontal cortex (83–96 ms; happy from fearful & neutral).

Likewise, Morel et al. (2009) found early differential responses to fearful, happy and neutral faces, around 40-50 ms over posterior regions with both EEG and MEG. They suggest that this effect may reflect the processing of low-level visual cues directly related to the emotional facial expression. Consistent with this, Vuilleumier and Pourtois (2007) have suggested that there may be a rapid extraction of visual information related to emotion that occurs before more detailed perceptual processes are complete.

Several studies have also reported later effects associated with the perception of emotional facial expressions, from around 200 ms post stimulus onset (Münte et al., 1998; Krolak-Salmon et al., 2001; Sato et al., 2001). Using MEG to investigate the processing of facial

emotional expressions, Streit (1999) found that neural activity related to attention to emotional facial expressions occurred between 140 and 530 ms after stimulus onset. They also showed that different neural structures including the fusiform gyrus, amygdala and inferior frontal cortex were involved in the processing of facial expressions at different latencies. Krolak-Salmon et al. (2001) also reported differential activity related to emotional and neutral expressions between 250 and 550 ms in occipital areas and between 550 and 750 ms in right occipito-temporal cortex.

In addition, Batty and Taylor (2003) reported a sustained response from 140 to 400 ms in middle and superior temporal gyri followed by later activity in more anterior regions. Several of these late ERP responses to emotional facial expressions have also been found to be sustained over prolonged periods of time following stimulus onset (Krolak-Salmon et al., 2001; Ashley et al., 2004), which do not seem specific to particular expressions and therefore may reflect more complex cognitive processes related to emotion processing (Vuilleumier and Pourtois, 2007).

Taken together these findings do not reliably support the modular view that distinct neural subsystems are dedicated to processing specific emotions. It seems more likely that common neural substrates are involved in the perception of multiple basic emotions at various different timepoints. The studies that will be presented in this thesis support this hypothesis, and it will be shown that common neural networks are generally involved in processing multiple facial stimuli over varying latencies and frequencies. It is also important to note that all of the studies discussed in this section have again used static face stimuli, which lack important dynamic information. To reiterate, dynamic stimuli would offer a better means of investigating the processing of facial expressions of emotion and this will be addressed in the present thesis.

1.3.5 A model of emotion recognition from faces

Adolphs' (2002) model of emotion recognition from facial expressions is an extension of Haxby et al.'s (2000) distributed human neural face perception system but adds an extra temporal dimension. Consistent with Haxby et al.'s (2000) model, Adolphs (2002) proposes that a distributed network of neural regions is involved in processing facial affect, but he further extends this to include information about the temporal processing

of facial expressions of emotion. According to Adolphs' (2002) model a given structure in a network may participate in processing multiple emotions over various time points. In this view, emotions are not static in the sense that one emotion is exclusively processed in one particular brain region, rather, several distinct neural structures are recruited to process emotions at different periods of time. Although Adolphs (2002) does suggest that different sets of neural structures within the network may be recruited to process different emotions. By adding this temporal dimension it accounts for the fact that some brain structures participate in different aspects of processing at different time points.

Similar to Haxby et al.'s (2000) model, Adolphs (2002b) proposes that early structural processing occurs in occipital cortex and feeds forward into temporal regions, where coarse categorisation takes place at around 100 ms post stimulus onset. A more detailed structural representation of the face is constructed in the fusiform gyrus from 170 ms after stimulus onset, while changeable facial features such as eye and mouth movements are processed in the STS around the same time. A perceptual representation of the facial expression is generated from the combined information from the fusiform gyrus and STS. Additional structures including the amygdala, orbitofrontal cortex, somatosensory cortex and insular cortex, are then recruited from around 300 ms post stimulus onset, to link the perceptual representation to conceptual knowledge of the emotional and social meaning of the perceived expression (see Figure 1.3.2).

Within this framework Adolphs (2002a) proposes three possible roles of combined amygdala and orbitofrontal function. First, the amygdala and orbitofrontal cortex may modulate emotion perception via feedback, for example upon encountering fearful stimuli vigilance may be increased by the amygdala and orbitofrontal cortex which feeds back to the visual cortex thus enhancing the sensitivity of early visual processing. Second, they may activate conceptual knowledge of an emotion in memory through connections with the hippocampal formation and neocortex. Third they may generate an emotional response via links to somatosensory and motor cortex thereby simulating or mimicking the observed emotional state. This is consistent with findings from non-human primate and human studies, revealing mirror neurons in premotor areas in inferior frontal cortex that respond during both action and the observation of action (Rizzolatti et al., 1996). Adolphs (2002) thus concludes that emotion recognition involves a diverse network of

regions that are differentially recruited over various periods of time, which are modulated by circumstances and experimental design.

An important characteristic of this model is the notion of feedback from higher order regions, which can modulate the processing of incoming stimuli. Feedback was also implied in Haxby et al.'s (2000) model by the bidirectional arrows between regions (see Figure 1.3.1), although Adolphs (2002) makes it more explicit by emphasising the fact that a given structure (e.g. V1) can participate in both early and late processing of emotional stimuli. Support for this comes from neuroimaging studies revealing increased activation in visual cortical regions, including the fusiform gyrus, to emotional face stimuli as a result of feedback from the amygdala and medial frontal cortices (Vuilleumier and Pourtois, 2007). This model therefore incorporates the important aspects of face perception and implies that it is an interactive dynamic process, that can be modulated by different experimental and task demands. However, as with Haxby et al. (2000), a major limitation of this model is that it is largely based on findings from studies using static facial stimuli, which neglect the important property of facial motion and consequently lack ecological validity.

1.3.6 Ecological validity of facial expression stimuli

As previously discussed, the dynamic property of facial expressions is an important factor that has largely been neglected in research on the perception of facial expressions of emotion to date. In everyday life, faces convey information about emotion as dynamic facial expressions change and unfold over time. Accordingly, these dynamic changes of facial musculature play an important role in the decoding of emotions from different facial expressions (Kamachi et al., 2001; Ambadar et al., 2005). However, the majority of early face perception studies have used static face stimuli, primarily from Ekman and Friesen's (1976) pictures of Facial Affect Collection.

While these stimuli have proved useful in face perception research, they lack ecological validity because they display static prototypes of highly intense emotional facial expressions at the apex of emotional expression (Carroll and Russell, 1997). Yet these types of facial expressions are rarely encountered in the real world (Carroll and Russell, 1997; Horstmann, 2002). Rather, social interactions involve interpreting brief dynamic facial

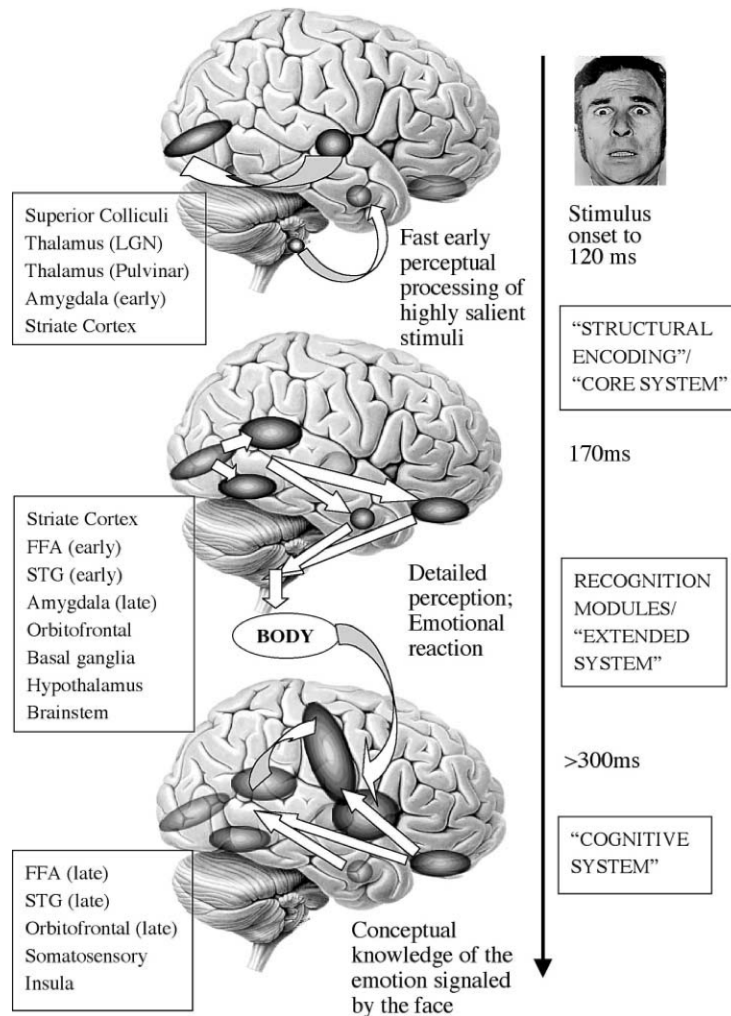


Figure 1.3.2: The neural system for recognising emotion from facial expressions, adapted from Adolphs (2002).

signals, which are constantly changing (Ambadar et al., 2005). In recent years many additional collections of facial stimuli have been created and used in face perception research in an attempt to create more realistic and diverse stimuli, such as the NimStim set of facial expressions (Tottenham et al., 2009). However the majority of these more recent collections still rely on static face stimuli.

Given the fact that the majority of studies have used these standard static face stimuli to investigate the perception of facial expressions it is possible that important aspects may have been overlooked (Bould and Morris, 2008). For example, the majority of knowledge about the neural correlates of face perception comes from either clinical studies, which have generally used static stimuli to probe deficits in patients, or neuroimaging studies using static stimuli to trigger face related activation as previously described. Also, both Haxby et al.'s (2000) model of face perception and Adolphs' (2002) model of emotion recognition were mainly derived from the results of studies using static face stimuli. While

these models provide an excellent framework for face perception research, they need to be tested empirically using more realistic dynamic face stimuli. This limitation was indeed acknowledged by Adolphs (2002), where he suggests that future studies should use tasks and stimuli with more ecological validity, particularly dynamic facial expressions of emotion. Recently a handful of neuroimaging studies have used dynamic face stimuli to investigate the neural correlates of dynamic face perception (see subsection 1.3.8 for discussion).

In sum, ecological validity is an important aspect of experimental research. Neuroscience research in general, but particularly vision and face perception research, is striving towards the use of more naturalistic and ecologically valid stimuli and experimental designs (Hasson et al., 2010). This is exemplified by the growing trend of studying neural activation under more natural viewing conditions, such as while watching movies (see Hasson et al., 2010 for review). This level of research is necessary as it aims to establish the functional significance of neural responses in natural conditions, which may have previously only been characterised with artificial stimuli (Felsen and Dan, 2005). In this context, naturalistic dynamic face stimuli provide a better means of representing the complex nature of perceiving emotions from facial expressions in the real world. Therefore authentic dynamic stimuli should be used to uncover the neural correlates of natural face perception, where the ultimate goal is to progress from an understanding of how static images of single faces are processed, to how real faces are perceived dynamically and interactively in the real world (Atkinson and Adolphs, 2011).

1.3.7 Biological motion perception

The perception of meaningful human body actions, also termed biological motion perception, is a critical cognitive ability as it provides information about the actions and intentions of others. It involves hand, eye, lip, or whole-body movements, which, together with faces, constitute crucial ingredients of social cognition and interaction (Blake and Shiffrar, 2007). The perception of facial expressions of emotion is an important aspect of biological motion perception. Therefore some of the key findings from studies of biological motion perception will be reviewed here, particularly in relation to localisation and timing, as these studies provide important insights into the processing of dynamic

information which can be used to inform theories of dynamic face perception.

Numerous behavioural studies of biological motion perception have used the point-light technique, developed by Johansson (1973), in order to examine how information from motion only (i.e. the pattern of motion) is processed without interference from form. In point-light displays a limited number of markers are placed on the joints of a body, which are animated to portray different human actions (Decety and Grèzes, 1999). Notably it is very difficult to identify the image as that of a human figure without animation. However, once the image is animated observers can correctly identify a range of different human attributes such as the identity and gender of a point-light defined walker, as well as the emotion portrayed by point-light animations of the whole body (for recent review see Blake and Shiffrar, 2007). From these point-light studies it is evident that humans are highly skilled at interpreting the motion information portrayed by different action patterns.

Recently, neuroimaging studies investigating the neural correlates of biological motion perception have reported a range of brain regions that are selectively responsive to different types of biological motion. Several studies have found that area MT in the posterior lateral temporal cortex is a common visual motion processing area and responds to all types of visual motion, but is not specialised for biological motion in particular (Decety and Grèzes, 1999; Grossman et al., 2010). For example, Grossman et al. (2000) found that displays of point-light actions and scrambled motion evoked equivalent activation in area MT/V5. In contrast, regions anterior and superior to MT along the posterior portion of the superior temporal sulcus appear to be selective for biological motion in particular. These regions in posterior superior temporal sulcus have consistently been shown to respond more to point-light displays portraying biological motion than similar displays containing scrambled or inverted motion (Howard et al., 1996; Grossman et al., 2000).

An interesting fMRI study by Beauchamp et al. (2002) compared neural responses to different types of tool and human motion stimuli. They found increased activation in the STS in response to the human motion stimuli, while observing the motion of tools evoked increased activation in MTG. Furthermore STS responded preferentially to complex articulated motion which is characteristic of human motion, whereas the MTG responded

to non-articulated motion characteristic of tool motion. Consistent with other researchers they have concluded that the STS is a crucial brain region involved in biological motion perception (Allison et al., 2000).

Regions in ventral temporal cortex have also been implicated in biological motion perception, including regions in the fusiform gyrus and inferior temporal sulcus (Vaina et al., 2001; Grossman and Blake, 2002). A region in lateral occipito-temporal cortex, termed the extrastriate body area has also been associated with the perception of human movements (Downing et al., 2001), although this region also supports the recognition of human form as well (Peelen et al., 2010). In a recent meta-analysis of the fMRI literature on human movement perception Grosbras et al. (2012) found that a number of regions in both dorsal and ventral temporal cortex were reliably engaged during the perception of human body movements. As expected, they found large clusters in the middle temporal gyrus and posterior superior temporal sulcus. They also report large clusters in the lateral occipito-temporal cortex, with the maximum peaks around the so-called extrastriate body area, as well as large clusters in the fusiform cortex.

While there are a wealth of studies that have identified the cortical areas involved in biological motion processing, relatively little consistent data exists on the time course of brain activity across this network of implicated regions. As discussed above, fMRI studies have identified area MT in posterior lateral temporal cortex as the canonical visual motion processing area, where it responds to all types of motion stimuli, while regions along posterior STS appear to respond to biological motion in particular (Beauchamp et al., 2002; Blake and Shiffrar, 2007). In a combined fMRI and MEG study of visual motion perception Ahlfors et al. (1999) found an early transient response in area MT at approximately 130 ms, followed by a later sustained response in the posterior STS over the latency range of 200–400 ms.

Similarly, Kawakami et al. (2002) performed a combined fMRI and MEG study to determine the neural mechanisms underlying visual motion detection. They also report a response in area MT but at a much faster timescale of 10 ms. These MEG studies provide converging evidence in support of the role of MT in visual motion processing as well as providing additional information on the timecourse of responses in MT to motion stimuli, which occur early within 200 ms of stimulus onset.

Recently, Hirai (2003) examined the neural dynamics in biological motion perception by comparing ERPs elicited by point-light displays of biological motion and scrambled motion. They report that both types of stimuli elicited peaks at around 200 ms (N200) and 240 ms (N240). Both of these peaks were larger in the biological motion condition compared to the scrambled motion condition over right occipito-temporal cortices. They speculate that the N200 response originates from extrastriate regions and the N240 from the STS.

Jokisch et al. (2005) also used EEG, along with source analysis measures, to investigate both the time course and sources of biological motion processing. They found two negative ERP components, at 180 ms (N170) and 230–360 ms (N300), which were greater in response to point-light displays of biological motion relative to the scrambled motion condition. Source analysis revealed that generators of the N170 were in the posterior cingulate gyrus and the left lingual gyrus, while the N300 response was localised to the right fusiform gyrus and the right superior temporal gyrus. They conclude that there are two distinct stages in biological motion processing, an early stage in visual regions occurs around 170 ms post stimulus onset followed by later processing in the fusiform gyrus and superior temporal gyrus around 300 ms post stimulus onset.

In a recent EEG study Krakowski et al. (2011) also report different stages of processing when contrasting biological to scrambled motion. The first stage was characterised by a right lateralised, positive ERP between 100–200 ms post stimulus onset, in the dorsal visual processing stream centred around area MT. The second stage was reported as a bilateral negative ERP within 200–350 ms of stimulus onset and located between area MT and STS. The authors suggest that this component roughly corresponds to the second component reported by Hirai (2003) and the N300 component reported by Jokisch et al. (2005).

In sum these studies provide converging evidence implicating regions of middle temporal and superior temporal cortex in biological motion processing. Furthermore, biological motion stimuli elicited earlier responses in visual regions, in area MT, occurring within 200 ms of stimulus onset, followed by later processing in the superior temporal sulcus around 300 ms post stimulus onset.

1.3.8 Dynamic face perception

The perception of facial expressions of emotion is an important aspect of biological motion perception. Although typically studied using static face stimuli, face processing is in fact dynamic by nature as it involves the interpretation of dynamic facial signals to decode the emotion messages conveyed in different facial action patterns. Behavioural studies using point-light displays of faces have shown that observers can correctly identify the facial expression being executed (Bassili, 1978) and also the gender of the actor (Hill et al., 2003). More recently, a handful of neuroimaging studies have investigated the neural network underlying the processing of dynamic face stimuli. An early Positron Emission Tomography (PET) study by Kilts et al. (2003) reported increased activation in the STS in response to dynamic compared to static face stimuli, along with greater activation in the amygdala and hippocampus.

In an fMRI study, LaBar et al. (2003) also reported increased activation in the STS, as well as in the fusiform gyrus and ventromedial prefrontal cortex, in response to dynamic expressions of emotion compared to neutral. Additionally, Sato et al. (2004) carried out an fMRI study using dynamic gray scaled morphed stimuli of fearful and happy faces, dynamic mosaics of scrambled faces and static controls. They found increased activation in the inferior occipital gyrus, middle temporal gyrus, STS and fusiform gyrus to dynamic facial expressions compared to the dynamic and static controls.

In a recent fMRI study Schultz and Pilz (2009) also found increased activation in middle temporal gyrus and STS when dynamic and static faces were contrasted. Interestingly, they also found increased activation to dynamic faces in bilateral fusiform gyrus and left inferior occipital gyrus, thereby implicating these regions in the processing of dynamic facial information, which is contrary to the predictions of Haxby et al.'s (2000) model. Conversely, Pitcher et al. (2011a) did not find a significant difference in responses between dynamic and static faces in functionally defined regions of the fusiform or occipital gyri (see chapter 2 for further discussion).

An MEG study by Watanabe et al. (2005) investigated spatiotemporal responses to the observation of different types of facial motion, specifically mouth and eye movements. They found a response to both types of facial motion with a peak latency of 160 ms in the lateral occipito-temporal region, corresponding to area MT. They found differential

responses in this region, characterised by a smaller response to mouth movements and suggest that area MT may possess multiple response characteristics.

Based on these findings a network of regions appears to be involved in processing dynamic facial displays at varying latencies. This network includes regions of occipital, temporal, limbic and prefrontal cortex (Pitcher et al., 2011a). The localisation of this network, its interactions, timing and frequency of responses, will all be investigated throughout the course of this thesis, using more naturalistic and ecologically valid dynamic face stimuli.

1.4 An integrative approach to face perception research

Up until recently, functional neuroimaging has primarily focused on the localisation of function to specific brain regions. This approach is exemplified in much of the previous face perception research discussed in this chapter (see subsection 1.3.1 and subsection 1.3.4), where a modular approach was adopted by studies emphasising the selectivity of particular neural regions for processing various aspects of faces and emotions (e.g. Kanwisher, 2000; Calder et al., 2001). However, recent advances in the field have highlighted the importance of understanding patterns of activation and the associated functional relations between brain areas, rather than merely examining isolated regional activity. Techniques such as multi-voxel pattern analysis (Haxby et al., 2001) and connectivity analysis (Fairhall and Ishai, 2007; Wicker et al., 2008) are examples of methods that have recently been applied to face perception research to investigate the patterns of responses and interactions within the face perception network.

Multi-voxel pattern analysis relies on pattern classification techniques to analyse distributed patterns of fMRI activity across multiple voxels, rather than evaluating absolute activation levels in individual voxels (Norman et al., 2006). These distributed patterns of fMRI activity are believed to contain more detailed information about different cognitive states and experimental conditions than the activity of individual voxels (Norman et al., 2006). An early study using multi-voxel pattern analysis showed that it was possible to determine which class of object participants were viewing based on their different respective patterns of neural activation (Haxby et al., 2001). In this seminal study, participants

were shown a range of different objects including faces, houses, and chairs, among others. Interestingly, each of these different object categories was associated with a specific and reliable pattern of activation within ventral temporal cortex. Yet this level of information was not evident from conventional univariate analysis.

More recently, Said et al. (2010) found that different facial expressions of emotion were associated with distinct patterns of activation in anterior and posterior superior temporal sulcus, and in the frontal operculum. Such patterns of activation are believed to represent the distributed population codes for each of the different facial expressions within these three regions (Said et al., 2010). Taken together, these results demonstrate the advantage of assessing patterns of neural activation, which provide additional information over measures of single voxel activity, in order to gain a better understanding of how faces are represented in the brain. Consequently, it has been proposed that information about faces is represented in a distributed fashion within a broad network of regions in the brain (Haxby et al., 2000; Ishai, 2008).

1.4.1 Connectivity analysis

The current view in cognitive neuroscience is that cognitive processes, including face perception, are implemented in the brain via networks of different brain regions (Haxby et al., 2000; Ishai, 2008) and thus depend fundamentally on interactions among these regions, rather than on isolated processes within regions (Friston, 2009). Therefore in order to obtain a better understanding of cognitive functions, such as face perception, the spatial and temporal relationships among the elements of these networks must be examined. This can be achieved through different measures of connectivity.

In the literature, distinctions have been made between three different types of connectivity measures (Horwitz, 2003). Anatomical connectivity refers to the structural link, or the presence of neural pathways between two areas, whereas functional connectivity is defined as statistical dependencies or temporal correlations between the neuronal activation patterns of different anatomic brain regions. Effective connectivity estimates the coupling between different brain regions and how this coupling is affected by experimental manipulations (Friston et al., 1997). Studies of neural integration, using structural, functional and effective connectivity measures have revealed interesting new findings about

the functional connections of specific brain regions and networks, and provide important new insights in to the overall organisation of functional communication in the human brain (Friston, 2009).

Structural analysis, in which the anatomical links between regions are considered, is typically accomplished through an analysis of white matter tracts. In recent years, an MR technology known as diffusion tensor imaging (DTI) has emerged as a powerful non-invasive tool used to delineate the anatomical connectivity between brain regions by exploring and characterising white matter structure in vivo (see Le Bihan et al. (2001) for review). To date the focus of many structural connectivity studies has been on brain regions that are well characterised from an anatomical perspective, such as motor and occipital cortex, which contain thick prominent fibre tracts and the structure of a number of different fibre pathways in these regions have been successfully analysed with DTI (Dougherty et al., 2005; Kim et al., 2006). More recently the anatomical connectivity of the face perception system has also been explored using DTI (Thomas et al., 2008, 2009; Gschwind et al., 2012).

In two separate studies Thomas et al. 2008; 2009 used structural connectivity measures to explore the relationship between face processing impairments and reduced connectivity within the face perception network. In their first study, Thomas et al. (2008) used DTI to examine whether age-related declines in face processing could be related to a reduction in white matter connectivity along two major tracts in ventral temporal cortex that pass through the fusiform gyrus. Consistent with their hypothesis, they found that there was a significant correlation between reduced white matter connectivity in the tract that connects posterior ventral cortex with regions of frontal cortex, and the decline in face processing. They therefore concluded that age-related difficulties in face processing are associated with changes in structural connectivity between right ventral temporal and frontal cortices.

In a second study, Thomas et al. (2009) used DTI to investigate whether congenital prosopagnosia was related to disrupted structural connectivity within the face perception network. They found a reduction in white matter fibre tracts within ventral occipito-temporal cortex in patients with congenital prosopagnosia and thus suggest that the face recognition impairments associated with congenital prosopagnosia may be due to a

disruption in structural connectivity in ventral occipito-temporal cortex. These studies provide important new insights into the architecture of the face perception network and how disruption in connectivity can lead to deficits in face processing.

Based on the assumption that brain structure determines function it is believed that structural connection patterns may provide major constraints on the dynamics of cortical networks, which are captured by functional and effective connectivity (Saygin et al., 2011). According to this rationale, the presence of a strong structural connection between specific regions makes a functional connection between the same regions more likely to occur (Rykhlevskaia et al., 2008). Therefore structural connectivity can be used to provide important constraints on functional models of the face perception network.

A recent study by (Gschwind et al., 2012) combined functional MRI with DTI to examine white-matter connectivity between regions of the face perception network. fMRI was used to identify regions of interest in the core face perception system (OFA, FFA, STS) and the extended face perception system (amygdala, posterior cingulate cortex), as well as a control region in primary visual area, in 22 participants. Then DTI was used to explore the white-matter pathways between those functionally defined regions.

They found significant white-matter connectivity between OFA and FFA, and between early visual regions and the amygdala, while the STS was connected to anterior temporal, superior parietal and frontal regions but not to the FFA or OFA. The authors therefore suggest that two separate processing pathways exist, a ventral extrastriate visual pathway that connects OFA and FFA, and a dorsal pathway that connects STS and frontoparietal regions. This finding of two separate processing pathways is consistent with Haxby et al. (2000)'s distributed model of face perception (see subsection 1.3.2), however the lack of connectivity between OFA and STS does not correspond with current theories of face processing (Haxby et al., 2000; Ishai, 2008).

Another recent study, which also combined structural (DTI) and functional (fMRI) methods to examine the face perception network, reported significant structural connectivity between regions of fusiform gyrus and inferior and superior temporal cortices. This is contrary to the findings of Gschwind et al. (2012) as they did not find significant white matter connectivity between FFA and STS. Nevertheless these studies demonstrate that fMRI and DTI can be successfully integrated and open up an avenue of future research,

which will be important in gaining a more complete understanding of the structural and functional architecture of the face perception network.

Researchers have also employed various different measures of functional and effective connectivity in fMRI research to estimate the neural coupling and functional organisation of the face perception network, and these will be discussed in detail in chapter 3. In brief, it has been shown that regions of the core face perception system are organised in a hierarchical network structure, where the inferior occipital gyrus feeds forward into both the fusiform gyrus and superior temporal sulcus, during passive viewing of static faces (Fairhall and Ishai, 2007). It has further been shown that coupling between regions of the core and extended face perception systems are modulated by various factors such as face type, emotional expression and experimental task demands (Summerfield et al., 2006; Fairhall and Ishai, 2007; Ishai, 2008). However, it is important to note that, once again, these data were derived from studies using static face stimuli, hence little is known about the functional coupling within the face perception system during the processing of naturalistic dynamic facial expressions (this will be addressed in chapter 3).

In sum, the importance of studies that assess the functional and structural connectivity between regions of the face perception network cannot be understated. The functional significance and relevance of connectivity analysis methods in face perception research has been demonstrated through their application to clinical populations. For example, Thomas et al. (2009) found that the face recognition impairments associated with congenital prosopagnosia may be due to a disruption in structural connectivity in ventral occipito-temporal cortex. Furthermore, Wicker et al. (2008) have shown that patients with autism exhibit abnormal patterns of connectivity within the network of neural structures involved in emotional face processing, relative to healthy controls.

Notably, in a recent article Rowe (2010) stresses the significance of using brain connectivity analyses to gain a better understanding of neurological disorders, and argues that conventional fMRI analyses of regional effects are impoverished and incomplete. It seems then that the analysis of distributed brain networks will prove to be a more appropriate and effective way to investigate the functional architecture of the face perception system in both health and disease.

1.5 A brief overview of applied methods

This section will provide an overview of the neuroimaging techniques used in the present thesis. The purpose of neuroimaging is to visualise the structure and function of brain areas that are engaged during certain tasks. Different neuroimaging techniques can be used to measure different types of source signals, which can change in time, space or frequency, as a result of neuronal activity. In general, neuronal activity is reflected by alterations in electrophysiological signals such as action potentials and post-synaptic activity. These changes in electrophysiological activity can be directly measured using neuroimaging techniques such as MEG and EEG. In addition, neuronal activity also induces changes in metabolic and haemodynamic processes, and these are the primary signals measured with fMRI. Both fMRI and MEG neuroimaging techniques are used in the present thesis. These are complementary techniques as they measure different source signals, where fMRI provides detailed spatial resolution and MEG offers excellent temporal resolution, and the benefits of each can be exploited and applied to face perception research. The basic principles of both techniques along with their relative advantages and disadvantages will be discussed in more detail in the following sections.

1.5.1 Basic principles of fMRI and the BOLD signal

Firstly the basic principles of magnetic resonance imaging (MRI) will be outlined, followed by a description of the blood oxygenation level dependent (BOLD) signal that is measured in fMRI and how this BOLD signal relates to the underlying neural activity. In MRI a strong and homogenous external magnetic field is applied, which causes various atomic nuclei, particularly the proton nucleus of hydrogen atoms, to align themselves with this magnetic field and reach a thermal equilibrium. The proton nuclei precess around the axis of the magnetic field at a characteristic frequency but a random phase from each other. Then when a radio frequency electromagnetic pulse is applied it disrupts the equilibrium introducing transient phase coherence and the net magnetisation rotates by 90° towards the transverse plane. This magnetisation can then be detected as a radio signal by a radiofrequency receiver coil and formed into an image. The magnetisation is short-lived and decays exponentially as a result of processes known as relaxation. Various types of tissue have different relaxation rates known as T1, T2, or T2*, depending on the specific

properties of the tissue. It is these differences that form the basis of image contrast. fMRI is based on this principle, and for most current fMRI, T2 is the primary contrast mechanism used to detect changes in relaxation times (T2*-weighted) due to differences in blood oxygenation across different epochs.

There are two important parameters that characterise the contrast and quality of an MR image. These are the repetition time (TR) and the echo time (TE). The repetition time, is the time interval between two successive RF excitation pulses, whereas the echo time is the time between the peak of the RF pulse and that of the recovered signal. During the rest period (TE) following the RF pulse, differences in MR signal intensity are detected, as tissues with longer T2 relaxation times will have stronger signals than those with shorter relaxation times, whose signals decay more rapidly. By modifying the pattern of the RF excitation pulse, known as the pulse sequence, various properties of the resulting MR signal can be modulated. Many different types of pulse sequences can be used, but the two most commonly applied in cognitive applications are the gradient-recalled echo and spin echo pulse sequences. Finally, a method known as echo-planar imaging (EPI) forms the basis for most fMRI applications. In echo-planar imaging multiple lines of imaging data are acquired following a single RF excitation pulse, hence it is a very fast imaging technique capable of acquiring a complete MR image in less than a second. The fMRI data that will be presented in chapter 2 and chapter 3 was acquired using gradient echo EPI.

fMRI acquisition is based on the detection of changes in haemoglobin, which is responsible for transporting oxygen through the bloodstream. Deoxygenated haemoglobin is paramagnetic and dephases quickly resulting in a fast T2* relaxation time, whereas oxygenated haemoglobin is diamagnetic and dephases more slowly with a slower T2* relaxation time. These properties of haemoglobin form the basis for the BOLD contrast signal that is measured with fMRI. The BOLD contrast was first described by Ogawa and colleagues in the early nineties (Ogawa et al., 1990), who found that cortical blood vessels became more visible on T2 weighted images as blood oxygen decreased. This is due to the paramagnetic nature of deoxygenated haemoglobin, which creates inhomogeneities in the magnetic field. It is argued that the signal increases detected in BOLD fMRI studies are due to the fact that neural activation causes increased cerebral blood flow that is larger than the oxygen

consumption rate of the active tissue, thus increasing the concentration of oxygenated haemoglobin and decreasing deoxygenated haemoglobin at that site. Hence the net effect of neural activation is a reduction in deoxygenated haemoglobin, which increases the BOLD signal strength (Fox and Raichle, 1986).

The BOLD signal is believed to reflect a number of components in addition to the concentration of deoxygenated haemoglobin (also known as the cerebral metabolic rate of oxygen consumption), including changes in cerebral blood flow and cerebral blood volume (Ogawa et al., 1993). It is based on the complex interaction of these different factors with a spatial scale representing hundreds of thousands of neurons in every MRI voxel. However, it is still not fully understood how the haemodynamic response is correlated with and reflects neuronal electrical activity. Results from combined physiological and fMRI experiments suggest that the BOLD response is more closely correlated with local field potentials, reflecting the synaptic processing of a given area, than with multi unit activity (Logothetis, 2002). Although it is now believed that the haemodynamic response is related to a range of factors, including both excitatory and inhibitory post-synaptic processing, neuronal spiking, and neuromodulation (Logothetis, 2008; Palmer, 2010).

1.5.2 fMRI data analysis

The aim of fMRI data analysis is to determine the brain regions (voxels) whose BOLD signal time course correlates with a particular experimental stimulus or task of interest. In the present thesis fMRI data were analysed using statistical parametric mapping (SPM2; <http://www.fil.ion.ucl.ac.uk/spm/>) which is an instantiation of the general linear model. In statistical parametric mapping, inferences are made by computing univariate statistical parametric tests at every voxel in the brain, these are then assembled into an image (Friston et al., 1995). The first stage of analysis involves applying a set of pre-processing transformations to the data. These include, correcting for head motion, normalising individual participants' data into a common template space to facilitate group level analysis, and finally, temporal and spatial smoothing can be applied. Following pre-processing, analysis is performed separately for each participant using the general linear model approach.

The general linear model aims to explain the variation of the time-course associated with

each voxel in terms of a linear combination of explanatory or predictor variables (i.e. experimental manipulations) and an error term. It can thus be described by the following equation in matrix form:

$$Y = X\beta + \varepsilon$$

Where Y represents the BOLD signal time series from each voxel.

X represents the design matrix where experimental manipulations which may explain the observed data are specified (i.e. the onset and offset times of the different experimental conditions).

β represents the parameter estimates of the contributions of each given predictor variable in X to response data Y .

Finally, ε is the residual error term which records the difference between the observed data Y and that predicted by the model $X\beta$.

This model is estimated at every voxel separately in order to obtain the parameters, β , that provide the best fit with the data. The optimal parameter estimates are calculated by minimising the sums of squares differences between the predicted model and the observed data. Once the parameter estimates have been obtained, particular effects of interest can be quantified by computing contrasts of specific parameter estimates (e.g. dynamic faces versus static faces), from which statistical inferences can be made, based on the assumption that the parameter estimates are normally distributed.

The results from each participant can then be entered into a group level analysis in order to make quantitative inferences about the average effects in the population (Friston et al., 1995). The results of the statistical analysis must then be corrected for multiple comparisons as a large number of non-independent univariate comparisons have been carried out. Hence the probability that any given region will exceed an uncorrected threshold by chance is high. However, the common Bonferroni correction method of dividing the threshold (e.g. 0.05) by the number of tests performed is believed to be overly conservative for functional images, because some of the voxels are spatially correlated, usually due to smoothness, and thus not independent. Standard procedures have been developed in SPM to correct for multiple comparisons based on gaussian random field theory, which uses a modified form of the Bonferroni correction to appropriately assess the number of independent voxels within the image (Friston et al., 1995).

1.5.3 Advantages and limitations of fMRI

The main advantages of fMRI are in its excellent spatial resolution, noninvasiveness and its capacity to image the entire network of brain areas involved in a particular task, making it a very popular tool in neuroscience research. fMRI, with its excellent spatial resolution, offers the advantages of investigating concurrent relationships between brain response, behavioural response and structural morphometry. Typical fMRI spatial resolution is approximately 3-5 mm, and spatial resolution of <1 mm can be achieved with advanced and specialised imaging sequences, which makes it possible to image smaller regions of interest. Furthermore, fMRI sequences and designs are continually evolving providing better quality images of neural networks. However, because fMRI measures changes in the haemodynamic signal it is only an indirect measure of neuronal activity, which makes interpretation of the response more difficult (see subsection 1.5.1). It also has relatively poor temporal resolution as it is limited by the haemodynamic response which peaks approximately 5 seconds after neural activity begins (Logothetis, 2008). Therefore fMRI cannot reliably be used to assess the dynamics of brain function, particularly transient cognitive responses.

1.5.4 Basic principles of MEG

Unlike fMRI, which uses an indirect measure of the haemodynamic response to infer neural activity, MEG can be used to directly measure neural activity with millisecond resolution. The primary sources of MEG (and EEG) signals are the electrical activity generated by the ionic currents flowing through the apical dendrites of large pyramidal neurons within cortical gray matter during synaptic transmission. EEG directly measures this electrical activity whereas MEG measures the corresponding magnetic field emanating from the brain. Due to the inherent properties of the magnetic field, MEG is capable of measuring currents that flow tangentially with respect to the head surface only. The magnetic fields produced by cells of radial orientation simply surround the cell and cannot be easily detected outside the head. Thus, the MEG signal primarily reflects the intracellular activity from pyramidal cells located on the sulci of the cortex that are orientated parallel to the surface of the head. In order for MEG to detect the neuronal activity from the cortical or head surface, a vast number of neurons, in the region of 50,000 must be activated

simultaneously and aligned in the same orientation (Okada, 1983).

The neuromagnetic signals that are produced by synaptic activity inside the brain are extremely small, in the order of 50-500 femtotesla (ft, 10-15). It is therefore necessary to use superconducting quantum interference devices (SQUIDs) to measure the very small variations in magnetic flux. Furthermore, because these neuromagnetic signals are relatively weak in comparison to environmental noise it is necessary to try to reduce the amount of external magnetic noise present. This can be achieved by placing the MEG system in a magnetically shielded room, which eliminates the majority of background environmental noise (Singh, 1995). The MEG data can then be recorded on a millisecond-by-millisecond scale with relatively little contamination from external noise.

1.5.5 MEG source localisation

Activity produced by a large number of neurons can be recorded by MEG instantaneously, accounting for its good temporal resolution, but it is also important to define the location of these neural sources of activation. This leads to what is known as the inverse problem, which refers to the estimation of primary sources of activation within the brain from the measured magnetic field outside of the head. Unfortunately, there is no unique solution to the inverse problem, as an infinite number of possible source configurations could potentially produce the same measured magnetic field. It is therefore described as an “ill-posed” problem. Different source analysis techniques can be used to try to solve this problem, but all are based on a certain set of assumptions and have their relative strengths and weaknesses (for reviews see Hillebrand et al., 2005; Barnes et al., 2006). In the MEG studies presented in the present thesis a beamforming strategy known as synthetic aperture magnetometry (SAM) has been implemented to localise sources of cortical activation in all MEG analyses.

Beamforming is a procedure that selectively weights the contribution of signals from pre-determined locations of interest within the brain (Van Veen et al., 1997; Robinson and Vrba, 1999). Essentially, a beamformer acts as a set of spatial filters that are tuned to each voxel in the brain. Before SAM source reconstruction can be computed a source space of the target locations must initially be defined. This involves using a coregistration procedure, which maps the functional MEG data onto a structural MRI for each

participant. In the present thesis this procedure was used to produce a structural image with 5 mm voxel resolution (for further details see section 4.2; Adjamian et al., 2004).

An optimal spatial filter is then constructed based on a set of beamformer weights that are determined for all of the different target locations (i.e., voxels), by linking activity at each voxel to the MEG system's sensor array (obtained from analysis of the data covariance matrix; see Van Veen et al., 1997; Robinson and Vrba, 1999; Barnes and Hillebrand, 2003). The output of the spatial filter for each voxel is a weighted sum of the recorded MEG sensor signals. By computing these spatial filters over the entire brain a volumetric image of the source power within a particular frequency range and time window can be produced. Furthermore, the spatial filter output at any voxel is similar to placing an invasive electrode at a given neural location, as it provides a millisecond-by-millisecond estimate of the electrical activity at that source, and as such, is often referred to as a virtual electrode (Barnes and Hillebrand, 2003).

One of the main advantages of SAM source analysis, and the beamforming technique in general, is that in contrast to dipole modelling, there are no a priori assumptions about the number of active sources (Supek and Aine, 1993), thus multiple (uncorrelated, see below) sources can potentially be constructed at any point in the brain within a given time interval (Singh et al., 2003). This is particularly important in relation to cognitive tasks, such as face processing, where a distributed network of neural regions may be active at any one time. Furthermore, SAM analysis can be used to image neural activity that is phase-locked as well as non-phase-locked to stimuli. This means that changes in spectral power that are not necessarily phase-locked to stimuli, including event related synchronisation (ERS) and event related desynchronisation (ERD) can be assessed (Pfurtscheller and Lopes da Silva, 1999). This is an important benefit of SAM analysis as it facilitates the use of MEG experimental paradigms that are comparable to fMRI (Singh et al., 2002, 2003). Notably, beamformer-based statistical parametric maps (SPMs) can be computed, similar to those produced in fMRI analyses, which represent task related changes in spectral power across the brain during various frequency bands and time windows.

Many of the MEG face perception studies to date have focused on temporal information by examining evoked responses and ignored the frequency information from ongoing neural oscillatory activity. However, it has been demonstrated that oscillatory activity

plays a key role in cortical function (Engel et al., 2001) and there is evidence to suggest that different frequency oscillations are involved in the emergence of percepts, memories, emotions, thoughts, and actions (Cantero and Atienza, 2005; Knyazev, 2007). It has also been shown that different cognitive tasks can induce both increases (ERS) and decreases (ERD) in oscillatory activity (Basar et al., 2001). These studies therefore highlight the importance of investigating ongoing neural oscillatory activity in order to obtain a better understanding of brain function. By using SAM analysis this important aspect of neural function can be assessed.

However, a limitation of the beamforming method is that it will be unable to localise signals from spatially separate sources if they are highly correlated (Van Veen et al., 1997; Barnes and Hillebrand, 2003). This is because the fundamental assumption behind beamformer analysis is that the time course from any cortical source is not linearly correlated with any other source i.e., the SAM algorithm tunes activation at each voxel by attenuating correlated power across the brain (Van Veen et al., 1997). However, simulations have shown that the temporal correlation between two source signals must be relatively high (>0.7) before cancellation occurs (Van Veen et al., 1997). This problem can be avoided if relatively long time windows are used when constructing the covariance matrix, as stimulus-related neural activity in various regions is less likely to be highly correlated over longer periods of time (Singh et al., 2003).

1.5.6 Group level analysis of MEG data

As described in the previous section the SAM beamformer algorithm creates differential images of source power across the brain, whereby, the differences in spectral power during two different experimental conditions are statistically assessed at each voxel using a pseudo t-statistic (Robinson and Vrba, 1999). This produces SAM volumetric images or so-called statistical parametric maps (SPMs) of cortical activation for each individual. In order to perform group level analyses in the present thesis, all of the volumetric SAM images for each participant were spatially normalised to a standard template brain in SPM99. This also facilitates direct comparison of the fMRI and MEG results, as they are both represented in the same standard template space. Significant group effects were assessed by nonparametric permutation analysis using the SnPM toolbox for SPM

(<http://www.fil.ion.ucl.ac.uk/spm/snpm/>; Nichols and Holmes, 2002). Nonparametric analyses were performed instead of the conventional parametric method because of the high variability in the magnitude of cortical oscillations across participants (Singh et al., 2003). Nonparametric permutation testing allows the statistical significance of voxel effects to be established without assuming that the data is normally distributed. Singh et al. (2003) found that nonparametric analysis of group MEG data was more sensitive and robust than the standard parametric approach.

1.5.7 Advantages and limitations of MEG

The primary advantage of MEG is its excellent temporal resolution, whereby events with time scales in the order of milliseconds can be resolved. Thus in contrast to fMRI, MEG has the necessary temporal resolution to study the dynamics of brain function and even transient cognitive responses can be detected. Furthermore, unlike fMRI, MEG provides a direct measure of neural activity. Hence it provides a more reliable account of brain activity and is less likely to be affected by other physiological confounding variables. However, MEG has relatively poor spatial resolution compared to fMRI. The inverse problem must be overcome in order to localise sources making it more difficult to reliably estimate sources of activation with MEG (see subsection 1.5.5).

1.6 Multimodal integration

In general, the goal of neuroimaging studies is to estimate when and where activation in relation to a specific task or experimental condition occurs in the brain. As described in section 1.5 different imaging techniques are better suited to measure one aspect or the other. MEG, which is based on direct measurements of neuronal electrical activity, provides excellent temporal resolution but relatively poor spatial resolution. Conversely, fMRI, which relies on indirect haemodynamic effects, has excellent spatial resolution but its temporal resolution is intrinsically limited by physiological factors. By adopting a multimodal approach of combining fMRI and MEG methods to investigate face processing, the benefits of both techniques can be exploited and will complement each other. Hence, it is possible to characterise face-related neural activity in the spatial, temporal and

frequency domains.

The majority of face perception research to date has focused on the spatial domain using fMRI to localise face-specific regions of activation (see section 1.3). The temporal domain has also received a great deal of attention, particularly in EEG studies using ERP methods, and to a lesser extent MEG studies examining evoked responses. However, as discussed in subsection 1.5.5, the frequency domain has been largely neglected in this field. Yet it is increasingly becoming clear that neural oscillations play an important role in brain function and the synchronised activity of oscillating neural networks is now believed to be the critical link between single neuron activity and behaviour (Engel et al., 2001; Buzsáki and Draguhn, 2004). It is therefore important to examine information in the frequency domain in addition to the spatial and temporal domains, in order to gain a thorough understanding of face processing in the brain.

As described in subsection 1.5.5, by using MEG with SAM source analysis, task-dependent and frequency specific oscillatory power changes can be investigated and localised both spatially and temporally. Several studies have used combined MEG (with SAM source analysis) and fMRI paradigms to investigate the relationship between neural oscillatory activity and the BOLD response, and have demonstrated that various oscillatory components of the MEG signal covary with the BOLD fMRI signal (Singh et al., 2002). For example, it has been shown that decreases in alpha and beta power during cognitive tasks are inversely correlated with increases in the BOLD response during the same tasks (Singh et al., 2002). While increases in higher frequency bands, such as gamma, appear to correlate with the BOLD response, particularly in visual cortices (Fawcett et al., 2004; Brookes et al., 2005; Muthukumaraswamy and Singh, 2008).

These studies reveal good spatial correspondence between these two different modalities. Hence, by combining different techniques such as fMRI and MEG, obtaining similar results validates both methods. In addition, connectivity analysis was also performed on the fMRI data in the present thesis adding another dimension to the level of information obtained. It is becoming increasingly more evident that the brain operates as an integrated network, thus by combining spatial, temporal, frequency and connectivity information a better understanding of the mechanisms involved in face processing can be gained.

1.7 Objectives

As discussed throughout the course of this chapter, facial motion is a key component of face perception, yet it has been largely neglected in face perception research to date. The importance of dynamic information in judgments of both facial identity and expression has been highlighted throughout this chapter. Thus, it has been argued that more naturalistic dynamic face stimuli should be used in face perception research in order to obtain a better understanding of how faces are processed when viewed naturally in the real world. Two compatible neural models of face perception and emotion recognition have been presented, which were mainly derived from studies of static faces. Using these models as a general guide and framework the present thesis aims to investigate the neural correlates of dynamic face perception, and thereby contribute to extending these models and the face perception literature to incorporate dynamic facial information.

It has also been shown that information about faces is represented in a distributed fashion within a broad network of neural regions over time (Haxby et al., 2000; Ishai, 2008). A major challenge for face perception research therefore is to try to disentangle these distributed patterns of information across time, space and frequency. To this end, a multimodal approach was adopted in the present thesis, whereby fMRI and MEG were used in two separate studies to explore the spatio-temporal and frequency characteristics of neural responses to dynamic faces. This approach combines the advantages of fMRI, as a neuroimaging technique which offers high spatial resolution, with MEG beamforming which offers exciting insights into the multidimensional structure of the neural signal. The rationale and experimental design of these studies will be described in detail in the following chapters.

To summarise, firstly in chapter 2 the superior spatial properties of fMRI will be exploited and used to localise the neural regions involved in processing dynamic facial expressions. Next, in chapter 3, measures of effective connectivity will be used to explore the relationships between the brain regions involved in processing dynamic faces, in order to gain a better understanding of the network interactions. Having localised the dynamic face perception network with fMRI, the temporal benefits of MEG will be exploited in chapter 4, to measure the timecourse of activation in response to dynamic facial stimuli compared to static displays, as well as examining the frequency of neural oscillations contributing to

these responses. In chapter 5, MEG will be used to further explore the effects of emotion-specific facial dynamics, whereby the time-frequency characteristics of responses to the different dynamic and static facial stimuli will be examined. Finally, the results from all four different analyses will be integrated and reviewed in the context of previous models in the concluding chapter 6.

Chapter 2

The neural substrates of dynamic face perception

2.1 Introduction

2.1.1 Overview

This chapter describes an fMRI study of dynamic face perception, where fMRI was used to identify regions of activation in response to different dynamic facial displays, including anger, happiness and speech.

2.1.2 Neuroimaging studies of dynamic face perception

Bruce and Young's (1986) influential model of face recognition has served as a general framework for the study of face perception for the last thirty years. Based largely on findings from behavioural observations, this model gives a modular description of the face processing system with different specialised modules for face recognition, facial expression analysis, facial speech analysis, among others, and an all encompassing cognitive system required to combine information from the different modules (see subsection 1.2.3 for further discussion of this model). Central to this model is the notion that analysis of facial expression and identity proceed independently of each other (see Figure 1.2.1). In addition to behavioural findings, evidence to support the functional division between facial expression and identity processing comes from neuropsychological studies of prosopagnosic

patients, who can interpret facial expressions correctly but are unable to correctly identify familiar faces (Humphreys et al., 1993). Importantly, the Bruce and Young (1986) model was primarily concerned with the functional components within the face perception system and did not provide a neural description of these areas.

Haxby et al. (2000) later provided a neurological description of face perception, where they described a distributed human neural system for face perception. This model consists of a core system and an extended system (see Figure 1.3.1). Within the core system, the initial perception of facial features occurs in the inferior occipital gyri. From here there are two functionally and neurologically distinct pathways based on the idea that facial structure is more important for identification purposes, while changeable aspects are necessary to facilitate social communication. Hence this model, like the earlier Bruce and Young (1986) model, proposes distinct pathways for the visual analysis of facial identity and expression. The perception of identity, the invariant aspect of a face, occurs in a ventral pathway that involves the lateral fusiform gyrus, whereas the superior temporal sulcus is part of the dorsal pathway that is implicated in the processing and representation of changeable facial features. The extended system incorporates additional brain regions such as, the amygdala, orbitofrontal cortex, and inferior frontal areas, which are recruited to support additional aspects of face processing, such as emotion recognition etc.

However, Haxby et al.'s (2000) distributed face perception model was mainly defined using evidence derived from static images of faces, hence very little is known about the neural structures involved in the perception of realistic dynamic facial expressions. Yet real life faces are dynamic by nature, particularly when expressing emotion. The posed static facial stimuli that have generally been used in face perception research do not reflect the unique temporal dynamics and information available from seeing a moving face in the real world. There is considerable behavioural evidence showing the importance of motion in face perception (see subsection 1.2.2.1). Hence the static facial stimuli that have traditionally been used in face perception research to date represent impoverished displays lacking natural facial motion (see subsection 1.3.6), which do not facilitate a complete interrogation of the face perception network, particularly the dorsal pathway which is implicated in the processing of facial dynamics. Dynamic stimuli would therefore offer a more suitable means of examining the neural basis of realistic natural face perception.

More recently researchers have begun to investigate the neural network underlying the processing of dynamic face stimuli (see subsection 1.3.8). Generally regions of middle temporal and superior temporal cortices have been shown to respond to biological motion including dynamic face stimuli (see subsection 1.3.7). Regions of the extended system including the amygdala and inferior frontal gyrus have also been shown to be involved in processing dynamic faces (Kilts et al., 2003; Fox et al., 2009; Pitcher et al., 2011a). Some studies have also reported increased activation in the fusiform gyrus, in the ventral pathway, to dynamic faces (LaBar et al., 2003; Sato et al., 2004; Schultz and Pilz, 2009), which suggests that the fusiform gyrus is not only involved in processing the invariant aspects of the face as predicted by Haxby's model, but may also be involved in processing changeable aspects as well. In light of these results, among others, the independence of the ventral pathway which processes the invariant aspects, and the dorsal pathway involved in processing the changeable aspects of faces has been questioned.

Calder and Young (2005) recently used principle component analysis to investigate the degree of separation between these two pathways and found that facial expressions and identity can be coded within a single multidimensional framework rather than relying on separate independent codes. Thus, it would appear that the roles of the fusiform gyrus and STS may not be as dissociable and distinct as previously thought. Connectivity analysis may help to inform this debate as highlighted in a recent study by Turk-Browne et al. (2010) where they found correlated resting connectivity between the fusiform gyrus and STS (see chapter 3) which they suggest explains the sparseness of evidence for a double dissociation between identity and emotion processing in the brain. Hence, an important update to Haxby et al.'s model is to emphasise that the segregation between the fusiform gyrus, in the ventral pathway, and the STS, in the dorsal pathway, is only partial (Said et al., 2011)

Despite the differences in activation patterns in regions in ventral temporal cortex, dynamic in contrast to static facial expressions reliably evoked increased activation in motion sensitive areas in the core face perception system, along middle temporal gyrus and STS (Kilts et al., 2003; Sato et al., 2004). This is consistent with Haxby et al.'s (2000) model and the biological motion perception literature (Grosbras et al., 2012). Furthermore, Fox et al. (2009) demonstrated that dynamic face stimuli improved localisation of face-

selective regions, not only in regions of the core face perception system, but also in regions of the extended system, such as the amygdala, inferior frontal gyrus and anterior cingulate cortex. This suggests that the processing of dynamic facial expressions recruits regions in the extended face perception system more reliably than static face stimuli (Fox et al., 2009; Trautmann et al., 2009).

Different dynamic facial expressions have also been shown to recruit different structures in the extended face perception system (Kilts et al., 2003; Trautmann et al., 2009), lending some support to the theory that dissociable brain areas are involved in the perception of different facial expressions of emotion (for review see Adolphs, 2002). However, due to the limited number of dynamic face perception studies and the different types of facial expression stimuli used, the extent to which regions in the extended system are involved in processing different dynamic facial expressions of emotion is still unclear. Not only have previous fMRI studies of dynamic face perception used different exemplars of facial expression stimuli, they have also employed different experimental designs and analysis techniques which complicate conclusions from individual experiments.

For example, some studies have used whole-brain analysis without examining the corresponding percent signal change in regions of the face perception network (Kilts et al., 2003; LaBar et al., 2003), while others have only examined responses in specific pre-defined regions of interest and have not acquired and analysed data from other brain regions (Pitcher et al., 2011a). In addition, some studies have collected their data in different scanning sessions which means that they cannot directly compare the brain activation in different conditions (Sato et al., 2004). This is a major limitation of Fox et al. (2009)'s study as they were not able to directly compare brain activation in response to dynamic and static face stimuli.

A further limitation of many of the dynamic face perception studies (LaBar et al., 2003; Sato et al., 2004) is that they have used morphed stimuli which were constructed from static face stimuli and may represent non-natural motion. Using such stimuli with artificial motion is unlikely to fully capture the mechanisms underlying the processing of natural facial motion as the response properties measured with these artificial stimuli may not generalise to natural stimuli (Felsen and Dan, 2005). Hence very little is known about the neural structures involved in the perception of realistic dynamic facial expressions.

2.1.3 Objectives and hypotheses

The objective of the present study was twofold. The first aim was to create and evaluate a set of naturalistic dynamic face stimuli to be used to investigate the neural correlates of dynamic face processing. Over forty different dynamic face stimuli were created and then evaluated psychometrically by 70 participants (see section 2.2 for full details). In addition, a motion capture technique was used to measure the amount of motion contained in the different stimuli. This was used as a control technique to eliminate any confounds of motion differences between the stimuli. The reason for this control condition was to ensure that there was not a perceived difference in the amount of motion in the different facial expression categories, but rather the pattern of that motion. So that identification of different emotions would be based on the latter rather than the former and any differences in cortical activation would be due to the stereotypical pattern of motion associated with that facial display and not differences in the amount of motion per se.

The second aim was to use fMRI to identify regions of activation in response to dynamic facial displays, including anger, happiness and speech. Angry and happy expressions were chosen in order to contrast positive and negative facial affects, while speech was chosen as a control for non-affective facial motion (see section 2.2 for full details). In the whole-brain subtractive analysis the BOLD activation response to all dynamic faces directly contrasted with static faces was examined. Planned pairwise comparisons were computed within each emotion category to examine the effects of motion on the processing of different face stimuli (i.e. dynamic angry versus static angry expressions, dynamic happy versus static happy expressions, and dynamic speech versus static speech displays). Contrasts were also computed to investigate the effects of emotion-specific facial dynamics by contrasting both of the dynamic affective expressions (i.e. angry and happy face stimuli) with dynamic speech facial displays. In addition to performing whole-brain group analyses, a regions of interest analysis was also carried out to estimate the amplitude of the responses to the different face stimuli within face-selective regions of the core and extended face perception systems.

It was hypothesised that dynamic facial expressions would elicit activation in the dorsal pathway of the face perception network. Dynamic face stimuli have previously been shown to activate regions in the dorsal pathway of the face perception network, such as regions

along middle temporal gyrus and STS, along with regions in the extended system, such as the amygdala and inferior frontal gyrus (Kilts et al., 2003; LaBar et al., 2003; Sato et al., 2004; Fox et al., 2009; Pitcher et al., 2011a). Thus, it was predicted that the dynamic facial expressions used in the present study would elicit activation in similar regions along this dorsal pathway, and also recruit regions in the extended system. Additionally, some studies have found differential activation for different facial expressions, particularly in the extended face perception system (Kilts et al., 2003; Trautmann et al., 2009). It is therefore hypothesised that different structures within Haxby et al.'s (2000) distributed face perception system may be selectively recruited to process dynamic angry, happy and speech facial displays.

2.2 Methods

2.2.1 Stimuli

In this study a unique set of stimuli were created in order to obtain examples of naturalistic facial expressions. Forty models were recruited from the psychology undergraduate student population and were filmed in a dedicated studio. All models were asked to remove facial piercings, earrings and headgear and none had any facial hair. The models were filmed sitting down against a uniform white background at a distance of 1.5 m. They were shown examples of prototypical facial expressions from the Ekman and Friesen (1976) collection and asked to use these as a reference guide when posing the expressions. They were also encouraged to imagine personal situations to evoke these emotions.

The models started emoting from a neutral expression and proceeded to each of the five basic emotion expressions (happy, anger, fear, disgust and surprise), and speech movements were also recorded by filming the models while counting from 1 to 10. A Canon ZR960 video camera was used to capture the video stream in colour. This was then transferred to a Dell PC for off-line editing. Each recording session lasted approximately 10 minutes. Windows Media Player was used to edit the video stream and create 2.5 sec clips for each different expression category for every participant (image size: 640 x 480 pixels, frame rate = 30 frames per second). Static stimuli were then created from a screenshot of the final frame of each expression.

Seventy-one additional participants from the psychology undergraduate student population were recruited to rate both the video stimuli and their static exemplars, to ensure that these stimuli depicted recognisable emotional expressions. They performed a five alternative forced choice task whereby they had to identify the facial expressions shown as one of the following; angry, happy, fear, disgust and surprise. Participants also evaluated emotional intensity on a 10-point Likert scale. They were instructed to “rate how intense the emotional expression is” where 1 = very low emotional intensity and 10 = very high emotional intensity. Both dynamic and static stimuli were displayed for 2.5 sec and participants were given 5 sec to respond to each stimulus before proceeding.

The number of correct responses within each emotion category was calculated across participants for both the dynamic and static conditions. This was then expressed as a percentage of the total number of stimuli shown within each affect condition. The data were then analysed using a mixed ANOVA with the percentage correct responses for each affect as a within participant factor with five levels (angry, happy, fear, disgust and surprise), and the motion category (either static or dynamic) as a between participant factor.

There was a significant main effect of motion, $F(1, 69) = 29.21, p < .001$ where dynamic facial expressions were recognised significantly better than static faces. There was also a main effect of affect, $F(4, 276) = 65.6, p < .001$. Post hoc contrast tests revealed that happy expressions were recognised significantly more accurately than all other expressions at $p < .001$: angry, $F(1, 69) = 78.5$, fear, $F(1, 69) = 228.23$, disgust, $F(1, 69) = 28.663$, and surprise, $F(1, 69) = 71.36$. Angry faces were recognised significantly better than fearful faces, $F(1, 69) = 53.53, p < .001$, there was no significant difference in recognition between angry and surprise facial expressions, and disgust facial expressions were recognised significantly better than angry expressions, $F(1, 69) = 23.14, p < .001$ (see Figure 2.2.1A). Due to the fact that fear and surprise had a low recognition rate they were excluded from subsequent study.

Mean intensity values were also calculated across participants for each affect, across both the dynamic and static conditions. Again an ANOVA was used to analyse the intensity ratings with the judged intensities of the correctly identified emotions for each of the affects as a within participant factor, and a between participants factor of motion category

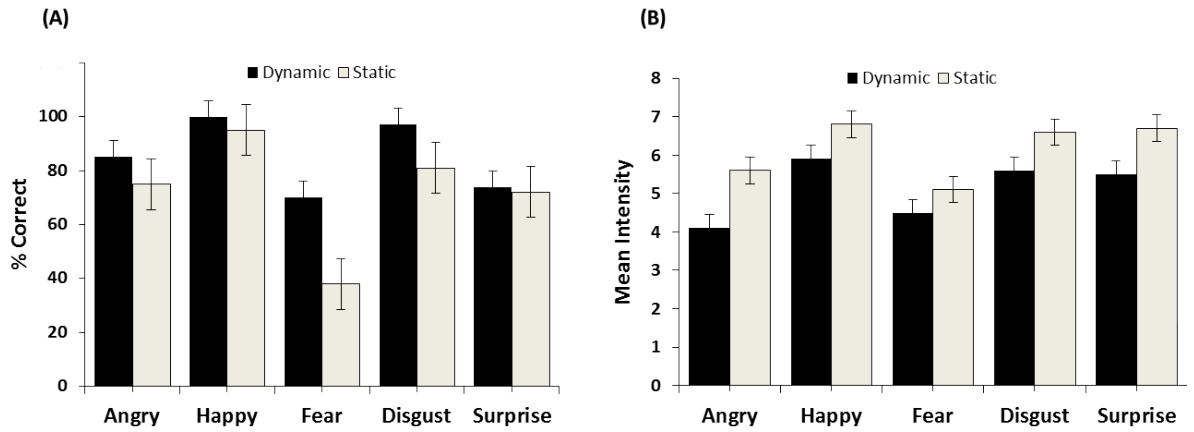


Figure 2.2.1: Behavioural face rating data showing: (A) % correct for each of the different dynamic and static facial affect stimuli (B) Mean intensity ratings for each of the different dynamic and static facial affect stimuli. Black bars indicate the dynamic stimulus condition and white bars denote the static stimulus condition, error bars indicate standard error of mean (S.E.M).

(either static or dynamic). Again there was a significant main effect of motion, $F(1, 69) = 19.03$, $p < .001$, where static faces were rated as more intense than dynamic faces. There was also a significant main effect of affect, $F(4, 272) = 67.35$, $p < .001$. Post hoc contrast tests revealed that happy facial expressions were rated as significantly more intense than angry expressions, $F(1, 69) = 110.62$, $p < .001$ (see Figure 2.2.1B).

In addition to this behavioural analysis a motion capture technique was used to assess whether the amount of facial motion was equivalent across the different facial expressions. This was important to ensure that any neurological distinction between the affects that may be identified with fMRI, would be due to differences in the type of affect specific motion not the amount of motion per se. Four additional models (2 males and 2 females) were recruited and as before they were asked to emote different facial expressions following the procedure described above. Seven retro-reflective markers were attached to each participant's face using double-sided adhesive tape. The marker locations were selected to track optimum facial motion and were placed at the following locations, left eyebrow, right eyebrow, nasion, left cheek, right cheek, left lip corner and right lip corner (Matsuzaki and Sato, 2008). The data were then recorded using three infrared light-emitting, ProReflex™ Motion Capture Units (MCU120; Qualisys Systems, Sweden). The cameras used the reflected data from the markers to calculate the position of the targets with high spatial resolution. The motion of the markers was recorded at 120 Hz and all data were low-pass filtered using a second order Butterworth Filter with 5 Hz cut-off frequency. The captured

data was then exported and analysed in Microsoft Excel.

The euclidean distance was calculated at each time point for every marker using the squareroot of the sum of the difference from point two to point one squared. The mean distance and standard deviation were calculated for each of the seven markers on each participant for each of the different expressions. The overall group means and standard deviations were then calculated for each of the affects. No significant difference was found in the amount of motion between angry (mean 0.09 mm and S.D. 0.02), happy (mean 0.11 mm and S.D. 0.05) and speech (mean 0.12 mm and S.D. 0.03) facial expressions (see Figure 2.2.2).

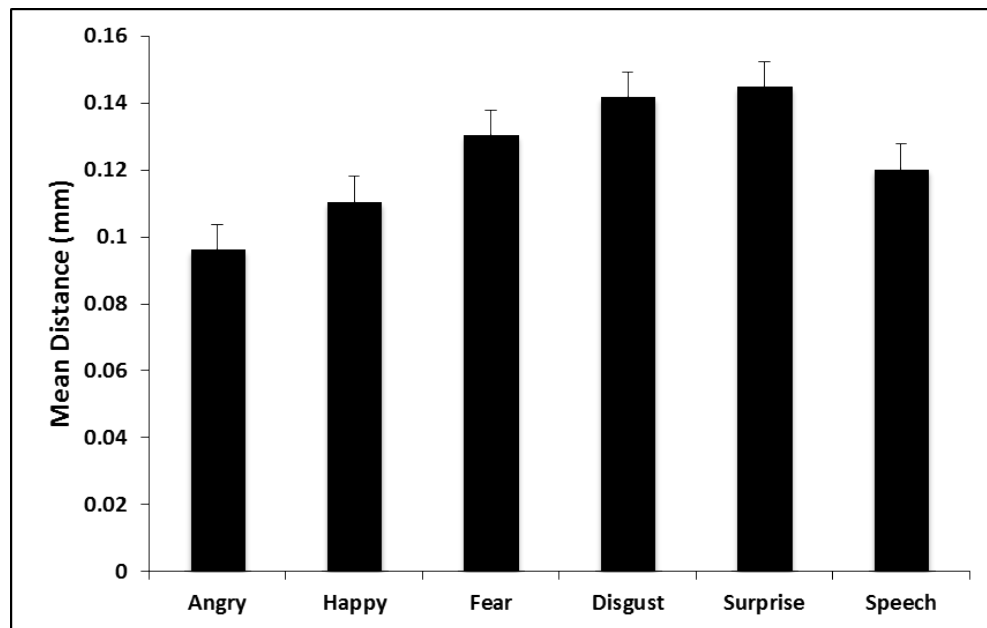


Figure 2.2.2: Group motion capture data ($n=4$) shows the mean amount of motion for each of the different facial affects. Error bars indicate standard error of mean (S.E.M).

2.2.2 fMRI participants

Fourteen healthy self-reported right-handed volunteers (6 male) with normal or corrected to normal vision (mean age 28.3, S.D. 3.67 years) gave full written informed consent to take part in the study, which was approved by the Aston University Human Science Ethical Committee.

2.2.3 Experimental design and imaging paradigm

A sample of twenty-four stimuli (twelve dynamic and twelve corresponding static images) was selected for the fMRI experiment, based on their highest intensity ratings and cor-

rectly identified as the target affect as described above. Two emotion categories were included, specifically, angry and happy, and a speech category was also included as a control for non-affective facial motion. In the dynamic condition four different stimuli were presented in each of the three emotion categories, and likewise in the static condition. The identities were matched across the dynamic and static conditions, as the static stimuli were created from a screenshot of the final frame of each of the dynamic excerpts including the speech controls.

Each stimulus was presented for 3 sec within a block of eight of the same condition. Hence, there were six different blocks of 24 sec duration (dynamic angry, static angry, dynamic happy, static happy, dynamic speech and static speech). A session of length 288 sec consisted of 24 sec blocks of no visual stimulation (fixation cross) alternating with the six 24 sec blocks of visual stimulation. Blocks were presented in a pseudo-random order around a Latin squares design within each session, and there were 6 sessions in total (1728 sec). Participants performed a 1-back memory task on the individual identity within each block, making all responses via the lumina response pad (see Figure 3.2.1). This task was designed to maintain vigilance and to control for attention which is known to modulate BOLD signals in many of the neural areas included in this study (see e.g. Beauchamp et al., 2002).

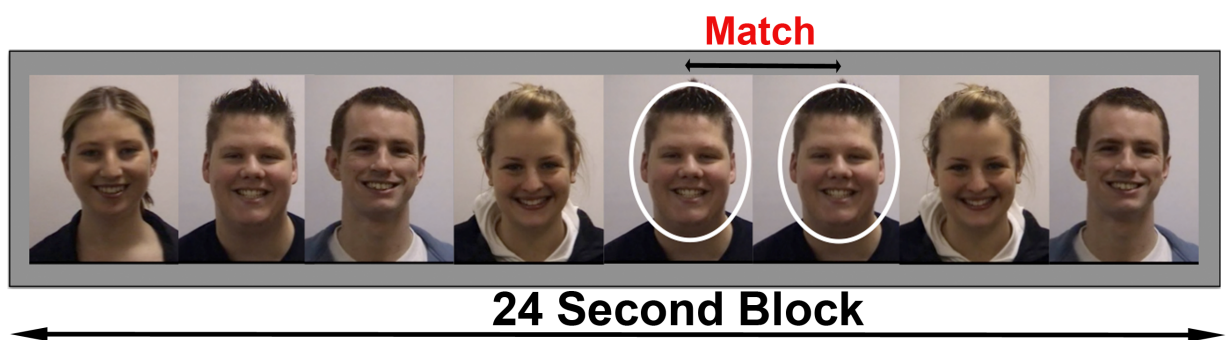


Figure 2.2.3: fMRI experimental design shows 24 s on-block where 8 stimuli were presented for 3 s within each block of the same condition. This alternated with a 24 s block of no visual stimulation (fixation cross). Participants (N=14) performed a 1-back memory task on the individual identity within each block, making all responses via the lumina response pad.

2.2.4 Imaging protocol

MR data were acquired on a 3 Tesla Siemens Magnetom Trio Scanner using an 8-channel radio frequency birdcage head-coil. A gradient echo planar sequence (EPI) was used to

acquire 44 contiguous 3 mm thick axial slices per whole brain volume in one time series of 576 scans, with the following parameters; echo time (TE) = 30 msec, repetition time (TR) = 3000 msec, field of view (FOV) = 192 mm, 64 x 64 pixels per inch matrix, resolution 3 x 3 mm in-plane resolution. A high resolution MPRAGE anatomical image with 1 x 1 x 1 voxel resolution was collected at the end of each scanning session. Visual stimuli were presented using Presentation Software (Neurobehavioral Systems, Inc.) and projected via LCD to a screen located in the back of the scanner bore behind the participant's head. Participants viewed the stimuli through a prism mirror mounted above their eyes on the head coil.

2.2.5 Image analysis

2.2.5.1 Subtractive analysis

Off-line data processing and analysis were performed using the Statistical Parametric Mapping software (SPM2; Wellcome Department of Cognitive Neurology, London, UK; www.fil.ion.ucl.ac.uk/spm) implemented within Matlab 7. All functional volumes were realigned to the first volume using rigid body transformations (the most accurate function for realignment in SPM2), to correct for any head motion. To facilitate group analysis all functional images were then spatially normalised into standard stereotactic space using the Montreal Neurological Institute (MNI) echo-planar imaging template proposed as default in SPM2, which approximates the standard stereotaxic space of Talairach and Tournoux (1988). Spatially normalised images were resliced to a final voxel size of 3 x 3 x 3 mm and smoothed using 7 mm full-width at half-maximum Gaussian kernel, and a high pass filter of 1/128 Hz was used to eliminate low-frequency components.

Realigned, spatially normalised, and smoothed functional images were analysed voxelwise using SPM2 in the framework of the general linear model (see section 1.5; Friston et al., 1995). A first-level, session-specific analysis was initially performed to accommodate for within-subject, between-scan variability. In the first-level analyses, block onsets were modelled as boxcars convolved with a canonical haemodynamic response function. All data were high-passed filtered with a cut-off frequency of 1 /128 Hz to remove low-frequency signal drifts and a correction for temporal autocorrelation was applied. Contrast images were created to identify voxels showing task-related increases in activity. The

following six contrasts were calculated: all dynamic versus all static faces, dynamic angry versus static angry faces, dynamic happy versus static happy faces, dynamic speech versus static speech faces, dynamic angry versus dynamic speech facial displays, and dynamic happy versus dynamic speech facial displays, which produced a statistical parametric map of the t statistic [SPM(t)].

Voxels were identified as significantly activated if they reached a threshold of $p < .001$ (uncorrected) with a spatial extent greater than or equal to 7 voxels. Then, the contrast images for each participant and each comparison were entered into a one-sample t-test for random effects analysis. This procedure accounts for possible participant-by-condition interactions and tests whether or not the population from which our set of participants is drawn possesses the hypothesised effect (Penny and Holmes, 2003). Voxels were identified as significantly activated if they reached a threshold of $p < .001$ (uncorrected) and corrected for multiple comparisons of the entire brain at a threshold of $p < .05$.

2.2.5.2 Regions of interest analysis

Regions of interest (ROI) were defined for each participant based on the contrast of all faces versus baseline fixation with a p value of $p < .001$ uncorrected, and coordinates were verified against previous face perception studies (Haxby et al., 2000; Fairhall and Ishai, 2007). These included the inferior occipital gyrus, superior temporal sulcus, amygdala, and inferior frontal gyrus. Percent signal change data were calculated by extracting the time series at the sites of peak activation within each of these regions of interest for each participant (spherical volumes of 6 mm radius) and then subtracting the mean baseline signal from the activation periods. A repeated measures ANOVA with two within participant factors: motion (dynamic and static), and facial display (angry, happy and speech), was then used to assess the differences in the amount of signal change within each ROI.

2.3 Results

2.3.1 Dynamic versus static facial expressions

As predicted, the contrast between dynamic and static facial expressions revealed significant activation in bilateral superior temporal sulci, bilateral middle temporal gyri and left middle occipital gyrus. In addition, bilateral inferior frontal gyri, bilateral middle frontal gyri, right precentral gyrus and the right amygdala were also significantly activated (see Table 2.1 and Figure 2.3.1). The contrast between dynamic and static angry

Table 2.1: Brain regions showing significant activations in response to all dynamic compared to all static expressions. Coordinates indicate local maxima in Talairach space. L = Left; R = Right. Multiple peaks within a cluster are shown on subsequent lines.

Region	Cluster Size	Z score	x, y, z
R Superior temporal sulcus (BA 22)	1986	5.46	56, -40, 10
R Middle temporal gyrus (BA 22)		4.81	50, -36, 2
R Middle temporal gyrus/MT/V5 (BA 37)		4.52	48, -62, 4
L Middle occipital gyrus/V5 (BA 19)	413	4.57	-42, -76, 4
L Superior temporal sulcus (BA 22)		4.48	50, -58, 16
L Middle temporal gyrus (BA 39)		4.43	-42, -58, 8
L Middle frontal gyrus (BA 6)	42	4.02	-48, 2, 56
R Middle frontal gyrus (BA 6)	63	3.93	48, 2, 42
R Precentral gyrus (BA 6)		3.35	44, -2, 48
R Inferior frontal gyrus (BA 47)	10	3.29	52, 24, -6
R Inferior frontal gyrus (BA 45)	17	3.21	56, 22, 14
L Inferior frontal gyrus (BA 47)	8	3.18	-38, 24, 2
R amygdala (BA 34)	7	3.16	20, -8, -16

faces also revealed significant activation in bilateral STS, bilateral middle temporal gyrus and the right amygdala, but also in bilateral middle occipital gyrus, and the right insula (see Table 2.2 and Figure 2.3.2). Dynamic happy faces compared to static happy faces revealed significant activation again in bilateral STS, and right middle temporal gyrus, but also in left middle occipital gyrus and left fusiform gyrus (see Table 2.3 and Figure 2.3.3). The comparison of the response to dynamic versus static speech revealed significant activation again in bilateral STS and middle temporal gyri, along with bilateral middle occipital gyri, but also bilaterally in the middle frontal gyri, right precentral gyrus and left inferior frontal gyrus (see Table 2.4 and Figure 2.3.4).

Table 2.2: Brain regions showing significant activations in response to dynamic angry compared to static angry expressions. Coordinates indicate local maxima in Talairach space. L = Left; R = Right. Multiple peaks within a cluster are shown on subsequent lines.

Region	Cluster Size	Z score	x, y, z
R Middle occipital gyrus (BA 19)	538	4.98	54, -70, -6
R Middle temporal gyrus (BA 37)		4.32	58, -62, 0
R Superior temporal sulcus (BA 22)		3.35	50, -58, 16
R Superior temporal sulcus (BA 22)	259	4.47	54, -40, 8
L Middle occipital gyrus/V5 (BA 19)	257	4.26	-46, -74, 4
L Middle temporal gyrus (BA 19)		3.52	-44, -62, 16
L Middle temporal gyrus (BA 21)	54	3.78	-58, -40, 2
L Superior temporal sulcus (BA 22)		3.47	-58, -44, 12
R Insula	9	3.5	48, -40, 22
R Amygdala	11	3.25	20, -8, -16

Table 2.3: Brain regions showing significant activations in response to dynamic happy compared to static happy expressions. Coordinates indicate local maxima in Talairach space. L = Left; R = Right. Multiple peaks within a cluster are shown on subsequent lines.

Region	Cluster Size	Z score	x, y, z
R Superior temporal sulcus (BA 41)	517	4.92	46, -40, 6
R Middle temporal gyrus (BA 22)		4.44	58, -44, 4
R Superior temporal sulcus (BA 22)		4.39	62, -32, 8
L Superior temporal sulcus (BA 22)	71	3.94	-50, -48, 12
L Middle occipital gyrus/V5 (BA 19)	22	3.51	-44, -76, 4
L Fusiform gyrus (BA 37)	11	3.33	42, -68, -10

Table 2.4: Brain regions showing significant activations in response to dynamic speech compared to static speech expressions. Coordinates indicate local maxima in Talairach space. L = Left; R = Right. Multiple peaks within a cluster are shown on subsequent lines.

Region	Cluster Size	Z score	x, y, z
L Middle temporal gyrus (BA 19)	489	4.99	-46, -62, 14
L Superior temporal sulcus (BA 21)		4.3	-60, -24, -2
L Superior temporal sulcus (BA 22)		4.12	-60, -44, 10
R Middle temporal gyrus (BA 21)	646	4.48	64, -38, 0
R Superior temporal sulcus (BA 22)		4.42	68, -36, 8
L Middle frontal gyrus (BA 9)	172	4.28	-52, 18, 30
L Middle frontal gyrus (BA 8)		3.35	-48, 10, 42
R Middle frontal gyrus (BA 6)	79	4.23	46, 65, 8
L Inferior frontal gyrus (BA 6)	33	4.11	-48, 18, -6
L Middle occipital gyrus/V5 (BA 19)	122	4.01	-42, -76, 4
R Middle occipital gyrus (BA 19)	88	4.01	54, -70, -8
R Middle frontal gyrus (BA 9)	182	3.97	52, 16, 30
R Precentral gyrus (BA 6)		3.4	44, -2, 46

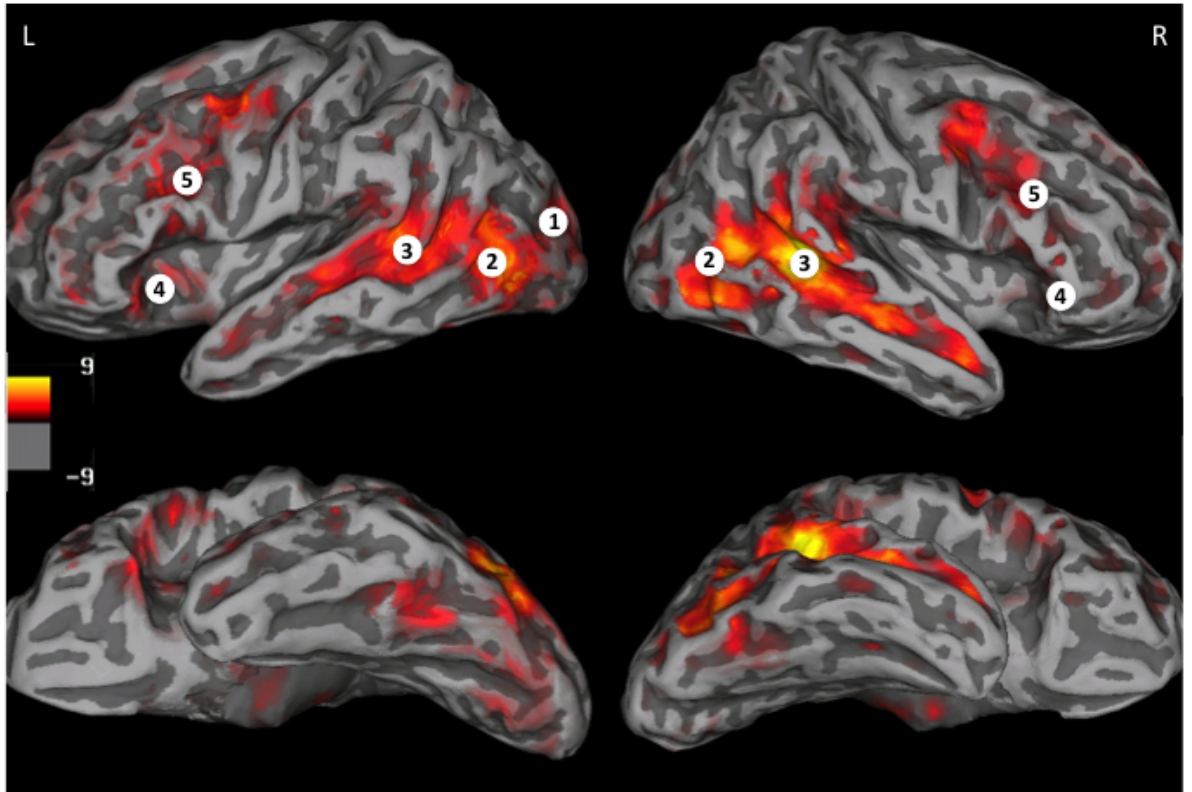


Figure 2.3.1: The dynamic face perception network. Results of whole brain group analysis (N=14) for the dynamic versus static condition projected onto the surface of an inflated standard brain, showing both lateral and ventral views. Bilateral activation is clearly shown on both left (L) and right (R) hemispheres in; (1) middle occipital gyri (2) middle temporal gyri (3) superior temporal sulci (4) inferior frontal gyri (5) and middle frontal gyri. Colour bar denotes T-statistic and images are thresholded at $p < .05$ corrected for multiple comparisons.

2.3.2 Dynamic facial expressions of emotion versus dynamic speech displays

The contrast of dynamic angry facial expressions with dynamic speech facial displays revealed significant activation in bilateral insula, right postcentral gyrus, right inferior frontal gyrus and right amygdala (see Table 2.5). The comparison of dynamic happy facial expressions with dynamic displays of speech revealed significant activation in bilateral inferior frontal gyri, bilateral middle occipital gyri and left fusiform gyrus (see Table 2.6).

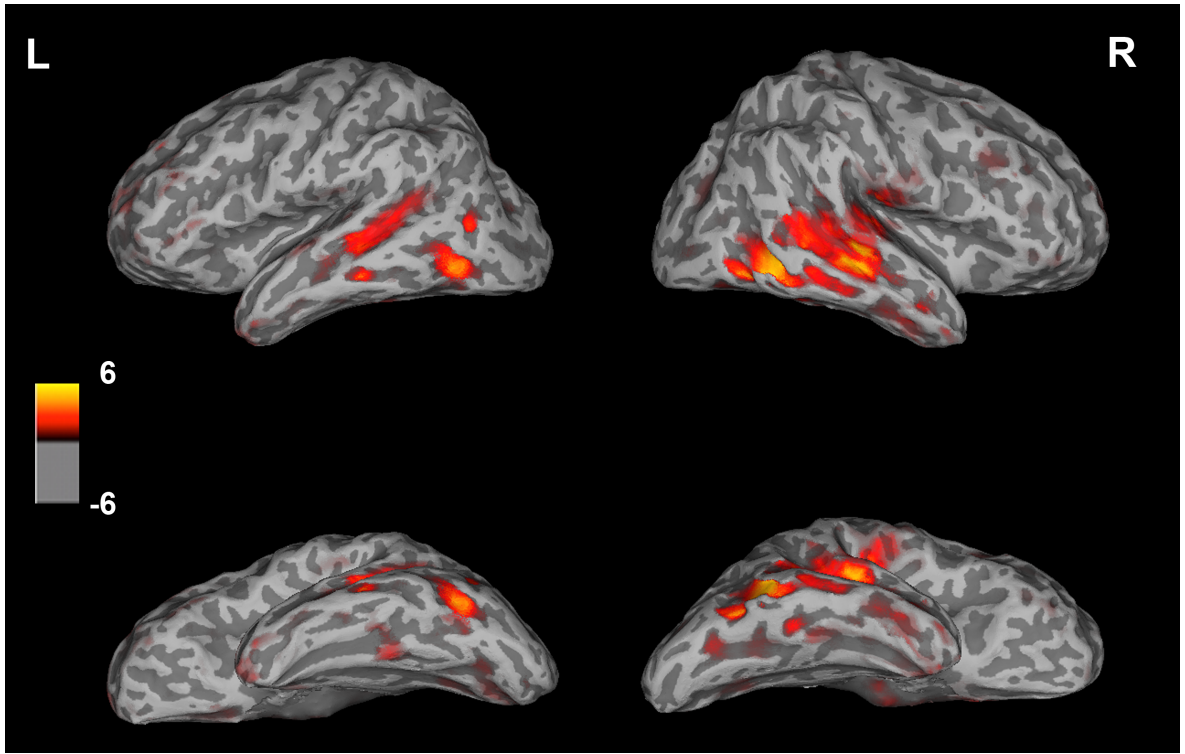


Figure 2.3.2: Results of whole brain group analysis (N=14) for the dynamic angry versus static angry condition projected onto the surface of an inflated standard brain, showing both lateral and ventral views (L=Left; R=Right). Activation is shown bilaterally in middle occipital gyri, middle temporal gyri, superior temporal sulci, as well as the right insula and right amygdala. Colour bar denotes T-statistic and images are thresholded at $p < .05$ corrected for multiple comparisons.

2.3.3 Regions of interest analysis

In comparing the dynamic and static conditions within the left and right inferior occipital gyri no significant differences were found in the amount of signal change, i.e. both conditions exhibited a similar response pattern for all faces. In both the left and right superior temporal sulci there was a significant main effect of motion, showing a significantly greater increase to dynamic faces, $F(1, 13) = 22$, $p < .05$ and $F(1, 13) = 6.63$, $p < .05$ respectively, but a main effect of affect was not revealed. On the other hand, the effect of motion was

Table 2.5: Brain regions showing significant activations in response to dynamic angry compared to dynamic speech facial displays. Coordinates indicate local maxima in Talairach space. L = Left; R = Right. Multiple peaks within a cluster are shown on subsequent lines.

Region	Cluster Size	Z score	x, y, z
R Insula (BA 13)	37	4.77	34, 4, 12
L Insula (BA 13)	40	4.28	-40, 0, 8
R Postcentral gyrus (BA 2)	28	4.19	48, -30, 34
R Inferior frontal gyrus (BA 44)	37	4.12	50, 2, 14
R Postcentral gyrus (BA 7)	§8	4.10	20, -48, 66
R Amygdala	17	3.89	20, -8, -16

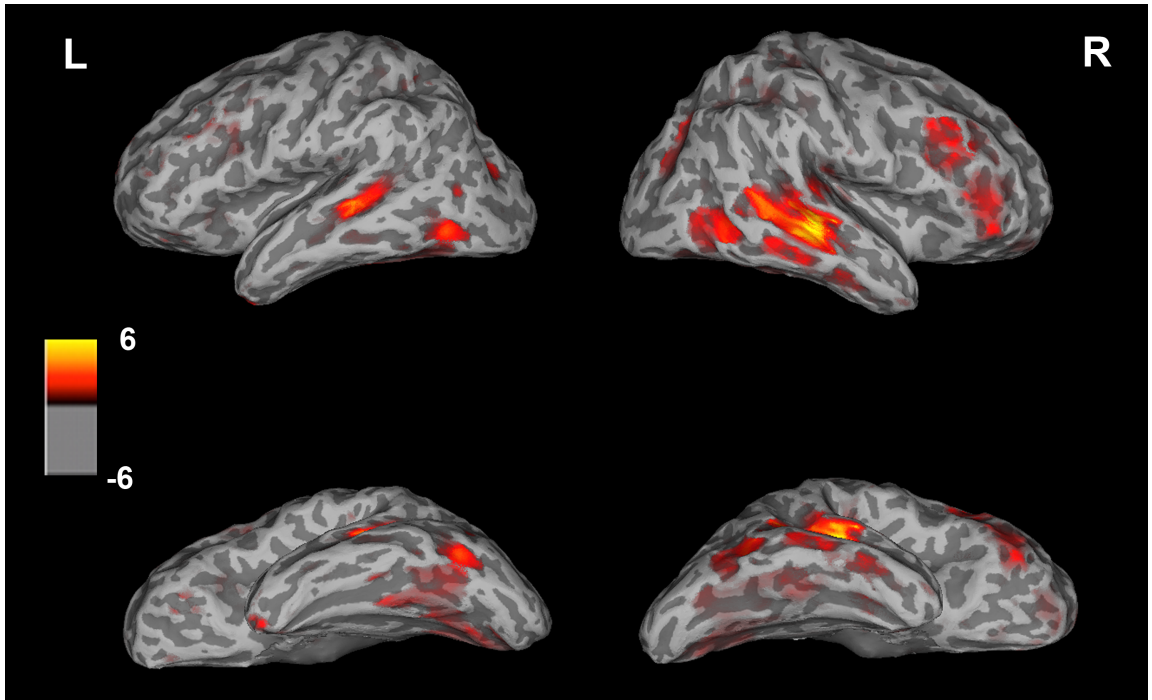


Figure 2.3.3: Results of whole brain group analysis (N=14) for the dynamic happy versus static happy condition projected onto the surface of an inflated standard brain, showing both lateral and ventral views (L=Left; R=Right). Activation is shown in left middle occipital gyrus, left fusiform gyrus, right middle temporal gyrus and bilateral superior temporal sulci. Colour bar denotes T-statistic and images are thresholded at $p < .05$ corrected for multiple comparisons.

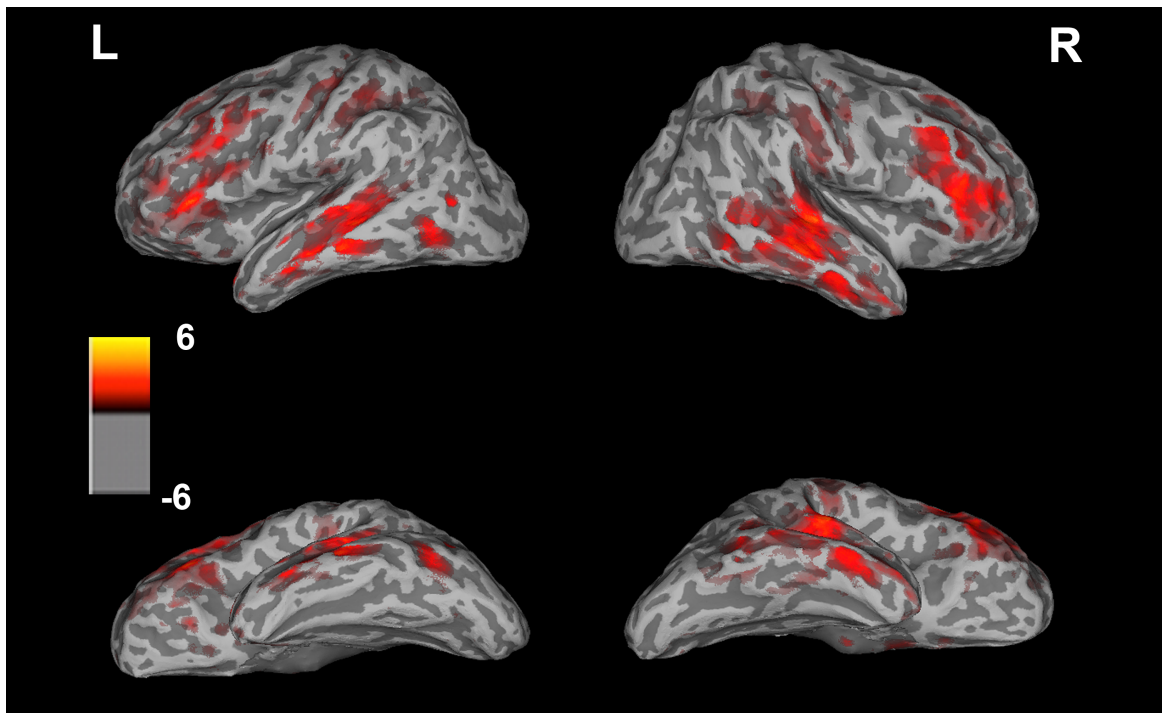


Figure 2.3.4: Results of whole brain group analysis (N=14) for the dynamic speech versus static speech condition projected onto the surface of an inflated standard brain, showing both lateral and ventral views (L=Left; R=Right). Activation is shown bilaterally in middle occipital gyri, middle temporal gyri, superior temporal sulci and middle frontal gyri, and in right precentral gyrus and left inferior frontal gyrus. Colour bar denotes T-statistic and images are thresholded at $p < .05$ corrected for multiple comparisons.

Table 2.6: Brain regions showing significant activations in response to dynamic happy compared to dynamic speech facial displays. Coordinates indicate local maxima in Talairach space. L = Left; R = Right. Multiple peaks within a cluster are shown on subsequent lines.

Region	Cluster Size	Z score	x, y, z
L inferior frontal gyrus (BA 9)	48	4.98	-54, 8, 18
R inferior frontal gyrus (BA 44)	36	4.63	50, 6, 18
L Middle occipital gyrus (BA 19)	66	4.46	-54, -68, -10
R Middle occipital gyrus (BA 18)	54	4.38	30, -78, 4
L Fusiform gyrus (BA 37)	24	3.75	46, -64, -8

not significant in neither the left nor right amygdalae, but there was a significant main effect of affect, $F(2, 26) = 9.92$, $p < .05$ and $F(2, 26) = 3.99$, $p < .05$, respectively.

In the left amygdala post hoc contrast tests revealed that there was no significant difference between the angry and happy conditions, whereas there was a significantly greater increase in signal strength to displays of anger relative to speech, $F(1, 13) = 20.71$, $p < .05$, and happy expressions relative to speech $F(1, 13) = 7.33$, $p < .05$. Similarly in the right amygdala post hoc contrast tests revealed that there was a significantly greater increase for angry expressions compared to speech, $F(1, 13) = 4.68$, $p < .05$, and happy expressions relative to speech, $F(1, 13) = 5.74$, $p < .05$, but no significant differences in signal change between the angry and happy conditions. Thus similar bilateral responses were observed in the left and the right amygdalae, where they exhibited greater responses to angry and happy expressions relative to speech. In the left and right inferior frontal gyri no significant differences were found for motion.

No significant differences were found for motion in bilateral inferior frontal gyri. However, there was a significant main effect of emotion in the right inferior frontal gyrus, $(F(2, 26) = 4.60$, $p < .05$, but not in the left inferior frontal gyrus. Post hoc contrast tests of the response in right inferior frontal gyrus revealed a significantly greater increase in signal strength for angry expressions compared to speech $F(1, 13) = 6.73$, $p < .05$, and happy expressions compared to speech $F(1, 13) = 5.36$, $p < .05$. In sum, superior temporal sulci and amygdalae showed sensitivity to motion and affect respectively, while the inferior occipital gyri and left inferior frontal gyrus did not. Right inferior frontal gyrus however, showed an increased response to affective facial displays (see Figure 2.3.5 and Table 2.7 for a list of ROI locations).

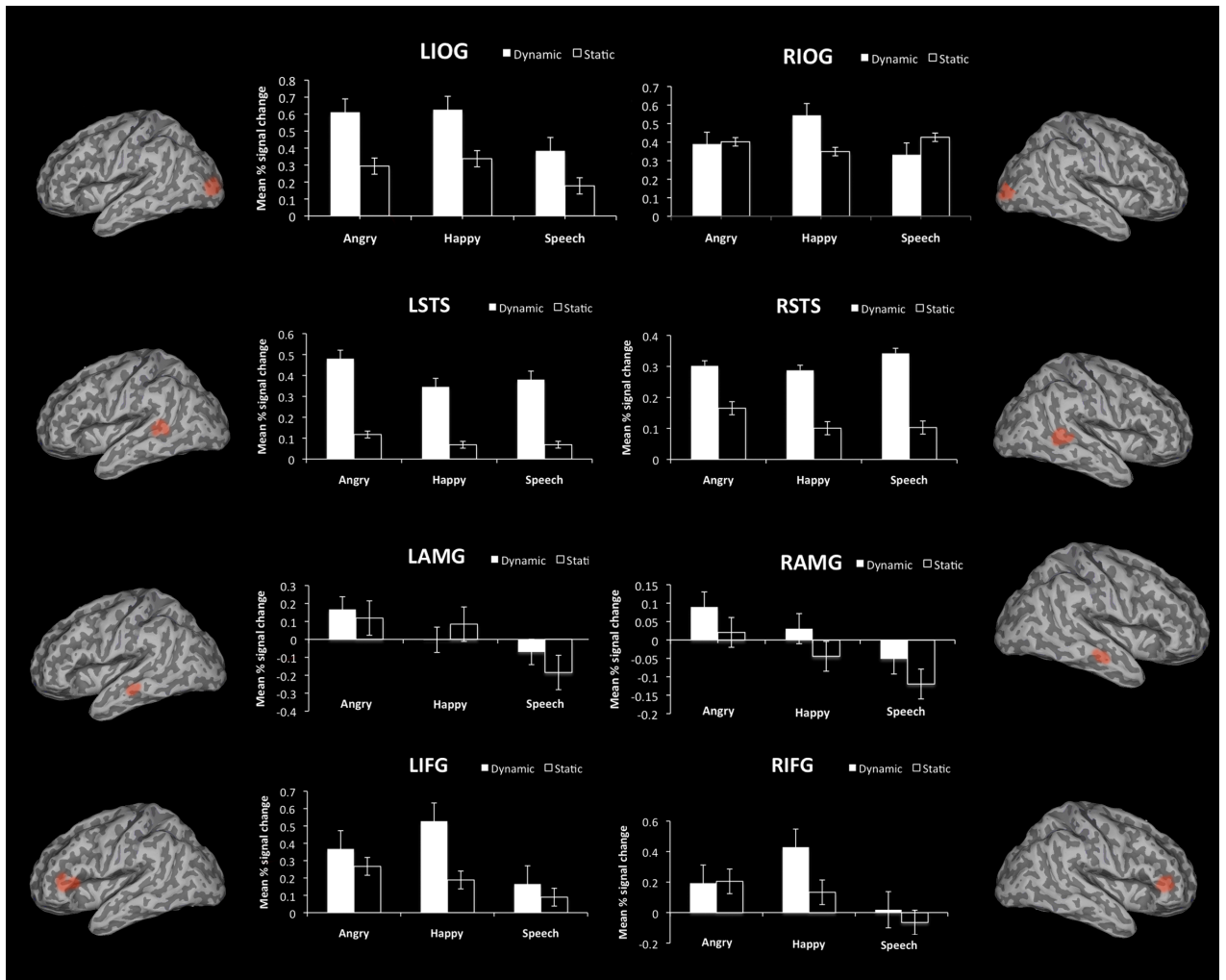


Figure 2.3.5: Regions of interest analysis shows mean percent signal change in left (L) and right (R) inferior occipital gyri (IOG), superior temporal sulci (STS), amygdalae (AMG) and inferior frontal gyri (IFG). White bars indicate the dynamic stimulus condition and black bars denote the static stimulus condition, error bars indicate standard error of mean.

2.4 Discussion

2.4.1 The common neural substrates of dynamic face perception

In this study a unique set of dynamic face stimuli were created in order to obtain examples of naturalistic facial expressions. These were then used to investigate brain activation in response to dynamic facial expressions of emotion, including angry, happy and speech facial displays. Dynamic face stimuli have previously been shown to activate regions in the dorsal pathway of the face perception network, such as regions along MTG and STS, along with regions in the extended system, such as the amygdala and IFG (Kilts et al., 2003; LaBar et al., 2003; Sato et al., 2004; Fox et al., 2009). Thus, it was predicted that the dynamic facial expressions used in the present study would elicit activation in similar regions along this dorsal pathway and also recruit regions in the extended system.

Table 2.7: Location of regions of interest within the face perception network. Coordinates are presented in Talairach space. L = Left; R =Right. N indicates the number of subjects who showed significant activation in each region. Standard error of the means are indicated in parentheses.

Region	N	Mean Coordinates		
		x	y	z
L Inferior occipital gyrus	14	-42 (2)	-84 (1)	-2 (3)
R Inferior occipital gyrus	14	40 (3)	-80 (2)	-4 (2)
L Superior temporal sulcus	14	-52 (2)	-54 (2)	12 (1)
R Superior temporal sulcus	14	52 (2)	-54 (1)	12 (1)
L Amygdala	12	-22 (2)	-6 (1)	-18 (2)
R Amygdala	13	20 (2)	-6 (2)	-18 (2)
L Inferior frontal gyrus	8	-46 (3)	18 (2)	22 (2)
R Inferior frontal gyrus	10	52 (3)	26 (3)	18 (2)

As expected, enhanced activation patterns in bilateral middle temporal gyrus, including area V5/MT, and extending along bilateral STS, were found for the perception of all dynamic facial expressions compared to their static counterparts, irrespective of the specific facial expression. Previous studies of motion perception have shown consistent activation of area MT in response to general motion processing, whereas STS shows a greater response to biological motion in particular (Beauchamp et al., 2002). In a recent meta-analysis of the fMRI literature on human motion perception, Grosbras et al. (2012) found that regions in bilateral middle temporal gyrus and STS were significantly activated across a range of studies on face movement perception.

While the STS has been implicated in biological motion perception it has also been associated more broadly with social communication (Allison et al., 2000). The posterior STS appears to be particularly sensitive to the dynamic aspects of a face, showing increased activation during the perception of eye and mouth movements (Puce et al., 1998), gaze discrimination (Hoffman and Haxby, 2000) and facial expression processing of static (Engell and Haxby, 2007) and dynamic stimuli (Kilts et al., 2003; LaBar et al., 2003; Sato et al., 2004). Further examination of the activation within bilateral STS, through analysis of the percent signal change, revealed that the STS showed sensitivity specifically to motion but not to affect. This was further confirmed by the absence of activation in the STS for the direct contrasts of both dynamic angry, and dynamic happy facial expressions with dynamic speech displays. Thus STS activations are not specifically related to the perceptions of emotion, but appear to be involved in general processing of dynamic social signals (Kilts et al., 2003), which supports the proposed role of the STS in socially

valenced motion perception (Grosbras et al., 2012).

According to Haxby et al.'s model, prior to processing in the STS, the first stage in the face perception process occurs in a region in inferior occipital gyrus, often referred to as the occipital face area, where an early structural description of a face is computed. Converging evidence from lesion and transcranial magnetic stimulation (TMS) studies provides support for the notion that the occipital face area is an essential component in the cortical face perception network (Rossion et al., 2003; Pitcher et al., 2008). However, while the occipital face area is believed to play a role primarily in early visual structural processing of faces, it has recently been implicated in higher level face processing.

For example, Pitcher et al. (2008) found that TMS delivered over the right occipital face area impaired facial expression discrimination, but interestingly not identity discrimination, which suggests that the occipital face area is involved in facial expression processing. Furthermore, Schultz and Pilz (2009) report increased activation in left inferior occipital gyrus in response to dynamic relative to static faces. However, in the present study the neural responses to dynamic and static facial expressions were not significantly different in bilateral inferior occipital gyri, which is more consistent with the view that the inferior occipital gyri represent the invariant properties of a face and thus are sensitive to faces in general, regardless of motion or facial display (Haxby et al., 2000; Pitcher et al., 2011b). In the extended face perception system then, dynamic facial expressions elicited increased activation in the right amygdala. Although this effect may be primarily driven by the dynamic angry facial expressions as shown by both of the dynamic angry contrasts (i.e. dynamic versus static angry expressions and dynamic angry versus dynamic speech displays). Previous neuroimaging studies have reported increased amygdala activation to dynamic facial expressions (LaBar et al., 2003; Sato et al., 2004, 2010; Trautmann et al., 2009) suggesting that dynamic stimuli may be more effective in engaging the amygdala during face perception tasks (LaBar et al., 2003). However, while the amygdala showed significantly greater activation for dynamic expressions in the whole brain analysis, further interrogation of the amygdala response through analysis of the percent signal change revealed that bilateral amygdalae were sensitive to affect in general (i.e., angry and happy expressions). This was revealed by a significant increase in the amygdala response to angry and happy expressions but not to speech, regardless of motion.

This is consistent with previous studies showing greater amygdala activation to emotional expressions in general (Breiter et al., 1996; Morris et al., 1996), and lesion studies showing that patients with bilateral ablation of the amygdala are impaired at processing facial affect (Young et al., 1995). Hence the amygdala may act as a multiprocessor of socially salient information, particularly from the face, where it is sensitive to affects with naturalistic facial motion. The difference in results between the whole brain analysis and the region of interest analysis may be due to a number of factors. The regions of interest analysis may be more sensitive as the regions are identified individually for each participant, which eliminates the between subject variation that is present in whole-brain group analysis. In addition, the multiple comparisons problem is greatly reduced in ROI analyses as a much smaller number of tests are being performed compared to testing all voxels in the brain, which allows more sensitive thresholds to be used in ROI analyses (Saxe et al., 2006).

In the extended system, frontal regions including bilateral inferior frontal gyri, bilateral middle frontal gyri and right precentral gyrus were significantly activated in response to dynamic faces. Middle frontal gyrus (BA 6; supplementary motor area) and precentral gyrus (BA 6) have been implicated in action observation and imitation and are believed to form part of the human mirror neuron system (Iacoboni et al., 1999). The mirror neuron system provides an action recognition mechanism through imitation and learning, whereby sensory representations of action are transformed into corresponding motor programmes (Rizzolatti and Craighero, 2004). Recent studies have shown activation in the mirror neuron system during passive observation of mouth, hand or foot movements (Buccino, 2004) and during passive observation of dynamic facial expressions of emotion (Kilts et al., 2003; Sato et al., 2004). Further evidence in support of the role of the mirror neuron system in emotion recognition comes from lesion studies where patients with lesions in frontal cortex show impairment in the recognition of emotional stimuli (Adolphs, 2002b). Previous face perception studies have implicated the inferior frontal gyrus, which is part of the extended face perception system, in processing static facial expressions (Ishai et al., 2005) as well as dynamic facial expressions (Kilts et al., 2003; Schultz and Pilz, 2009; Trautmann et al., 2009). Furthermore, Pitcher et al. (2011a) and Fox et al. (2009) found increased activation in inferior frontal gyri in response to dynamic facial expressions relat-

ive to static. In the present study bilateral inferior frontal gyri showed significantly greater activation to dynamic relative to static faces in the whole brain subtractive analysis. However, examination of the percent signal change in bilateral inferior frontal gyri did not show a significant effect of motion. Interestingly, a main effect of emotion was found in right inferior frontal gyrus only, where there were significantly greater responses to the affective stimuli, angry and happy, relative to speech regardless of motion. Additionally, when both of the affective displays (dynamic angry and dynamic happy) were contrasted with dynamic speech displays significant activation was found in inferior frontal gyri. This suggests enhanced processing of dynamic affective expressions in regions of inferior frontal gyri.

2.4.2 Distinct neural substrates associated with the perception of different dynamic facial expressions

In the previous section the common neural substrates for the perception of all of the dynamic facial expressions were described, involving middle temporal gyrus, superior temporal sulcus, amygdala and inferior frontal gyrus. Planned pairwise comparisons were computed to investigate the effects of motion on the processing of different face stimuli by explicitly contrasting dynamic and static stimuli for each of the different affects. In addition, the effects of emotion-specific facial dynamics were examined by contrasting each of the dynamic affective stimuli with the dynamic speech stimuli. In this context, the dynamic speech stimuli represented dynamic neutral stimuli as they contained neutral expressions without an emotional component and were thus used to control for general facial motion responses.

Furthermore, a motion capture technique was used to ensure that all of the dynamic stimuli contained similar amounts of motion. This control measure was used to ensure that any differences in neural responses to the different facial affects identified with fMRI, would be due to differences in the type of affect specific motion, not the amount of motion per se. Based on previous research showing dissociable systems involved in processing emotional facial expressions it was predicted that dynamic angry and happy facial expressions may recruit distinct regions of the extended face perception system relative to speech (Kilts et al., 2003; Sato et al., 2004; Trautmann et al., 2009).

The direct comparison of dynamic and static angry expressions revealed significant activation bilaterally in the core system, in the middle occipital gyri extending into the MTG and STS. Significantly greater activation was also found in the extended system, in the amygdala and insula, in response to dynamic angry expressions. The contrast of dynamic angry versus dynamic speech facial displays also revealed significant activation in the amygdala and insula, as well as in postcentral and inferior frontal gyri. The persistence of these activations in the amygdala and insula suggests that these activations are specifically related to the processing of dynamic angry expressions and not attributable to general motion processing. Taken together these results imply that the regions of the core system are involved in general motion processing while the amygdala, insula and regions of prefrontal cortex are specifically involved in processing the affective information from dynamic angry expressions.

Previous neuroimaging studies have reported increased amygdala activation to both static angry and dynamic angry expressions (Kilts et al., 2003; LaBar et al., 2003; Sato et al., 2004). Kilts et al. (2003) also reported increased activation in a similar set of regions when they contrasted dynamic and static angry expressions using PET. The insula is believed to play an important role in emotion perception through its projections to the inferior prefrontal cortex and amygdala, and it modulates amygdala activity by relaying signals from cortical regions through efferent pathways (Phelps et al., 2001). While the insular cortex is known to be involved in emotional processing, it has generally been associated with the processing of expressions of disgust (Phillips et al., 1997; Wicker et al., 2003).

However, Fusar-Poli et al. (2009) carried out a meta-analysis of over one hundred fMRI studies of emotional face processing and report insula activation to angry facial expressions in static images as well as to expressions of disgust. It has recently been proposed that the insula may act as a relay centre between action and emotion areas during the observation of action (Montgomery and Haxby, 2008). In this case, it may be that the dynamic angry stimuli evoke neural activation patterns in the right insula which then modulates activity in the right amygdala to facilitate emotion processing.

Compared to static displays, the perception of happiness in dynamic expressions was once again associated with increased activation in the core system in right middle temporal gyrus extending into STS and in the left middle occipital gyrus and STS. Similarly, Kilts

et al. (2003) reported increased activation in visual regions in temporal and occipital gyri in response to dynamic happy facial expressions relative to static. Furthermore a cluster was identified in the left fusiform gyrus, which showed significant activation in response to dynamic happy facial expressions. The contrast of dynamic happy facial expressions with dynamic speech facial displays also revealed significant activation in the fusiform gyrus, as well as in middle occipital gyri and inferior frontal gyri.

The persistence of activation in the fusiform gyrus suggests that it is involved specifically in processing the happy facial expressions rather than in general structural or motion processing. This is consistent with Trautmann et al. (2009) who also reported increased activation in the fusiform gyrus in response to dynamic happy facial expressions. Furthermore, Hennenlotter et al. (2005) have reported increased fusiform activation to dynamic stimuli of smiling faces relative to dynamic neutral faces. Previous studies of dynamic face perception have reported increased fusiform activation to different dynamic face stimuli (LaBar et al., 2003; Sato et al., 2004; Fox et al., 2009; Schultz and Pilz, 2009), however in the present study increased fusiform activation was only found for dynamic happy expressions. Again the increased activation in inferior frontal gyrus in response to dynamic happy facial expressions is consistent with its proposed role in affective face processing (Fairhall and Ishai, 2007; Ishai, 2008).

When dynamic speech displays were directly contrasted with static speech displays significant activation was again found in the core system in bilateral middle occipital gyrus, MTG and STS. Significant activation was also found in regions of the extended system including, bilateral middle frontal gyrus (BA 6, 8, 9), left inferior frontal gyrus (BA 6) and right precentral gyrus (BA 9) for dynamic speech displays. These results are similar to those obtained by Campbell et al. (2001) where they contrasted dynamic stimuli displaying lip movements with still faces. These regions of premotor and supplementary motor areas are believed to form part of the mirror neuron system. Thus the processing of dynamic displays of speech relative to static appears to elicit greater activation in regions associated with the mirror neuron system.

Taken together these results reveal a common core system, including middle occipital gyri, middle temporal gyri and superior temporal sulci, that is involved in processing all of the dynamic facial expressions. However there appears to be differences between activation

patterns for each of the different dynamic facial expressions, particularly in regions of the extended system. For example, processing of dynamic angry facial expressions involves the amygdala and insula, whereas processing of dynamic happy expressions is associated with greater fusiform activation, and dynamic speech perception relies on regions of premotor and supplementary motor areas. This suggests that partly dissociable neural networks are involved in processing different dynamic facial expressions of emotion (Hennenlotter and Schroeder, 2006).

2.4.3 Summary

In conclusion, these findings extend Haxby et al.'s (2000) model to include naturalistic dynamic facial motion. A dynamic face perception network has emerged (see Figure 2.3.1), comprising early visual regions, such as IOG, which is insensitive to motion or affect but sensitive to the visual stimulus. The STS, which is specifically sensitive to motion, and the amygdala in the extended system, which is recruited to process affect. Notably, functional dissociations were found within the STS and the amygdala, where the STS is sensitive to facial motion regardless of affect and conversely the amygdala is sensitive to facial affect regardless of motion. However, the amygdala showed a trend towards increased activation for dynamic angry expressions.

Frontal regions in the extended system are involved in additional face processing, where IFG is involved in processing the affective information from dynamic facial expressions of emotion. Furthermore, different activation patterns were reported for each of the different dynamic facial expressions where processing of dynamic angry facial expressions involves the amygdala and insula, whereas processing of dynamic happy expressions is associated with greater fusiform activation, and dynamic speech perception relies on regions of premotor and supplementary motor areas. This suggests that partly dissociable neural networks are involved in processing different dynamic facial expressions of emotion (Hennenlotter and Schroeder, 2006).

Chapter 3

Connectivity analysis of the dynamic face perception network

3.1 Introduction

3.1.1 Overview

This chapter will assess connectivity within the dynamic face perception network. The effective connectivity within the distributed face perception system will be examined with realistic dynamic facial expressions of emotion. In the previous chapter fMRI was used to examine specific regional effects related to dynamic face processing. A dynamic face perception network was identified which extends Haxby et al. (2000)'s distributed neural system for face perception. This network includes early visual regions, such as IOG, which is insensitive to motion or affect but sensitive to the visual stimulus. The STS, which is specifically sensitive to motion, the amygdala in the extended system, which is recruited to process affect, and frontal regions which are recruited for additional affective processing.

However, while this level of investigation localised the function of the components of the dynamic face perception network quite well, it did not explicitly measure the relationships between these brain regions. Beyond identifying the functional properties of each individual node in a network, it is also important to understand their connections in order to fully characterise face processing in the brain (Wiggett and Downing, 2008). Thus, it is important to assess how, and to what extent the face perception network is func-

tionally integrated (Said et al., 2011). Functional integration is usually inferred on the basis of correlations among measurements of neuronal activity through different forms of connectivity analysis (Friston, 2009). Studies of neural functional integration, using both functional and effective connectivity measures have revealed interesting new findings about the functional connections of specific brain regions and networks, and provide important new insights in to the overall organisation of functional communication in the human brain (Friston, 2009). These studies will be discussed in detail in the following sections.

3.1.2 Functional connectivity within the distributed face perception network

In recent years an increasing number of neuroimaging studies have explored neural functional connectivity by measuring the level of co-activation of resting-state fMRI time-series between different brain regions. This fMRI technique measures spontaneous, low-frequency (< 0.1 Hz) BOLD signal fluctuations while participants are at rest (i.e. performing no explicit task). A number of so-called resting-state networks have been reported (e.g., visual, auditory, somatomotor, default, attention) where temporal correlations in the BOLD signal of distributed brain regions were found (Biswal et al., 1995; Greicius et al., 2003; Fox et al., 2005, 2006). These temporal correlations are presumed to reflect the intrinsic functional connectivity among anatomically related discrete regions within these neural networks. Essentially this means that brain regions that are generally activated in unison during tasks will also display temporal coherence in their spontaneous activity while at rest (Corbetta et al., 2008).

Recently Zhang et al. (2009) used resting state functional connectivity analysis to examine whether regions of the distributed face perception network maintain a significant degree of temporal coherence in their spontaneous activity in the resting state (i.e. in the absence of any external stimulation). They did this by comparing the resting state functional connectivity of the face perception network with the active state during passive viewing of static objects and faces. Whole brain functional connectivity MRI analysis revealed that the functional connectivity between regions in the core face perception system (i.e. IOG, FG and STS) was similar during rest and while passively viewing faces. However

the functional connectivity among regions in the extended system was modulated by the passive viewing task. They therefore conclude that the regions of the core but not the extended face perception network are functionally connected in the resting state.

Turk-Browne et al. (2010) also examined resting connectivity within the face perception network but primarily focused on assessing the intrinsic connectivity between the FG and the STS. Based on evidence showing that both the FG and STS are key structures involved in face processing, Turk-Browne et al. (2010) suggest that the relationship between these two regions may in fact be the most important connection in any larger network. They used localiser scans, where participants were presented with static pictures of faces and scenes, to define specific regions of interest for each participant in right FG and posterior STS, along with a control region in parahippocampal cortex. The activation time series in these regions were then compared while at rest, having controlled for confounds such as sources of whole-brain noise.

Consistent with their predictions, Turk-Browne et al. (2010) found significant resting correlations between FG and posterior STS. Zhang et al. (2009) also observed significant resting connectivity between FG and STS, which provides converging evidence for the existence of resting state functional connectivity between these two regions. This has important implications for models of face perception such as Haxby et al's model which proposes distinct pathways for the visual analysis of facial identity occurring in the FG and expression analysis in the STS, as it suggests that these pathways are only partially segregated (Said et al., 2011; see chapter 2).

3.1.3 Effective connectivity analysis of the face perception network

The previous studies on face-related resting state functional connectivity provide valuable information on the baseline intrinsic connectivity of the face perception network (Turk-Browne et al., 2010). However, they do not provide any direct insight into how these face-specific connections are modulated by external stimulation. Measures of effective connectivity, such as dynamic causal modelling (DCM) or psychophysiological interaction (PPI) analysis, are required for this level of investigation. DCM treats the brain as an input-state-output system, whereby the neural activity in a given region (output)

is characterised in terms of driving inputs, such as face stimuli, combined with intrinsic connections and task-related modulations of connectivity with other brain regions (Friston et al., 2003). Face perception studies using DCM analysis have demonstrated that different tasks and face stimuli can influence the coupling among face-selective regions (Fairhall and Ishai, 2007). For example, Mechelli et al., 2004 used DCM to investigate changes in neuronal interactions between occipito-temporal cortex and prefrontal cortex during two different cognitive tasks, specifically passive viewing and visual imagery of faces and objects. They found that during visual perception of faces there was an increase in feed-forward connectivity from early visual regions to occipito-temporal cortex, whereas there was an increase in effective connectivity from prefrontal cortex to occipito-temporal cortex during visual imagery of faces.

Similarly, Summerfield et al. (2006) reported patterns of differential connectivity between prefrontal cortex and face-sensitive visual areas during a perceptual decision task. They found that perceptual decisions about faces were associated with a significant increase in effective connectivity between ventral medial frontal cortex and the FG and amygdala, but there was no significant effect of bottom-up modulation from FG or amygdala to the frontal cortex during the same task. Rotshtein et al. (2007) also used DCM to examine changes in connectivity in the face perception network across different stimulus conditions. They focused on the differential effects of high and low spatial frequency properties of face stimuli on the coupling among regions of occipito-temporal cortex. Interestingly, they found that low spatial frequency faces were associated with a significant increase in connectivity between middle occipital gyrus and FG. Whereas visual processing of high spatial frequency faces was associated with an increase in connectivity between inferior occipital gyrus, inferior temporal gyrus and the FG. They conclude from this that different regions in occipito-temporal cortex are sensitive to different visual cues, whereby high and low spatial frequency information from face stimuli are processed separately and then converge in the FG for integration.

Furthermore, a recent DCM study by Fairhall and Ishai (2007) demonstrated that the effective connectivity between the FG and various regions of the face perception network was modulated by different types of static face stimuli. They presented photographs of unfamiliar, famous and emotional faces in a passive viewing task and found that all

faces exerted a strong and significant influence on the effective connectivity between IOG and both FG and STS. Emotional and famous faces significantly modulated the coupling between IOG and FG, but not between IOG and STS. They also found that the FG exerted influences on the amygdala, inferior frontal gyrus and orbitofrontal cortex. They concluded from this that the extraction of the changeable aspects of face stimuli, within limbic and prefrontal regions, is enabled via the FG in the ventral pathway rather than the STS. However this may be due to the fact that static images of faces were used, indeed the authors themselves predict that the STS in the dorsal pathway would exert a greater effective influence on the extended system during the perception of dynamic faces.

PPI analysis is another form of connectivity analysis that has been used to assess face-related changes in effective connectivity among regions of the face perception network (Das et al., 2005; Nummenmaa et al., 2009). PPI analysis measures how activity in a particular brain region of interest modulates activity in other brain regions, in response to an experimental condition (Friston et al., 1997). It has an advantage over DCM analysis because it does not require prior specification of the anatomical model. Rather a ‘source’ or ‘seed’ region is selected and regions of interaction with this ‘source’ are identified based on the experimental condition. This allows effects throughout the whole brain to be assessed rather than being limited to specific regions of interest.

In a recent study, Nummenmaa et al. (2009) used PPI analysis to identify brain regions showing changes in effective connectivity with regions of the core face perception network, when viewing eye gaze shifts relative to control eye movements. Haxby et al.’s model predicts that the STS would be primarily involved in gaze perception, while other regions such as the FG and IOG would not. By selecting three ‘seed’ regions in the core face perception system, in IOG, FG and STS, they tested these predictions by assessing the extent to which these regions are involved in gaze perception. As predicted they found significant correlations between the STS and MT/V5, intraparietal sulcus, frontal eye fields, superior temporal gyrus, supramarginal gyrus, and middle frontal gyrus. Consistent with Haxby et al.’s model, they did not find any significant changes in connectivity with the IOG and other brain regions as a function of gaze. However, the FG did show significant correlations with the superior temporal gyrus and middle frontal gyrus, demonstrating the contribution of both dorsal and ventral core face areas to gaze perception.

3.1.4 Objectives and hypotheses

Taken together these connectivity analysis studies of face perception have shown interesting task-specific modulations of the effective connectivity within the face perception network. However, all of them have used impoverished static face stimuli, thus little is known about the effective connectivity of the dynamic face perception network. This will be examined in the present study, through the use of PPI analysis. By choosing 'source' regions in the core (IOG and STS) and extended systems (amygdala and IFG) the effective connectivity within Haxby et al.'s (2000) distributed face model can be examined with realistic dynamic facial expressions of emotion.

The data used in this analysis are the same as that used in the previous fMRI chapter 2, thus the stimuli consist of dynamic and static angry, happy and speech facial displays. Preplanned comparisons were computed to assess the effective connectivity within the dynamic face perception network related to the following contrasts of interest: all dynamic versus all static faces, dynamic angry versus static angry facial expressions, dynamic happy versus static happy facial expressions, dynamic speech versus static speech facial displays, dynamic angry versus dynamic speech displays, and dynamic happy versus dynamic speech displays.

It is hypothesised that PPI analysis will reveal correlations between early visual regions such as IOG and regions in the dorsal pathway, such as the STS, in response to dynamic face stimuli. It is also predicted that activation in STS will be correlated with regions in the extended network such as the amygdalae and IFG when viewing dynamic facial expressions of emotion only. Furthermore, the regions beyond the distributed face perception network that are implicated in processing dynamic facial displays will be examined, in a hypothesis generating fashion, using PPI analysis. Based on the results from chapter 2 it is predicted that the different facial expressions will exhibit different effective connectivity patterns within the dynamic face perception network.

During the perception of dynamic angry facial expressions it is predicted that STS and amygdala activation will be correlated. It is further hypothesised that activation in the amygdala will be correlated with the insula, based on anatomical connections between these regions (Phelps et al., 2001; see subsection 2.4.2), to facilitate emotional processing of the dynamic angry face stimuli. It is also predicted that IOG activation will be cor-

related with the FG when processing dynamic happy expressions based on the significant fusiform activation reported in the previous chapter. Finally, it is hypothesised that activation in STS will be correlated with regions of prefrontal cortex around Brodmann area 6, including precentral gyrus, which is known to be involved in speech processing.

An additional form of effective connectivity analysis known as physiophysiological interaction (PYPI) analysis will also be performed on the data. PYPI analysis is distinct from PPI analysis in that it is used to assess how the activity in a particular brain region is modulated by the physiological interaction of two other brain regions, rather than by the interaction between one brain region and an experimental condition. The physiophysiological interaction of brain regions in the core and extended systems of the face perception network will be examined in both left and right hemispheres.

In the core system the interaction between IOG and STS will be examined, along with the interaction between STS and amygdala, and amygdala and IFG in the extended system. Based on the resting state functional connectivity analysis studies by Turk-Browne et al. (2010) and Zhang et al. (2009) it is predicted that IOG and STS activation will be correlated with FG activation. Also based on the results in chapter 2 showing STS and middle temporal gyrus activation to dynamic faces, it is hypothesised that IOG and STS activation will correlate with activation in middle temporal gyrus. Furthermore, it is predicted that STS and amygdala activation will correlate with frontal regions in the extended system.

3.2 Methods

3.2.1 fMRI participants

Fourteen healthy self-reported right-handed volunteers (6 male) with normal or corrected to normal vision (mean age 28.3, S.D. 3.67 years) gave full written informed consent to take part in the study, which was approved by the Aston University Human Science Ethical Committee. These are the same participants as those described in chapter 2.

3.2.2 Experimental design and imaging paradigm

The stimuli and experimental design are the same as those described in chapter 2, but for ease of reading the details will be outlined again here. A sample of twenty-four stimuli (twelve dynamic and twelve corresponding static images) was selected for the fMRI experiment, based on their highest intensity ratings and correctly identified as the target affect as described in chapter 2. Two emotion categories were included, specifically, angry and happy, and a speech category was also included as a control for non-affective facial motion. In the dynamic condition four different stimuli were presented in each of the three emotion categories, and likewise in the static condition. The identities were matched across the dynamic and static conditions, as the static stimuli were created from a screenshot of the final frame of each of the dynamic excerpts including the speech controls. Each stimulus was presented for 3 seconds within a block of eight of the same condition. Hence, there were six different blocks of 24 seconds duration (dynamic angry, static angry, dynamic happy, static happy, dynamic speech and static speech).

A session of length 288 seconds consisted of 24 second blocks of no visual stimulation (fixation cross) alternating with the six 24 second blocks of visual stimulation. Blocks were presented in a pseudo-random order around a Latin squares design within each session, and there were 6 sessions in total (1728 seconds). Participants performed a 1-back memory task on the individual identity within each block, making all responses via the lumina response pad (see Figure 3.2.1). This task was designed to maintain vigilance and to control for attention which is known to modulate BOLD signals in many of the neural areas included in this study (see e.g. Beauchamp et al., 2002).

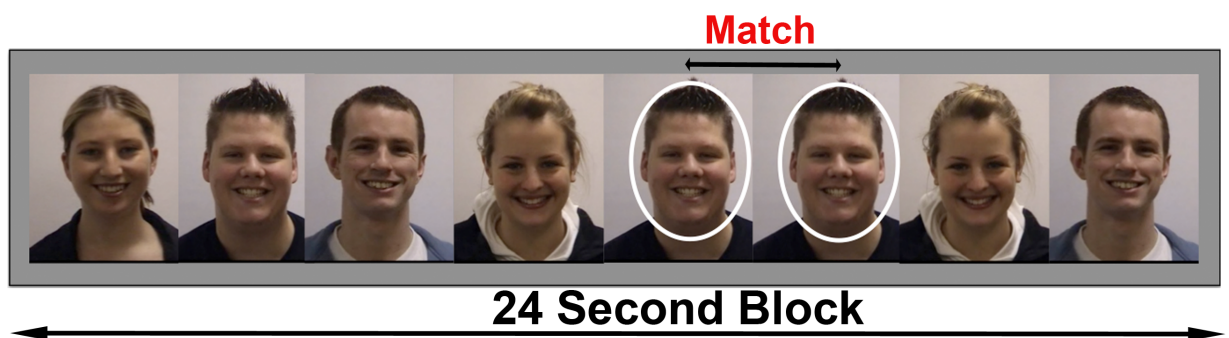


Figure 3.2.1: fMRI experimental design shows 24 s on-block where 8 stimuli were presented for 3 s within each block of the same condition. This alternated with a 24 s block of no visual stimulation (fixation cross). Participants (N=14) performed a 1-back memory task on the individual identity within each block, making all responses via the lumina response pad.

3.2.3 Imaging protocol

As before MR data were acquired on a 3 Tesla Siemens Magnetom Trio Scanner using an 8-channel radio frequency birdcage head-coil. A gradient echo planar sequence (EPI) was used to acquire 44 contiguous 3 mm thick axial slices per whole brain volume in one time series of 576 scans. With the following parameters echo time (TE) = 30 ms, repetition time (TR) = 3000 ms, field of view (FOV) = 192 mm, 64 x 64 pixels per inch matrix, resolution 3 x 3 mm in-plane resolution. A high resolution MPRAGE anatomical image with 1 x 1 x 1 voxel resolution was collected at the end of each scanning session. Visual stimuli were presented using Presentation Software (Neurobehavioral Systems, Inc.) and projected via LCD to a screen located in the back of the scanner bore behind the participant's head. Participants viewed the stimuli through a prism mirror mounted above their eyes on the head coil.

3.2.4 Image analysis

Off-line data processing and analysis were performed using the Statistical Parametric Mapping software (SPM2; Wellcome Department of Cognitive Neurology, London, UK; www.fil.ion.ucl.ac.uk/spm) implemented within Matlab 7. All functional volumes were realigned to the first volume using rigid body transformations (the most accurate function for realignment in SPM2), to correct for any head motion. To facilitate group analysis all functional images were then spatially normalised into standard stereotactic space using the Montreal Neurological Institute (MNI) echo-planar imaging template proposed as default in SPM2, which approximates the standard stereotaxic space of Talairach and Tournoux (1988). Spatially normalised images were resliced to a final voxel size of 3 x 3 x 3 mm and smoothed using 7 mm full-width at half-maximum Gaussian kernel. and a high pass filter of 1/128 Hz was used to eliminate low-frequency components.

Realigned, spatially normalised, and smoothed functional images were analysed voxelwise using SPM2 in the framework of the general linear model (see section 1.5; Friston et al., 1995). A first-level, session-specific analysis was initially performed to accommodate for within-subject, between-scan variability. In the first-level analyses, block onsets were modelled as boxcars convolved with a canonical haemodynamic response function. All data were high-passed filtered with a cut-off frequency of 1/128 Hz to remove low-frequency

signal drifts and a correction for temporal autocorrelation was applied. Contrast images were created to identify voxels showing task-related increases in activity.

As previously described in chapter 2, regions of interest (ROI) were defined for each participant based on the contrast of all faces versus baseline fixation with $p < .001$ uncorrected, and coordinates were verified against previous face perception studies (Haxby et al., 2000; Fairhall and Ishai, 2007). The regions of interest identified were bilateral IOG, STS, amygdalae, and IFG. The time series at the sites of peak activation within each of these regions of interest were extracted for each participant (spherical volumes of 6 mm radius) and subsequently used to assess task-dependent changes in functional connectivity between brain regions using a psychophysiological interaction (PPI) model (Friston et al., 1997).

3.2.4.1 Connectivity analysis

Psychophysiological interaction (PPI) connectivity analyses were carried out separately for each region in both hemispheres, therefore eight separate PPI analyses were conducted in bilateral IOG, STS, amygdalae, and IFG for the contrast of dynamic versus static faces. Firstly, left IOG (-42 -84 -2) was chosen as the source region in order to interrogate the core face perception system under the dynamic and static conditions, followed by the right IOG (40 -80 -4). The time series of activity in the IOG was extracted for each participant, based on a sphere of 6 mm radius centred on the most significant voxel of activation which was specific for each participant. Here the PPI analysis produced an interaction term between the IOG time series and the psychological condition (i.e., dynamic versus static faces). The psychophysiological interaction term, or the “PPI regressor”, was computed as the element-by-element product of the deconvolved extracted IOG time series and a vector coding for the main effect of task condition (Friston et al., 1997). It was necessary to deconvolve the BOLD time series with a model of the haemodynamic response function in order to represent the interaction at the neuronal level (Gitelman et al., 2003).

The PPI regressor was then convolved with the canonical haemodynamic response function and entered into the regression model along with a second regressor P, representing the contrast for the main effect of dynamic versus static faces (i.e., the psychological variable), and a third regressor y, representing the extracted ROI time series (i.e., the

physiological variable). Model estimation was performed and the effect of the interaction term was evaluated using the following contrast [1 0 0], where the first column represents the interaction term, the second represents the psychological variable and the third represents the time series of the source region. This essentially tests for positive slopes of the PPI regressor which identifies the brain areas receiving context-dependent influences from the IOG that were stronger during processing of dynamic than static faces.

The resulting SPM then shows areas with significant differential connectivity to the IOG due to context manipulations. PPI analysis was carried out for each participant and the resulting contrast images were then used to perform a second level random effects group analysis (using a one-sample t test) with a statistical threshold of $p < .001$ (uncorrected) and an extent threshold of 7 voxels per cluster. This same procedure was repeated for all of the other regions of interest, and for the following contrasts; dynamic angry versus static angry expressions, dynamic happy versus static happy expressions, dynamic speech versus static speech facial displays, dynamic angry versus dynamic speech facial displays, and dynamic happy versus dynamic speech displays.

Physiophysiological interaction (PYPI) connectivity analysis was also performed on the data. PYPI analysis is distinct from PPI analysis in that it is used to assess how the activity in a particular brain region is modulated by the physiological interaction of two other brain regions, rather than by the interaction between one brain region and an experimental condition. As with PPI analysis, this analysis was carried out separately for the regions in both hemispheres. PYPI analysis was computed to assess the effect of interaction between the IOG and STS, the STS and amygdala, and finally the amygdala and IFG. The analysis steps are the same as those described for the PPI analysis, but in this case the interaction term is based on the time series extracted from the two source regions (i.e. IOG and STS) rather than one source region and the experimental condition.

3.3 Results

3.3.1 Psychophysiological interaction results

Using psychophysiological interaction analysis (PPI) the effective connectivity between different regions within the face perception network was examined. PPI analysis provides

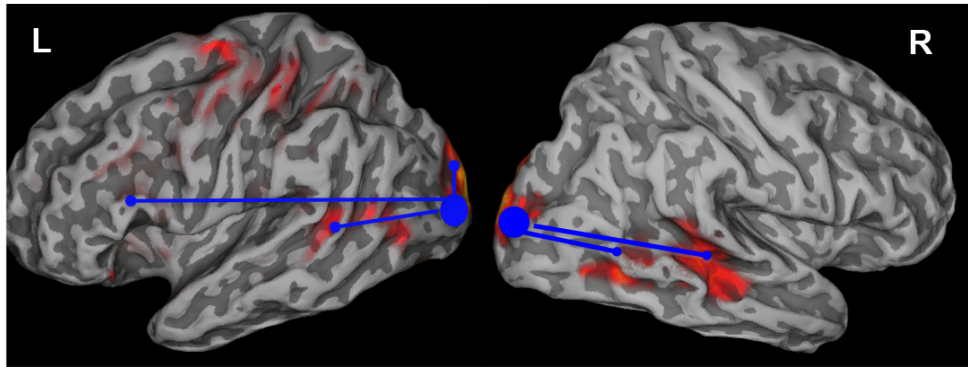
a means of assessing possible interactions between selected regions of interest, within the face perception network, in response to dynamic and static faces. The interpretation of a significant PPI is that there are different engagements of anatomical connections as a function of psychological context, in this case viewing dynamic or static faces (Friston et al., 1997).

3.3.1.1 Inferior occipital gyri

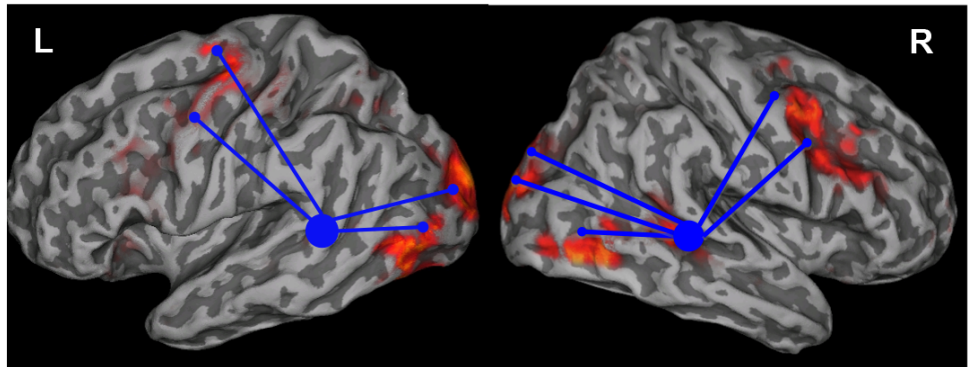
A seed voxel was firstly placed in left IOG (-42 -84 -2; see Table 3.1) and the regions of covariation under the condition of all dynamic faces compared to all static faces were examined. This revealed significant correlations with bilateral STS, left IFG and middle occipital gyrus, along with right middle frontal gyrus, superior frontal gyrus and precentral gyrus, for all dynamic faces compared to all static faces (see Figure 3.3.1 (a) and Table 3.1 A). When the dynamic and static displays of anger were contrasted there were significant correlations between the seed region in left IOG and left precentral gyrus, superior frontal gyrus, STS, lingual gyrus and IFG, along with right middle temporal gyrus and middle frontal gyrus (see Figure 3.3.2 (a) and Table 3.1 B).

The contrast of dynamic happy and static happy expressions revealed significant correlations between left IOG and bilateral middle occipital gyri, and left fusiform gyrus (see Figure 3.3.2 (b) and Table 3.1 C). The contrast of dynamic and static displays of speech revealed significant correlations between left IOG and left STS, middle temporal gyrus and precentral gyrus (see Figure 3.3.2 (c) and Table 3.1 D). The contrast of dynamic angry and dynamic speech displays revealed significant correlations between left IOG and left middle occipital gyrus, left amygdala, right precentral gyrus and bilateral insula (see Table 3.1 E). Finally, the contrast of dynamic happy and dynamic speech facial displays revealed significant correlations between left IOG and bilateral fusiform gyri, bilateral IFG, left middle occipital gyrus, and left middle temporal gyrus (see Table 3.1 F).

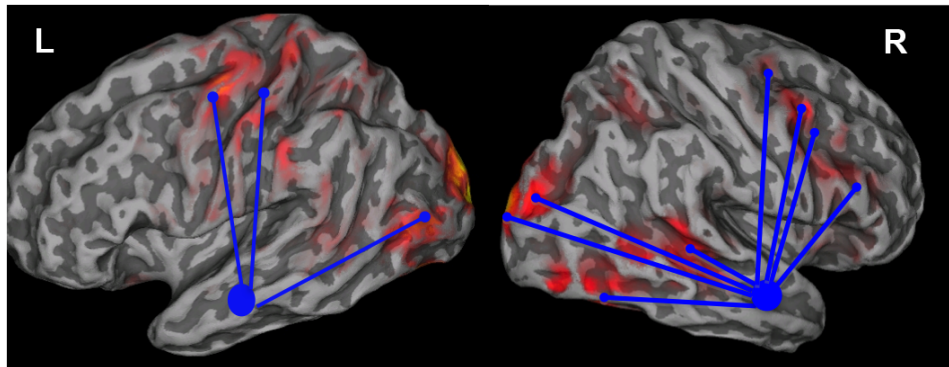
A seed region in right IOG (40, -80, -4; see Table 3.2), was correlated with bilateral middle temporal gyri and STS for the dynamic versus static face contrast (see Figure 3.3.1 (a) and Table 3.2 A). When the dynamic and static displays of anger were compared there were significant correlations between right IOG and right middle occipital gyrus, STS, middle frontal gyrus, and superior frontal gyrus as well as the left superior parietal lobule



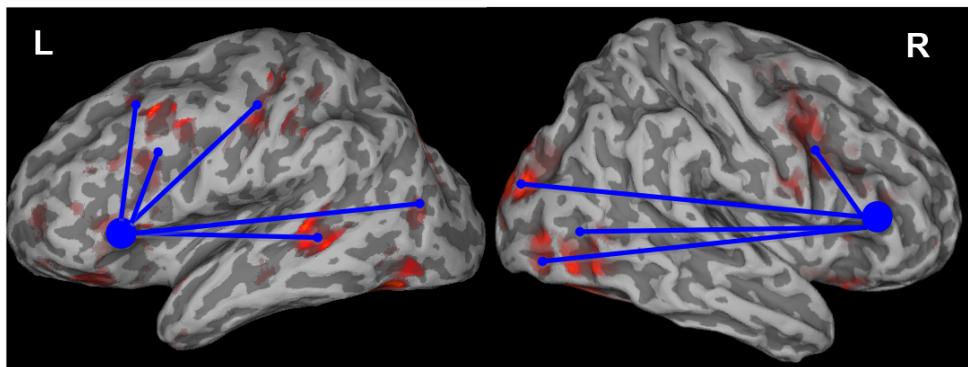
(a) Seed voxels in left (L) and right (R) inferior occipital gyri.



(b) Seed voxels in left (L) and right (R) superior temporal sulci.



(c) Seed voxels in left (L) and right (R) amygdalae.



(d) Seed voxels in left (L) and right (R) inferior frontal gyri.

Figure 3.3.1: Effective connectivity of the four main seed voxels in the dynamic face perception network: (a) Inferior occipital gyri; (b) Superior temporal sulci; (c) Amygdalae; (d) Inferior frontal gyri. Results are thresholded at $p < .001$ for the dynamic versus static contrast for all 14 participants. L=Left; R=Right.

(see Figure 3.3.2 (a) and Table 3.2 B).

Comparison of the dynamic and static happy facial expressions revealed significant correlations with right inferior frontal gyrus and middle frontal gyrus (see Figure 3.3.2 (b) and Table 3.2 C). When activation in response to the dynamic and static displays of speech was examined significant correlations were found between right IOG and the right superior frontal gyrus and left STS (see Figure 3.3.2 (c) and Table 3.2 D). The contrast of dynamic angry and dynamic speech displays revealed significant correlations between right IOG and right middle occipital gyrus, bilateral middle occipital gyri, right middle frontal gyrus and right superior temporal gyrus (see Table 3.2 E). Finally the contrast of dynamic happy and dynamic speech displays revealed significant correlations between right IOG and bilateral middle temporal gyri, bilateral superior temporal gyri, and right middle frontal gyrus (see Table 3.2 F).

3.3.1.2 Superior temporal sulci

Next a seed voxel was placed in the left dorsal pathway, in the left STS (-52 -54 12; see Table 3.3). When all dynamic and static faces were compared, the left STS showed significant correlations with bilateral middle occipital gyri and IOG, right middle frontal gyrus, right STS, left precentral gyrus and left superior frontal gyrus (see Figure 3.3.1 (b) and Table 3.3 A). The contrast of dynamic angry and static angry expressions revealed significant correlations between the left STS and bilateral IOG, and middle occipital gyri, left postcentral gyrus, and amygdala, as well as right precentral gyrus and right STS (see Figure 3.3.2 (a) and Table 3.3 B). The comparison of dynamic and static displays of happiness revealed significant correlations between left STS and bilateral middle occipital gyri, left IOG, along with right middle frontal gyrus and right middle temporal gyrus (see Figure 3.3.2 (b) and Table 3.3 C). The contrast of dynamic and static displays of speech revealed significant correlations between left STS and bilateral lingual gyri and middle occipital gyri, and right STS and middle frontal gyrus (see Figure 3.3.2 (c) and Table 3.3 D). The contrast of dynamic angry and dynamic speech facial displays revealed significant correlations between left STS and right postcentral gyrus, left precentral gyrus, right middle frontal gyrus, left middle temporal gyrus and right insula (see Table 3.3 E). Finally, the contrast of dynamic happy and dynamic speech displays revealed significant

correlations between left STS and right postcentral gyrus, left fusiform gyrus, right medial frontal gyrus and left inferior frontal gyrus (see Table 3.3 F).

A seed voxel was also placed in the right STS (52, -54, 12; see Table 3.4). Again all dynamic were compared to all static facial expressions, which revealed significant correlations between the right STS and bilateral lingual gyri and precentral gyri, right IOG, middle temporal gyrus, and superior frontal gyrus, along with left middle occipital gyrus (see Figure 3.3.1 (b) and Table 3.4 A). The comparison of the dynamic and static angry expressions revealed significant correlations with the right lingual gyrus, IOG and middle frontal gyrus, as well as left precentral gyrus and middle occipital gyrus (see Figure 3.3.2 (a) and Table 3.4 B). While the comparison of dynamic and static displays of happiness revealed significant correlations with the right lingual gyrus and left IOG and precentral gyrus (see Figure 3.3.2 (b) and Table 3.4 C). When the dynamic and static displays of speech were compared, activation in the right STS was significantly correlated with activation in bilateral lingual gyri, right middle occipital gyrus and left superior frontal gyrus (see Figure 3.3.2 (c) and Table 3.4 D). The contrast of dynamic angry and dynamic speech facial displays revealed significant correlations between right STS and bilateral IOG, right lingual gyrus and right amygdala (see Table 3.4 E). Finally, the contrast of dynamic happy and dynamic speech displays revealed significant correlations between right STS and right postcentral gyrus, right middle occipital gyrus, right middle temporal gyrus, right precentral gyrus and left fusiform gyrus (see Table 3.4 F).

3.3.1.3 Amygdalae

The next seed voxel was placed in the left extended system, in the left amygdala (22 -6 -18; see Table 3.5), and again the regions of covariation under the condition of all dynamic versus all static facial expressions were examined. This revealed significant correlations between activation in the left amygdala and bilateral cingulate gyri, left lingual gyrus, precentral and postcentral gyri, as well as right middle temporal gyrus and middle occipital gyrus (see Figure 3.3.1 (c) and Table 3.5 A). When dynamic angry and static angry expressions were contrasted significant correlations were found between the left amygdala and bilateral lingual gyri, left IOG, and right STS and cingulate gyrus (see Figure 3.3.2 (a) and Table 3.5 B). Significant correlations were found between the left amygdala and

bilateral superior frontal gyri in response to dynamic happy and static happy expressions (see Figure 3.3.2 (b) and Table 3.5 C). Dynamic versus static displays of speech revealed significant correlations between the left amygdala and bilateral superior frontal gyri, left lingual gyrus and precentral gyrus and also right middle temporal gyrus (see Figure 3.3.2 (c) and Table 3.5 D). The contrast of dynamic angry and dynamic speech facial displays revealed significant correlations between left amygdala and bilateral medial frontal gyri, left middle temporal gyrus, left precentral gyrus and right STS (see Table 3.5 E). Finally, the contrast of dynamic happy and dynamic speech displays revealed significant correlations between left amygdala and right STS, left middle occipital gyrus, right middle frontal gyrus and left fusiform gyrus (see Table 3.5 F).

A seed voxel was also placed in a region in the right amygdala (20, -6, - 18; see Table 3.6). The contrast of all dynamic and static faces revealed significant correlations between the right amygdala and bilateral lingual gyri and precentral gyri, right middle occipital gyrus, STS, fusiform gyrus, cingulate gyrus, IFG, middle frontal gyrus, and superior frontal gyrus (see Figure 3.3.1 (c) and Table 3.6 A). Comparing activation in response to dynamic and static angry facial expressions revealed significant correlations with bilateral middle temporal gyri, right IFG, cingulate gyrus, middle frontal gyrus and left precentral gyrus (see Figure 3.3.2 (a) and Table 3.6 B). When activation in response to the dynamic and static facial expressions of happiness was examined a significant correlation between the right amygdala and the right precentral gyrus only was found (see Figure 3.3.2 (b) Table 3.6 C). When the dynamic and static displays of speech were compared activation in the right amygdala was significantly correlated with activation in the right middle temporal gyrus and cingulate gyrus, and left precentral and postcentral gyri (see Figure 3.3.2 (c) and Table 3.6 D). The contrast of dynamic angry and dynamic speech facial displays revealed significant correlations between the right amygdala and right middle frontal gyrus, bilateral precentral gyri, and bilateral middle temporal gyri (see Table 3.6 E). Finally, the contrast of dynamic happy and dynamic speech displays revealed significant correlations between the right amygdala and right IFG, right middle frontal gyrus and right middle temporal gyrus (see Table 3.6 F).

3.3.1.4 Inferior frontal gyri

Another seed voxel was placed in the extended face perception system, in the left IFG (-46 18 22; see Table 3.7), and as before all the dynamic and static facial expressions were compared, revealing significant correlations between the left IFG and left superior frontal gyrus, precentral gyrus, middle occipital gyrus, STS and middle frontal gyrus, along with right IFG, middle occipital gyrus and middle temporal gyrus (see Figure 3.3.1 (d) and Table 3.7 A). The comparison of the dynamic and static angry expressions revealed significant correlations between the left IFG and bilateral cingulate gyri, postcentral gyri, middle temporal gyri and middle frontal gyri, as well as right inferior parietal lobule (see Figure 3.3.2 (a) and Table 3.7 B). The comparison of the dynamic and static happy expressions revealed significant correlations between the left the IFG and bilateral middle occipital gyri and bilateral frontal gyri, left lingual gyrus, left cingulate gyrus, left precentral and postcentral gyri, and right fusiform gyrus (see Figure 3.3.2 (b) and Table 3.7 C). The contrast of dynamic and static displays of speech revealed significant correlations between the left IFG and bilateral middle occipital gyri, right STS, right lingual gyrus and right precentral gyrus (see Figure 3.3.2 (c) and Table 3.7 D). The contrast of dynamic angry and dynamic speech facial displays revealed significant correlations between the left IFG and right insula, left postcentral gyrus and bilateral middle frontal gyri (see Table 3.7 E). Finally, the contrast of dynamic happy and dynamic speech displays revealed significant correlations between the left IFG and bilateral middle frontal gyri, left postcentral gyrus and right fusiform gyrus (see Table 3.7 F).

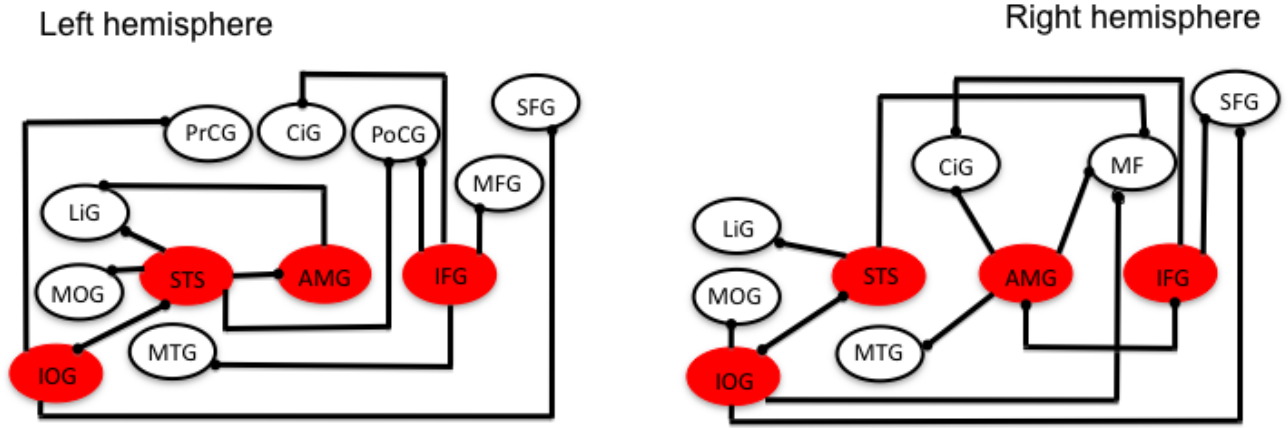
Finally, a seed voxel was placed in the right IFG (52, 26, 18; see Table 3.8). The contrast of all dynamic faces relative to static faces showed significant correlations between the right IFG and right middle occipital gyrus, middle temporal gyrus, fusiform gyrus and middle frontal gyrus (see Figure 3.3.1 (d) and Table 3.8 A). The comparison of the dynamic and static angry expressions revealed significant correlations between the right IFG and the right amygdala, cingulate gyrus and superior frontal gyrus (see Figure 3.3.2 (a) and Table 3.8 B). While the comparison of the dynamic and static expressions of happiness revealed a correlation with the right fusiform gyrus only (see Figure 3.3.2 (b) and Table 3.8 C). The comparison of the activation in response to the dynamic and static displays of speech revealed significant correlations between the right IFG and the right lingual gyrus

and middle temporal gyrus (see Figure 3.3.2 (c) and Table 3.8 D). The contrast of dynamic angry and dynamic speech facial displays revealed significant correlations between the right IFG and bilateral superior frontal gyri, right medial frontal gyrus and right amygdala (see Table 3.6 E). Finally, the contrast of dynamic happy and dynamic speech displays revealed significant correlations between the right IFG and bilateral middle frontal gyri and right fusiform gyrus (see Table 3.6 F).

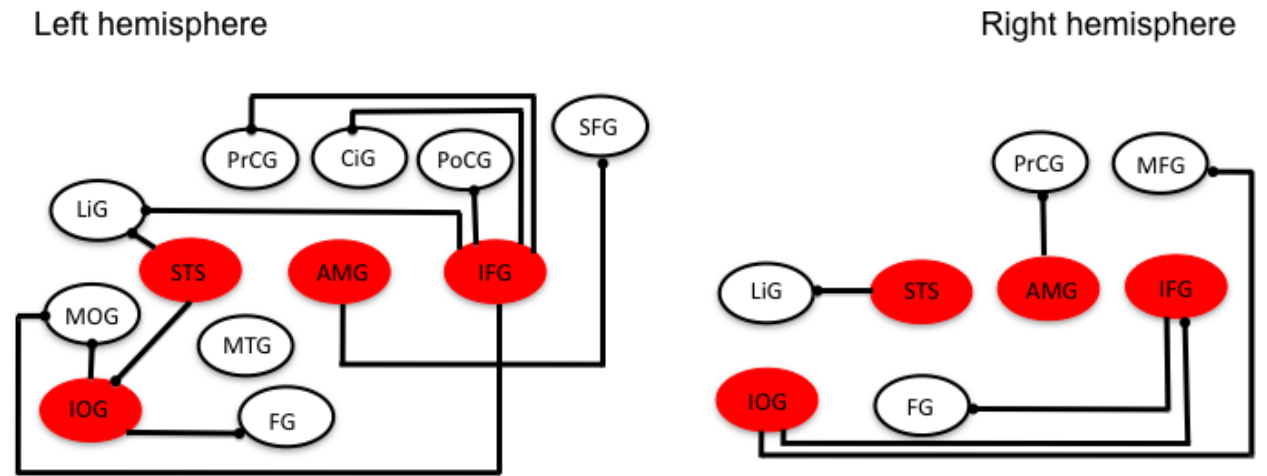
3.3.2 Physiophysiological interaction results

Physiophysiological interaction analysis (PYPI) was used to examine the effect of interaction between two different brain regions. Firstly the effect of the interaction between the left IOG and left STS was examined. This interaction revealed significant correlations with right middle temporal gyrus, right STS, right amygdala and left middle occipital gyrus (see Table 3.9 A). The interaction between the left STS and left amygdala revealed significant correlations with right precentral gyrus, right lingual gyrus, right IFG, right amygdala, left middle occipital gyrus, right STS and right fusiform gyrus (see Table 3.9 B). Finally, the interaction between the left amygdala and left IFG revealed a significant correlation with left posterior cingulate, left precentral gyrus, and left middle temporal gyrus (see Table 3.9 C).

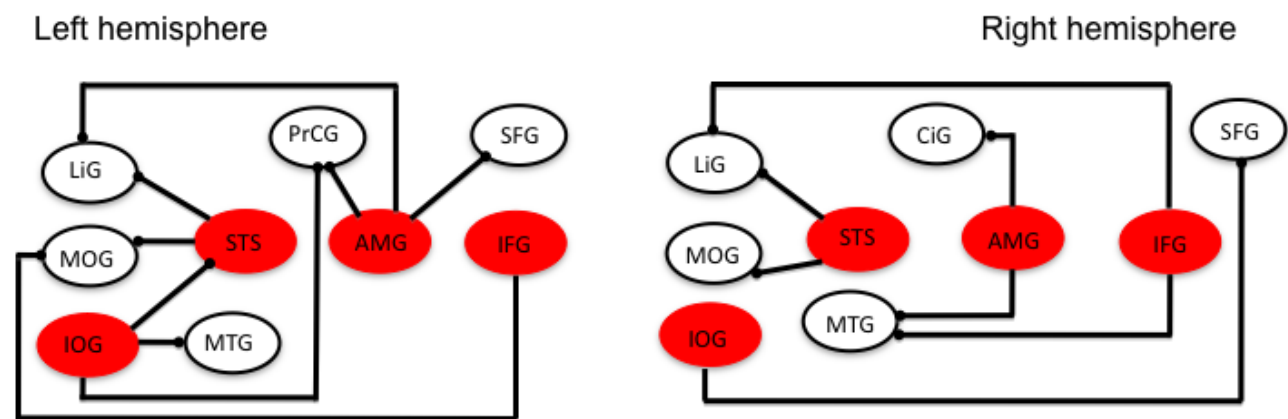
The same interactions were examined in the right hemisphere. The interaction between the right IOG and right STS showed significant correlations with bilateral middle temporal gyri, right middle frontal gyrus, right amygdala and right IFG (see Table 3.10 A). The interaction between right STS and right amygdala was assessed next, this revealed significant correlations with right middle temporal gyrus, right middle frontal gyrus, right postcentral gyrus, right IFG, and right precentral gyrus, along with left middle occipital gyrus, left IOG, and left fusiform gyrus (see Table 3.10 B). The interaction between right amygdala and right IFG was also examined and revealed significant correlations with bilateral anterior cingulate, bilateral middle temporal gyri, right posterior cingulate, right middle occipital gyrus and right STS (see Table 3.10 C).



(a) Dynamic angry versus static angry facial expressions.



(b) Dynamic happy versus static happy facial expressions



(c) Dynamic speech versus static speech facial displays.

Figure 3.3.2: Connectivity maps for (a) Dynamic angry versus static angry expressions; (b) Dynamic happy versus static happy facial expressions; (c) Dynamic speech versus static speech facial displays. Red sections indicate the seed voxels in the PPI analysis shown separately for left and right hemispheres.

Table 3.1: Brain regions showing effective connectivity with left IOG under condition of (A) All dynamic compared to all static expressions; (B) Dynamic angry compared to static angry expressions; (C) Dynamic happy compared to static happy expressions; (D) Dynamic speech compared to static speech expressions; (E) Dynamic angry compared to dynamic speech displays; (F) Dynamic happy compared to dynamic speech displays. Coordinates indicate local maxima in Talairach space. L = Left; R = Right. Multiple peaks within a cluster are shown on subsequent lines.

Region	Cluster Size (mm)	Z score	x, y, z
<i>(A) All dynamic versus all static faces</i>			
L Superior temporal sulcus (BA 39)	68	4.09	-50, -52, 14
R Middle frontal gyrus (BA 6)	38	3.94	38, 2, 64
L Inferior frontal gyrus (BA 47)	29	3.79	-46, 16, -8
L Middle occipital gyrus (BA 18)	68	3.55	-16, -96, 16
R Superior frontal gyrus (BA 6)	27	3.42	2, 4, 66
R Superior temporal sulcus (BA 22)	24	3.38	54, -44, 12
R Precentral gyrus (BA 6)	10	3.37	50, 2, 50
<i>(B) Dynamic angry versus static angry faces</i>			
L Precentral gyrus (BA 6)	41	4.52	-58, 4, 18
L Superior frontal gyrus (BA 6)	107	3.74	0, 0, 70
R Middle temporal gyrus (BA 21)	97	3.75	58, -50 4
L Superior temporal sulcus (BA 39)	143	3.84	-46, -52, 6
L Lingual gyrus (BA 18)	65	3.62	-4, -90, -18
R Middle frontal gyrus (BA 6)	80	3.6	48, 6, 48
L Inferior frontal gyrus (BA 47)	18	3.53	-48, 16, -6
<i>(C) Dynamic happy versus static happy faces</i>			
L Middle occipital gyrus (BA 19)	150	3.66	-20, -96, 14
L Fusiform gyrus (BA 37)	11	3.43	-40, -54, -18
R Middle occipital gyrus	13	3.3	18, -100, 14
<i>(D) Dynamic speech versus static speech faces</i>			
L Superior temporal sulcus (BA 22)	147	4.43	-56, -38, 10
L Middle temporal gyrus (BA 39)		3.58	-54, 56, 14
L Precentral gyrus (BA 6)	85	4.15	-50, -2, 54
<i>(E) Dynamic angry versus dynamic speech faces</i>			
L Middle occipital gyrus (BA 19)	54	4.15	-38 -78 4
L Amygdala	22	3.75	-22 -8 -12
R precentral gyrus (BA 6)	23	3.89	64, -4, 34
L Insula (BA 13)	12	3.49	34, 4, 12
R Insula (BA 13)	10	3.42	-40, 4, 8
<i>(F) Dynamic happy versus dynamic speech faces</i>			
L Fusiform (BA 19)	59	4.36	-42, -66, -10
R Inferior frontal gyrus (BA 47)	18	4.27	48, 16, -6
L Middle temporal gyrus (BA 39)	32	4.21	-54, 56, 14
L Middle occipital gyrus (BA 18)	45	3.79	-40, -90, 10
R Fusiform gyrus (BA 37)	34	3.82	40, -54, -16
L Inferior frontal gyrus (BA 47)	17	3.76	-45, 16, -8

Table 3.2: Brain regions showing effective connectivity with right IOG under condition of (A) All dynamic compared to all static expressions; (B) Dynamic angry compared to static angry expressions; (C) Dynamic happy compared to static happy expressions; (D) Dynamic speech compared to static speech expressions; (E) Dynamic angry compared to dynamic speech displays; (F) Dynamic happy compared to dynamic speech displays Coordinates indicate local maxima in Talairach space. L = Left; R = Right. Multiple peaks within a cluster are shown on subsequent lines.

Region	Cluster Size (mm)	Z score	x, y, z
<i>(A) All dynamic versus static faces</i>			
L Superior Temporal Sulcus (BA 22)	11	3.47	-58, -60, 14
L Middle Temporal Gyrus (BA 39)	8	3.40	-54, -70, 14
R Middle Temporal Gyrus (BA 22)	28	3.35	60, -40, 6
R Superior Temporal Sulcus (BA 22)	44	3.28	54, -46, 12
<i>(B) Dynamic angry versus static angry faces</i>			
R Superior Frontal Gyrus (BA 6)	12	3.87	4, 2, 70
R Middle Occipital Gyrus (BA 18)	24	3.84	46, -78, -8
R Superior Temporal Sulcus (BA 22)	16	3.82	56, -40, 12
L Superior Parietal Lobule (BA 7)	13	3.5	-30, -62, 50
R Middle Frontal Gyrus (BA 6)	9	3.37	46, 4, 44
<i>(C) Dynamic happy versus static happy faces</i>			
R Inferior Frontal Gyrus (BA 44)	26	3.7	52, 16, 10
R Middle Frontal Gyrus (BA 6)	22	3.28	38, 2, 50
<i>(D) Dynamic speech versus static speech faces</i>			
R Superior Frontal Gyrus (BA 6)	31	3.43	4, 2, 70
L Superior Temporal Sulcus (BA 22)	28	3.17	-54, -38, 10
<i>(E) Dynamic angry versus dynamic speech faces</i>			
R Middle temporal gyrus (BA 39)	62	4.33	48, -56, 6
L Middle occipital gyrus (BA 19)	43	3.91	-52, -76, 2
R Middle occipital gyrus (BA 18)	15	3.59	18, -88, 18
R Middle frontal gyrus (BA 6)	42	3.55	46, 4, 46
R Superior temporal sulcus (BA 38)	33	3.42	28, 10, -28
<i>(F) Dynamic happy versus dynamic speech faces</i>			
L Middle temporal gyrus (BA 19)	61	4.16	-44, -62, 12
R Superior temporal gyrus (BA 22)	36	3.90	64, -42, 18
R Middle temporal gyrus (BA 21)	19	3.61	62, -54, 8
L Superior temporal gyrus (BA 39)	28	3.57	-46, -50, 10
R Middle frontal gyrus (BA 6)	22	3.51	40, 2, 50

Table 3.3: Brain regions showing effective connectivity with left STS under condition of (A) All dynamic compared to all static expressions; (B) Dynamic angry compared to static angry expressions; (C) Dynamic happy compared to static happy expressions; (D) Dynamic speech compared to static speech expressions; (E) Dynamic angry compared to dynamic speech displays; (F) Dynamic happy compared to dynamic speech displays Coordinates indicate local maxima in Talairach space. L = Left; R = Right. Multiple peaks within a cluster are shown on subsequent lines.

Region	Cluster Size (mm)	Z score	x, y, z
<i>(A) All dynamic versus all static faces</i>			
L Middle occipital gyrus (BA 19)	217	4.96	-40, -80, 2
R Middle occipital gyrus (BA 19)		4.90	46, -72, -6
R Inferior occipital gyrus (BA 18)	54	4.68	44, -88, -2
L Inferior occipital gyrus (BA 18)	189	4.30	-50, -78, 0
R Middle frontal gyrus (BA 6)	94	4.27	48, 6, 56
R Superior temporal sulcus (BA 22)	50	3.84	52, -42, 12
L Precentral gyrus (BA 6)	26	3.70	-38, -14, 68
L Superior frontal gyrus (BA 6)	65	3.67	-2, 8, 52
<i>(B) Dynamic angry versus static angry faces</i>			
R Precentral gyrus (BA 9)	394	4.4	38, 6, 32
R Inferior occipital gyrus (BA 19)	260	4.34	44, -72, -4
L Inferior occipital gyrus (BA 18)	34	4.02	-46, -80, -10
L Postcentral gyrus (BA 3)	24	3.98	-44, -18, 62
R Middle occipital gyrus (BA 19)	32	3.90	44, -80, 6
L Amygdala (BA 28)	26	3.82	-18, -8, -16
R Superior temporal sulcus (BA 22)	40	3.71	52, -40, 10
L Lingual gyrus (BA 19)	8	3.44	-14, -60, -2
L Middle occipital gyrus (BA 18)	35	3.19	-10, -102, 16
<i>(C) Dynamic happy versus static happy faces</i>			
R Middle occipital gyrus (BA 19)	819	5.36	48, -74, -6
L Middle occipital gyrus (BA 19)	211	4.52	-40, -84, 4
R Middle frontal gyrus (BA 6)	40	4.22	48, 4, 56
L Inferior occipital gyrus (BA 18)	41	3.83	-44, -80, -10
R Middle temporal gyrus (BA 21)	17	3.72	50, -42, 12
<i>(D) Dynamic speech versus static speech faces</i>			
R Superior temporal sulcus (BA 22)	90	4.17	54, -40, 8
L Lingual gyrus (BA 18)	120	4.07	-6, -86, -6
R Lingual gyrus (BA 17)	87	4.06	6, -90, 2
R Middle frontal gyrus (BA 6)	34	4.06	40, 2, 64
R Middle occipital gyrus (BA 18)	16	3.50	-44, -78, -12
L Middle occipital gyrus (BA 18)	36	3.38	-16, -102, 16
<i>(E) Dynamic angry versus dynamic speech faces</i>			
R postcentral gyrus (BA 2)	34	4.13	52, -18, 30
L precentral gyrus (BA 6)	29	4.10	-22, -18, 52
R Middle frontal gyrus (BA 11)	36	4.02	24, 36, -8
L Middle temporal gyrus (BA 21)	45	3.97	-58, -58, 4
R Insula (BA 13)	19	3.83	44, -18, 24
<i>(F) Dynamic happy versus dynamic speech faces</i>			
R Postcentral gyrus (BA 1)	47	4.10	66, -22, 34
L Fusiform gyrus (BA 37)	32	3.89	-46, -48, -14
R Medial frontal gyrus (BA 6)	29	3.81	2, -24, 70
L Inferior frontal gyrus (BA 47)	17	3.75	44, 20, -14

Table 3.4: Brain regions showing effective connectivity with right STS under condition of (A) All dynamic compared to all static expressions; (B) Dynamic angry compared to static angry expressions; (C) Dynamic happy compared to static happy expressions; (D) Dynamic speech compared to static speech expressions; (E) Dynamic angry compared to dynamic speech displays; (F) Dynamic happy compared to dynamic speech displays Coordinates indicate local maxima in Talairach space. L = Left; R = Right. Multiple peaks within a cluster are shown on subsequent lines.

Region	Cluster Size (mm)	Z score	x, y, z
<i>(A) All dynamic versus all static faces</i>			
R Lingual gyrus (BA 17)	380	4.74	12, -90, 2
L Lingual gyrus (BA 18)		4.73	-2, -88, -8
R Inferior occipital gyrus (BA 19)	129	4.1	50, -80, -4
R Superior frontal gyrus (BA 6)	31	3.75	6, 14, 50
R Precentral gyrus (BA 6)	77	3.7	50, 2, 50
L Middle occipital gyrus (BA 19)	22	3.65	-48, -78, -4
L Precentral gyrus (BA 6)	46	3.59	-30, -16, 72
R Middle temporal gyrus (BA 22)	107	3.26	50, -40, 6
<i>(B) Dynamic angry versus static angry faces</i>			
R Lingual gyrus (BA 17)	211	5.31	6, -92, -2
R Middle frontal gyrus (BA 6)	94	4.02	46, 6, 44
L Precentral gyrus (BA 6)	126	3.96	-42, -12, 64
R Inferior occipital gyrus (BA 17)	34	3.82	52, -80, -4
L Middle occipital gyrus (BA 19)	13	3.57	-46, -74, 6
<i>(C) Dynamic happy versus static happy faces</i>			
R Lingual gyrus (BA 17)	311	4.9	8, -88, 4
L Inferior occipital gyrus (BA 18)	28	3.87	-50, -78, 0
L Precentral gyrus (BA 6)	11	3.39	-38, -6, 60
<i>(D) Dynamic speech versus static speech faces</i>			
R Lingual gyrus (BA 17)	565	3.95	14, -92, 2
L Lingual gyrus (BA 17)		3.73	-6, -88, -6
L Superior frontal gyrus (BA 6)	15	3.65	-2, 0, 64
R Middle occipital gyrus (BA 18)	54	3.48	22, -98, 22
<i>(E) Dynamic angry versus dynamic speech faces</i>			
R Inferior occipital gyrus (BA 18)	48	4.09	50, -84, -12
R Lingual gyrus (BA19)	37	4.02	28, -70, -2
L Inferior occipital gyrus (BA 18)	31	3.98	48, -82, -10
R Amygdala	10	3.71	22, -8, -16
L Inferior frontal gyrus (BA 47)	18	3.64	-32, 26, -10
<i>(F) Dynamic happy versus dynamic speech faces</i>			
R Postcentral gyrus (BA 5)	36	4.05	40, -48, 66
R Middle occipital gyrus (BA 19)	42	4.01	38, -80, 6
R Middle temporal gyrus (BA 39)	27	3.98	38, -74, 16
R Precentral gyrus (BA 6)	24	3.87	48, 0, 36
L Fusiform gyrus (BA 37)	19	3.73	-42, -50, -10

Table 3.5: Brain regions showing effective connectivity with the left amygdala under condition of (A) All dynamic compared to all static expressions; (B) Dynamic angry compared to static angry expressions; (C) Dynamic happy compared to static happy expressions; (D) Dynamic speech compared to static speech expressions; (E) Dynamic angry compared to dynamic speech displays; (F) Dynamic happy compared to dynamic speech displays Coordinates indicate local maxima in Talairach space. L = Left; R = Right. Multiple peaks within a cluster are shown on subsequent lines.

Region	Cluster Size (mm)	Z score	x, y, z
<i>(A) All dynamic versus all static faces</i>			
L Lingual gyrus (BA 17)	114	3.64	-26, -68, 4
L Precentral gyrus (BA 6)	67	3.12	-40, -12, 66
R Middle temporal gyrus (BA 22)	326	3.02	50, -46, 2
R Middle occipital gyrus (BA 19)	65	2.97	30, -88, 12
L Postcentral gyrus (BA 3)	27	2.61	-40, -28, 58
L Cingulate gyrus (BA 15)	15	2.61	-2, -20, 26
R Cingulate gyrus (BA 23)	16	2.59	8, -32, 26
R Inferior frontal gyrus (BA 9)	21	2.59	54, 16, 24
<i>(B) Dynamic angry versus static angry faces</i>			
L Inferior occipital gyrus (BA 18)	28	3.92	-46, -82, -2
R Lingual gyrus (BA 19)	9	3.78	26, -60, -2
R Superior temporal sulcus (BA 22)	27	3.60	60, -42, 12
R Cingulate gyrus (BA 23)	8	3.32	6, -30, 26
L Lingual gyrus (BA 17)	35	3.15	-6, -74, 0
<i>(C) Dynamic happy versus static happy faces</i>			
L Superior frontal gyrus (BA 6)	17	2.55	-10, 10, 72
R Superior frontal gyrus (BA 6)	10	2.48	12, 4, 68
<i>(D) Dynamic speech versus static speech faces</i>			
L Superior frontal gyrus (BA 6)	10	4.02	-4, -4, 66
R Superior frontal gyrus (BA 6)	42	3.94	6, 14, 54
L Lingual gyrus (BA 17)	413	3.54	-6, -64, 4
L Precentral gyrus (BA 14)	14	3.42	-50, -12, 58
R Middle temporal gyrus (BA 39)	12	3.41	46, -70, 10
<i>(E) Dynamic angry versus dynamic speech faces</i>			
L Medial frontal gyrus (BA 6)	91	4.34	-6, 4, 50
R Medial frontal gyrus (BA 6)	28	3.78	12, 8, 50
L Middle temporal gyrus (BA 39)	19	3.62	-44, -70, 10
L Precentral gyrus (BA 4)	23	3.56	-34, -24, 54
R Superior temporal sulcus (BA 22)	26	3.51	64, -42, 18
<i>(F) Dynamic happy versus dynamic speech faces</i>			
R Superior temporal sulcus (BA 22)	48	4.12	56, -43, 10
L Middle occipital gyrus (BA 18)	32	3.97	-14, -98, 16
R Middle frontal gyrus (BA 6)	25	3.78	40, -2, 46
L Fusiform gyrus (BA 37)	22	3.69	-40, -60, -14

Table 3.6: Brain regions showing effective connectivity with the right amygdala under condition of (A) All dynamic compared to all static expressions; (B) Dynamic angry compared to static angry expressions; (C) Dynamic happy compared to static happy expressions; (D) Dynamic speech compared to static speech expressions; (E) Dynamic angry compared to dynamic speech displays; (F) Dynamic happy compared to dynamic speech displays. Coordinates indicate local maxima in Talairach space. L = Left; R = Right. Multiple peaks within a cluster are shown on subsequent lines.

Region	Cluster Size (mm)	Z score	x, y, z
<i>(A) All dynamic versus all static faces</i>			
R Superior temporal sulcus (BA 22)	442	4.03	58, -44, 12
R Superior frontal gyrus (BA 6)	106	3.92	4, 12, 48
R Lingual gyrus (BA 18)	425	3.8	8, -72, 4
R Middle occipital gyrus (BA 18)		3.66	10, -90, 12
R Middle frontal gyrus (BA 46)	78	3.76	46, 18, 22
R Fusiform gyrus (BA 19)	23	3.74	22, -60, -10
R Inferior frontal gyrus (BA 44)	17	3.63	62, 8, 18
L Lingual gyrus (BA 18)	26	3.62	-2, -88, -10
R Cingulate gyrus (BA 30)	7	3.54	12, -66, 8
R Precentral gyrus (BA 6)	7	3.42	54, -2, 42
L Precentral gyrus (BA 6)	15	3.41	-40, -8, 58
<i>(B) Dynamic angry versus static angry faces</i>			
R Inferior frontal gyrus (BA 44)	52	4.06	60, 10, 14
R Cingulate gyrus (BA 23)	17	3.98	10, -28, 28
R Inferior frontal gyrus (BA 46)	67	3.94	54, 32, 10
R Middle temporal gyrus (BA 22)	97	3.8	62, -38, 8
L Middle temporal gyrus (BA 39)	7	3.61	-56, -70, 10
R Middle frontal gyrus (BA 6)	23	3.5	28, -8, 58
L Precentral gyrus (BA 6)	7	3.38	-56, 0, 26
<i>(C) Dynamic happy versus static happy faces</i>			
R Precentral gyrus (BA 6)	21	3.71	49, 0, 52
<i>(D) Dynamic speech versus static speech faces</i>			
R Cingulate gyrus (BA 23)	33	4.24	4, -10, 26
R Middle temporal gyrus (BA 22)	66	3.65	58, -44, 4
L Postcentral gyrus (BA 1)	19	3.58	-52, -24, 56
L Precentral gyrus (BA 6)	20	3.53	-50, 2, 54
<i>(E) Dynamic angry versus dynamic speech faces</i>			
R Middle frontal gyrus (BA 6)	43	3.93	34, 0, 46
L Precentral gyrus (BA 4)	22	3.73	-26, -24, 54
R Precentral gyrus (BA 6)	19	3.58	50, -2, 40
R Middle temporal gyrus (BA 37)	16	3.56	56, -64, 8
L Middle temporal gyrus (BA 37)	21	3.49	-42, -66, 6
<i>(F) Dynamic happy versus dynamic speech faces</i>			
R Inferior frontal gyrus (BA 46)	57	4.09	50, 36, 8
R Middle frontal gyrus (BA 10)	28	3.72	34, 52, 0
R Middle temporal gyrus (BA 37)	21	3.64	54, -66, 4

Table 3.7: Brain regions showing effective connectivity with the region in left inferior frontal gyrus under condition of (A) All dynamic compared to all static expressions; (B) Dynamic angry compared to static angry expressions; (C) Dynamic happy compared to static happy expressions; (D) Dynamic speech compared to static speech expressions; (E) Dynamic angry compared to dynamic speech displays; (F) Dynamic happy compared to dynamic speech displays Coordinates indicate local maxima in Talairach space. L = Left; R = Right. Multiple peaks within a cluster are shown on subsequent lines.

Region	Cluster Size (mm)	Z score	x, y, z
<i>(A) All dynamic versus all static faces</i>			
L Superior frontal gyrus (BA6)	122	3.56	0, 6, 54
R Inferior frontal gyrus (BA 9)	106	3.47	46, 6, 28
R Middle occipital gyrus (BA 19)	172	3.40	52, -68, 8
R Middle temporal gyrus (BA 19)		2.72	50, -78, 14
L Precentral gyrus (BA 6)	49	3.22	-38, -10, 66
L Middle occipital gyrus (BA 19)	48	3.17	-44, -86, 6
L Superior temporal sulcus (BA 39)	26	3.14	-52, -52, 10
L Middle frontal gyrus (BA11)	17	3.09	-30, 42, -10
<i>(B) Dynamic angry versus static angry faces</i>			
R Inferior parietal lobule (BA 40)	170	3.38	46, -44, 56
R Postcentral gyrus (BA 2)		3.33	48, -36, 62
L Cingulate gyrus (BA23)	45	3.13	-4, -24, 30
R Cingulate gyrus (BA 23)	34	3.12	4, -28, -26
L Postcentral gyrus (BA5)	101	3.05	-36, -46, 58
R Middle frontal gyrus (BA 6)	14	2.97	32, 0, 64
R Middle temporal gyrus (BA 39)	63	2.93	50, -66, 10
L Middle temporal gyrus (BA 19)	47	2.92	-58, -64, 14
L Middle frontal gyrus (BA 10)	18	2.80	-28, 42, 26
<i>(C) Dynamic happy versus static happy faces</i>			
L Lingual gyrus (BA 17)	413	4.00	0, -86, 6
R Superior frontal gyrus (BA 9)	50	3.52	28, 40, 30
L Middle occipital gyrus (BA 19)	9	3.47	-42, -84, 10
R Middle occipital gyrus (BA 19)	39	3.23	42, -84, 6
R Middle frontal gyrus (BA 6)	15	3.09	48, 8, 44
L Middle frontal gyrus (BA9)	22	3.06	-28, 42, 36
R Fusiform gyrus (BA 37)	46	3.03	42, -52, -18
L Cingulate gyrus (BA30)	17	3.02	-22, -66, 8
L Precentral gyrus (BA 6)	59	2.98	-32, -8, 70
L Postcentral gyrus (BA 40)	18	2.67	-42, -32, 54
<i>(D) Dynamic speech versus static speech faces</i>			
R Superior temporal sulcus (BA 38)	15	3.76	54, 12, -14
R Lingual gyrus (BA 18)	789	3.58	14, -100, -4
L Middle occipital gyrus (BA19)	33	2.98	-46, -84, 0
R Precentral gyrus (BA 6)	16	2.95	32, -10, 72
R Middle occipital gyrus (BA 19)	28	2.86	50, -78, 6
<i>(E) Dynamic angry versus dynamic speech faces</i>			
R Insula (BA 13)	15	4.23	40, 18, 4
L Postcentral gyrus (BA 2)	23	4.14	-48, -24, 28
L Middle frontal gyrus (BA 6)	19	4.08	-28, -8, 62
R Middle frontal gyrus (BA 46)	17	3.98	46, 40, 22
<i>(F) Dynamic happy versus dynamic speech faces</i>			
R Middle frontal gyrus (BA 10)	24	4.08	36, 42, 20
L Middle frontal gyrus (BA 6)	21	3.97	-20, 6, 50
L Postcentral gyrus (BA 2)	27	3.86	-48, -18, 26
R Fusiform gyrus (BA 37)	16	3.74	36, -42, -8

Table 3.8: Brain regions showing effective connectivity with the region in right inferior frontal gyrus under condition of (A) All dynamic compared to all static expressions; (B) Dynamic angry compared to static angry expressions; (C) Dynamic happy compared to static happy expressions; (D) Dynamic speech compared to static speech expressions; (E) Dynamic angry compared to dynamic speech displays; (F) Dynamic happy compared to dynamic speech displays Coordinates indicate local maxima in Talairach space. L = Left; R = Right. Multiple peaks within a cluster are shown on subsequent lines.

Region	Cluster Size (mm)	Z score	x, y, z
<i>(A) All dynamic versus all static faces</i>			
R Middle frontal gyrus (BA 6)	122	3.56	44, 0, 60
R Middle occipital gyrus (BA 19)	172	3.4	52, -68, 8
R Middle temporal gyrus (BA 19)		2.72	50, -78, 14
R Fusiform gyrus (BA 37)	41	3.23	44, -56, -18
L Precentral gyrus (BA 6)	49	3.22	-38, -10, 68
R Middle temporal gyrus (BA 22)	28	3.19	58, -40, 6
L Middle occipital gyrus (BA 19)	48	3.17	-44, -86, 6
L Superior frontal gyrus (BA 6)	122	2.59	0, 6, 54
L Superior temporal sulcus (BA 39)	10	2.53	-52, -52, 10
<i>(B) Dynamic angry versus static angry faces</i>			
L Superior temporal sulcus (BA 38)	15	3.85	-42, 18, -30
L Postcentral gyrus (BA 5)	9	3.66	-24, -40, 64
R Amygdala	11	3.59	18, -2, -18
L Superior frontal gyrus (BA 6)	16	3.51	-4, -6, 64
R Cingulate gyrus (BA 30)	29	3.45	6, -52, 16
L Insula (BA 13)	12	3.49	-40, 0, 16
R Superior frontal gyrus (BA 6)	12	3.43	12, 0, 66
<i>(C) Dynamic happy versus static happy faces</i>			
L Lingual gyrus (BA 18)	170	3.38	-26, -72, -8
L Precentral gyrus (BA 4)	24	2.91	-40, -20, 58
L Superior frontal gyrus (BA 6)	38	2.83	0, -2, 66
R Fusiform gyrus (BA 37)	34	2.76	26, -60, -8
L Inferior frontal gyrus (BA 47)	8	2.59	-46, 22, -14
L Middle occipital gyrus (BA 18)	15	2.59	-42, -90, 14
<i>(D) Dynamic speech versus static speech faces</i>			
R Lingual gyrus (BA18)	135	4.37	10, -96, -8
L Lingual gyrus (BA 18)		4.02	-6, -90, -10
R Middle temporal gyrus (BA 22)	59	3.84	62, -40, 4
L Superior temporal sulcus (BA 22)	16	3.72	-60, -38, 12
L Inferior occipital gyrus (BA 19)	13	3.22	-48, -78, -4
<i>(E) Dynamic angry versus dynamic speech faces</i>			
R Superior frontal gyrus (BA 10)	23	4.12	16, 52, 18
R Medial frontal gyrus (BA 10)	19	4.04	10, 56, 8
R Amygdala	10	3.67	20, -4, -18
L Superior frontal gyrus (BA 6)	14	3.60	-10, -12, 64
<i>(F) Dynamic happy versus dynamic speech faces</i>			
R Middle frontal gyrus (BA 6)	15	3.98	44, 0, 60
R fusiform gyrus (BA 19)	19	3.86	26, -60, -6
L Middle frontal gyrus (BA 6)	22	3.74	-42, 2, 58

Table 3.9: Physiophysiological interaction results in the left hemisphere.

Region	Cluster Size (mm)	Z score	x, y, z
<i>(A) PYPI between left inferior occipital gyrus and left superior temporal sulcus</i>			
R Middle temporal gyrus (BA 37)	473	4.66	58, -62, -2
R Superior temporal sulcus (BA 38)	15	3.85	38, 8, -30
R Amygdala (BA)	14	3.75	18, -2, -18
L Middle occipital gyrus (BA 19)	26	3.61	-42, -76, 4
<i>(B) PYPI between left superior temporal sulcus and left amygdala</i>			
R Precentral gyrus (BA 6)	56	3.23	36, -8, 66
R Lingual gyrus (BA 18)	20	3.09	20, -80, -4
R Inferior frontal gyrus (BA 47)	27	3.03	50, 30, -8
R Amygdala	18	3.03	20, -2, -20
L Middle occipital gyrus (BA 18)	26	2.92	-44, -84, 2
R Superior temporal sulcus (BA 38)	10	2.62	36, 18, -34
R Fusiform gyrus (BA 37)	10	2.61	38, -46, -16
<i>(C) PYPI between left amygdala and left inferior frontal gyrus</i>			
L Cingulate gyrus (BA 29)	27	4.58	-2, -46, 10
L Precentral gyrus (BA 4)	6	3.66	-46, -14, 48
L Middle temporal gyrus (BA 21)	20	3.49	-60, -38, 2

Table 3.10: Physiophysiological interaction results in the right hemisphere.

Region	Cluster Size (mm)	Z score	x, y, z
<i>(A) PYPI between right inferior occipital gyrus and right superior temporal sulcus</i>			
R Middle frontal gyrus (BA 46)	115	3.92	44, 34, 18
R Middle temporal gyrus (BA 37)	32	3.89	46, -66, 6
L Middle temporal gyrus (BA 39)	72	3.84	-50, -68, 12
R Amygdala	15	3.59	20, -2, -20
R Inferior frontal gyrus (BA 44)	17	3.45	50, 16, 10
<i>(B) PYPI between right superior temporal sulcus and right amygdala</i>			
L Middle occipital gyrus (BA 19)	27	3.55	-32, -96, 20
L Fusiform gyrus (BA 20)	57	3.27	-42, -2, -24
R Middle temporal gyrus (BA 21)	37	3.19	50, -44, 6
R Middle frontal gyrus (BA 46)	65	3.14	56, 34, 14
L Inferior occipital gyrus (BA 18)	45	3.10	-42, -82, -2
R Postcentral gyrus (BA 1)	18	3.09	66, -22, 42
R Inferior frontal gyrus (BA 47)	17	3.03	48, 30, -12
<i>(C) PYPI between right amygdala and right inferior frontal gyrus</i>			
R Anterior Cingulate gyrus (BA 33)	10	4.08	8, 22, 16
L Anterior Cingulate gyrus (BA 32)	19	3.80	-22, 28, 20
L Middle temporal gyrus (BA 21)	10	3.50	-60, -46, 8
R Middle occipital gyrus (BA 19)	11	3.40	36, -82, 16
R Middle temporal gyrus (BA 21)	12	3.31	44, -36, 0
R Superior temporal sulcus (BA 22)	9	3.16	46, -36, 6

3.4 Discussion

Having previously defined the regional brain activation patterns mediating dynamic face perception in chapter 2, the objective of this study was to examine the associations between these brain regions. To this end, PPI connectivity analysis was used to examine the covariance of changes in activity between different brain regions within the previously defined dynamic face perception network. PPI analysis confirmed the hypothesis that brain activation in early visual regions, such as IOG, would be correlated with regions in the dorsal pathway, such as the STSi, when viewing dynamic face stimuli. Furthermore, it was predicted that activation in STS would be correlated with regions in the extended network such as the amygdala and IFG when viewing dynamic facial expressions of emotion. This was also confirmed through PPI analysis.

3.4.1 Dynamic versus static faces

During the perception of all dynamic stimuli, activation in the region in right IOG was correlated with activation in bilateral MTG and STS. Similarly activation in the region in left IOG was also correlated with bilateral STS. Based on Haxby et al.'s (2000) model this is part of the core system where early visual and motion processing takes place, and the STS is involved in processing facial motion (see chapter 2). This supports previous studies that have shown increases in MTG and STS activations in response to facial motion (Sato et al., 2004; Schultz and Pilz, 2009) and further extends them by providing evidence of effective connectivity between IOG and the dorsal MTG and STS regions when processing dynamic face stimuli. When the effective connectivity with the STS was examined it was also found to covary with IOG activation, thus implying reciprocal connections between these two regions. Fairhall and Ishai (2007) however, found that emotional and famous faces significantly modulated the coupling between IOG and FG in the ventral pathway, but not between IOG and STS when static faces were processed. This suggests that the coupling between IOG and STS observed in the present study is as a result of the specific facial motion properties of the stimuli.

Activation in the left IOG was also correlated with regions in prefrontal cortex, including left IFG, right middle frontal gyrus and superior frontal gyrus. This may reflect top-down processing where these regions in prefrontal cortex modulate visual attention to the

dynamic face stimuli (Mechelli et al., 2004; Summerfield et al., 2006). PPI analysis does not provide information on the direction of these connections thus it is also possible that this correlation could be due to bottom-up processing from IOG to prefrontal cortex, or potentially a combination of top-down and bottom up processing. Recently, Pitcher et al. (2011b) have shown that IOG, or the occipital face area as it is commonly referred to, is an essential component of the face perception network. These findings extend Haxby et al.'s model, which proposes connections from IOG to STS and FG, to include effective connectivity between IOG and prefrontal cortex during dynamic face processing.

STS activation in both hemispheres was correlated with activation in early visual regions such as the lingual gyrus, middle occipital gyrus and middle temporal gyrus (MT/V5). Similarly, a recent meta-analysis by Fusar-Poli et al. (2009) reports lingual gyrus and middle occipital gyrus activation in response to face stimuli, independent of emotional valence. Nummenmaa et al. (2009) also found significant correlations between STS activation and area MT when viewing eye gaze shifts, supporting the contention that these regions are involved in processing the changeable aspects of the face (Haxby et al., 2000). In addition, STS activity covaried with frontal regions, including superior frontal gyrus and precentral gyrus. This is consistent with Hein and Knight (2008)'s proposal that a covariation between STS and premotor activity facilitates motion processing.

Activation in the amygdala was correlated with early visual regions, lingual gyri, right middle occipital gyrus, MTG, the STS in the dorsal pathway, as well as the fusiform gyrus in the ventral pathway. This correlation between amygdala and fusiform gyrus activity is consistent with previous research which proposes direct feedback signals from the amygdala to the fusiform gyrus during the processing of emotional faces (Vuilleumier and Pourtois, 2007). The amygdala was also correlated with the cingulate gyri, precentral gyri and frontal regions including right IFG, middle frontal gyrus and superior frontal gyrus. This correlation between amygdala and frontal regions is consistent with (Adolphs, 2002b) theory of emotion recognition, where the amygdala and the mirror neuron system work together to link perceptual representations of the face to the generation of knowledge about the particular emotion signalled. Similarly, activation in the IFG was correlated with visual regions including middle occipital gyri, middle temporal gyri, STS, and fusiform gyrus as well as frontal regions including middle frontal gyrus, superior frontal gyrus

and precentral gyrus. The effective connectivity observed here between IFG and early visual regions may be as a result of top down modulatory processes on visual processing (Mechelli et al., 2004; Summerfield et al., 2006).

3.4.2 Dynamic facial expressions of anger

In the previous chapter the perception of dynamic angry relative to static angry expressions was associated with significant increases in activation in regions of the core face perception system including middle occipital gyri, middle temporal gyri and STS, along with the amygdala and insula, in the extended system (see subsection 2.3.1). The persistence of activation in the amygdala and insula during the contrast of dynamic angry expressions with dynamic speech displays suggests that these regions are specifically involved in processing dynamic angry facial expressions, whereas regions of occipital and temporal gyri are involved in more general motion processing. Based on these results it was expected that activation in IOG would be correlated with regions in the dorsal pathway of the core face perception system such as MTG and STS during the perception of dynamic angry expressions. It was also predicted that STS and amygdala activation would be correlated, during the processing of dynamic angry facial expressions. It was further hypothesised that activation in the amygdala would be correlated with the insula, based on anatomical connections between these regions (Phelps et al., 2001; subsection 2.4.2), to facilitate emotional processing of the dynamic angry face stimuli.

As predicted, activation in IOG was correlated with activation in middle occipital gyrus, middle temporal gyrus and the STS. Interestingly, IOG activation was also correlated with a number of frontal regions including inferior, middle and superior frontal gyri, along with the superior parietal lobule and precentral gyrus. This is similar to the results described in the previous section for all dynamic faces and is again consistent with the view that IOG is an important structure in the face perception network, which may be involved in multiple stages of face processing rather than just the early structural encoding stage (Atkinson and Adolphs, 2011).

Furthermore a recent DCM study by Dima et al. (2011) found that facial affect, particularly facial expressions of anger, significantly modulated the effective connectivity between IOG and a region of ventral prefrontal cortex in the vicinity of the inferior frontal gyrus.

The authors therefore propose that the functional coupling between visual cortical and prefrontal regions may be important in facilitating facial affect processing. In addition, activation in IOG was correlated with activation in the amygdala and insula for the direct contrast of dynamic angry and dynamic speech displays, which again supports the notion that these structures are specifically involved in processing the affective information within dynamic angry expressions.

STS was reciprocally connected with IOG, thereby linking early stimulus perception in visual regions to the STS in the dorsal pathway for motion processing (Decety and Grèzes, 1999). The STS feeds back into regions such as the middle occipital and lingual gyri, which are involved in visual processing, but also connects to regions of the extended system including the amygdala, insula, middle frontal gyri, precentral and postcentral gyri. While the STS is consistently implicated in social perception (Allison et al., 2000), in chapter 2 it was shown that the STS was sensitive to the motion properties of the stimuli not the specific affect. Thus, it may be that the STS facilitates social perception of different facial expressions by acting as a relay centre between regions involved in early visual perceptual processing and emotional processing such as the amygdala (Hein and Knight, 2008).

Similar to the STS, activation in the amygdala was also correlated with visual regions including the lingual gyrus, IOG, as well as MTG and STS in the dorsal pathway. The amygdala was also effectively connected with frontal regions such as IFG, middle frontal gyri, precentral gyri and the cingulate gyrus during the perception of dynamic angry facial expressions. The IFG and amygdala are reciprocally connected, and both are effectively connected to the right cingulate, hence these structures may work together to process the emotional content of the dynamic angry facial expressions. IFG was also effectively connected with frontal regions such as the postcentral and superior frontal gyri which are believed to form part of the mirror neuron system (Montgomery and Haxby, 2008). Interestingly, IFG showed significant correlations with activity in the insula during the perception of dynamic angry expressions, but the amygdala was not effectively connected to the insula. This is contrary to our hypothesis that amygdala and insula activation would be correlated. Possibly the IFG mediates the interaction between the amygdala and the insula during the processing of dynamic angry facial expressions.

3.4.3 Dynamic facial expressions of happiness

In chapter 2 the perception of dynamic happy expressions was associated with increased activation in the core system in middle occipital gyri, MTG and STS. In addition, increased activation was also found in a ventral region in the fusiform gyrus, which showed significantly greater activation specifically in response to dynamic happy expressions relative to both, static happy facial expressions and dynamic displays of speech (see subsection 2.3.1). Based on these results it was predicted that activation in IOG would once again be correlated with regions in the dorsal pathway of the core face perception system such as MTG and STS during the perception of dynamic happy facial expressions. It was also predicted that IOG activation would be correlated with ventral regions in the fusiform gyrus when processing dynamic happy expressions based on the significant fusiform activation reported in chapter 2.

As predicted, IOG activation was correlated with regions of the core system including middle occipital gyri, MTG and STS, as well as with the fusiform gyrus, which is consistent with our findings from chapter 2. Additionally, IOG activation was also correlated with regions in prefrontal cortex, including middle frontal and IFG. This provides further support for the theory that the coupling between IOG and ventral prefrontal cortex facilitates emotional face processing (Dima et al., 2011), for both positive and negative affects.

Activation in STS was correlated with IOG activation and other visual regions, including the lingual gyrus, middle occipital gyrus and MTG. Activation in STS was also correlated with frontal regions, including middle frontal gyrus and precentral gyrus. Again the STS may act as a relay centre between early visual regions and regions in prefrontal cortex involved in action observation and interpretation (Montgomery and Haxby, 2008). Notably, in contrast to the perception of dynamic angry expressions the STS was not correlated with amygdala activation during the perception of dynamic happy facial expressions. However, activation in the STS was correlated with activation in the fusiform gyrus during the processing of dynamic happy facial expressions relative to dynamic displays of speech. Correlations between STS and fusiform activation have previously been reported during resting state studies (Zhang et al., 2009; Turk-Browne et al., 2010). However, the results here revealed changes based on experimental modulation, where STS and

fusiform activations were only correlated during the processing of dynamic happy facial expressions.

Interestingly, activation in the amygdala was also correlated with activation in the fusiform gyrus for the contrast of dynamic happy expressions with dynamic speech facial displays, as well as with dorsal regions of the core system including MTG and STS. In addition amygdala activation was correlated with frontal regions, including IFG, middle frontal gyrus, precentral gyrus and bilateral superior frontal gyri. The connectivity between amygdala and fusiform gyrus described here is in accordance with previous studies that have shown increased activation in the fusiform gyrus to emotional face stimuli as a result of feedback from the amygdala (Vuilleumier et al., 2001; Vuilleumier and Pourtois, 2007).

Activation in the IFG was correlated with frontal regions including middle frontal gyrus, superior frontal gyrus, precentral and postcentral gyri, all regions involved in the mirror neuron system (Montgomery and Haxby, 2008). IFG activation was also correlated with visual regions including the middle occipital gyrus and lingual gyrus. In addition, activation in the right IFG was correlated with activation in the right fusiform gyrus, whereas in the case of dynamic angry expressions the right IFG was reciprocally connected to the amygdala. It would therefore appear in this network that the fusiform gyrus and IFG are involved in processing dynamic happy facial expressions to a greater extent than the amygdala. Dima et al. (2011) also report significant coupling between the fusiform gyrus and IFG in the processing of static facial expressions of emotion. However, they only used examples of negative facial affect. The results of the present connectivity analysis show that the coupling between the fusiform gyrus and IFG may facilitate the processing of dynamic facial expressions of happiness.

3.4.4 Dynamic speech versus static speech facial displays

Dynamic displays of speech were previously associated with increased activation in the core face perception system including middle occipital gyri, middle temporal gyri and STS, along with regions of the extended system including left IFG, bilateral middle frontal gyri and right precentral gyrus (see subsection 2.3.1). Based on these results effective connectivity was predicted between IOG and dorsal regions of the core face perception system, including MTG and STS during the perception of dynamic speech facial displays.

It was further hypothesised that activation in STS would be correlated with regions of prefrontal cortex around brodmann area 6, including precentral gyrus, which is known to be involved in speech processing.

As expected, activation in IOG was correlated with activation in MTG and STS, as well as with superior frontal gyrus and precentral gyrus activation. In contrast to the dynamic angry and happy conditions, IOG activation was not correlated with IFG activation during the perception of dynamic speech stimuli. Activation in the STS was again correlated with visual and frontal regions including lingual gyri, middle occipital gyri, middle frontal and superior frontal gyri. Surprisingly, activation in the STS was not correlated with the MTG, whereas activation in the amygdala was correlated with the right MTG. Amygdala activation was also correlated with activation in the lingual gyrus, the right posterior cingulate gyrus, precentral and postcentral gyri. While activation in the IFG correlated with visual regions only, including lingual gyri, middle occipital gyrus, MTG, and STS.

An important difference between this network and both of the affective networks is the lack of effective connectivity between the IOG and IFG and vice versa, during the perception of dynamic speech displays, which do not contain any affective components. This lends further support to the proposal that the effective connectivity between the IOG and IFG facilitates affective processing from facial expressions of emotion (Dima et al., 2011). Processing of dynamic speech displays may rely more on connections between the IOG and precentral gyrus. Also the amygdala showed effective connectivity with precentral and postcentral gyri. This is consistent with literature on speech perception showing the involvement of premotor cortex in the perception of speech (Campbell et al., 2001).

3.4.5 Physiophysiological interactions

Physiophysiological interaction analysis measures how activity in one brain region is modulated by the physiological interaction between two other brain regions (Friston et al., 1997). The physiophysiological interaction between the right IOG and right STS was examined first, showing significant correlations with bilateral MTG, right middle frontal gyrus, right amygdala and right IFG. This is consistent with Haxby et al. (2000)'s distributed face perception network, which proposes that regions of the core visual system and the extended system are recruited to process faces. In this case activation in IOG

and STS predicts activation in MTG in the core system, which is involved in processing biological motion, as well as the amygdala, and inferior frontal gyri which are recruited to process emotion.

It is interesting that IOG and STS activity did not correlate with FG activation, which is a key component of the face perception network. However, the interaction between the right STS and right amygdala did correlate with FG activation. Turk-Browne et al. (2010) report functional connectivity between the FG and STS at rest, however they focused their analysis on these two regions only and therefore could not assess the connectivity between the FG, STS and the amygdala. Based on the present results it appears that the FG, STS and amygdala are functionally connected. Previous studies have reported modulatory feedback from the amygdala to the fusiform gyrus during emotional face processing (Vuilleumier and Pourtois, 2007). These results suggest that both the STS and amygdala may modulate fusiform activity. The interaction between right STS and right amygdala also revealed significant correlations with visual regions, IOG, middle occipital gyrus and MTG, as well as frontal regions, including IFG, middle frontal gyrus, postcentral gyrus, and precentral gyrus. Finally the interaction between right amygdala and right IFG showed significant correlations again with regions of the core system including middle occipital gyrus, MTG, and STS, as well as with anterior and posterior cingulate.

In the left hemisphere then, the interaction between the left IOG and left STS showed significant correlations with right MTG, right STS, right amygdala and left MOG. This is again consistent with Haxby et al.'s model showing that the IOG and STS interact with regions in the core system (MTG and MOG), as well as feed forward connections to the extended system (amygdala) during face processing. The interaction between the left STS and left amygdala again predicted activation in regions of the core and extended systems, but predominantly in the right hemisphere, including right lingual gyrus, right STS and right FG, in the core system, and right precentral gyrus, right IFG and the right amygdala in the extended system. This interaction between the left STS and left amygdala only predicted activation in one region in the left hemisphere in the left middle occipital gyrus. The right hemisphere bias reported here is consistent with numerous studies showing that face perception is more right lateralised (Clark et al., 1996; Kanwisher et al., 1997). Interestingly, again STS and amygdala activation predict activation in the

fusiform gyrus. Finally, the interaction between left amygdala and left IFG revealed significant correlations with left MTG, left posterior cingulate, and left precentral gyrus.

3.4.6 Summary

In chapter 2 it was shown that broadly similar regions were involved in processing the different dynamic stimuli, particularly in the core face perception system. Consistent with this, the measures of effective connectivity defined in the present chapter revealed that the effective connectivity when viewing dynamic facial stimuli in general was associated with specific increases in connectivity between early visual regions, such as IOG, and the STS in the dorsal pathway, which was broadly similar for all of the different dynamic face stimuli. However, the coupling between regions of the core and the extended system varied depending on the type of expression that was processed. Similarly, Fairhall and Ishai (2007) found that the effective connectivity between the core system and regions of the extended system, such as the amygdala and orbitofrontal cortex, were modulated by different face stimuli. Furthermore, Zhang et al. (2009) found reliable resting state functional connectivity within the core face perception system but not in the extended system.

Processing dynamic facial expressions of anger was associated with increases in effective connectivity between IOG and STS, and reciprocal connections between STS and the amygdala, as well as reciprocal connections between the amygdala and IFG. In addition inferior frontal gyri were effectively connected to the insula. While dynamic happy expressions were associated with effective connectivity between IOG and IFG, and IFG and fusiform gyri, as well as between STS and FG, and amygdala and FG, among others. Thus, the amygdala and insula appear to play a greater role in processing dynamic angry facial expressions. Whereas the fusiform gyrus appears to be more involved in processing dynamic happy facial expressions, which was revealed by the greater extent of connectivity between the 'seed' regions of the face perception network and the fusiform gyrus.

Interestingly, both the dynamic angry and dynamic happy networks displayed effective connectivity between IOG and inferior frontal gyri, which may facilitate emotional processing (Dima et al., 2011). In contrast, viewing dynamic speech stimuli, which lack any emotional content, were associated with increases in connectivity between IOG and pre-

central gyrus. The STS was effectively connected with visual regions, lingual gyri and middle occipital gyri, and IFG were coupled with lingual gyri and MTG, regions involved in motion processing and motor movements.

Chapter 4

The time-course of cortical oscillatory responses to dynamic faces

4.1 Introduction

4.1.1 Overview

As previously discussed in chapters 1, 2 and 3, faces are processed by an anatomically distributed neural network (Haxby et al., 2000) and the localisation of these neural substrates has been extensively described (see chapter 1 and chapter 2). In chapter 2 a dynamic face perception network was identified which extends Haxby et al. (2000)'s distributed neural system for face perception. In chapter 3 the effective connectivity within this dynamic face perception network was assessed, revealing coupling between the IOG and the STS during the perception of dynamic faces. While these analyses provided valuable information on the neural substrates of dynamic face perception, they did not provide any information on the temporal sequence of regional activations involved in face processing. This is because this level of information cannot be obtained from fMRI due to its relatively poor temporal resolution. MEG on the other hand, is more suited to identifying the detailed temporal processing of such information. In this chapter, MEG will be used to interrogate the dynamic face perception network by examining location, temporal structure and frequency information of the implicated neural regions i.e. to examine where, when, and in what

frequency band dynamic face processing takes place.

4.1.2 Timecourse and oscillatory responses to dynamic faces

Electrophysiological studies of face perception have shown that just as information about faces is spatially distributed across cortical sites, faces are also processed at various temporal scales (Vuilleumier and Pourtois, 2007). These studies were discussed in detail in chapter 1 (see subsection 1.3.4.1) so only the main findings will be presented here. In brief, the findings from these electrophysiological studies have converged on a network of brain regions that are known to contribute to face perception and have provided additional information on the temporal processing in these regions.

An early evoked response has been identified in early visual regions such as lingual and inferior occipital gyri at approximately 100 ms post stimulus onset (N/M100), followed by later evoked responses in STS and fusiform gyrus at approximately 170 ms (N/M170) (Liu et al., 2000; Itier et al., 2006; Vuilleumier and Pourtois, 2007). However, as with much of the face perception literature to date, the studies described so far have used static images of faces, which lack important temporal information (see subsection 1.2.2.1). These static facial stimuli represent impoverished displays lacking natural facial motion, therefore they do not allow a complete description of the temporal structure of face specific neural activities to be made. Dynamic stimuli would offer a more suitable means of examining the neural basis of realistic natural face perception.

fMRI studies of biological motion perception have provided valuable information on the processing of motion stimuli. Regions of middle and superior temporal cortices were shown to be involved in processing dynamic stimuli, area MT in posterior lateral temporal cortex was identified as the canonical visual motion processing area, where it responds to all types of motion stimuli, while regions along posterior STS respond to biological motion in particular (Beauchamp et al., 2002; Blake and Shiffrar, 2007). Electrophysiological studies have also implicated regions of middle temporal and superior temporal cortices in biological motion processing. For example, Ahlfors et al. (1999) found an early transient response in area MT at approximately 130 ms, followed by a later sustained response in the posterior STS over the latency range of 200–400 ms. Consequently, it has been proposed that there are two distinct stages in biological motion processing, an early stage

in visual regions occurs around 170 ms post stimulus onset followed by later processing in the superior temporal gyrus and fusiform gyrus around 300 ms post stimulus onset (Jokisch et al., 2005)

While these studies have provided valuable information on the time course of activation related to face and motion perception, they do not explore the frequency content of these neural responses. Additional information about the spatio-temporal dynamics of cognitive processes can be gained by exploring the frequency characteristics of the signal. In the frequency domain, MEG/EEG signals can be used to analyse task-specific or event related changes in cortical oscillatory power. The power changes in rhythmic oscillations occurring within a certain frequency band can show either a decrease (event related desynchronisation, ERD) or an increase (event related synchronisation, ERS) in power (Pfurtscheller, 2001). It has been suggested that the ERD reflects activation of the underlying cortex while ERS reflects inactivation or return to the resting state (Shibasaki, 2008).

An influential study by Singh et al. (2002) used MEG and the SAM beamformer source localisation technique, to investigate changes in cortical synchronisation in response to biological motion. They found a decrease in oscillatory power in 5-15 Hz and 15-25 Hz frequency bands. In the biological motion condition these responses were found in known motion sensitive areas such as area MT and STS. They also found that the BOLD response was inversely related to cortical synchronisation for the 5-15 Hz and 15-25 Hz bands when SAM analysis was used, supporting the theory that neural activation is represented by decreases in cortical power particularly in these low frequency bands (Singh et al., 2002). Muthukumaraswamy et al. (2006) later examined neural oscillatory responses to oro-facial stimuli using MEG and SAM source localisation. They found decreased alpha (8-15 Hz) and beta (15-35 Hz) power in response to different biological motion stimuli, including biological motion, object directed action and linguistic motion in lateral sensorimotor areas and bilateral occipito-parietal regions. These decreases in low frequency power responses to biological motion are consistent with Singh et al. (2002)'s findings. Like Singh et al. the authors suggest, based on the theory that decreases in power in these frequency bands represent an active state, that these results signify an increase in neural activity during movement observation.

More recently, Lee et al. (2010) investigated the spatial distribution of neural oscillations in response to a set of dynamic face stimuli portraying rigid motion that conveyed shifts in social attention, using fMRI and MEG with SAM source analysis. These dynamic stimuli were contrasted with both static face stimuli and moving scrambled stimuli. They report a decrease in high frequency power (30–80 Hz) in bilateral STS in response to the dynamic face stimuli during the movement time period of (240–480 ms). However, they did not find a decrease in low frequency power (5–30 Hz) in the STS. They did however find low frequency power decreases in ventral visual areas including the fusiform gyrus, in response to both dynamic and static face stimuli. This low frequency response was greater in magnitude and spatial extent for the dynamic face stimuli.

Again like Singh et al. (2002) and Muthukumaraswamy et al. (2006), they interpreted these oscillatory power decreases as representing increases in cortical activation, in both ventral and dorsal streams during passive viewing of face stimuli. While this study provides valuable information about the sources and frequencies of neural oscillations that contribute to rigid dynamic face perception, it only applies to rigid facial motion such as head turns, but not to non-rigid facial motion such as a moving expressing face. Furthermore, because the authors only analysed the responses within a specific time window (240–480 ms) corresponding to the time of the head turns, they could not detail the temporal progression of activation within the face perception network over different latencies (i.e. early and late responses). Hence very little is known about the temporal and frequency response characteristics of neural regions during the processing of realistic dynamic facial expressions.

4.1.3 Objectives and hypotheses

As highlighted above, there are very few studies that have investigated neural responses to dynamic face stimuli. In the studies that have used dynamic stimuli some studies, such as Watanabe et al. (2005), have focused more on the time domain, while others including Muthukumaraswamy et al. (2006) and Lee et al. (2010), on the frequency domain. The aim of this study was to thoroughly interrogate the dynamic face perception network by examining location, temporal structure and frequency information of the implicated neural regions i.e. to examine where, when and in what frequency band dynamic face

processing takes place. Having previously established the spatial profile of the haemodynamic response to dynamic faces (see chapter 2) this study used MEG as a direct measure of neural activity to address these research questions. Thus, MEG and SAM were used to assess the main effect of motion by identifying regions of differential neural responses to dynamic relative to static face stimuli and examining the timing and frequency of oscillations contributing to these responses.

As described above, decreased oscillatory power in frequencies between 5-25 Hz has been observed with MEG when participants viewed biological motion stimuli (Singh et al., 2002; Muthukumaraswamy et al., 2006). Hence, the main hypothesis tested in the present study is that processing of dynamic face stimuli will result in decreased beta band power in regions of the dynamic face perception network, which will be spatially coincident with those identified previously with fMRI i.e. IOG, MTG, STS, and IFG (see chapter 2). It is also predicted that regions such as IOG will show early responses, followed by later responses in area MT and regions in STS, based on previous research (Ahlfors et al., 1999; Jokisch et al., 2005).

4.2 Methods

4.2.1 MEG participants

Fourteen healthy self-reported right-handed volunteers (5 male) with normal or corrected to normal vision (mean age 29.2, S.D. 2.45 years) gave full written informed consent to take part in the study, which was approved by the Aston University Human Science Ethical Committee. These were naive participants who had not participated in the previous fMRI study described in chapters 2 and 3.

4.2.2 Experimental design and imaging paradigm

In order to facilitate comparisons between the fMRI and MEG studies the same stimuli were used in both studies (see chapter 2 for details). The paradigm was altered slightly from the block design that was used in the fMRI study to an event related design, to optimise results from the SAM analysis. A sample of twenty-four stimuli (twelve dynamic

and twelve corresponding static images) were presented in an event related design and participants were instructed to maintain central fixation throughout the experiment. Stimuli were completely randomised and presented for 2.5 seconds with 2.5 seconds of baseline (fixation cross) presented before each stimulus. There were 240 trials in an experimental run. Each trial consisted of a single stimulus presentation of 2.5 seconds (active state) and an inter-stimulus interval fixation cross of 2.5 seconds (passive state). Participants performed a 1-back memory task and responded via the lumina response pad as to whether the identity in the current image matched that of the previous image. This is the same task that was used in the fMRI study and as described in chapter 2 it was designed to maintain vigilance and to control for attention (see Figure 4.2.1).

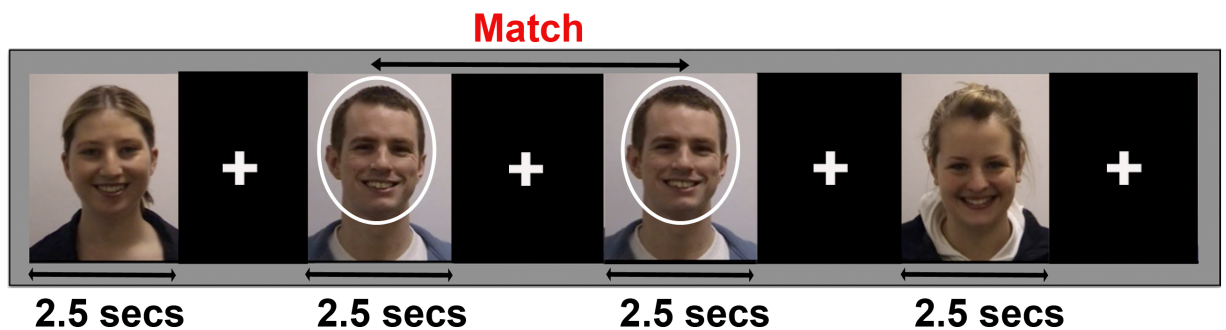


Figure 4.2.1: MEG experimental design: 120 dynamic and 120 static images were presented for 2.5 s in a random sequence, alternating with a 2.5 s fixation cross. Participants (N=14) performed a 1-back memory task and responded via button press as to whether the identity of the current image matched the previous image.

MEG data were recorded using a 275 channel CTF system using 3rd order gradiometer configuration with a sample rate of 600 Hz. Three electromagnetic localisation coils were attached to the participant's head at the nasion and bilateral pre-auricular points in order to localise their head relative to the MEG sensors. Participants were seated in an upright position in the MEG scanner. Visual stimuli were presented using Presentation (Neurobehavioral Systems, Inc.) and participants viewed the computer monitor directly through a window in the shielded room. A polhemus Isotrak 3D digitiser was used to map the surface shape of each participant's head and localise the electromagnetic head coils with respect to that surface. Each participant's head shape file was then extracted and coregistered to a high-resolution T1-weighted anatomical image, which was acquired for each participant prior to the MEG recording, on a 3 Tesla Siemens Magnetom Trio Scanner using an 8-channel radio frequency birdcage head-coil. Coregistration was performed using in-house software based on an algorithm designed to minimise the squared Euc-

clidean distance between the polhemus surface and the MRI surface. This coregistration is accurate to within 5 mm (for further details see Adjamian et al., 2004).

4.2.3 Data analysis

Data for each participant were edited and filtered to remove environmental and physiological artefacts, a 50 Hz powerline filter was used and DC offset was removed, 3rd order gradient noise reduction was also used to remove environmental noise from the data that was picked up by reference coils during acquisition. The MEG data were then analysed using Synthetic Aperture Magnetometry (SAM), which is a spatial filtering ‘beamformer’ technique that can be used to generate statistical parametric maps of stimulus or event-related changes in cortical oscillatory power (see section 1.5). A boxcar experimental design was used to assess spectral power between active (dynamic faces) and passive (static faces) states in beta (12-30 Hz) band power. The difference between the active and passive spectral power estimates was assessed for each voxel using a pseudo t-statistic (Robinson and Vrba, 1999). This produced a 3-D SAM image of cortical activity for each participant under each condition. SAM analysis was computed using 500 ms time windows to assess the main effect of motion by directly comparing power changes in low frequency bands between dynamic and static faces, starting from stimulus onset at 0 ms (0-500, 500-1000, 1000-1500, 1500-2000, 2000-2500 ms). Rather than using a long time window of 2.5 s to cover the length of stimulus display these 500 ms time windows were chosen in order to investigate the temporal progression within the network at multiple time points.

Each participant’s data were normalised and converted to Talairach space using statistical parametric mapping (SPM99, <http://www.fil.ion.ucl.ac.uk/spm>) for group-level comparisons. Non-parametric permutation analysis using SnPM (<http://www.fil.ion.ucl.ac.uk/spm>) was computed to assess significant group effects. Regions of interest were determined based on significant group effects ($p < .05$, corrected) from SnPM showing significant peaks of activation within the face perception network. Virtual electrodes were constructed at the peak locations identified for each participant in the SnPM analysis. These virtual electrodes were based on a covariance matrix constructed using a 5 s window from 2.5 s prior to stimulus onset, to 2.5 s after stimulus onset, with a bandwidth of 12-30 Hz.

Time windows for baseline estimation were of equal duration to the time window of interest to achieve balanced covariance estimation. Time-frequency wavelet plots were then computed on the virtual electrode for a window beginning at 0 s to 2.5 s after stimulus onset. Percent power change from baseline (the 1 s preceding stimulus onset) was computed at each frequency for both dynamic and static stimuli to give mean (across epochs and participants) power increases and decreases for dynamic and static face stimuli. Dynamic and static face stimuli were directly contrasted at each region of interest from 0 s to 2.5 s after stimulus onset, thresholded at $p < .05$.

An important aspect of this study is the direct comparison of two ‘active’ states in the SAM analysis, rather than ‘active’ versus ‘passive’, as used in previous MEG and SAM studies (Singh et al., 2002; Muthukumaraswamy et al., 2006; Lee et al., 2010). In this study dynamic faces were directly compared to static faces not to baseline. This methodology was employed in order to use a more robust control for the dynamic face stimuli (Kaiser et al., 2008) and to maintain consistency with the fMRI study. However, in order to correctly interpret the results from the direct comparison of the dynamic versus static face conditions the baseline comparisons must also be computed. This is because an overall decrease in the dynamic versus static face comparison may be driven by either a decrease in power for dynamic faces or an increase in power for static faces, hence time-frequency plots for the direct comparison along with the two baseline conditions were computed.

4.3 Results

4.3.1 Source analysis results

SAM was computed across five different 500 ms time windows, to identify sources of differential activity between dynamic and static face stimuli across the length of stimulus presentation in the beta frequency band (12 - 30 Hz). Group analysis was performed using SnPM to identify significantly clustered peaks across the group of participants in response to dynamic versus static face stimuli. As predicted group SnPM analysis identified significant decreases in low frequency power in the beta band for dynamic relative to static faces, in regions within the distributed face perception network across

the group of fourteen participants (see Table 4.1 and Figure 4.3.1).

The first time window analysed was from 0 to 500 ms post stimulus onset and this revealed an early decrease in low frequency power in bilateral IOG in response to dynamic relative to static faces. The later time window of 500 ms to 1000 ms again revealed decreases in low frequency power in bilateral IOG, along with bilateral MTG, right STS and left IFG. Within the time window from 1000 ms to 1500 ms, decreases in low frequency power were seen in bilateral IOG, right MTG, right STS, right lingual gyrus, right IFG and left insula. Notably, responses are more right lateralised during this time period and responses in the lingual gyrus, MTG and STS show higher levels of activation as indexed by the higher *t*-values. Interestingly, right STS shows a sustained response from approximately 500 ms to 1500 ms. From 1500 ms to 2000 ms low frequency power decreases were localised to right MTG, bilateral STS, right IOG, right middle occipital gyrus and right IFG. Again these responses appear to be more right lateralised. Finally, from 2000 ms to 2500 ms low frequency power decreases were found in right middle occipital gyrus, right STS, left MTG, left precentral gyrus, right middle frontal gyrus and left IFG (see Table 4.1 and Figure 4.3.1).

4.3.2 Time frequency results

Virtual electrodes were constructed to map the time-frequency characteristics of the regions of interest within the dynamic face perception network. The specific regions of interest selected were bilateral IOG, bilateral MTG and bilateral STS, as these were the most robust regions identified across the group of participants in the SAM source analysis, which also corresponded to the regions identified in the fMRI study in chapter 2 (see Table 4.2 for coordinates of virtual electrodes).

4.3.2.1 Inferior occipital gyri

The virtual electrode constructed in the region in the left IOG (see Figure 4.3.2 a) showed, at the group level, a sustained power decrease within 200 ms of stimulus onset for dynamic faces relative to baseline in the 10–20 Hz frequency range. Static faces compared to baseline showed a slight power increase at approximately 80 ms between 20–30 Hz, followed by a power decrease between 10–25 Hz which was not quite as sustained as the

Table 4.1: Brain regions showing decreases in beta power (12-30Hz) in response to all dynamic compared to static faces within the following time windows (A) 0 to 500 ms (B) 500 to 1000 ms (C) 1000 to 1500 ms (D) 1500 to 2000 ms (E) 2000 to 2500 ms. Co-ordinates indicate local maxima in Talairach space. L = Left; R = Right. Clusters are significant at $p < .05$.

Region	Pseudo t-value	x	y	z
<i>(A) 0 to 500 ms</i>				
L Inferior occipital gyrus (BA 17)	- 3.6	-12	-93	-18
R Inferior occipital gyrus (BA 18)	- 3.24	18	-82	-11
<i>(B) 500 to 1000 ms</i>				
L Middle temporal gyrus (BA 37)	- 4.35	42	-63	0
R Middle temporal gyrus (BA 39)	- 3.83	48	-66	15
L Inferior occipital gyrus (BA 18)	- 3.54	-27	-99	-18
R Inferior occipital gyrus (BA 18)	- 3.47	27	-81	-9
R Superior temporal sulcus (BA 22)	- 2.8	54	-15	0
<i>(C) 1000 to 1500 ms</i>				
L Inferior occipital gyrus (BA 18)	- 6.03	-30	-81	-3
R Middle temporal gyrus (BA 37)	- 5.97	42	-63	9
R Superior temporal sulcus (BA 22)	- 5.35	54	-15	0
R Inferior occipital gyrus (BA 17)	- 5.23	12	-87	-6
L Superior temporal sulcus (BA 13)	- 4.83	-51	-39	18
R Inferior frontal gyrus (BA 46)	- 4	36	30	21
L Insula (BA 13)	- 2.93	-36	21	12
<i>(D) 1500 to 2000 ms</i>				
R Middle temporal gyrus (BA 19)	- 4.96	45	-63	12
R Superior temporal sulcus (BA 22)	- 4.5	57	-9	3
R Inferior occipital gyrus (BA 17)	- 4.1	12	-87	-6
L Superior temporal sulcus (BA 13)	- 3.74	-51	-39	18
R Middle occipital gyrus (BA 18)	- 3.32	15	-99	18
R Inferior frontal gyrus (BA 47)	- 2.85	57	27	-6
R Inferior frontal gyrus (BA 10)	- 2.33	42	39	12
<i>(E) 2000 to 2500 ms</i>				
R Middle occipital gyrus (BA 18)	- 4.34	30	-84	-3
R Superior temporal sulcus (BA 22)	- 3.15	60	-15	0
L Precentral gyrus (BA 6)	- 3.11	-9	-24	68
L Middle temporal gyrus (BA 37)	- 2.71	-45	-45	-60
R Superior temporal sulcus (BA 38)	- 2.43	48	21	-30
R Middle frontal gyrus (BA 10)	- 2.38	39	45	21

Table 4.2: Mean stereotactic co-ordinates for the virtual electrodes in Talairach space. N = number of participants showing a significant peak in a particular region.

Region	N	x	y	z
Left Inferior occipital gyrus	12	-12	-93	-18
Right Inferior occipital gyrus	12	20	-81	-11
Left Middle temporal gyrus	8	-45	-45	-60
Right Middle temporal gyrus	8	42	-63	9
Left Superior temporal sulcus	8	-51	-39	18
Right Superior temporal sulcus	9	57	-9	3

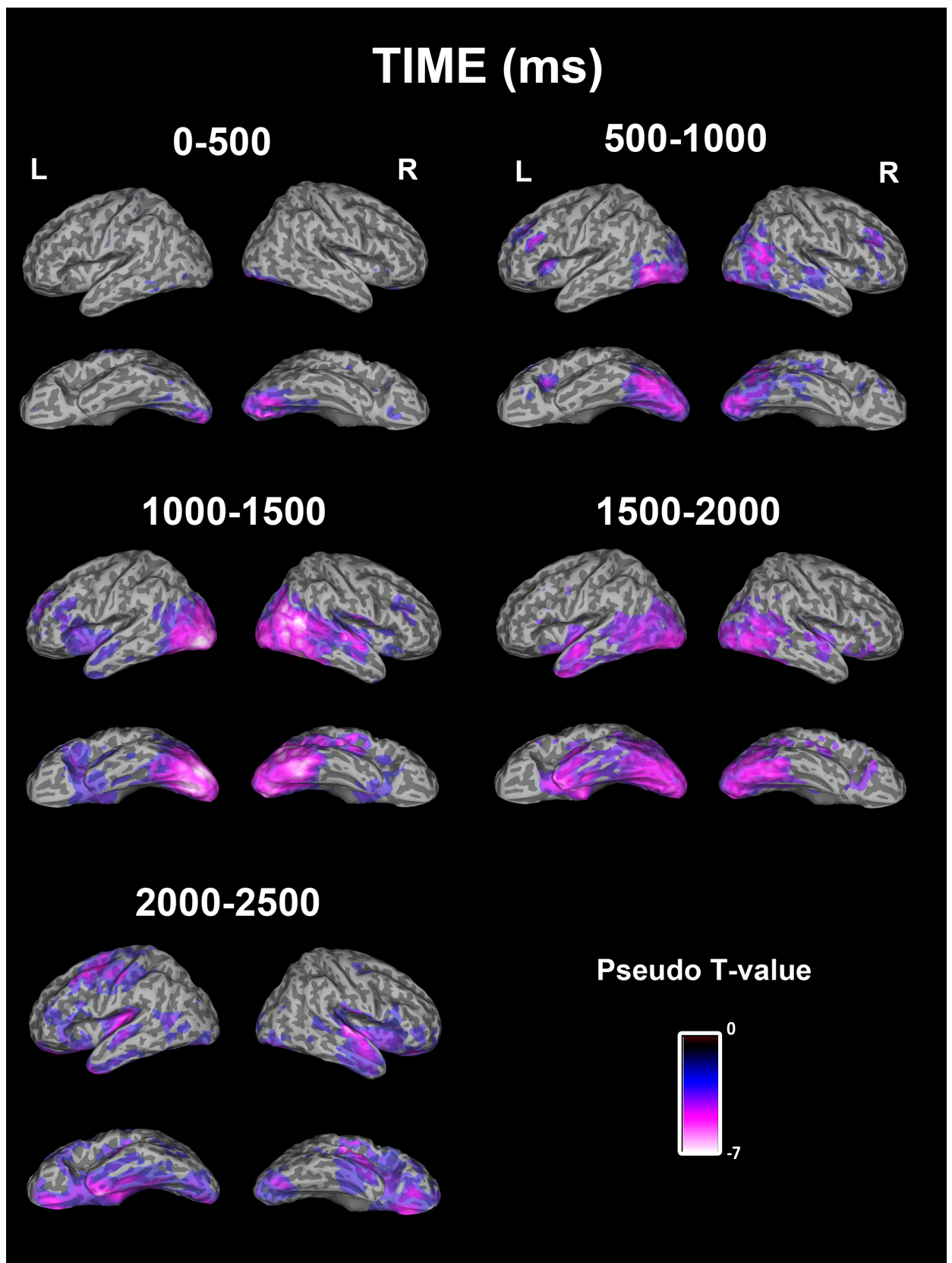


Figure 4.3.1: Group SAM image (N=14) shows decreases in beta power (12–30 Hz) within 5 different time windows 0-500; 500-1000; 1000-1500; 1500-2000; and 2000-2500 ms post stimulus onset. Shows progression of activation within the face perception network over time. Activation is shown in bilateral IOG, MTG, STS, and IFG. Blue-purple-white colour scale represents a decrease in signal power ($p < .05$).

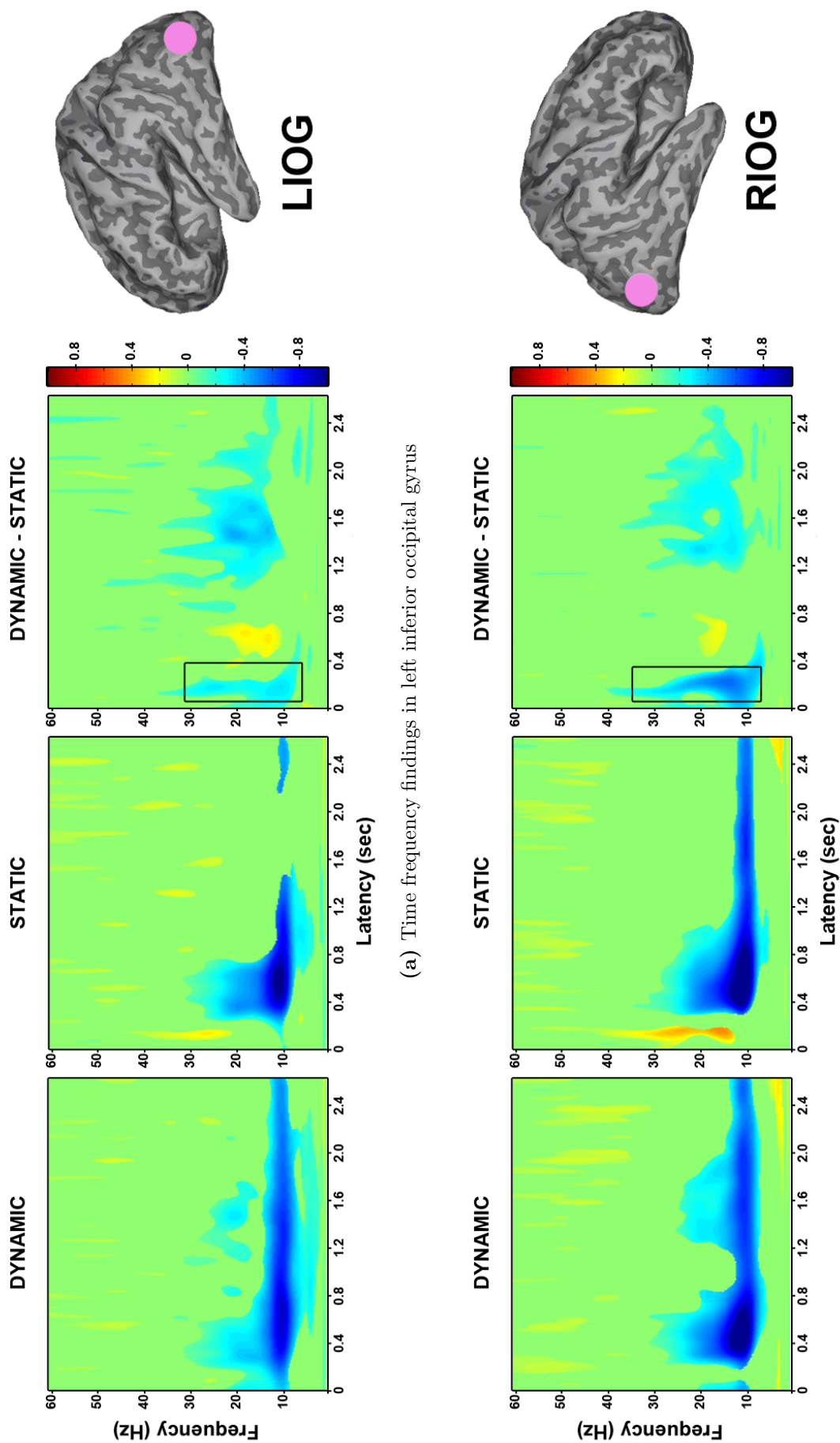
decrease to dynamic faces. The direct comparison of dynamic and static faces showed an early power decrease within the first 200 ms between 10-30Hz followed by a slight increase and then a sustained decrease from approximately 700 ms onwards.

The time frequency characteristics of the virtual electrode constructed in the right IOG were extremely similar to those of the left IOG described above (see Figure 4.3.2 b). When dynamic faces were compared to baseline a sustained power decrease within 200 ms of stimulus onset was found in the 10–20 Hz frequency range. Again static faces compared to baseline showed a slight power increase around 80 ms between 10–30 Hz, followed by a power decrease around 200 ms between 10–20 Hz. When the response to dynamic and static faces was directly compared, an early power decrease within the first 200 ms between 5-30 Hz was found, followed by a later decrease around 800 ms in the 10-20 Hz range.

4.3.2.2 Middle temporal gyri

The virtual electrode constructed in the left MTG (see Figure 4.3.3 a) revealed, at the group level, a sustained decrease in power from approximately 200 ms in the 20–30 Hz frequency range for dynamic faces relative to baseline, followed by a stronger sustained decrease in power from approximately 500 ms between 10-15 Hz. Static faces compared to baseline also showed a power decrease in the 20–30 Hz frequency range, but this was at a slightly later time of 400 ms and was not sustained. A similar decrease in power between 10-15 Hz was also revealed at 500 ms but again it was not as strong or sustained. When dynamic and static faces were directly compared an early power decrease occurred at 200 ms between 12–25 Hz, followed by a decrease in power between 800 ms and 1500 ms in the 10-25 Hz frequency range.

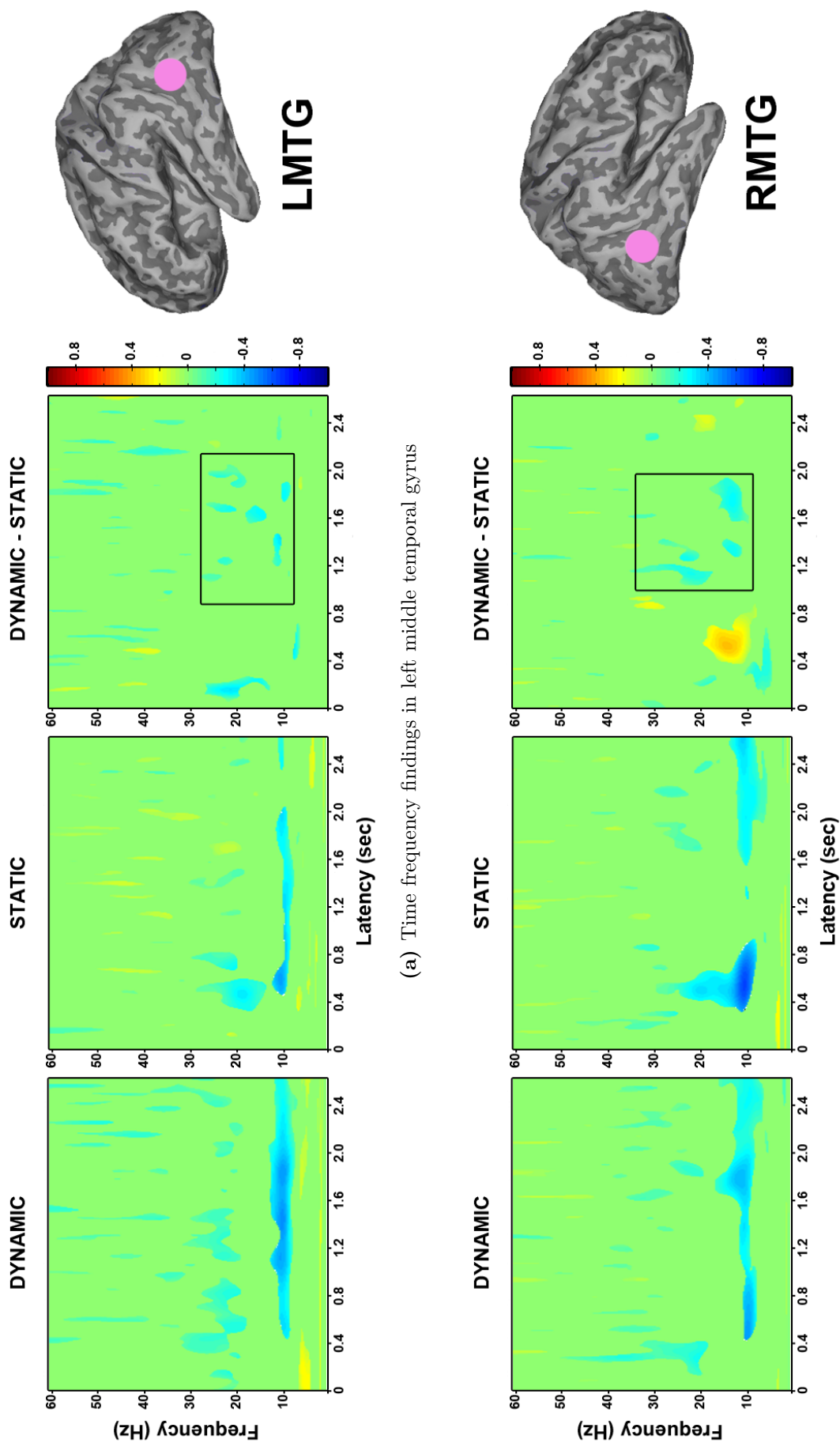
In the right MTG (see Figure 4.3.3 b) the dynamic faces compared to baseline showed a sustained decrease in power from approximately 500 ms, between 10–30 Hz. Static faces compared to baseline revealed a decrease in power between 400 ms and 800 ms in the 10-30 Hz range, followed by a later decrease in power from 1600 ms between 8-25 Hz. The direct contrast of dynamic and static faces showed a power increase from 400 ms to 800 ms between 10–20 Hz, which was driven by the corresponding decrease in power at this time for the static faces. This was followed by a decrease in power between 900 ms



(a) Time frequency findings in left inferior occipital gyrus

(b) Time frequency findings in right inferior occipital gyrus

Figure 4.3.2: Group time frequency findings in: (a) Left inferior occipital gyrus (N=12) shows an early decrease in low frequency power. Left: Dynamic faces compared to baseline shows sustained power decrease within 200 ms of stimulus onset between 10-30 Hz. Middle: Static faces compared to baseline shows slight power increase at 80 ms followed by power decrease between 10-25 Hz. Right: Direct comparison of dynamic and static faces shows early power decrease within first 200 ms between 10-30 Hz; (b) Right inferior occipital gyrus (N=12) shows an early decrease in low frequency power. Left: Dynamic faces compared to baseline shows sustained power decrease within 200 ms of stimulus onset between 10-30 Hz. Middle: Static faces compared to baseline shows slight power increase at 80 ms followed by power decrease between 10-20 Hz. Right: Direct comparison of dynamic and static faces shows early power decrease within 200 ms between 5-30 Hz.



(a) Time frequency findings in left middle temporal gyrus

(b) Time frequency findings in right middle temporal gyrus

Figure 4.3.3: Group time frequency findings in: (a) Left middle temporal gyrus (N= 8). Left: Dynamic faces compared to baseline shows sustained power decrease from 200 ms between 20–30 Hz and sustained power decrease from 500 ms between 10–15 Hz. Middle: Static faces compared to baseline shows power decrease from 400 ms between 20–30 Hz. Right: Direct comparison of dynamic and static faces shows power decrease around 200 ms between 12–25 Hz and power decrease from 800–1500 ms between 10–25 Hz; (b) Right middle temporal gyrus (N= 8). Left: Dynamic faces compared to baseline shows sustained power decrease from 500 ms between 10–30 Hz. Middle: Static faces compared to baseline shows power decrease from 400–800 ms between 10–30 Hz and a later decrease from 1600 ms between 8–25 Hz. Right: Direct comparison of dynamic and static faces shows power increase from 400–800 ms between 10–20 Hz, and a power decrease from 900 ms between 12–30 Hz.

and 2000 ms in the beta frequency range (12-30 Hz) due to the more sustained decrease in power for dynamic faces.

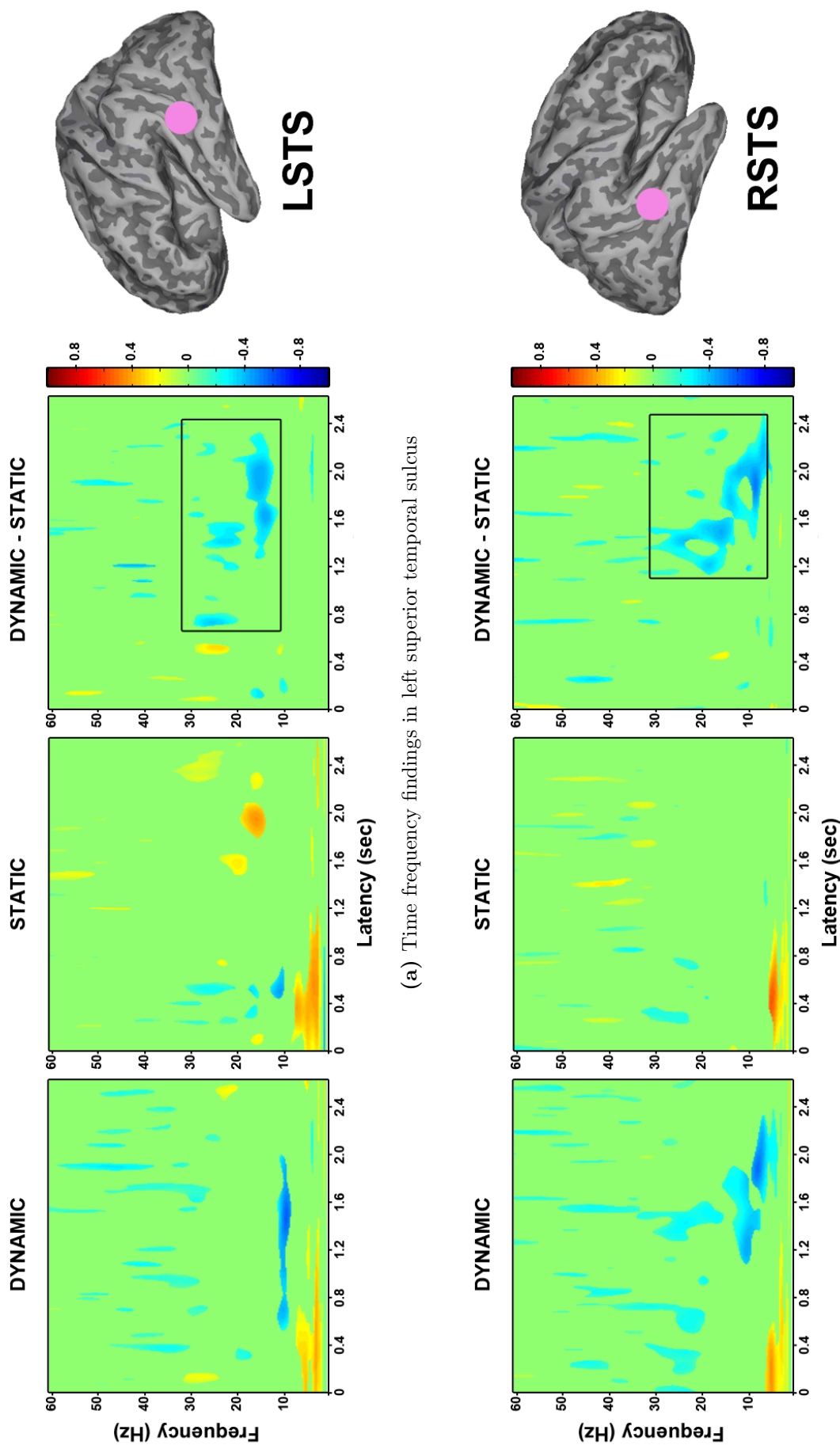
4.3.2.3 Superior temporal sulci

When a virtual electrode was constructed in the left STS (see Figure 4.3.4 a), the contrast of dynamic faces with baseline showed at the group level, a sustained decrease in power from 600 ms onwards around 12 Hz. The static faces elicited a power decrease between 200 ms and 600 ms in the 10–30 Hz range. The direct comparison of dynamic and static faces showed a short power increase at ~500 ms followed by a stronger and more sustained decrease from 800 ms onwards between 10-30 Hz due to the more sustained decrease in power in the dynamic condition.

The virtual electrode constructed in the right STS (see Figure 4.3.4 b) revealed a broad decrease in power between 20–60 Hz from around 200 ms until 1600 ms for the dynamic faces compared to baseline, as well as a more sustained decrease in lower frequency power (5-13 Hz) from 1000 ms onwards. Static faces compared to baseline showed a slight power decrease at 200 ms and again at 600 ms between 20–30 Hz. Finally, the direct contrast of dynamic and static faces revealed a sustained decrease in power from 800 ms onwards between 8-30Hz due to the decrease in power for dynamic faces.

4.4 Discussion

In this chapter MEG and SAM were used to identify neural responses to dynamic compared to static face stimuli and to examine the frequency of oscillations contributing to these responses over various time periods. Based on previous research by Singh et al. (2002), it was hypothesised that responses to dynamic face stimuli would be characterised by decreases in low frequency power in the regions of the distributed neural face perception network that were identified in the fMRI study in chapter 2. As expected, SAM analysis revealed a number of regions showing differential activation to dynamic versus static faces in the distributed face network, including IOG, MTG, STS and IFG, all regions that were previously identified with fMRI in chapters 2 and 3. This was characterised by decreases in cortical oscillatory power in the beta band (12–30 Hz) in these



(a) Time frequency findings in left superior temporal sulcus

(b) Time frequency findings in right superior temporal sulcus

Figure 4.3.4: Group time frequency findings in: (a) Left superior temporal sulcus (N=8). Left: Dynamic faces compared to baseline shows sustained power decrease from 400-2000 ms around 12 Hz. Middle: Static faces compared to baseline shows power decrease from 200-600 ms between 10-30 Hz, and decreases in low frequency power 3-8 Hz from onset to 1000 ms. Right: Direct comparison of dynamic and static faces shows power increase around 500 ms followed by a sustained power decrease from 800 ms onwards between 10-30 Hz; (b) Right superior temporal sulcus (N=9). Left: Dynamic faces compared to baseline shows power decrease (20-60 Hz) between 200-1600 ms, and a sustained decrease in low frequency power (5-13 Hz) from 1000 ms onwards. Middle: Static faces compared to baseline shows slight power decrease between 20-30 Hz at 200 ms and 600 ms. Right: Direct comparison of dynamic and static faces shows a sustained decrease in power from 800 ms onwards between 8-30 Hz.

regions. It was further hypothesised that responses in these different regions would display different temporal patterns of activation, whereby regions centred around the IOG would display early responses, followed by later responses in regions such as MTG and STS. This was confirmed through both the SAM and time frequency analysis.

4.4.1 Temporal progression within the dynamic face perception network

Within the first 500 ms of stimulus onset SAM analysis revealed two regions in left and right IOG, that showed significant decreases in beta band power in response to dynamic versus static face stimuli. This region in IOG forms part of the core system for visual analysis of faces in Haxby et al. (2000)'s model. Furthermore this early response in IOG is consistent with some of the evoked potential studies that localised the M100 to occipital regions (Itier and Taylor, 2002; Liu et al., 2002), although they were using static faces only. Further interrogation of this response through time frequency analysis revealed a number of interesting results. Firstly these two regions, left and right, showed strikingly similar response patterns. Also, there was a decrease in response to both the static and dynamic stimuli within 200 ms of stimulus onset, but overall a greater and more sustained decrease in power to the dynamic stimuli. Interestingly, there was a slight power increase in the static condition. This suggests that the IOG is involved in processing both the static and dynamic face stimuli, but additional processing was required for the dynamic stimuli.

This is consistent with fMRI data showing increased activation in IOG to dynamic faces (Fox et al., 2009; Schultz and Pilz, 2009). The sustained response in IOG has important implications for hierarchical feed forward face perception models, as it suggests that IOG is not only involved in early visual analysis but also plays a role in higher level processing (Atkinson and Adolphs, 2011) such as facial expressions analysis (Pitcher et al., 2008), possibly due to feedback connections from the STS as described in chapter 3.

From 500 ms to 1000 ms a number of additional regions were identified that showed significant decreases in beta power in response to dynamic compared to static face stimuli. Along with bilateral IOG, bilateral MTG and the right STS, also showed power decreases. The area identified here as MTG, that includes area MT, is a well-known region in motion

processing in both the fMRI and MEG literature (e.g. Ahlfors et al., 1999) and we have also previously shown with fMRI that it plays an important role in dynamic face perception (see Foley et al., 2012; and chapter 2). Watanabe et al. (2005) identified area MT as a key region involved in facial motion processing using MEG. They found both eye and mouth movements elicited responses in this region around 170 ms post stimulus onset, with a larger response to eye movements. Krakowski et al. (2011) also found that area MT responded to biological motion between 100 and 200 ms of stimulus onset. Additionally, Singh et al. (2002) report a decrease in low frequency power in the MTG when participants viewed point light displays of biological motion, which is consistent with the results reported here.

Neuroimaging studies have consistently identified the STS as an essential structure in general motion processing, which also incorporates biological motion and dynamic face processing (see chapter 2 and chapter 3). In an MEG study of motion processing Ahlfors et al. (1999) found a sustained response in the STS over the latency range of 200–400 ms. Krakowski et al. (2011), along with Jokisch et al. (2005) and Horovitz et al. (2004), all report that evoked responses to biological motion were generated in the STS. Also, Singh et al. (2002) found decreases in low frequency power in the STS in their biological motion condition. Similarly, Muthukumaraswamy et al. (2006) found decreases in low frequency power in the STS to oro-facial motion. Lee et al. (2010) also found decreased oscillatory responses in the STS to turning heads, although this was in the higher gamma frequency range. Surprisingly, they did not find a similar decrease in the low frequency range. However, they still propose that this decrease in oscillatory power signifies enhanced cortical processing of the dynamic stimuli.

Further interrogation of the response in the STS through time frequency analysis revealed similar response patterns between the left and right STS. There was a short decrease in power between 10-30 Hz, at ~500 ms in both the static and dynamic conditions, but this was followed by a stronger sustained response from 800 ms onwards in the dynamic condition only. Hence the direct comparison of dynamic versus static faces revealed a sustained power decrease at 800 ms between 10-30 Hz. It would appear then that the STS contributes largely to the processing of dynamic faces and to a lesser extent static faces. This is consistent with the results of the fMRI study described in chapter

2, wherein the STS showed significantly greater activation to dynamic faces relative to static. Similarly a recent fMRI study by Pitcher et al. (2011a) report a region in the right posterior STS which responded almost three times more strongly to dynamic relative to static faces. Also, the long duration of the STS response is consistent with Ahlfors et al. (1999) who also found a sustained response in STS to motion stimuli. Furthermore, significant coupling between the STS and both visual regions and frontal regions was found in chapter 3, suggesting that the STS may act as a relay centre between regions involved in early visual perceptual processing and emotion processing. The sustained response in the STS provides converging evidence for this, as it may represent multiple activations which facilitate the integration of information from multiple input areas (Hein and Knight, 2008).

In the time window from 1000 ms to 1500 ms, sources of differential activity were again localised in IOG, MTG and in bilateral STS this time, whereas only right STS was active in the previous time window. Additional regions within the distributed face perception system were also recruited, such as the right IFG and the left insula. Furthermore the core regions such as IOG, MTG, and STS appear to show the largest differences in peak power during this time period compared to previous and subsequent time windows. This may be because the dynamic stimuli are approaching peak expression around this time. The insula was previously identified as showing enhanced activation to dynamic angry stimuli in the fMRI study (see chapter 2 and chapter 3). This analysis provides additional information about the time-course of insula activity, which appears to respond relatively late. Similarly, the IFG was also identified as a structure in the dynamic face perception network in the previous fMRI study. While the insula and IFG have been identified in fMRI studies of face perception, there is little MEG data on these structures. However a recent MEG study by Bayle and Taylor (2010) report an M170 in IFG when participants viewed static fearful faces.

In the subsequent time window from 1500 ms to 2000 ms responses are predominantly right lateralised in IOG, MTG, middle occipital gyrus and IFG, with the exception of the STS which has a bilateral response. In this case the middle occipital gyrus is the only extra region activated in this time period. The middle occipital gyrus is known to play a role in visual processing of stimuli. Again this region was identified in the fMRI study

described in chapters 2 and 3. Finally then in the time window from 2000 ms to 2500 ms regions in middle occipital gyrus, MTG and STS were identified as before, notably the IOG was absent. Additional regions include the right middle frontal gyrus and the left precentral gyrus. Both middle frontal gyrus and precentral gyrus were also reported in the fMRI study (see chapter 2), believed to form part of the mirror neuron system.

Taken together these results reveal a distributed network of brain regions showing differential responses to dynamic relative to static stimuli as characterised by decreases in low frequency power. Furthermore, early differential responses were identified in bilateral IOG within 200 ms, followed by later responses in regions such as MTG and STS within 800 ms of stimulus onset. This early response in IOG followed by later responses in STS is consistent with the findings from a recent MEG study by Furl et al. (2010). They used MEG to examine the effects of dynamic facial expressions, which varied in their predictability and found that predictable expression dynamics evoked very early effects in early visual regions (165 ms), followed by heightened activity in right posterior STS (237 ms). They suggest that early visual regions accumulate information over shorter time intervals and thus respond faster, while the STS accumulates information over longer time intervals resulting in a later response and enabling the integration of information from multiple sites. Additional regions, including the insula, IFG and middle occipital gyri all showed decreased beta responses to dynamic face stimuli at relatively late latencies from 1000 ms.

An important aspect of this study that may have influenced the results is that two ‘active’ states were compared in the SAM analysis rather than ‘active’ versus ‘passive’ i.e. dynamic faces were compared to static faces not to baseline. In the majority of studies using SAM analysis an ‘active’ state is compared with a ‘passive’ state, generally represented by a pre-stimulus baseline period (Singh et al., 2002; Muthukumaraswamy et al., 2006; Lee et al., 2010). However in this MEG study a direct comparison between two active states was made between the dynamic and the static face stimuli. This methodology was employed in order to use a more robust control for the dynamic face stimuli and to maintain consistency with the fMRI study described in chapter 2. A recent study by Kaiser et al. (2008) report that direct contrasts may yield more focal oscillatory activations than comparing pre-versus post-stimulus responses. Hence the patterns of activation seen here may be more

focal than previous studies.

Notably, all the regions identified during the SAM analysis as showing decreased beta responses to dynamic stimuli correspond very closely with the regions of the dynamic face perception network that were previously identified with fMRI in chapter 2 (see Table 2.1 and Table 4.1). This shows strong concordance between these two different imaging techniques and further extends Haxby et al. (2000)'s model by demonstrating the temporal progression and frequency of responses that contribute to dynamic face perception. This will be discussed further in chapter 6.

4.4.2 Summary

Early differential responses to dynamic face stimuli were identified in bilateral IOG within 200 ms, followed by later responses in MTG and STS, within 800 ms of stimulus onset. These were all characterised by decreases in beta band oscillatory power. Additional regions including the insula, IFG and middle occipital gyri also showed decreases in beta band power in response to dynamic relative to static face stimuli from ~1000 ms post stimulus onset.

Chapter 5

The timecourse and oscillatory responses to facial displays of emotion

5.1 Introduction

5.1.1 Overview

In the previous chapter MEG and SAM were used to identify regions of differential activation in response to dynamic relative to static faces, where the timing and frequency of oscillations contributing to these responses were examined. This revealed a network of regions showing differential responses to dynamic face stimuli over different latencies. Early differential responses were identified in bilateral IOG within 200 ms, followed by later responses in regions such as MTG and STS, within 800 ms of stimulus onset, which were all characterised by decreases in beta band oscillatory power. Additional regions including the insula, IFG and middle occipital gyri also showed decreases in beta band power for dynamic relative to static face stimuli from ~1000 ms onwards. Furthermore, despite the differences between MEG and fMRI imaging techniques, the regions localised by SAM corresponded closely with the regions of the dynamic face perception network that were identified with fMRI in chapter 2.

However, because the aim of chapter 4 was to assess the main effect of motion, the individual facial expression categories were not differentiated during the analysis. Therefore

the effects of motion on the processing of different face stimuli was not examined and the effects of emotion-specific facial dynamics were not explored. This will be addressed in the present chapter by explicitly contrasting the dynamic and static stimuli for each of the different affects, as well as contrasting the dynamic affects with dynamic speech displays, and examining the time frequency characteristics of the responses. Planned pairwise comparisons were computed within each emotion category to examine the effects of motion on the processing of different face stimuli (i.e. dynamic angry versus static angry expressions, dynamic happy versus static happy expressions, and dynamic speech versus static speech displays). Contrasts were also computed to investigate the effects of emotion-specific facial dynamics by contrasting both of the dynamic affective expressions (angry and happy) with dynamic speech facial displays.

5.1.2 Emotional face perception

In chapter 2 it was shown that broadly similar regions within occipito-temporal cortex were involved in processing the different dynamic stimuli, particularly in the core face perception system, including middle occipital gyri, MTG and STS. Consistent with this, the measures of effective connectivity defined in chapter 3 revealed that the effective connectivity when viewing dynamic facial stimuli in general was associated with specific increases in connectivity between early visual regions, such as IOG, and the STS in the dorsal pathway, which was broadly similar for all of the different dynamic stimuli. However, some differences between activation patterns for each of the different dynamic facial expressions, particularly in regions of the extended system were found.

There has been some debate over the extent to which distinct neural sub-systems are involved in the processing of specific emotions. Some researchers have proposed that distinct neural sub-systems exist that are specialised to process specific facial emotions (Calder et al., 2001). This theory is largely based on the fact that many neuroimaging studies on emotional processing, in particular fMRI studies, have implicated differing brain regions for different emotions (Adolphs, 2002b). However, these studies do not take the timing of emotional face processing into account. It is possible that rather than separate emotion-specific networks specialised in processing distinct emotions, it may be that brain regions involved in emotion processing become active in emotion-specific time

sequences (Esslen et al., 2004). Thus, the time course of emotional face processing should be explored in order to gain a better understanding of emotion processing in the brain. MEG is an ideal tool to use because of its excellent temporal resolution, this combined with SAM source analysis means reliable localisation can also be obtained.

The timecourse of facial expression processing was discussed in detail in chapter 1 (see subsection 1.3.4.1). To recap briefly, electrophysiological studies of emotional face perception have demonstrated emotion effects arising at both early and late latencies (Vuilleumier and Pourtois, 2007). Many of these studies have focused on the face selective N170 or M170 by using EEG or MEG to examine the effect of emotion on this face-selective component. A number of studies have reported some emotional modulations on the amplitude and latency of the N170 (Vuilleumier and Pourtois, 2007). On the other hand, some researchers have found that the N170 component is not affected by emotional facial expressions (Krolak-Salmon et al., 2001; Münte et al., 1998).

Some studies have also reported an influence of emotional expression on very early brain responses even prior to the N170 at approximately 100 ms (Pizzagalli et al., 1999; Eger et al., 2003). Additionally, several studies have reported later effects associated with the perception of emotional facial expressions, from around 200 ms post-stimulus onset (Münte et al., 1998; Krolak-Salmon et al., 2001; Sato et al., 2001). Many of these late ERP responses to emotional facial expressions have also been found to be sustained over prolonged periods of time following stimulus onset (Krolak-Salmon et al., 2001; Ashley et al., 2004), which do not seem specific to particular expressions and therefore may reflect more complex cognitive processes related to emotion processing (Vuilleumier and Pourtois, 2007).

5.1.3 Frequency characteristics of emotional face processing

While ERP and fMRI studies have provided valuable information on the temporal and spatial localisation of brain processes involved in emotional face processing (see chapter 1), the frequency characteristics of the underlying processes have been less studied (Knyazev et al., 2008). More recently the analysis of ERPs has been complemented by the analysis of oscillatory brain activity. One great advantage of analysing induced oscillatory activity is the fact that processes do not need to be precisely time-locked to an event. This is

particularly relevant when using natural dynamic visual stimuli, such as those used in the present study, as they vary in the development of the motion, thus not providing a clear emotion recognition point. Although brain oscillations have recently been investigated in various sensory modalities, their role for brain functioning remains unclear. However, it has been proposed that emotional content may be indexed by oscillatory activity and the full range of frequency bands including, delta (0.5–3.5 Hz), theta (4–7 Hz), alpha (8–12 Hz), beta (13–30 Hz) and gamma (>30 Hz), have been associated with face and emotion processing in one way or another (Güntekin and Basar, 2009).

In a recent EEG study Balconi and Lucchiari (2006) explored brain oscillations involved in emotional face processing by measuring changes in power across different frequency bands in response to different facial expressions of emotion (angry, happy, sad, fear and neutral) during a passive viewing task. They reported desynchronisation of alpha and beta oscillations upon presentation of all facial stimuli, while theta and delta frequencies responded specifically to emotional faces. They found a sustained synchronisation in delta oscillations over posterior regions from 150–350 ms followed by a gradual desynchronisation, notably there was greater synchronisation to emotional stimuli from 150–250 ms, but from 250–350 ms synchronisation was elicited by all face stimuli. They observed frontal theta synchronisation during emotional stimulus presentation at a slightly earlier latency followed by an earlier desynchronisation at 250 ms.

In a subsequent EEG study Balconi and Pozzoli (2009) explored changes in oscillatory power specifically in delta, theta, alpha and gamma bands, during the processing of emotional (angry, happy, sad, fearful) and neutral facial expressions. Once again they found that delta and theta responses were significantly modulated by the emotional stimuli, in addition gamma band modulations by emotion were also reported, while alpha power was not responsive to emotion specifically, rather to all face stimuli. Delta and theta bands displayed similar response patterns as before, where again they both showed a greater synchronisation in the 150-250 ms time interval to the emotional stimuli relative to neutral, but differed in the successive time interval from 250–350 ms, as theta band activity was related to the emotional content while delta responded similarly to all stimuli. In the gamma band then, the pattern of results were the same as in the theta band, as gamma synchronisation was mainly present within the second time window (with a peak latency

of 240 ms), and was observed to be sensitive to the high arousing emotions, such as anger and fear in comparison with happiness and sadness.

Luo et al. (2007) also found that gamma band synchronisation was associated with emotional face processing, specifically with negative facial expressions of emotion. They used MEG and SAM source analysis to examine gamma oscillatory responses to facial expressions of fear, anger and neutral facial expressions during a gender discrimination task. They found significant gamma band synchronisation in different areas of the brain including occipito-temporal cortex, amygdala and prefrontal cortex in response to the different facial stimuli. Gamma band synchronisation in occipito-temporal cortex, including the fusiform gyrus, showed a similar profile for all three facial displays, with an early onset of 40 ms. Gamma band synchronisation in the amygdala occurred very early for fearful faces within 20–30 ms and at a later latency for angry faces at approximately 150–160 ms. There was no significant gamma synchronisation in the amygdala or prefrontal cortex for neutral faces. Angry faces elicited a significant increase in gamma power in right anterior cingulate cortex at ~200 ms and left orbitofrontal cortex at a similar time of 200 ms. The authors suggest that gamma oscillatory responses are involved in higher-level emotional and cognitive processing.

Beta oscillatory responses have also been associated with emotional face processing and have previously been shown to play an important role in face recognition and the differentiation of known and unknown faces (Ozgoren et al., 2005). In an EEG study Güntekin and Basar (2007) examined neural oscillatory responses to emotional facial expressions of anger and happiness relative to neutral, during a passive viewing paradigm. They also assessed participants level of emotional involvement through questionnaire after the experiment. They found significant differences in oscillatory responses to angry and happy facial expressions in the alpha (9–13 Hz) and beta (15–24 Hz) frequency ranges, but only for highly arousing expressions. Angry faces evoked higher amplitude responses in alpha and beta bands compared to happy expressions. Alpha responses were found in posterior cortical regions, whereas beta responses were found in anterior regions. This is in contrast to the study by Balconi and Lucchiari (2006) where they did not find differences in beta power, but Güntekin and Basar (2007) attributes these conflicting results to differences in valence and arousal related to the different stimuli used.

However, as noted in previous chapters, an important aspect that has been overlooked in all of the studies described so far is the inherent dynamic nature of facial expressions of emotion. As most of these studies have used static facial stimuli, many from the Ekman and Friesen (1976) collection, the question arises which brain regions are involved in the processing of more natural dynamic emotional stimuli and do they display similar temporal and frequency responses as static faces? It appears that only one study so far has used dynamic stimuli to investigate the spatiotemporal profile of emotion processing. In a recent EEG study Jessen and Kotz (2011) used dynamic audiovisual stimuli to explore the temporal processing of multimodal emotional expressions of fear, anger and neutral faces.

In this study auditory stimuli were presented as sounds of different emotional interjections such as “ah”, visual stimuli were video clips displaying emotional body language, and the audiovisual stimuli were the video clips presented with their corresponding interjections. Participants performed two tasks one was an explicit emotion judgement task and the other was an implicit task. In the alpha band emotional modulation was only observed in the visual condition but not in the audio or audiovisual conditions. In the visual condition the comparison of both, angry and fearful displays relative to the neutral condition showed significant decreases in alpha power at bilateral posterior electrodes between 300 and 700 ms. In the beta band there was a greater decrease in power in response to emotional stimuli relative to neutral in all three conditions. The contrast of angry emotional displays to neutral displays revealed two significant clusters of decreased beta power in the right hemisphere, one between 250 and 500 ms and one between 650 and 900 ms. Displays of fearful body language contrasted with neutral stimuli revealed a decrease in beta power bilaterally in posterior regions. Unfortunately they did not perform source analysis in this study so it is difficult to precisely localise these responses.

5.1.4 Objectives and hypotheses

As described above there are a number of studies investigating many different aspects of emotional face processing, many have used conventional ERP methods which provide excellent temporal resolution but poor spatial resolution, others have investigated frequency characteristics but lack source localisation, and only one study (Jessen and Kotz, 2011)

has used dynamic stimuli but with no source localisation. The present study aims to thoroughly investigate the neural processes involved in emotional face perception by examining location, temporal structure and frequency information of the implicated neural regions, using more natural dynamic stimuli. Also, to assess to what extent emotion-specific networks are involved in processing different dynamic facial expressions of emotion, or if similar neural regions are involved but are activated at different time points. Planned pairwise comparisons were computed within each emotion category (matching those used in the fMRI analysis in chapters 2 and 3) to examine the effects of motion on the processing of different facial expressions (i.e. dynamic angry versus static angry expressions, dynamic happy versus static happy expressions, and dynamic speech versus static speech displays). Contrasts were also computed to investigate the effects of emotion-specific facial dynamics by contrasting both of the dynamic affective expressions (angry and happy) with dynamic speech facial displays.

The spatial haemodynamic response profiles of the different dynamic facial expressions were previously established with fMRI in chapters 2 and 3. In this chapter then, MEG and SAM will be used to interrogate these responses further by examining the timing and frequency of oscillations contributing to them. It is predicted that dynamic angry, happy and speech displays will elicit larger decreases in alpha and beta oscillatory power, relative to their static counterparts, in those regions previously identified with fMRI in chapter 2, due to enhanced neural processing for dynamic expressions (Singh et al., 2002; Jessen and Kotz, 2011). It is also predicted that delta and theta frequency bands will show emotional modulations for angry and happy facial stimuli, based on findings from Balconi and Lucchiari (2006) and Balconi and Pozzoli (2009) showing greater synchronisation to emotional facial displays in these frequency bands. It is evident from the literature that emotional face processing can occur over both short and extended periods of time and within multiple frequency bands. Therefore a wide frequency band (1–80 Hz) was used in this analysis over multiple short time windows in order to perform a thorough analysis of emotional face processing.

5.2 Methods

5.2.1 MEG participants

Fourteen healthy self-reported right-handed volunteers (5 male) with normal or corrected to normal vision (mean age 29.2, S.D. 2.45 years) gave full written informed consent to take part in the study, which was approved by the Aston University Human Science Ethical Committee. Again these are the same participants that were described in chapter 4 and were naive participants who had not participated in the previous fMRI study described in chapters 2 and 3.

5.2.2 Experimental design and imaging paradigm

The stimuli and experimental design are the same as those described in chapter 4, but for ease of reading the details will be outlined again here. In order to facilitate comparisons between the fMRI and MEG studies the same stimuli were used in both studies (see chapter 2 for details). The paradigm was altered slightly from the block design that was used in the fMRI study to an event related design, to optimise results from the SAM analysis. A sample of twenty-four stimuli (twelve dynamic and twelve corresponding static images) were presented in an event related design and participants were instructed to maintain central fixation throughout the experiment. Consistent with the fMRI study (see chapter 2 and chapter 3) two emotion categories were included, specifically, angry and happy, along with a speech category which was included as a control for non-affective facial motion.

In the dynamic condition four different stimuli were presented in each of the three emotion categories, and likewise in the static condition. Stimuli were completely randomised and presented for 2.5 seconds with 2.5 seconds of baseline (fixation cross) presented before each stimulus. There were 240 trials in an experimental run. Each trial consisted of a single stimulus presentation of 2.5 seconds (active state) and an inter-stimulus interval fixation cross of 2.5 seconds (passive state). Participants performed a 1-back memory task and responded via the lumina response pad as to whether the identity in the current image matched that of the previous image. This is the same task that was used in the fMRI study and as described in chapter 2 it was designed to maintain vigilance and to

control for attention (see Figure 5.2.1).

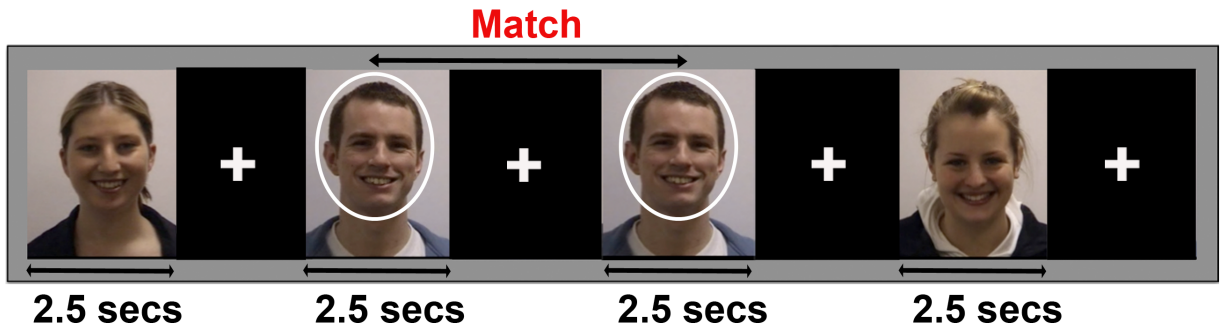


Figure 5.2.1: MEG experimental design: 120 dynamic and 120 static images were presented for 2.5 s in a random sequence, alternating with a 2.5 s fixation cross. Participants (N=14) performed a 1-back memory task and responded via button press as to whether the identity of the current image matched the previous image.

MEG data were recorded using a 275 channel CTF system using 3rd order gradiometer configuration with a sample rate of 600 Hz. Three electromagnetic localisation coils were attached to the participant's head at the nasion and bilateral pre-auricular points in order to localise their head relative to the MEG sensors. Participants were seated in an upright position in the MEG scanner. Visual stimuli were presented using Presentation (Neurobehavioral Systems, Inc.) and participants viewed the computer monitor directly through a window in the shielded room. A polhemus Isotrak 3D digitiser was used to map the surface shape of each participant's head and localise the electromagnetic head coils with respect to that surface. Each participant's head shape file was then extracted and coregistered to a high-resolution T1-weighted anatomical image, which was acquired for each participant prior to the MEG recording, on a 3 Tesla Siemens Magnetom Trio Scanner using an 8-channel radio frequency birdcage head-coil. Coregistration was performed using in-house software based on an algorithm designed to minimise the squared Euclidean distance between the polhemus surface and the MRI surface. This coregistration is accurate to within 5 mm (for further details see Adjamian et al., 2004).

5.2.3 Data analysis

Data for each participant were edited and filtered to remove environmental and physiological artefacts, a 50 Hz powerline filter was used and DC offset was removed, 3rd order gradient noise reduction was also used to remove environmental noise from the data that was picked up by reference coils during acquisition. The MEG data were then analysed

using Synthetic Aperture Magnetometry (SAM), which is a spatial filtering ‘beamformer’ technique that can be used to generate statistical parametric maps of stimulus or event-related changes in cortical oscillatory power. A boxcar experimental design was used to assess spectral power between different active and passive states, this time within a broad frequency band from 1-80 Hz. Consistent with the fMRI analyses preplanned comparisons were computed for the following five different contrasts of active and passive states: dynamic angry versus static angry expressions, dynamic happy versus static happy expressions, dynamic speech versus static speech displays, dynamic angry versus dynamic speech facial displays, and dynamic happy versus dynamic speech facial displays.

The difference between the active and passive spectral power estimates was assessed for each voxel using a pseudo t-statistic (Robinson and Vrba, 1999). This produced a 3-D SAM image of cortical activity for each participant under each condition. SAM analysis was computed using 200 ms time windows to directly compare power changes in a broad frequency band (1-80 Hz) for the three different contrasts, starting from stimulus onset at 0 ms (0 - 200, 200–400, 400–600, 600–800, 800–1000, 1000-1200, 1200-1400, 1400-1600, 1600-1800, 1800-2000, 2000-2200, 2200-2400 ms). These short time windows were used for two reasons, firstly because a broadband SAM was used it is advantageous to use a narrower time window to construct the covariance matrix. Secondly, to investigate the temporal progression within the network at different time points where early, late and intermediate effects can be detected.

Each participant’s data were normalised and converted to Talairach space using statistical parametric mapping (SPM99, <http://www.fil.ion.ucl.ac.uk/spm>) for group-level comparisons. Non-parametric permutation analysis using SnPM (<http://www.fil.ion.ucl.ac.uk/spm>) was computed to assess significant group effects. Regions of interest were determined based on significant group effects ($p < .05$, corrected) from SnPM showing significant peaks of activation within the face perception network. Virtual electrodes were constructed at the peak locations identified for each participant in the SnPM analysis. These virtual electrodes were based on a covariance matrix constructed using a 4.8 second window from 2.4 s prior to stimulus onset, to 2.4 s after stimulus onset, with a bandwidth of 1-80 Hz. Time windows for baseline estimation were of equal duration to the time window of interest to achieve balanced covariance estimation. Time-frequency wavelet plots were

then computed on the virtual electrode for a window beginning 0 ms to 2400 ms after stimulus onset. Percent power change from baseline (the 1 s preceding stimulus onset) was computed at each frequency for both dynamic and static stimuli to give mean (across epochs and participants) power increases and decreases for the different active and control stimuli. Then active and control face stimuli were directly contrasted at each region of interest from 0 ms to 2400 ms after stimulus onset, thresholded at $p < .05$.

Similar to the analysis method used in chapter 4, two 'active' states are directly compared in the SAM analysis, rather than 'active' versus 'passive', as used in previous MEG and SAM studies (Singh et al., 2002; Muthukumaraswamy et al., 2006; Lee et al., 2010). For example, in this study dynamic angry faces were directly compared to static angry faces rather than to baseline fixation. This methodology was employed in order to use a more robust control for the dynamic face stimuli (Kaiser et al., 2008) and to maintain consistency with the fMRI study (see chapter 2). However, in order to correctly interpret the results from the direct comparisons of the dynamic facial stimuli with their static counterparts and with dynamic speech, the baseline comparisons must also be computed. This is because, for example an overall decrease in the dynamic angry versus static angry facial expression comparison may be driven by either a decrease in power for dynamic angry faces or an increase in power for static angry faces, hence time-frequency plots for the direct comparison along with the two baseline conditions were computed.

5.3 Results

5.3.1 Dynamic facial expressions of anger

5.3.1.1 Source analysis results

SAM was computed across twelve different 200 ms time windows using a wide frequency band of 1-80 Hz, to identify sources of differential activity between dynamic angry and static angry facial expressions across the length of stimulus presentation. Group analysis was performed using SnPm to identify significantly clustered peaks across the group of participants in response to dynamic versus static angry face stimuli. In the first time window from 0 to 200 ms two regions were identified, one in left IOG and the other in right STS, that showed significant decreases in oscillatory power for dynamic angry

relative to static angry expressions across the group.

The next time window showing significant peaks of differential activity was from 400–600 ms post-stimulus onset, where regions in both left middle occipital gyrus and right MTG, showed significantly greater power in response to dynamic angry relative to static angry displays. In the following time window from 600–800 ms a peak was found in left superior frontal gyrus which showed a significant decrease in power to dynamic angry relative to static angry expressions. Two further regions were identified in the next time window from 800–1000 ms in bilateral IOG, which showed significantly less power in response to dynamic relative to static angry expressions. The final time window showing significant peaks of activation was from 1800 to 2000 ms where regions in left middle frontal gyrus and right superior frontal gyrus showed significantly less power in response to dynamic angry relative to static angry expressions. No significant differences were found in any of the other time windows analysed (see Table 5.1).

Table 5.1: Brain regions showing significant differences in oscillatory power in response to dynamic angry versus static angry facial expressions within the following time windows: (A) 0–200 ms (B) 400–600 ms (C) 800–1000 ms (D) 1800–2000 ms. Co-ordinates indicate local maxima in Talairach space. Clusters are significant at $p < .05$. N = number of participants showing a peak in that region. L= Left, R = Right.

Region	N	Pseudo t	x	y	z
<i>(A) 0–200 ms</i>					
L Inferior occipital gyrus (BA 18)	12	- 5.37	-30	-86	-15
R Superior temporal sulcus (BA 39)	11	- 5.78	48	-52	12
<i>(B) 400–600 ms</i>					
L Middle occipital gyrus (BA 19)	10	+ 5.89	-27,	-78	18
R Middle temporal gyrus (BA 39)	12	+ 5.2	42	-63	18
<i>(C) 800–1000 ms</i>					
L Inferior occipital gyrus (BA 18)	11	- 4.87	-30	-84	-9
R Inferior occipital gyrus (BA 18)	10	- 5.64	36	-87	-9
<i>(D) 1800–2000 ms</i>					
L Middle frontal gyrus (BA 10)	8	- 3.97	-33	42	18
R Superior frontal gyrus (BA 8)	8	- 3.86	21	18	45

SAM was also computed across twelve different 200 ms time windows using a wide frequency band of 1–80 Hz, to identify sources of differential activity between dynamic angry and dynamic speech facial displays across the length of stimulus presentation. Once again group analysis was performed using SnPm to identify significantly clustered peaks across the group of participants (see Table 5.2). Two regions were identified as showing significantly greater power for dynamic angry relative to dynamic speech displays in the 200–400

ms time window, one in left IFG and the other in right IFG. A region in right STS was identified as showing significantly less power for dynamic angry relative to dynamic speech displays in the 600-800 ms time window. Two regions in bilateral IOG showed significantly less power for dynamic angry versus dynamic speech displays from 800-1000 ms. Finally, a region in the right insula showed significantly greater power for dynamic angry compared to dynamic speech displays during the 800-1000 ms time windows. No significant differences were found in any of the other time windows analysed.

Table 5.2: Brain regions showing significant differences in oscillatory power in response to dynamic angry facial expressions versus dynamic speech facial displays within the following time windows: (A) 200-400 ms (B) 600-800 ms (C) 800-1000 ms. Co-ordinates indicate local maxima in Talairach space. Clusters are significant at $p < .05$. N = number of participants showing a peak in that region. L= Left, R = Right.

Region	N	Pseudo t	x	y	z
<i>(A) 200-400 ms</i>					
L Inferior frontal gyrus (BA 46)	12	+3.55	-50	20	12
R Inferior frontal gyrus (BA 45)	11	+3.43	48	18	14
<i>(B) 600-800 ms</i>					
R Superior temporal sulcus (BA 22)	12	-3.42	50	-54	16
<i>(C) 800-1000 ms</i>					
L Inferior occipital gyrus (BA 18)	13	-4.27	-32	-86	-15
R Inferior occipital gyrus (BA 18)	14	-4.54	3	-86	-12
R Insula (BA 13)	8	+3.45	36	22	12

5.3.1.2 Time frequency results

Dynamic angry versus static angry facial expressions. Virtual electrodes were constructed at the peak locations identified by SAM in order to examine the time-frequency characteristics of these regions of interest. Virtual electrodes were only constructed for those participants who showed a peak at the selected location in the SAM volume. The first virtual electrode was constructed in the left IOG where an early difference between dynamic angry and static angry expressions was found within 200 ms of stimulus onset in twelve of the fourteen participants (see Figure 5.3.1). This difference appears to be due to the strong decrease in power to dynamic angry faces which occurs from stimulus onset. The time-frequency maps show a sustained decrease in power to dynamic angry faces relative to baseline from stimulus onset in the 8-20 Hz range, while static faces show a decrease in power slightly later at ~200s in a similar frequency band from 8-20 Hz, with a shorter latency until ~1s and also an increase in power around 100

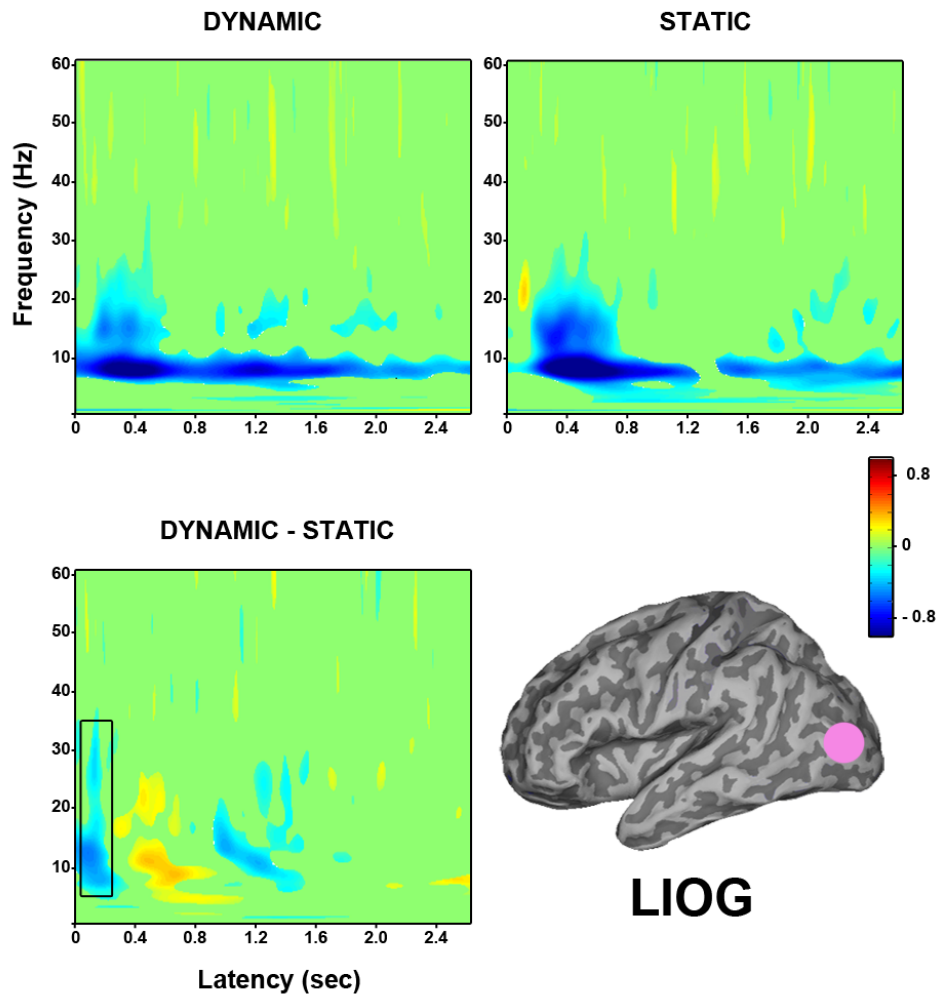


Figure 5.3.1: Group time frequency findings in left inferior occipital gyrus (N=12), shows early differences between dynamic angry and static angry expressions around 200 ms. This is due to a larger decrease in power for dynamic angry expressions between 8-35 Hz within 0-200 ms. Top left: Dynamic angry faces versus baseline fixation; Top right: Static angry faces versus baseline fixation; Bottom left: Dynamic versus static angry faces.

ms from 25-35 Hz. Dynamic versus static angry faces then, show an early power decrease from 8-35 Hz due to the early decrease in the dynamic condition and the increase to static faces around 100 ms.

An early difference was also found in the right STS again within 200 ms of stimulus onset in eleven of the fourteen participants (see Figure 5.3.2). Again this difference is due to the early decrease in power in response to dynamic angry expressions, where they elicit an early decrease within 100 ms of stimulus onset sustained until ~1500 ms in the 10–40 Hz range. Static angry expressions elicit a shorter decrease in power from around 200–500 ms at 10–40 Hz. The direct comparison of dynamic and static angry expressions reveals an early power decrease at ~10 Hz and 22–30 Hz within 200 ms of stimulus onset, which

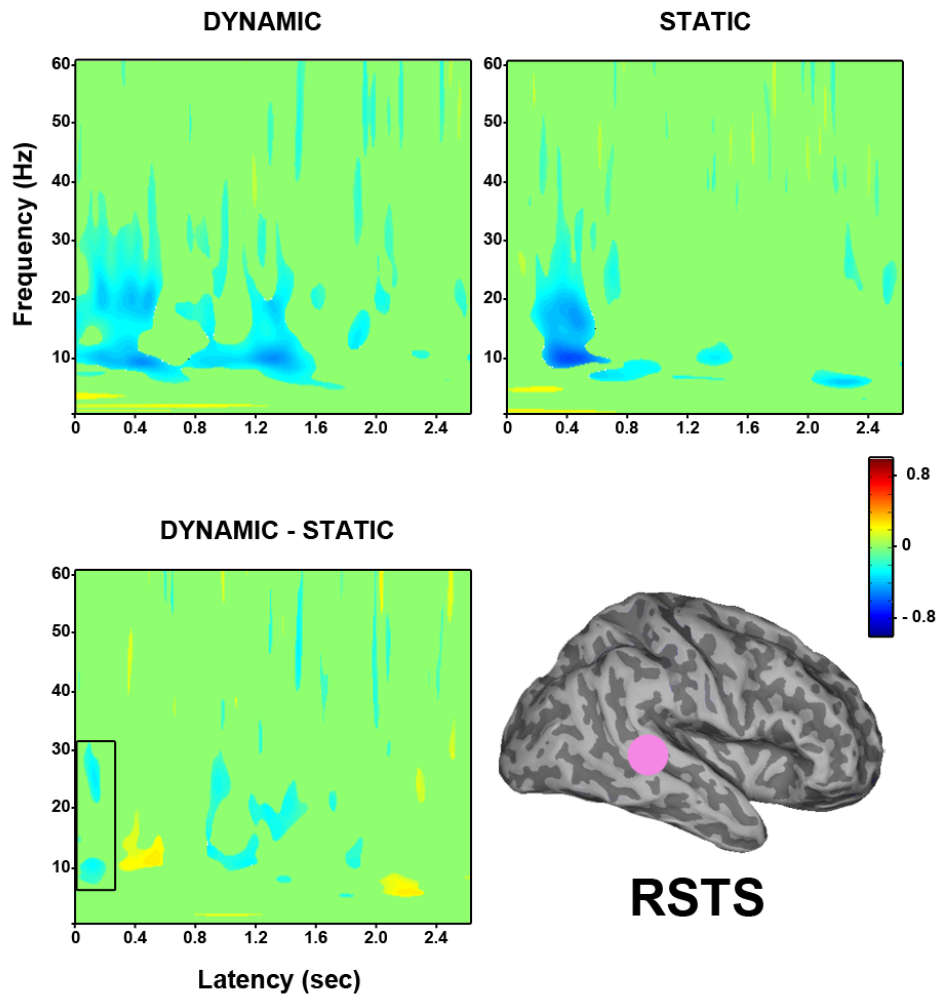


Figure 5.3.2: Group time frequency findings in right superior temporal sulcus (N=11), shows early differences between dynamic angry and static angry expressions within 200 ms. This is due to a larger decrease in power for dynamic angry expressions between 8-30 Hz within 0-200 ms. Top left: Dynamic angry faces versus baseline fixation; Top right: Static angry faces versus baseline fixation; Bottom left: Dynamic versus static angry faces.

is due to the early decrease in the dynamic angry condition.

A region in the left middle occipital gyrus showed a significant difference between dynamic and static angry expressions during the 400-600 ms time window (see Figure 5.3.3), with greater power in the dynamic angry condition this time, in twelve of the fourteen participants. A virtual electrode constructed at this region shows a decrease in power to dynamic angry expressions from 200-500 ms in the 10-25 Hz range, while static faces show a larger decrease from 300-600 ms between 8-28 Hz. Dynamic versus static angry expressions show an early decrease from 5-35 Hz followed by an increase centred around 500 ms from 10-22 Hz which is due to the greater decrease in power to static angry expressions.

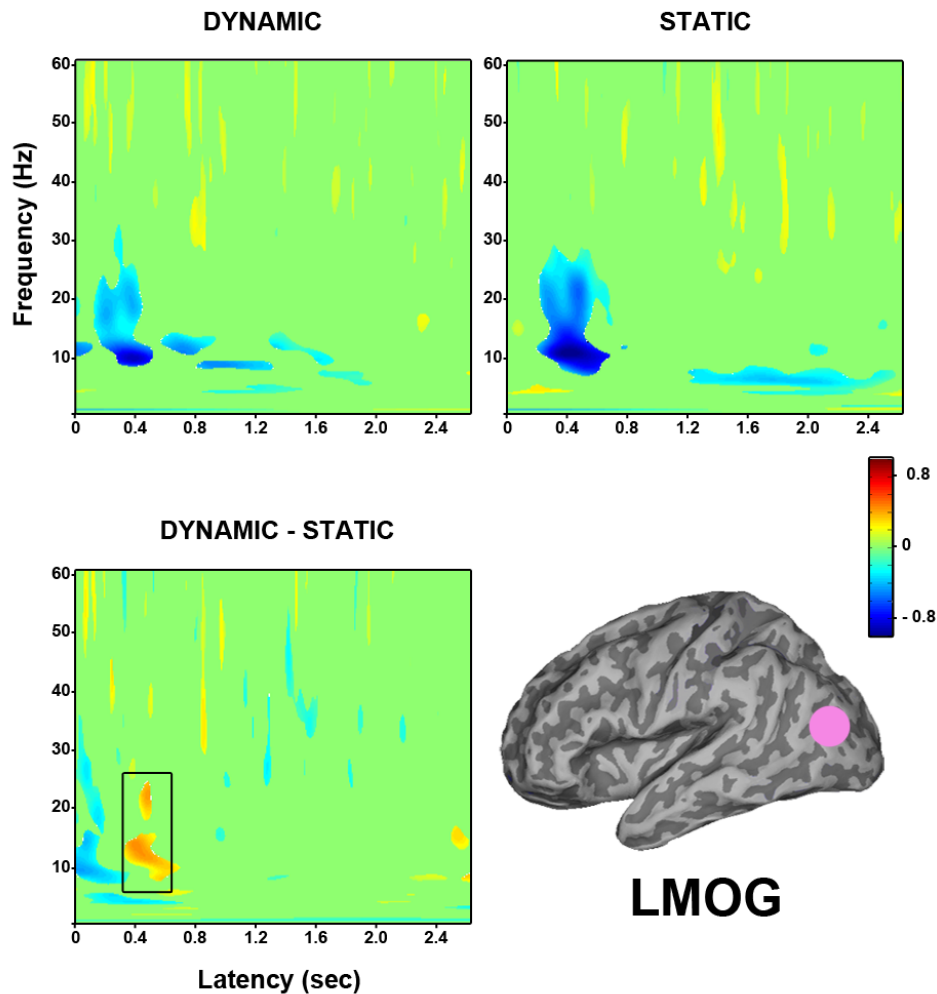


Figure 5.3.3: Group time frequency findings in left middle occipital gyrus (N=10), shows greater power for dynamic angry relative to static angry expressions from 400-600 ms, between 10-22 Hz. This is due to a greater peak decrease in power (8-28 Hz) for static angry expressions around 400 ms. Top left: Dynamic angry faces versus baseline fixation; Top right: Static angry faces versus baseline fixation; Bottom left: Dynamic versus static angry faces.

A region in right MTG also showed differences in the 400-600 ms time window, again with greater power in the dynamic angry condition (see Figure 5.3.4). A virtual electrode constructed here revealed a very similar response pattern to the region in left middle occipital gyrus previously described. Once again, dynamic angry faces elicited a sustained decrease in power mainly between 10–30 Hz, static angry faces elicited a decrease at a slightly later time of 300 ms and of stronger amplitude from 300–600 ms around 10-40 Hz. Dynamic versus static angry expressions again show an early decrease from 10-30 Hz, followed by an increase centred around 500 ms ranging from 10-40 Hz, which is due to the greater power decrease to static angry expressions. This is then followed by a further power decrease (10-20 Hz) around 800 ms due to the more sustained response to dynamic angry expressions.

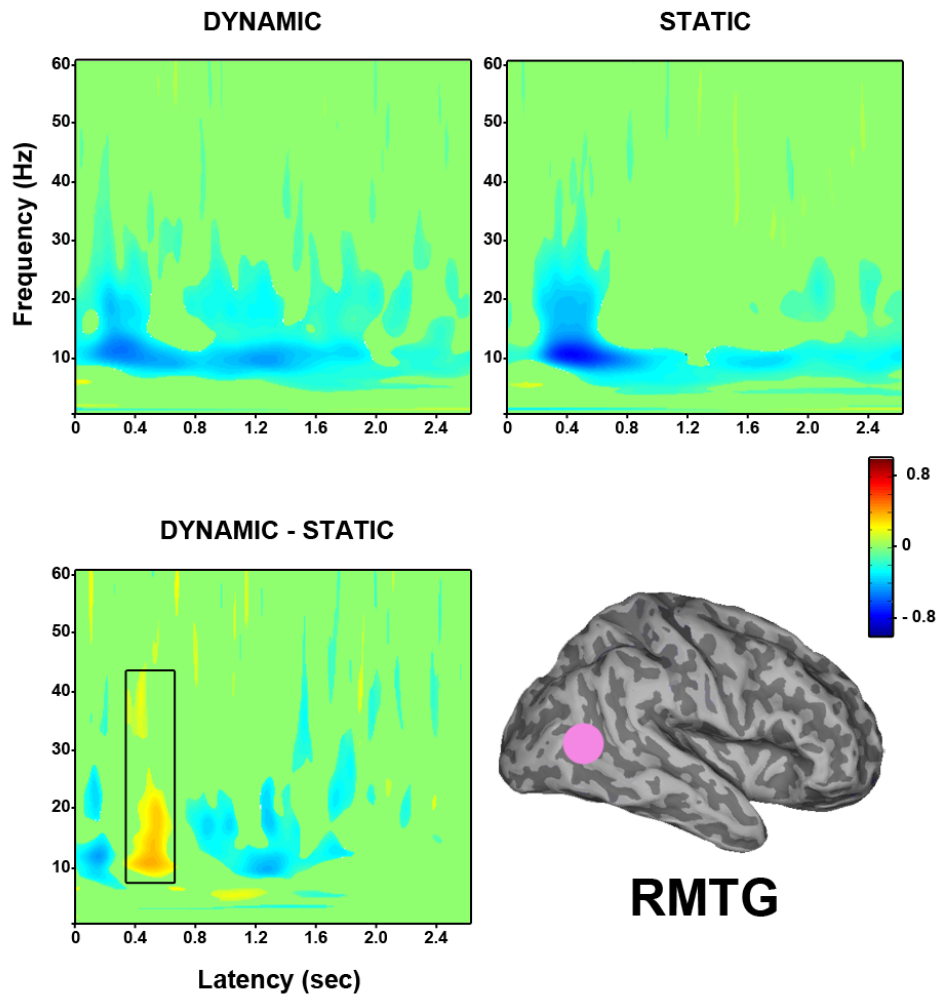


Figure 5.3.4: Group time frequency findings in right middle temporal gyrus (N=12), shows greater power for dynamic angry relative to static angry expressions from 400-600 ms, between 10-40 Hz. This is due to a greater peak decrease in power (10-40 Hz) for static angry expressions around 400 ms. Top left: Dynamic angry faces versus baseline fixation; Top right: Static angry faces versus baseline fixation; Bottom left: Dynamic versus static angry faces.

A virtual electrode was then constructed in the left IOG where differences were found during the 800-1000 ms time interval (see Figure 5.3.5). Once again the dynamic angry faces showed a very similar response pattern as before, displaying a strong sustained decrease in power in the 10–20 Hz range from stimulus onset. Static angry faces again display a sustained decrease in power from around 300 ms in the 10–25 Hz range, this was sustained until 600 ms then reduced to a more narrowband around 10 Hz. The direct comparison of dynamic versus static angry faces revealed an early power decrease from onset to 500 ms in the 5–25 Hz range, followed by a slight increase in power from 10-20 Hz around 500 ms and a decrease from 800-1200 ms between 10–30 and 40-50 Hz which was due to the greater decrease in power to dynamic angry faces.

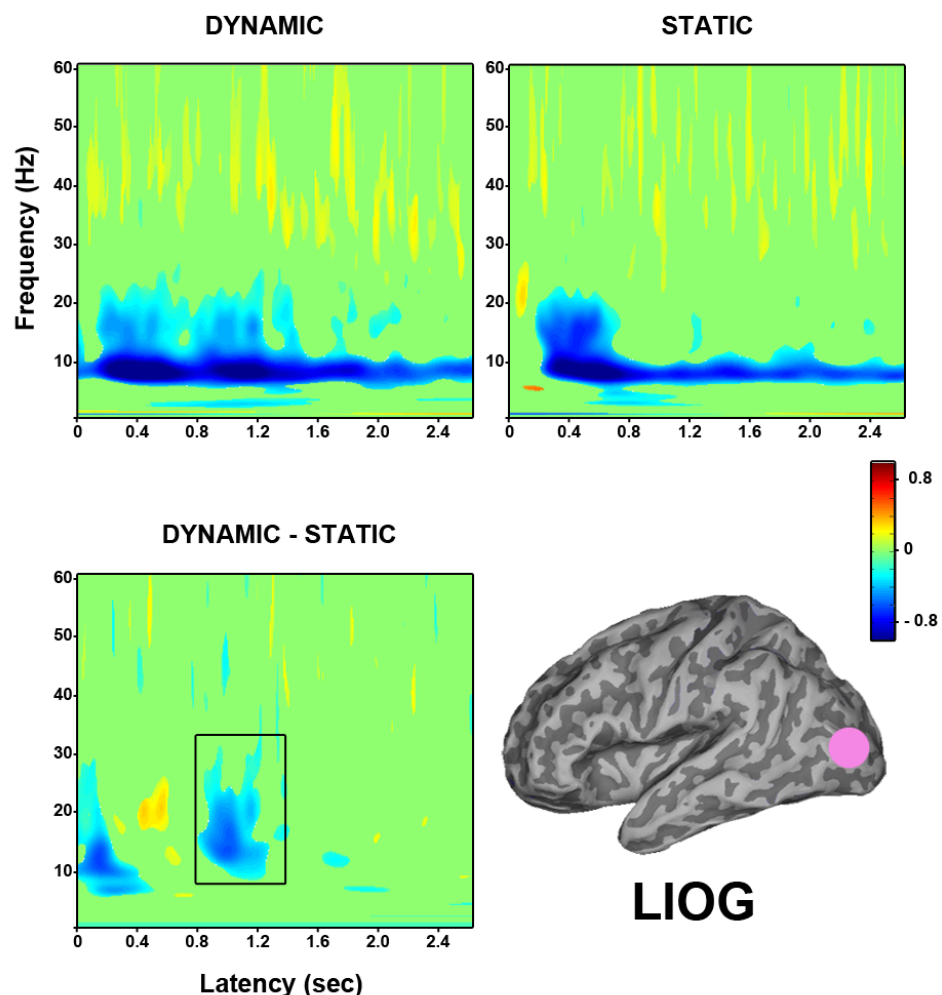


Figure 5.3.5: Group time frequency findings in left inferior occipital gyrus (N=11), shows significantly less power for dynamic angry relative to static angry expressions from 800-1000 ms, between 10-30 Hz. This is due to a greater and more sustained peak decrease in power for dynamic angry expressions around 800 ms. Top left: Dynamic angry faces versus baseline fixation; Top right: Static angry faces versus baseline fixation; Bottom left: Dynamic versus static angry faces.

A virtual electrode was also constructed in the right IOG where differences were also found in the 800-1000 ms time window (see Figure 5.3.6). This region showed a very similar response pattern to that of the left IOG previously described. Dynamic angry faces elicited a strong sustained power decrease in the 5-30 Hz range from stimulus onset, while static angry expressions elicited a short increase in power around 200 ms at 5 Hz and 20-35 Hz followed by a sustained decrease in power from ~400 ms in the 8-30 Hz range reducing to 8-12 Hz from 800 ms onwards. The comparison of dynamic angry to static angry expressions revealed a power decrease from onset to 400 ms in the 5-40 Hz range, followed by an increase in power from 10-22 Hz around 500 ms and once again followed by a decrease in power from 800 ms in the 5-30 Hz range which was due to the to the greater decrease in power in the dynamic angry condition.

The final time window where differences between dynamic angry and static angry expressions were found was from 1800-2000 ms (see Figure 5.3.7). Two frontal regions were identified, one in left middle frontal gyrus and one in right superior frontal gyrus, during this time window both showed significantly less power for dynamic angry relative to static angry expressions. A virtual electrode constructed in the left middle frontal gyrus revealed a decrease in power from 15-25 Hz around 1800 ms in the dynamic angry condition, while static angry expressions elicited an increase in power at ~10 Hz around 1800 ms. The direct comparison of dynamic and static angry expressions revealed a decrease at 1800 ms around 10 Hz and between 20–25Hz, which seems to be driven by the increase to the static angry faces at 10 Hz and the decrease in the dynamic angry face condition around 18–25 Hz.

Finally, the virtual electrode constructed in the region in right superior frontal gyrus (see Figure 5.3.8) revealed a broadband (10-60 Hz) decrease to dynamic angry expressions around 1800 ms, while static angry expressions elicited an increase in low frequency power (~5Hz) around 1800 ms. The direct contrast of dynamic and static angry expressions revealed a decrease in low frequency power (~5 Hz) due to the increase in the static angry condition, along with a broadband (10-60 Hz) decrease due to the decrease to dynamic angry expressions.

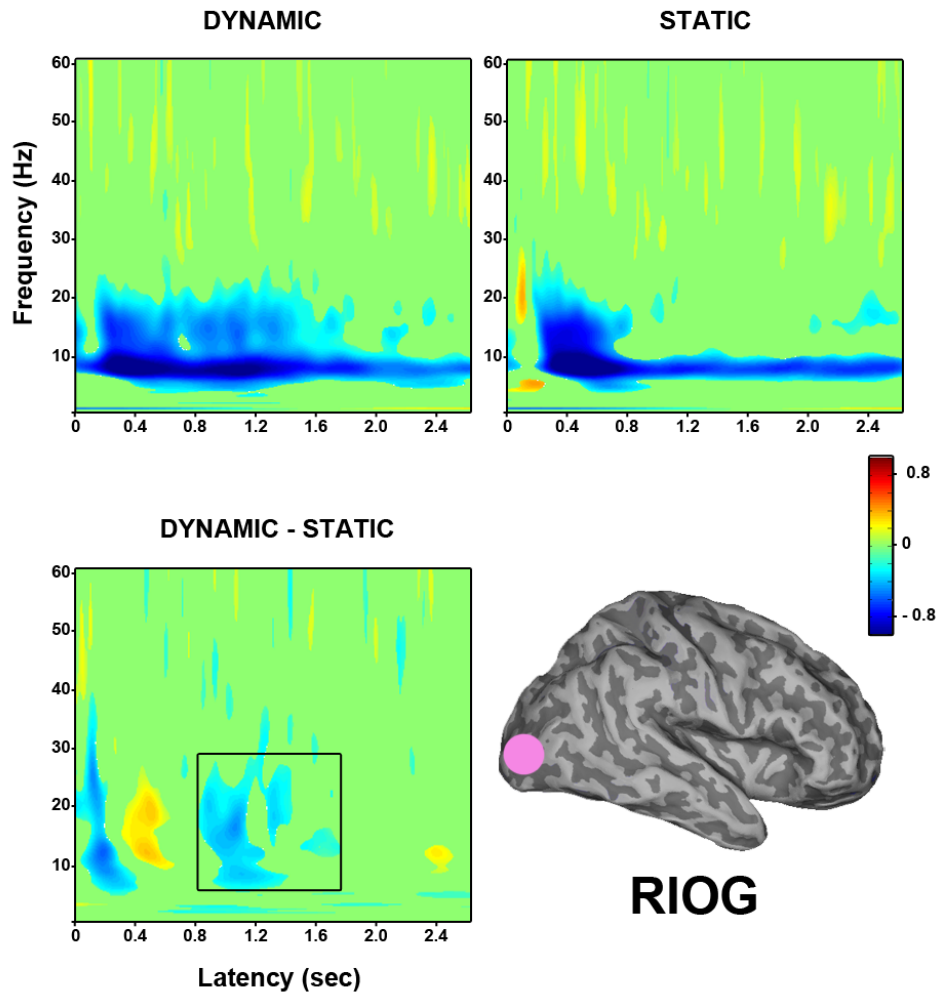


Figure 5.3.6: Group time frequency findings in right inferior occipital gyrus (N=10), shows significantly less power for dynamic angry relative to static angry expressions from 800-1000 ms, between 5-30 Hz. This is due to a greater and more sustained peak decrease in power for dynamic angry expressions around 800 ms. Top left: Dynamic angry faces versus baseline fixation; Top right: Static angry faces versus baseline fixation; Bottom left: Dynamic versus static angry faces.

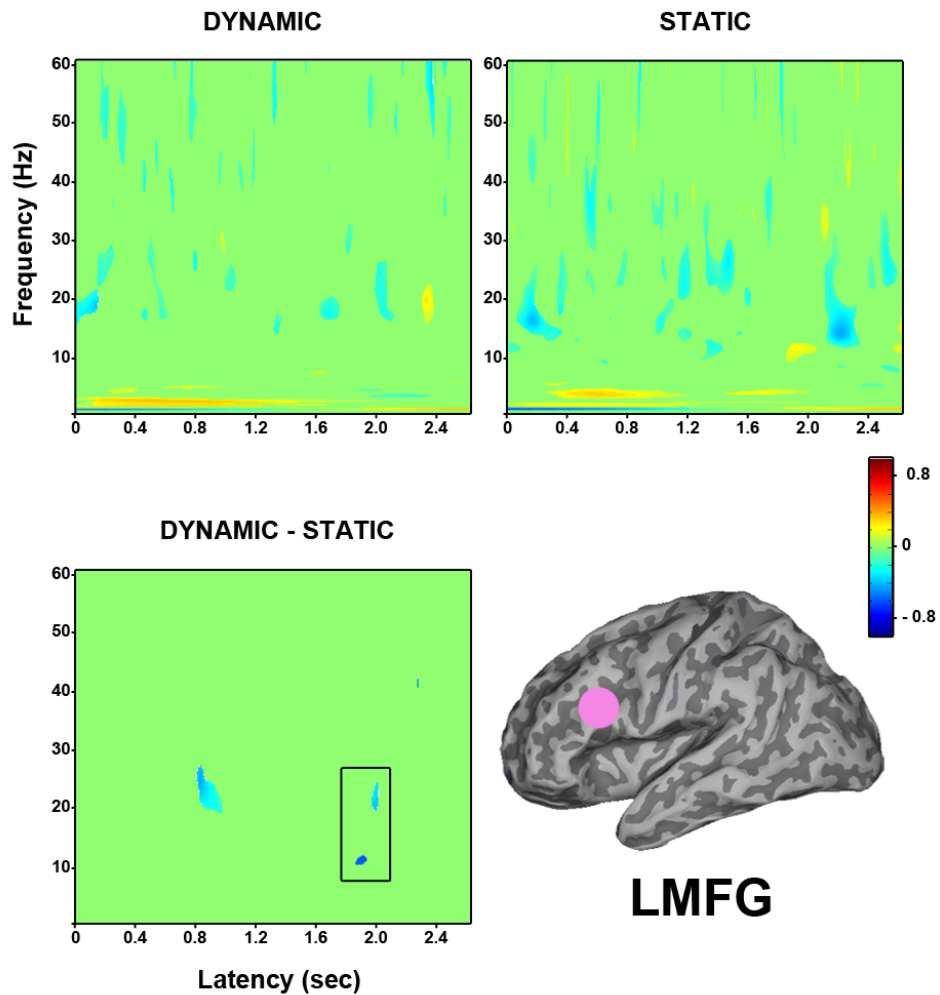


Figure 5.3.7: Group time frequency findings in left middle frontal gyrus (N=8), shows significantly less power for dynamic angry relative to static angry expressions from 1800-2000 ms, between 10-25 Hz. This is due to a greater peak decrease in power for dynamic angry expressions around 1800 ms. Top left: Dynamic angry faces versus baseline fixation; Top right: Static angry faces versus baseline fixation; Bottom left: Dynamic versus static angry faces.

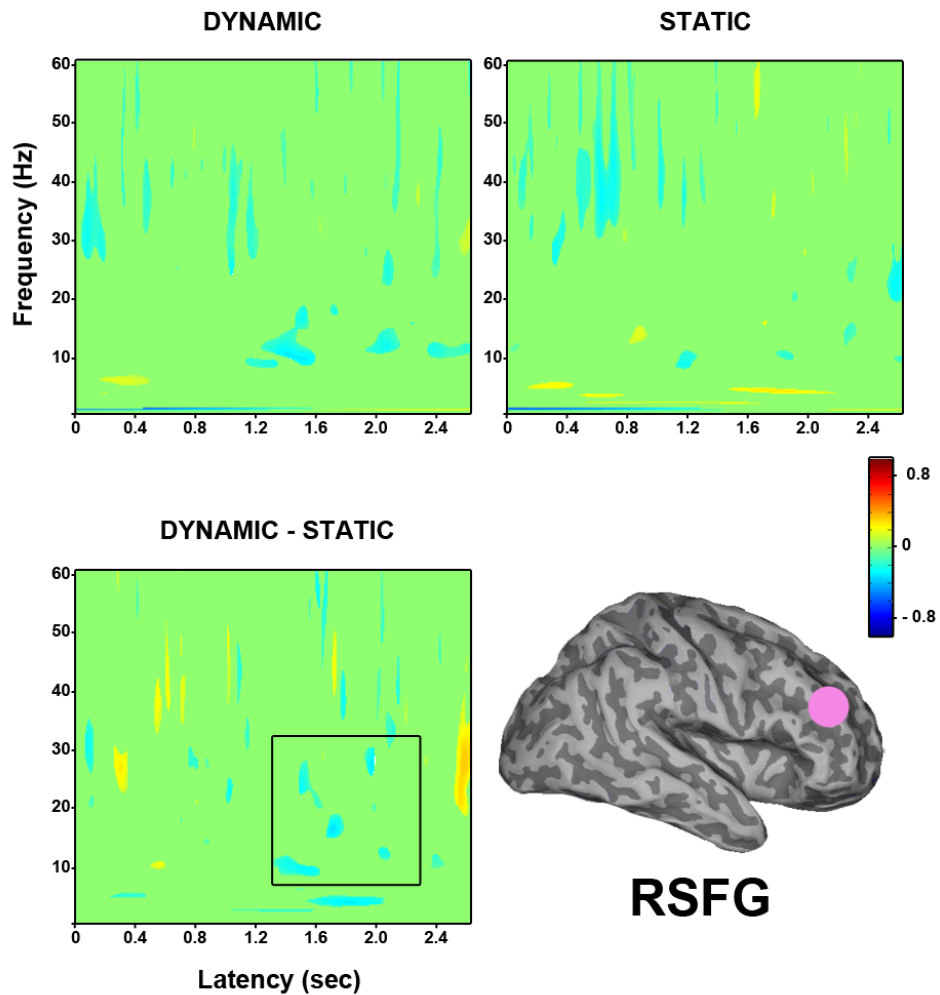


Figure 5.3.8: Group time frequency findings in right superior frontal gyrus (N=8), shows significantly less power for dynamic angry relative to static angry expressions from 1800-2000 ms between 10-30 Hz. This is due to a greater decrease in power for dynamic angry expressions from 1400 ms onwards. Top left: Dynamic angry faces versus baseline fixation; Top right: Static angry faces versus baseline fixation; Bottom left: Dynamic versus static angry faces.

Dynamic angry versus dynamic speech facial displays. Virtual electrodes were constructed at the peak locations identified by SAM in order to examine the time-frequency characteristics of these regions of interest. Virtual electrodes were only constructed for those participants who showed a peak at the selected location in the SAM volume. The first virtual electrode was constructed in the left IFG where early differences were found between dynamic angry and dynamic speech displays within 400 ms of stimulus onset in twelve of the fourteen participants (see Figure 5.3.9). This was due to a greater increase in low frequency power between 2-6 Hz from around 200 ms in the dynamic angry condition. The next virtual electrode was constructed in the right IFG where early

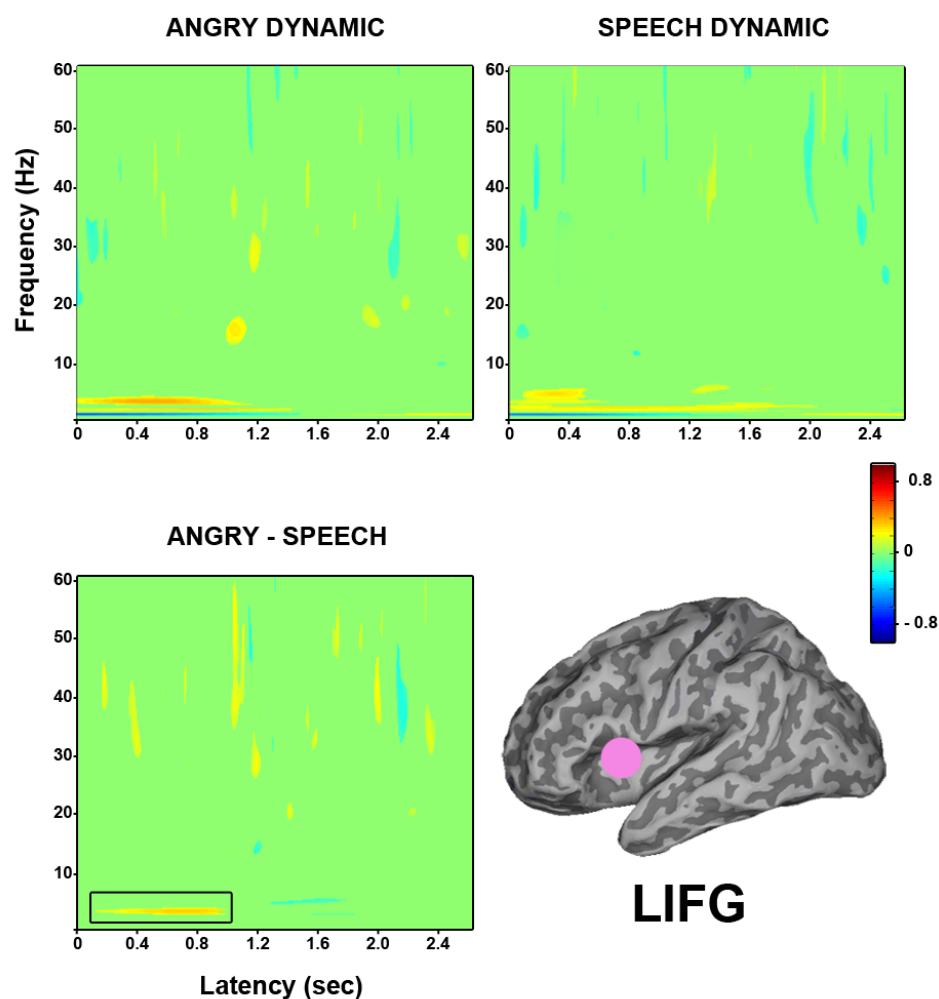


Figure 5.3.9: Group time frequency findings in left inferior frontal gyrus (N=12), shows significantly greater power (2-6 Hz) for dynamic angry relative to dynamic speech displays from 200-1000 ms between. This is due to a greater increase in low frequency power (2-6 Hz) for dynamic angry expressions from 200 ms onwards. Top left: Dynamic angry faces versus baseline fixation; Top right: Dynamic speech faces versus baseline fixation; Bottom left: Dynamic angry versus dynamic speech displays.

differences were also found between dynamic angry and dynamic speech displays within

400 ms of stimulus onset in eleven of the fourteen participants (see Figure 5.3.10). This was also due to a greater increase in low frequency power (2-8 Hz) from around 100 ms in the dynamic angry condition.

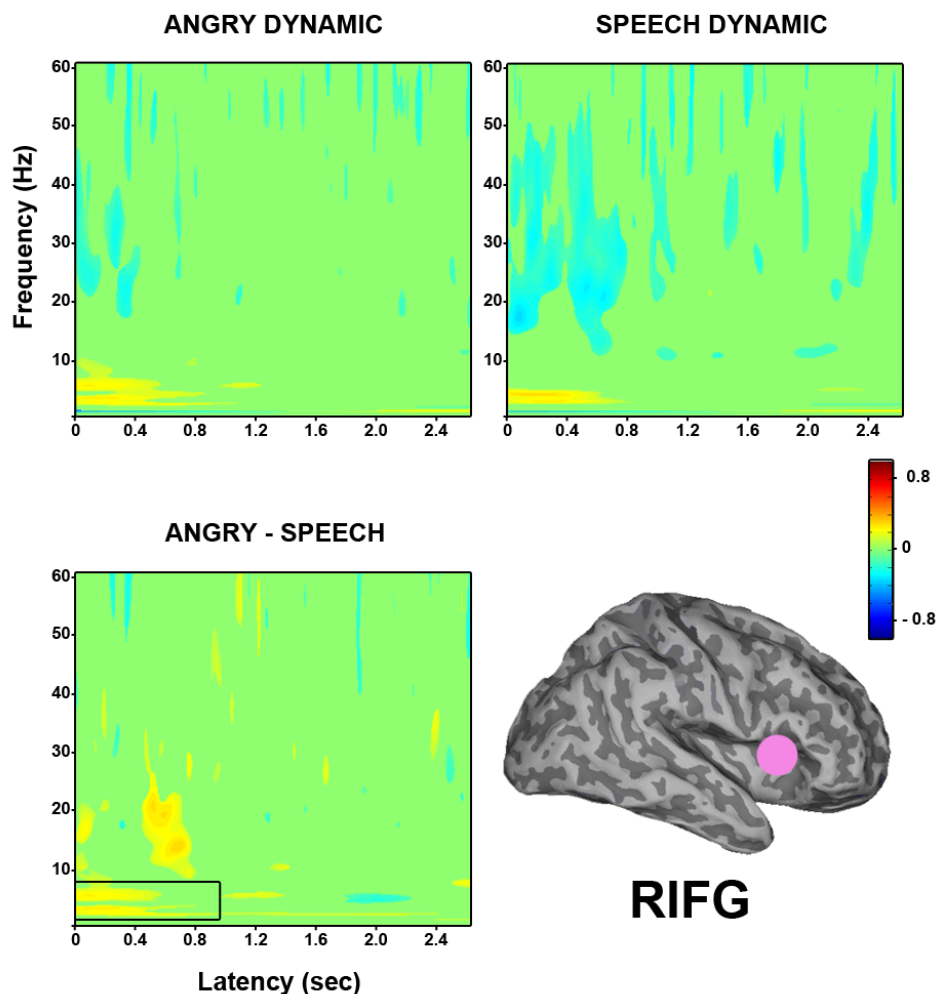


Figure 5.3.10: Group time frequency findings in right inferior frontal gyrus (N=11), shows significantly greater power (2-8 Hz) for dynamic angry relative to dynamic speech displays from 0-800 ms. This is due to a greater increase in power (2-8 Hz) for dynamic angry expressions from 0-800 ms. Top left: Dynamic angry faces versus baseline fixation; Top right: Dynamic speech faces versus baseline fixation; Bottom left: Dynamic angry versus dynamic speech displays.

A region in right STS showed significantly less power for dynamic angry relative to dynamic speech displays in the 600-800 ms time window. A virtual electrode constructed in this region revealed that the difference was due to greater decreases in power (10-30 Hz) around 400 ms for dynamic angry faces (see Figure 5.3.11). Regions were identified in bilateral IOG in the 800-1000 ms time window. A virtual electrode constructed in left IOG revealed significantly greater decreases in power (8-30 Hz) for dynamic angry faces between 800-1200 ms (see Figure 5.3.12). Similarly, a virtual electrode constructed in

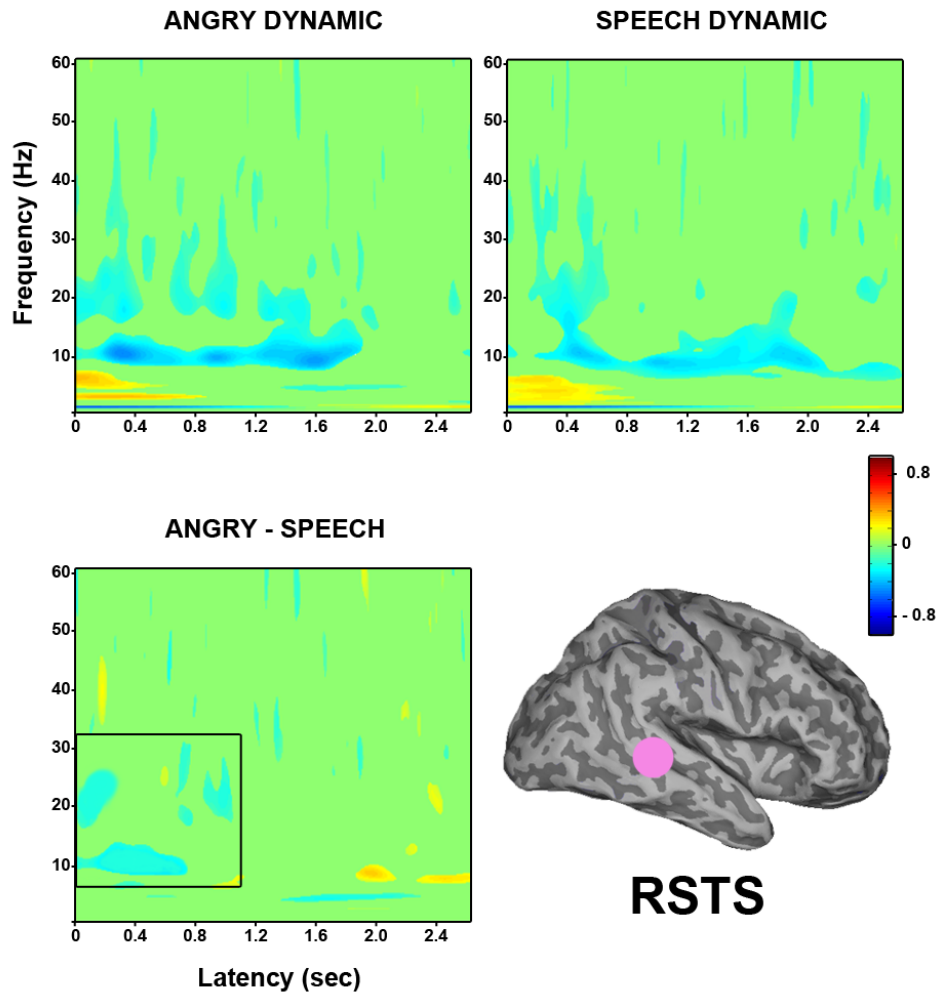


Figure 5.3.11: Group time frequency findings in right superior temporal sulcus (N=12), shows significantly less power (8-30 Hz) for dynamic angry relative to dynamic speech displays from 0-1000 ms. This is due to a greater decrease in power (8-30 Hz) for dynamic angry expressions between 0-800 ms. Top left: Dynamic angry faces versus baseline fixation; Top right: Dynamic speech faces versus baseline fixation; Bottom left: Dynamic angry versus dynamic speech displays.

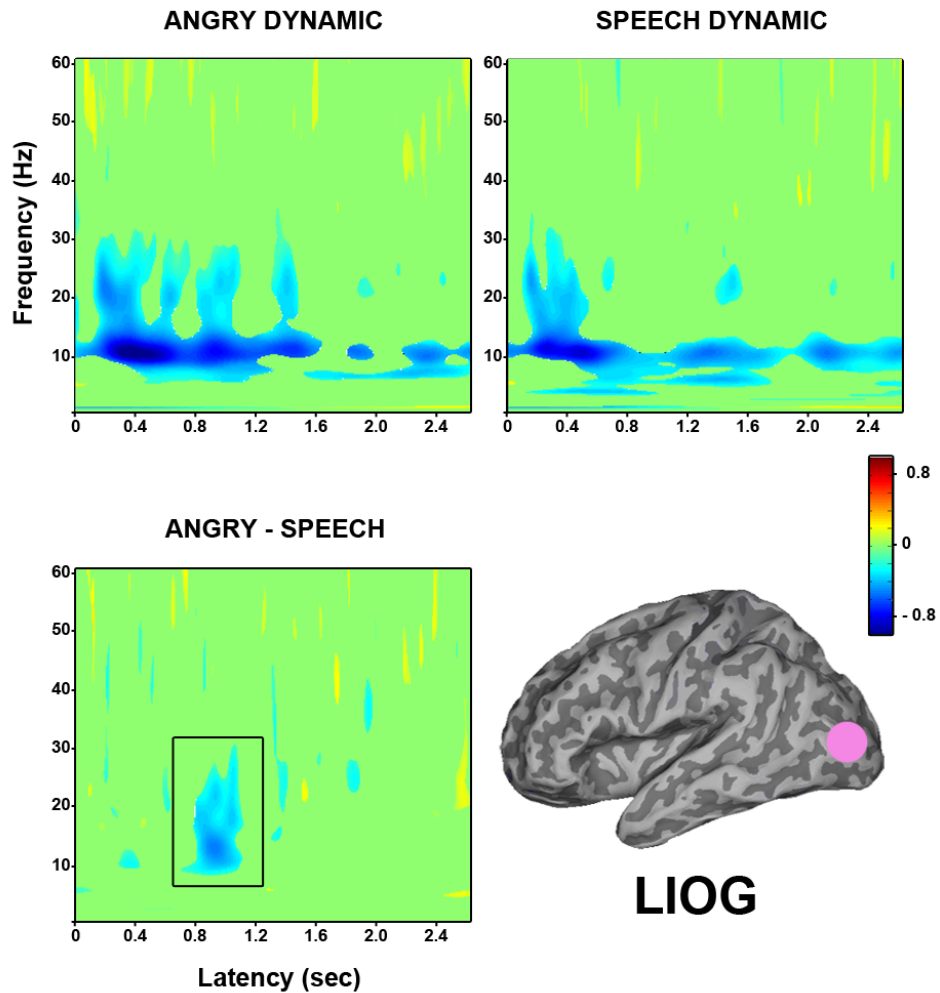


Figure 5.3.12: Group time frequency findings in left inferior occipital gyrus (N=13), shows significantly less power (8-30 Hz) for dynamic angry relative to dynamic speech displays from 800-1200 ms. This is due to a greater decrease in power (8-30 Hz) for dynamic angry expressions between 800-1200 ms. Top left: Dynamic angry faces versus baseline fixation; Top right: Dynamic speech faces versus baseline fixation; Bottom left: Dynamic angry versus dynamic speech displays.

right IOG revealed significantly greater decreases in power (10-30 Hz) for dynamic angry faces between 800-1400 ms (see Figure 5.3.13). Finally, a virtual electrode was construc-

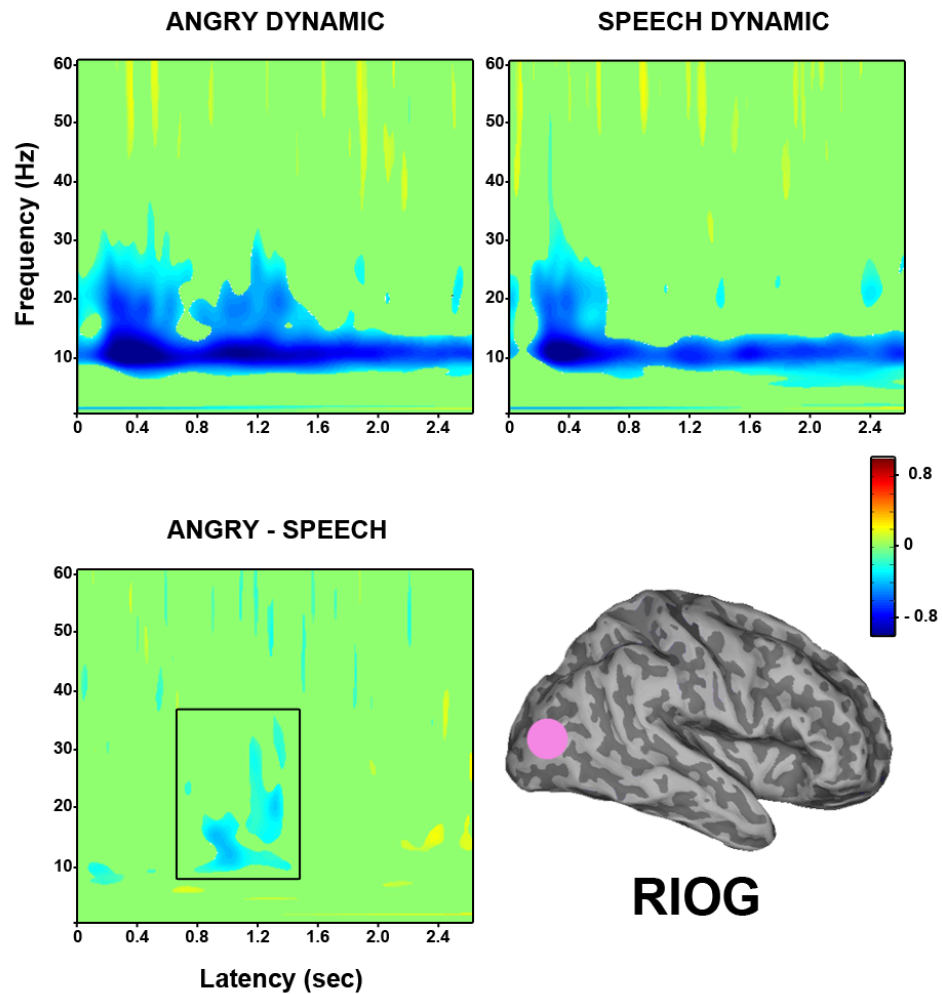


Figure 5.3.13: Group time frequency findings in right inferior occipital gyrus (N=14), shows significantly less power (10-30 Hz) for dynamic angry relative to dynamic speech displays from 800-1400 ms. This is due to a greater decrease in power (10-30 Hz) for dynamic angry expressions between 800-1400 ms. Top left: Dynamic angry faces versus baseline fixation; Top right: Dynamic speech faces versus baseline fixation; Bottom left: Dynamic angry versus dynamic speech displays.

ted in the right insula, this revealed significantly greater increases in low frequency power (3-12 Hz) for dynamic angry expressions between 400-1200 ms (see Figure 5.3.14).

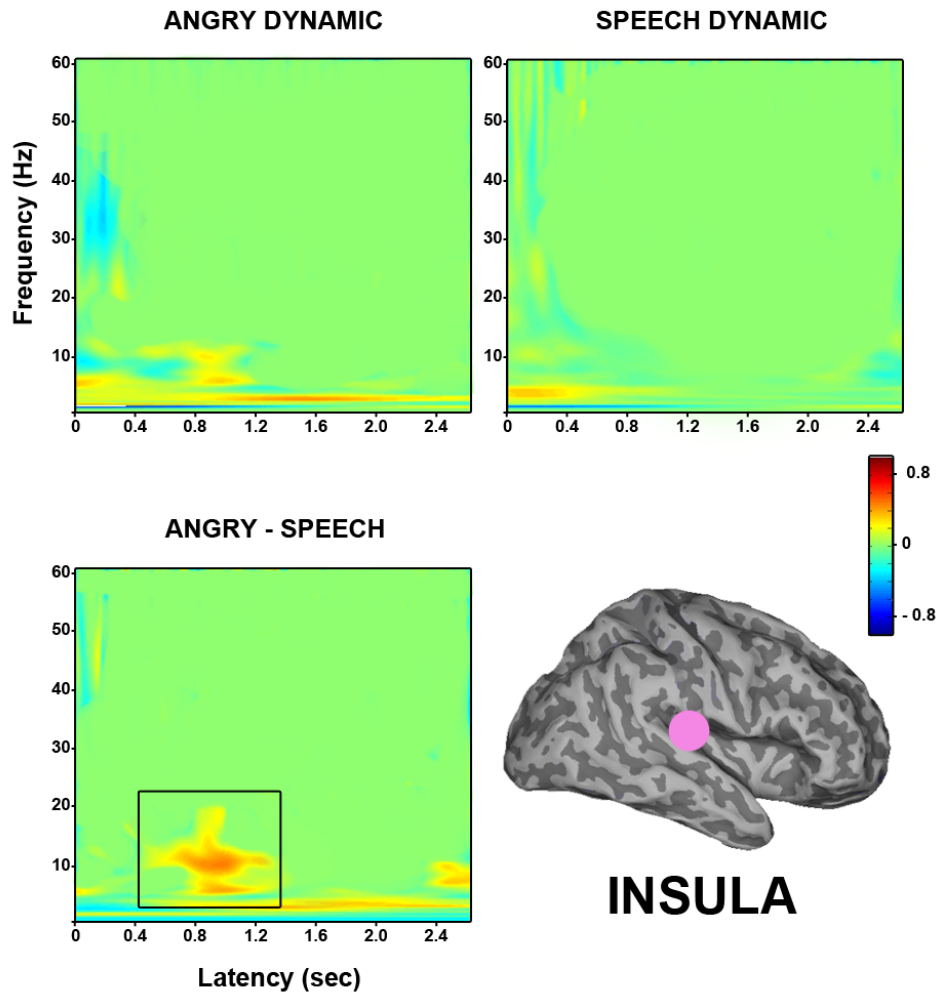


Figure 5.3.14: Group time frequency findings in right insula (N=8) shows significantly greater power (3-20 Hz) for dynamic angry relative to dynamic speech displays from 400-1600 ms between. This is due to a greater increase in low frequency power (3-12 Hz) for dynamic angry expressions around 800 ms. Top left: Dynamic angry faces versus baseline fixation; Top right: Dynamic speech faces versus baseline fixation; Bottom left: Dynamic angry versus dynamic speech displays.

5.3.2 Dynamic facial expressions of happiness

5.3.2.1 Source analysis results

Once again SAM was computed across twelve different 200 ms time windows using a wide frequency band of 1-80 Hz, to identify sources of differential activity between dynamic happy and static happy facial expressions, across the length of stimulus presentation. Group analysis was performed using SnPm to identify significantly clustered peaks across the group of participants in response to dynamic happy versus static happy face stimuli (see Table 5.3). In the first time window from 0 to 200 ms peaks were identified in bilateral IOG that showed significant decreases in oscillatory power for dynamic happy relative to static happy expressions across the group, while a region in right IFG showed significant increases in power for dynamic happy compared to static happy facial expressions.

In the following time window from 200 to 400 ms a significant peak was found in right middle occipital gyrus showing significantly greater power for dynamic happy relative to static happy expressions. In the next time window from 400 to 600 ms significant peaks were identified in bilateral fusiform gyri, and left postcentral gyrus, all showing greater power for dynamic happy relative to static happy expressions, while a region in left IFG showed significantly less power for dynamic happy expressions relative to static. A peak in left postcentral gyrus was also identified in the subsequent time window from 600 to 800 ms, again showing significantly greater power for dynamic happy expressions relative to static happy expressions.

A region in left middle occipital gyrus showed significantly less power for dynamic happy expressions compared to static in the 800–1000 ms time window. Peaks were identified in left MTG and right STS showing significantly less power for dynamic happy relative to static happy expressions in the time interval from 1000 to 1200 ms. In the following time window from 1200 to 1400 ms, peaks were found in bilateral fusiform gyri, again showing significantly less power for dynamic happy expressions relative to static. Finally, in a later time window from 2000 to 2200 ms a peak was found in left STS that showed significantly less power for dynamic happy relative to static happy expressions. No significant differences were found in any of the other time windows analysed.

SAM was also computed across twelve different 200 ms time windows using a wide frequency band of 1-80 Hz, to identify sources of differential activity between dynamic happy

Table 5.3: Brain regions showing significant differences in oscillatory power in response to dynamic happy versus static happy facial expressions within the following time windows: (A) 0-200 ms (B) 200-400 ms (C) 400-600 ms (D) 600-800 ms (E) 800-1000 ms (F) 1000-1200 ms (G) 1200-1400 ms (H) 2000-2200 ms. Co-ordinates indicate local maxima in Talairach space. Clusters are significant at $p < .05$. N = number of participants showing a peak in that region. L= Left; R = Right.

Region	N	Pseudo t	x	y	z
<i>(A) 0-200 ms</i>					
R Inferior frontal gyrus (BA 45)	10	+ 3.96	51	24	15
L Inferior occipital gyrus (BA 18)	12	- 4.87	-48	-84	-9
R Inferior occipital gyrus (BA 18)	12	- 5.97	42	-84	-12
<i>(B) 200-400 ms</i>					
R Middle occipital gyrus (BA 19)	9	+ 5.42	27	-86	12
<i>(C) 400-600 ms</i>					
L Fusiform gyrus (BA 37)	11	+ 5.71	-40	-45	-16
R Fusiform gyrus (BA 37)	10	+5.44	51	-45	-16
L Inferior frontal gyrus (BA 13)	9	- 4.51	-42	27	6
L Postcentral gyrus (BA 3)	8	+3.89	-48	-18	40
<i>(D) 600-800 ms</i>					
L Postcentral gyrus (BA 2)	9	+3.69	-42	-27	33
<i>(E) 800-1000 ms</i>					
L Middle occipital gyrus (BA 19)	11	- 4.49	-54	-81	8
<i>(F) 1000-1200 ms</i>					
L Middle temporal gyrus (BA 21)	10	- 5.7	-48	3	-20
R Superior temporal sulcus (BA 22)	11	- 4.9	52	-40	12
<i>(G) 1200-1400 ms</i>					
R Fusiform gyrus (BA 37)	12	- 4.7	50	-45	-12
<i>(H) 2000 - 2200 ms</i>					
L Superior temporal sulcus (BA 22)	8	- 4.45	-55	-45	15

and dynamic speech facial displays across the length of stimulus presentation. Once again group analysis was performed using SnPm to identify significantly clustered peaks across the group of participants (see Table 2.6). Two regions were identified as showing significantly greater power for dynamic happy relative to dynamic speech displays in the 0-200 ms time window, one in left IFG and the other in right IFG. A region in left middle occipital gyrus was identified as showing significantly less power for dynamic happy compared to dynamic speech displays between 200-400 ms. Lastly a region in the left fusiform gyrus showed significantly less power for dynamic happy compared to dynamic speech displays in the time window between 1000-1200 ms. No significant differences were found in any of the other time windows analysed.

Table 5.4: Brain regions showing significant differences in oscillatory power in response to dynamic happy facial expressions versus dynamic speech facial displays within the following time windows: (A) 0-200 ms (B) 200-400 ms (C) 1000-1200 ms. Co-ordinates indicate local maxima in Talairach space. Clusters are significant at $p < .05$. N = number of participants showing a peak in that region. L= Left, R = Right.

Region	N	Pseudo t	x	y	z
<i>(A) 0-200 ms</i>					
L Inferior frontal gyrus (BA 45)	8	+3.63	-50	18	14
R inferior frontal gyrus (BA 46)	9	+3.84	42	14	18
<i>(B) 200-400 ms</i>					
L Middle occipital gyrus (BA 19)	12	-3.98	-57	-75	-3
<i>(C) 1000-1200 ms</i>					
L Fusiform gyrus (BA 37)	12	-3.37	-40	-56	-12

5.3.2.2 Time frequency results

Dynamic happy versus static happy facial expressions. Virtual electrodes were again constructed at the peak locations identified by SAM in order to map the time-frequency characteristics of these regions of interest. Virtual electrodes were only constructed for those participants who showed a peak at the selected location in the SAM volume. The first virtual electrode was constructed in a region in right IFG where an early difference between dynamic happy and static happy expressions was found within 200 ms of stimulus onset (see Figure 5.3.15), showing greater power for dynamic happy expressions relative to static. In the dynamic happy condition the time-frequency map shows an early increase in low frequency power (3-6 Hz) from 0-500 ms and a shorter power increase from 8-12 Hz within 200 ms of stimulus onset. Static faces relative to baseline

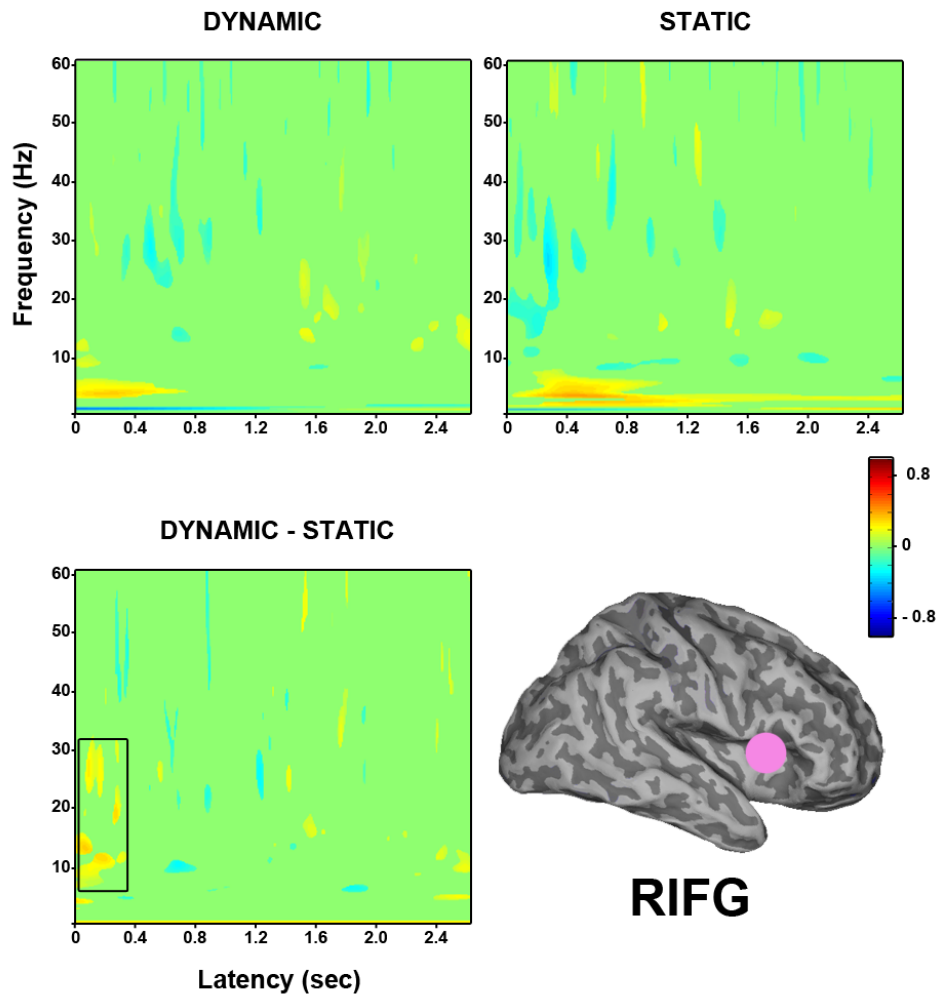


Figure 5.3.15: Group time frequency findings in right inferior frontal gyrus (N=10), shows early differences between dynamic happy and static happy expressions around 200 ms between 5-30 Hz. This is due to an increase in power (3-6 Hz) for dynamic happy faces and a decrease in power for static happy expressions (10-45 Hz) within 0-200 ms. Top left: Dynamic happy faces versus baseline fixation; Top right: Static happy faces versus baseline fixation; Bottom left: Dynamic versus static happy faces.

show a sustained increase between 2–6 Hz from 100 ms, along with a power decrease in the 10-45 Hz range. The direct comparison of dynamic versus static happy expressions shows an early increase in power within 200 ms ranging from 5 Hz to 30 Hz, which is due to both the low frequency power increase to dynamic happy expressions and the broader power decrease in the happy static condition.

An early difference was also found in a region in left IOG within 200 ms of stimulus onset (see Figure 5.3.17). A virtual electrode constructed at this region revealed that this difference is due to an early decrease in power in response to dynamic happy expressions, where they elicited an early sustained decrease from stimulus onset in the 8–30 Hz frequency range but centred around 10 Hz. Static happy faces showed a small power

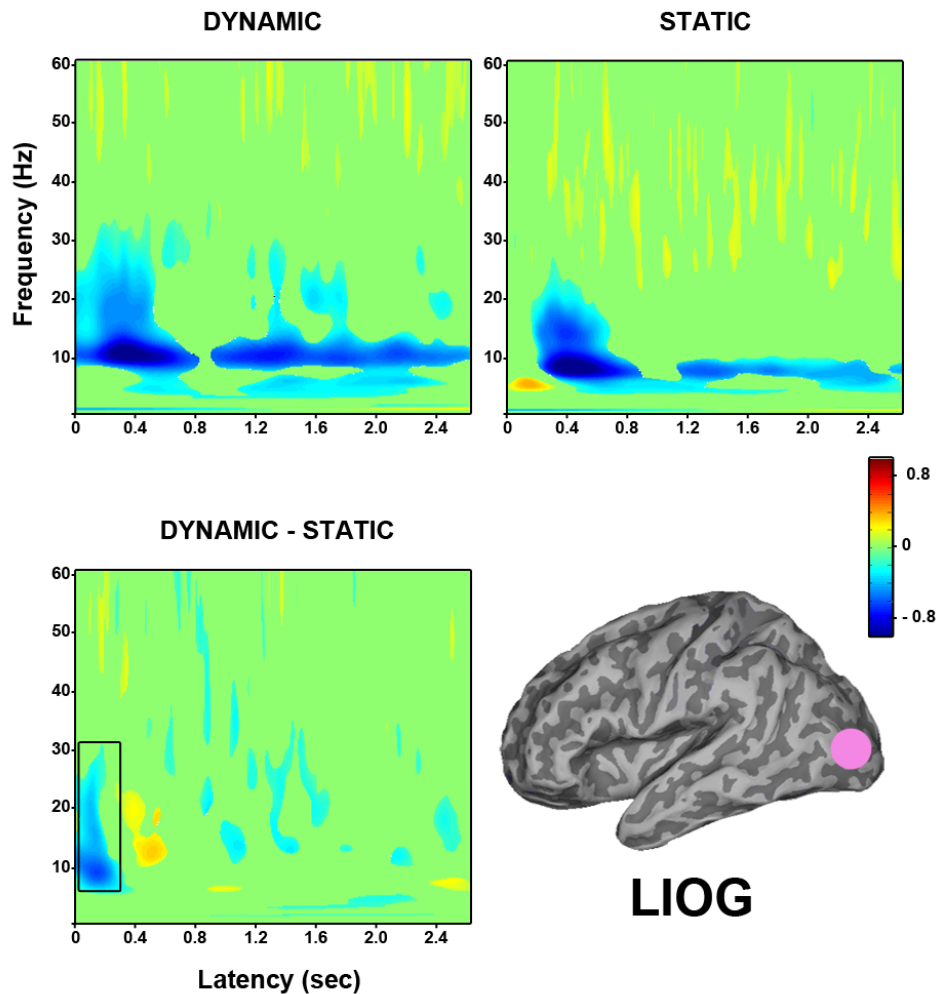


Figure 5.3.16: Group time frequency findings in left inferior occipital gyrus (N=12), shows early differences between dynamic happy and static happy expressions around 200 ms between 8-30 Hz. This is due to a greater decrease in power (8-30 Hz) for dynamic happy faces within 0-200 ms. Top left: Dynamic happy faces versus baseline fixation; Top right: Static happy faces versus baseline fixation; Bottom left: Dynamic versus static happy faces.

increase around 5 Hz within 200 ms of stimulus onset followed by a later decrease in power from 300 ms in the 8–30 Hz range. The direct comparison of dynamic happy and static happy expressions shows an early decrease from stimulus onset until around 400 ms in the 8-30 Hz range due to the decrease in power to dynamic happy expressions (see Figure 5.3.16). A virtual electrode was also placed in a region in right IOG which again showed early differences between dynamic and static happy expressions within 200 ms. Dynamic happy expressions relative to baseline show a sustained early decrease in power from stimulus onset, centred around 10 Hz and spanning 8–30 Hz. Static happy expressions again elicited a small increase in power around 5 Hz within 200s, followed by a sustained decrease in power from around 300 ms in the 8-30 Hz range. Dynamic versus static happy expressions again show an early power decrease within 200 ms from 8–30 Hz

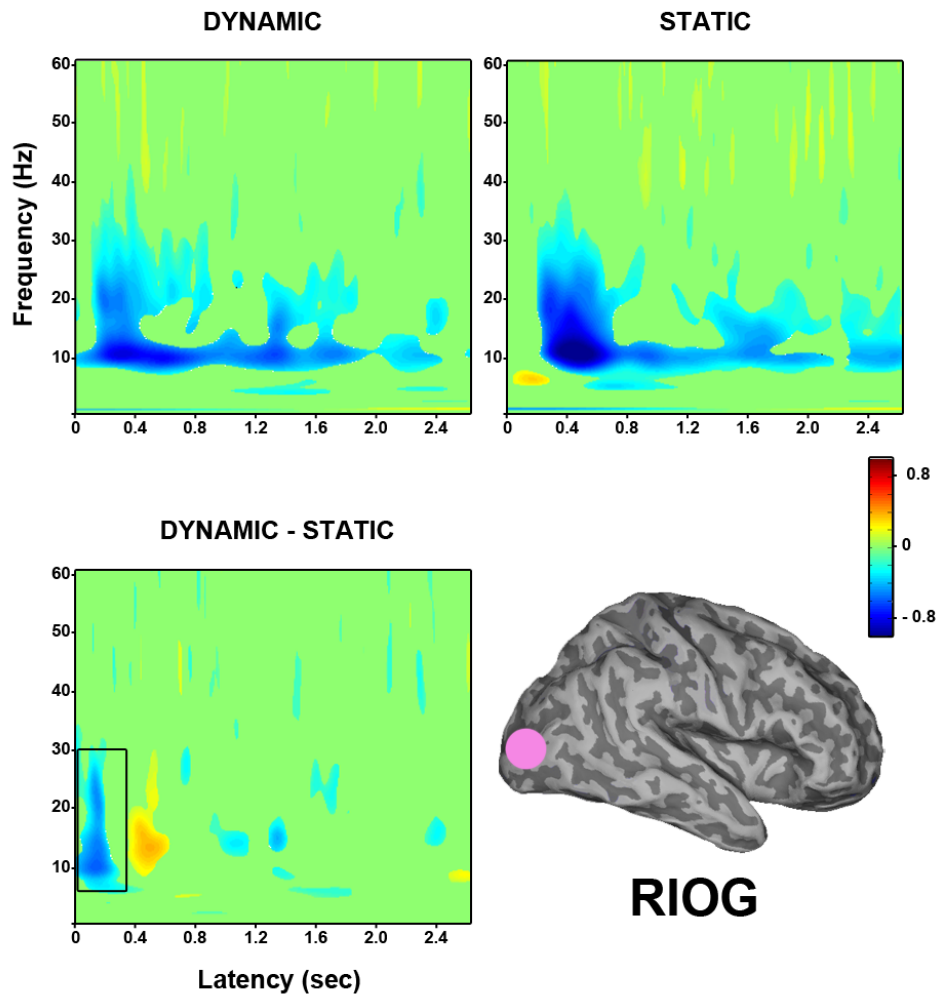


Figure 5.3.17: Group time frequency findings in right inferior occipital gyrus (N=12), shows early differences between dynamic happy and static happy expressions around 200 ms between 8-30 Hz. This is due to a greater decrease in power (8-30 Hz) for dynamic happy faces within 0-200 ms. Top left: Dynamic happy faces versus baseline fixation; Top right: Static happy faces versus baseline fixation; Bottom left: Dynamic versus static happy faces.

due to the decrease in power in the dynamic happy condition.

A virtual electrode was then constructed in a region in right middle occipital gyrus which was identified in the 200-400 ms time interval as showing greater power for dynamic happy relative to static happy faces (see Figure 5.3.18). Dynamic happy faces relative to baseline showed a sustained decrease in power from stimulus onset in the 8-30 Hz range, while static happy expressions elicited a sustained decrease in power from 200 ms again in the 8-30 Hz range, showing a strong decrease from 400 to 600 ms. The direct contrast of dynamic and static happy expressions shows an early decrease within 200 ms from 5-30 Hz followed by an increase from 300 to 600 ms in the 8-35 Hz range which is due to the greater decrease in power in the static happy condition at this time interval .

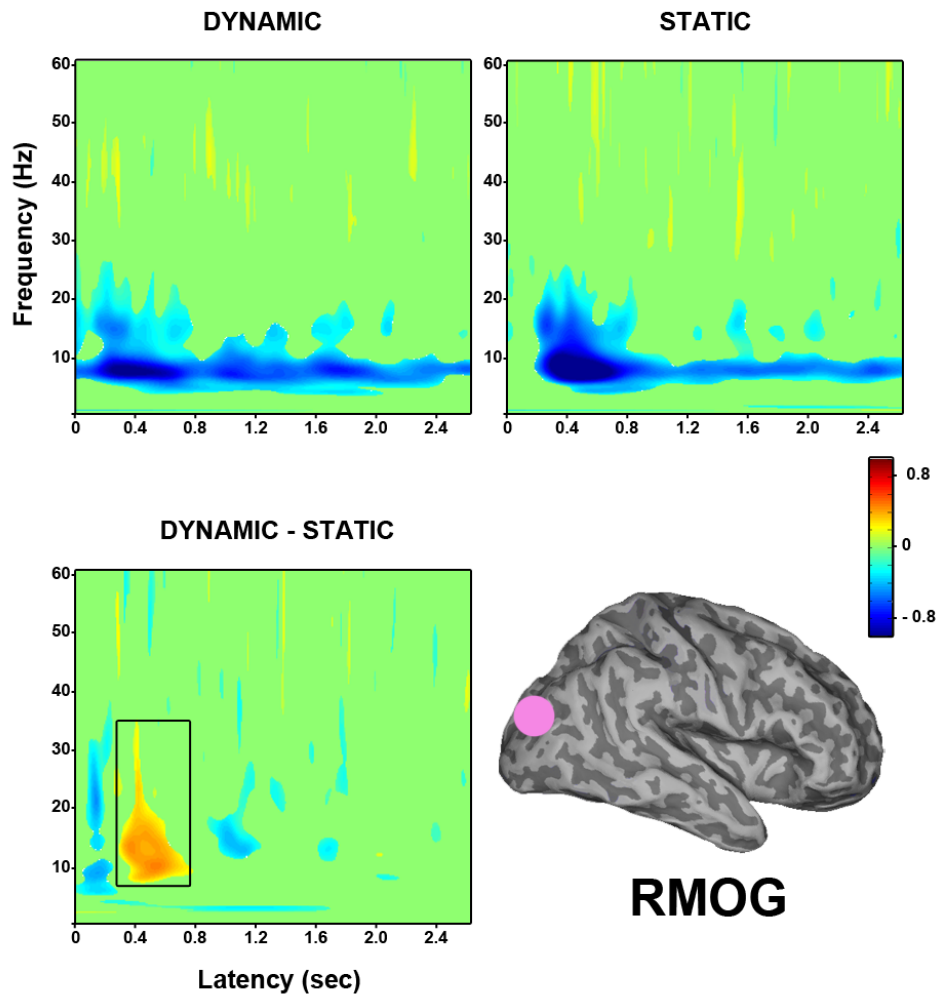


Figure 5.3.18: Group time frequency findings in right middle occipital gyrus (N=9), shows greater power for dynamic happy relative to static happy expressions within 200-400 ms between 8-30 Hz. This is due to a greater peak decrease in power (8-30 Hz) for static happy faces within 200-400 ms. Top left: Dynamic happy faces versus baseline fixation; Top right: Static happy faces versus baseline fixation; Bottom left: Dynamic versus static happy faces.

A region in left fusiform gyrus showed greater power for dynamic happy expressions in the 400-600 ms time window (see Figure 5.3.19). A virtual electrode constructed here revealed that dynamic happy expressions relative to baseline elicited an early sustained power decrease in the range of 8-28 Hz, centred around 10 Hz. Static happy faces elicited an early increase in power at ~5 Hz and also 25–35 Hz, followed by a strong sustained power decrease from around 400 ms again in the range of 8-28 Hz and centred around 10 Hz. The direct contrast of dynamic versus static happy expressions revealed a decrease in power within 200 ms in the range of 5-35 Hz, followed by an increase in power from 400 to 600 ms in the 12-40 Hz range as a result of the strong power decrease to static happy expressions during this time period.

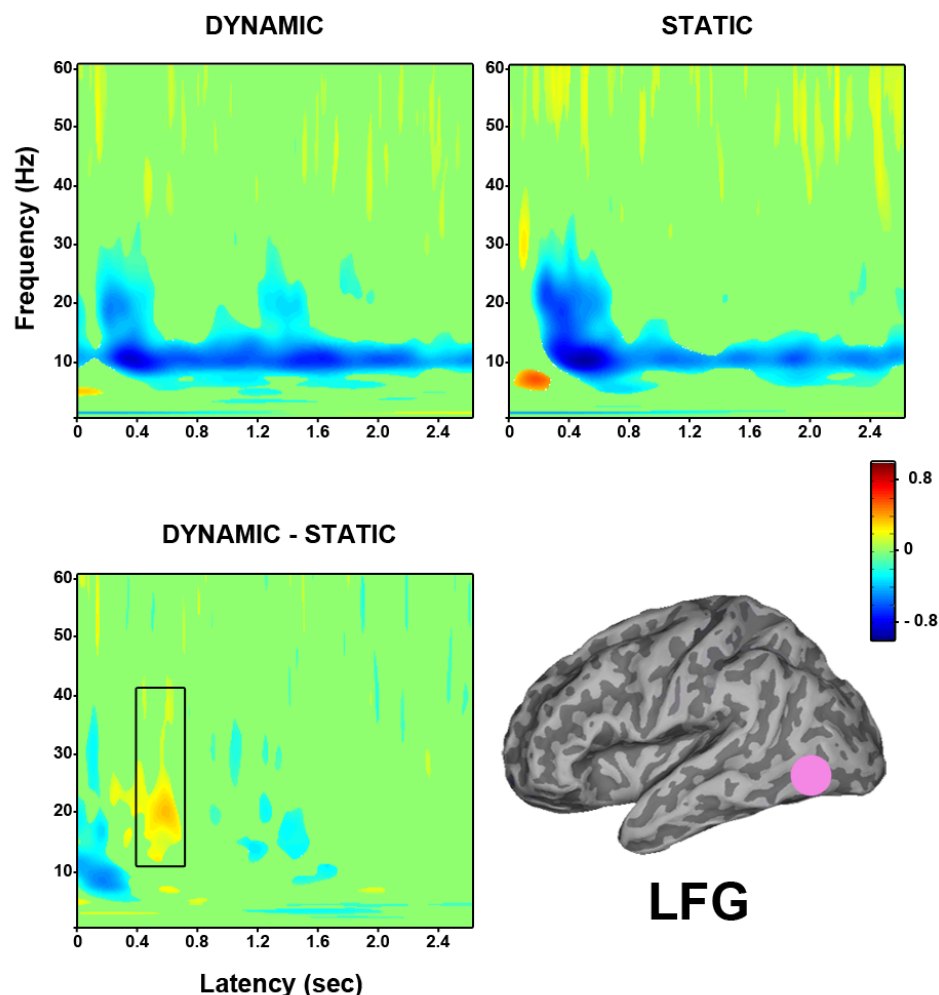


Figure 5.3.19: Group time frequency findings in left fusiform gyrus (N=11), shows greater power for dynamic happy relative to static happy expressions within 400-600 ms between 12-40 Hz. This is due to a greater peak decrease in power (8-28 Hz) for static happy faces around 500 ms. Top left: Dynamic happy faces versus baseline fixation; Top right: Static happy faces versus baseline fixation; Bottom left: Dynamic versus static happy faces.

Similarly, a region in right fusiform gyrus showed greater power for dynamic happy expressions in the 400-600 ms time window (see Figure 5.3.20). A virtual electrode constructed here revealed that dynamic happy expressions relative to baseline elicited an early sustained power decrease again centred around 10 Hz along with a slight increase in low frequency power (2-6 Hz) within 200 ms. Static happy expressions also showed an early increase in low frequency power (2-6 Hz) within 200 ms. Static happy expressions also showed an early increase in low frequency power (2-6 Hz), this was followed by a strong decrease in power from around 300–800 ms in the 8-30 Hz range. Dynamic versus static happy expressions show an early decrease in power from 5-35 Hz within 300 ms, followed by an increase between 400–800 ms in the 8-25 Hz range, which is due to the strong decrease in the static happy condition during this time period.

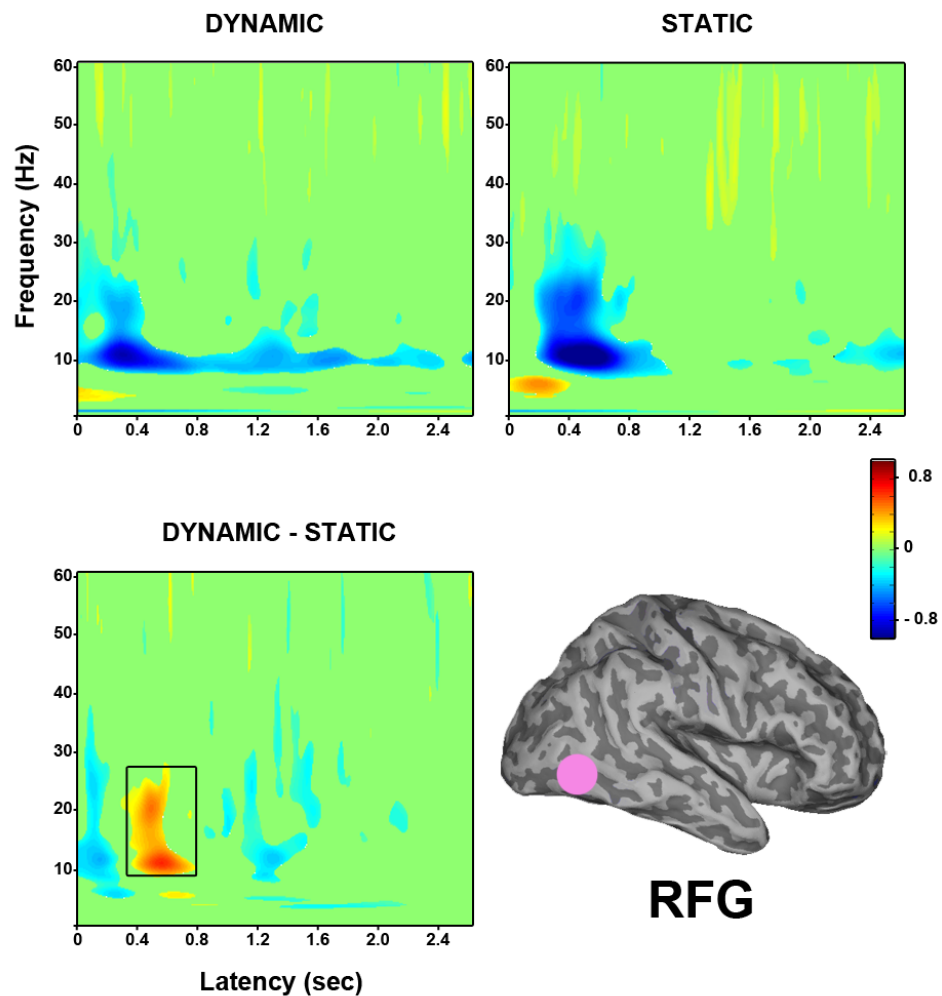


Figure 5.3.20: Group time frequency findings in right fusiform gyrus (N=10), shows greater power for dynamic happy relative to static happy expressions within 400-600 ms between 8-25 Hz. This is due to a greater peak decrease in power (8-30 Hz) for static happy faces around 500 ms. Top left: Dynamic happy faces versus baseline fixation; Top right: Static happy faces versus baseline fixation; Bottom left: Dynamic versus static happy faces.

A region in left IFG was also identified as showing differences in the 400-600 ms time window, but this time it was due to significantly less power for dynamic happy expressions relative to static (see Figure 5.3.21). A virtual electrode revealed an early increase in low frequency power (1-5 Hz) from 0–500 ms, along with a decrease ranging from 10-30 Hz within 500 ms in the dynamic happy condition relative to baseline. The static happy expressions elicited a stronger increase in low frequency power (1-7 Hz) from 300–1000 ms, along with a decrease from 300–800 ms in the 16-30 Hz range. The direct comparison of dynamic and static happy expressions showed a decrease in low frequency power (2-10 Hz) around 400 ms due to the increase in power in the static happy condition, as well as a decrease in the 15-22 Hz range at 500s as a result of the corresponding decrease in power in the dynamic happy condition.

The next virtual electrode was constructed in a region in left postcentral gyrus which showed greater power for dynamic happy relative to static happy expressions during the same time window from 400-600 ms (see Figure 5.3.22). Here, dynamic happy expressions elicited a decrease in power from 100–500 ms in the 20–60 Hz range, while static happy expressions showed a stronger decrease in power from 100–700 ms in the 15–60 Hz range. Dynamic versus static happy expression showed an increase in power between 400 and 800 ms in the 5-50 Hz range, due to the greater decrease in power to static happy expressions during this time period.

The next virtual electrode was also constructed in a region in left postcentral gyrus, which showed greater power for dynamic happy faces during the 600-800 ms time window (see Figure 5.3.23). Dynamic happy expressions elicited an early decrease in power from stimulus onset to 600 ms within a broad frequency range of ~8-50 Hz, while static happy expressions elicited a short increase in low frequency power (4-6 Hz) at 200 ms followed by a broader decrease in power (10-40 Hz) from 400 ms. The direct comparison of dynamic and static happy expressions revealed an early decrease in power from 6-12 Hz and 20-25 Hz within 200 ms followed by a broader increase in power (10-40 Hz) from 500–900 ms as a result of the stronger power decrease in the static happy condition during this time period.

A region in left middle occipital gyrus was identified as showing less power in the dynamic happy condition relative to static during the 800-1000 ms time interval (see Figure 5.3.24).

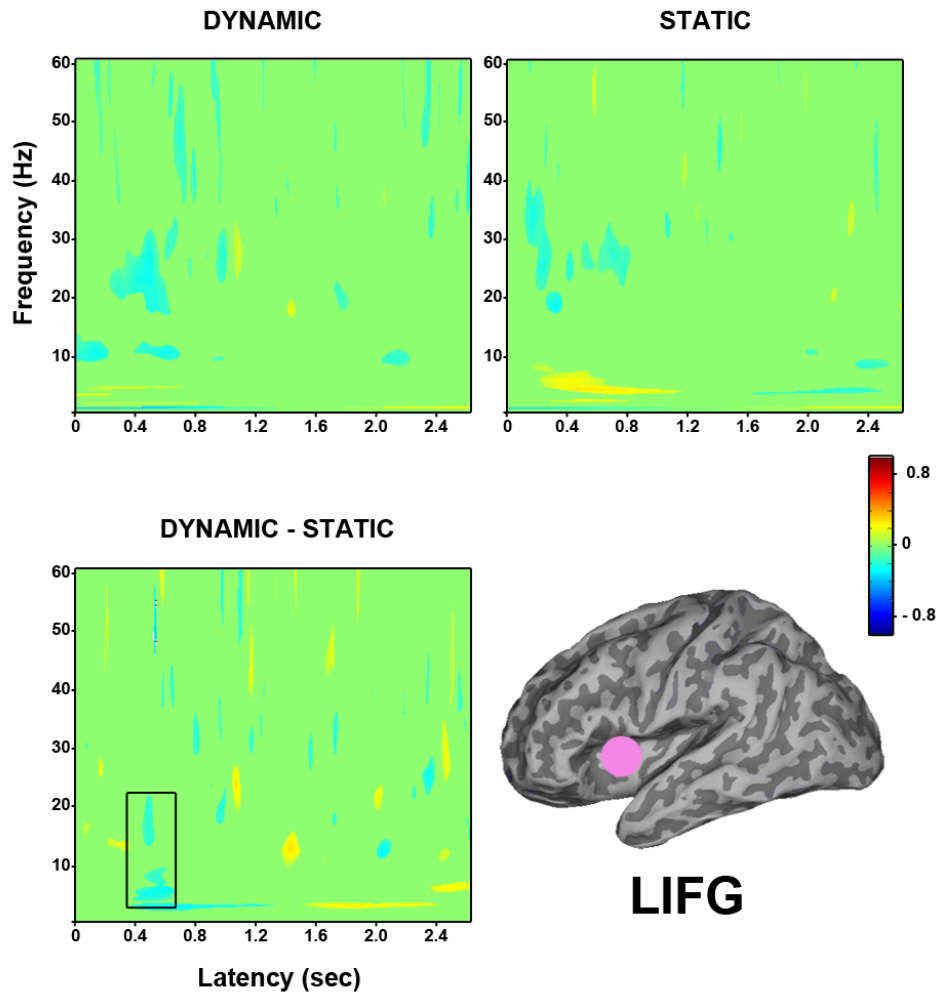


Figure 5.3.21: Group time frequency findings in left inferior frontal gyrus (N=9), shows decreased power for dynamic happy relative to static happy expressions within 400-600 ms between 2-22 Hz. This is due to an increase in low frequency power (2-10 Hz) and a decrease in power (15-22 Hz) for dynamic happy faces around 400 ms. Top left: Dynamic happy faces versus baseline fixation; Top right: Static happy faces versus baseline fixation; Bottom left: Dynamic versus static happy faces.

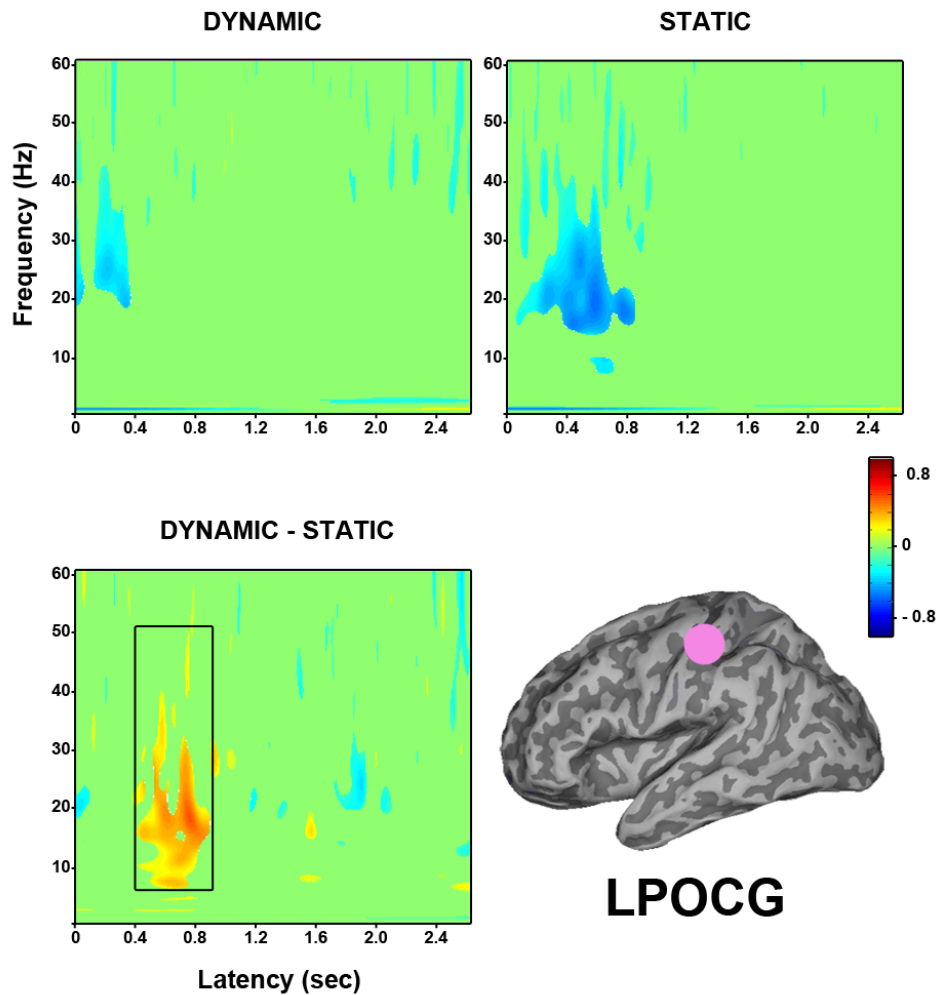


Figure 5.3.22: Group time frequency findings in left postcentral gyrus (N=8), shows greater power for dynamic happy relative to static happy expressions within 400-600 ms between 5-50 Hz. This is due to a greater decrease in power (15-60 Hz) for static happy faces around 500 ms. Top left: Dynamic happy faces versus baseline fixation; Top right: Static happy faces versus baseline fixation; Bottom left: Dynamic versus static happy faces.

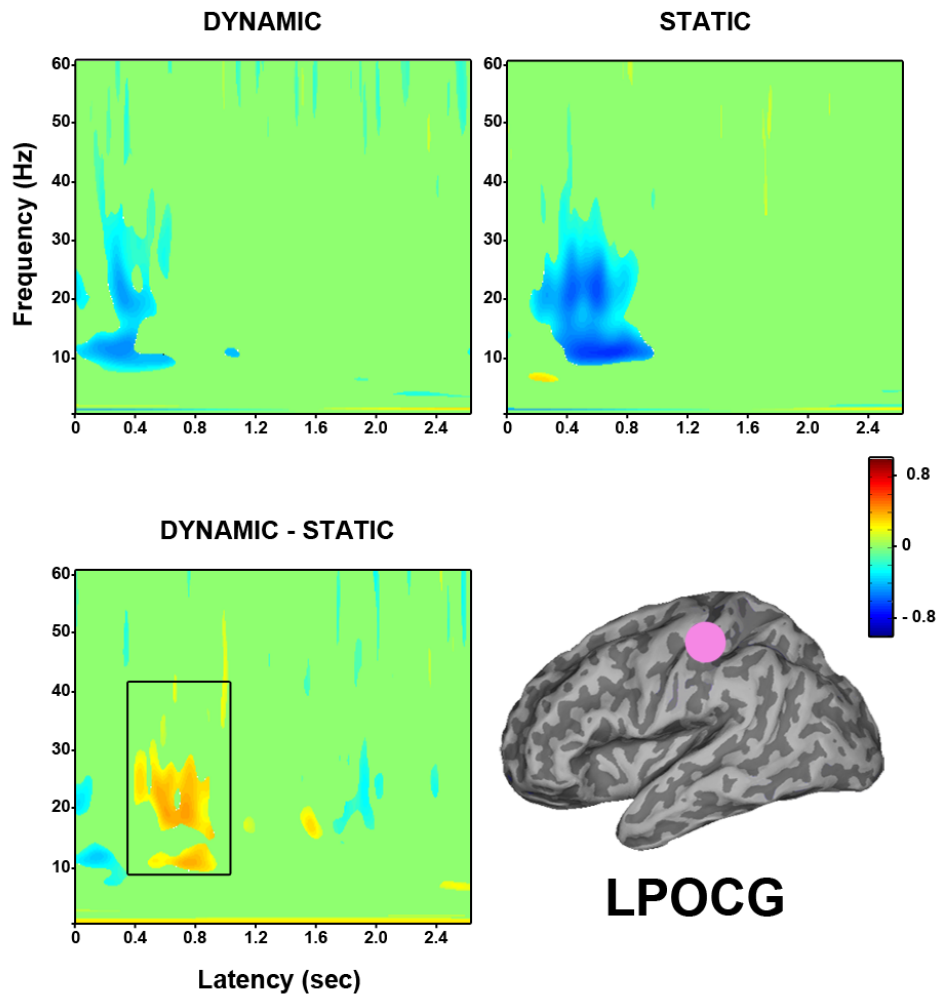


Figure 5.3.23: Group time frequency findings in left postcentral gyrus (N=9), shows greater power for dynamic happy relative to static happy expressions within 600-800 ms between 10-40 Hz. This is due to a greater decrease in power (10-40 Hz) for static happy faces around 600 ms. Top left: Dynamic happy faces versus baseline fixation; Top right: Static happy faces versus baseline fixation; Bottom left: Dynamic versus static happy faces.

A virtual electrode constructed in this region revealed that dynamic faces once again elicited an early sustained power decrease from stimulus onset ranging from 8-30 Hz and centred around 10 Hz. Static happy expressions also elicited a sustained response but with a slightly later onset around 100 ms, again ranging from 8-30 Hz and centred around 10 Hz, however this response reduced from 800 ms onwards. The direct contrast of dynamic versus static happy expressions revealed an early power decrease in the range of 8–40 Hz within 200 ms, followed by a power increase from 300–600 ms in the 10-20 Hz range, which was then followed by a decrease in power in the range of 12-35 Hz at 800 ms which was due to the greater decrease in power to dynamic happy faces at this time.

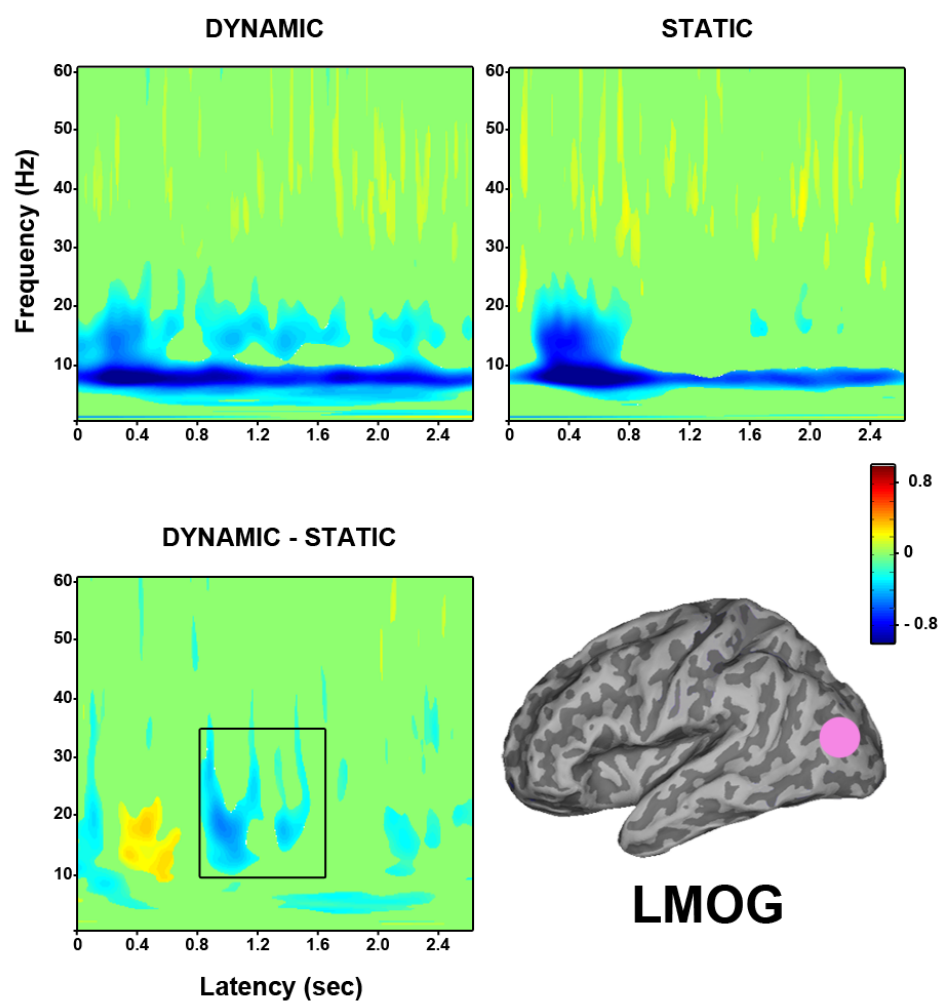


Figure 5.3.24: Group time frequency findings in left middle occipital gyrus (N=11), shows decreased power for dynamic happy relative to static happy expressions within 800-1000 ms between 12-35 Hz. This is due to a greater peak decrease in power (12-35 Hz) for dynamic happy faces from 800 ms onwards. Top left: Dynamic happy faces versus baseline fixation; Top right: Static happy faces versus baseline fixation; Bottom left: Dynamic versus static happy faces.

A region in left MTG showed less power in response to dynamic happy relative to static

happy expressions during the 1000-1200 ms time window (see Figure 5.3.25). A virtual electrode constructed here showed that dynamic happy expressions relative to baseline once again elicited an early sustained decrease in power in the range of 10-40 Hz centred around 10 Hz, while static happy faces showed a short increase in low frequency power (5 Hz) around 200 ms, followed by a decrease in higher frequency power (8-30 Hz) from 200–1000 ms, along with a short power increase around 1000 ms at 15 Hz. The direct comparison of dynamic and static happy expressions showed an early power decrease (10–20 Hz) within 200s, followed by a power increase ranging from 4-22 Hz at around 500 ms. This was then followed by a broad decrease in power ranging from 8-35 Hz at ~1000 ms as a result of the decrease in power to dynamic happy expressions.

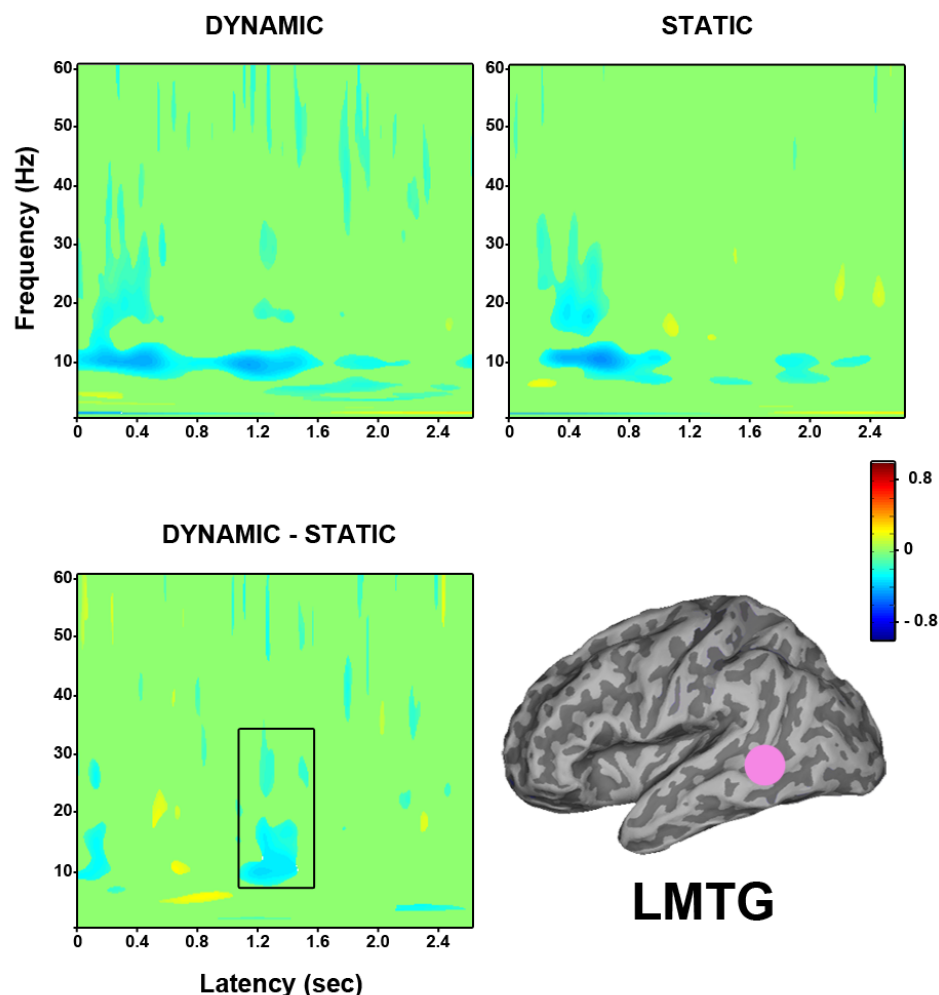


Figure 5.3.25: Group time frequency findings in left middle temporal gyrus (N=10), shows decreased power for dynamic happy relative to static happy expressions within 1000-1200 ms between 8-35 Hz. This is due to a greater decrease in power (10-40 Hz) for dynamic happy faces from 800 ms onwards. Top left: Dynamic happy faces versus baseline fixation; Top right: Static happy faces versus baseline fixation; Bottom left: Dynamic versus static happy faces.

A region in right STS also showed a power decrease in response to dynamic happy relative to static happy expressions during the 1000-1200 ms time window (see Figure 5.3.26). A virtual electrode constructed here showed that dynamic happy faces again elicited an early sustained decrease in power in the range of 8-40 Hz, primarily centred around 12 Hz for stimulus duration, along with a decrease in low frequency power (4-6 Hz) from 600-2000 ms. Static happy faces showed a decrease from 200-800 ms in the range of 8-30 Hz followed by a later power decrease of reduced amplitude from 1400-2500 ms in the 10-20 Hz range. Dynamic happy relative to static happy expressions showed an early decrease in power within 200s from 5–40 Hz, followed by a power increase around 500 ms from 10-40 Hz, which was then followed by a broader power decrease (5-35 Hz) from around 800 ms due to the sustained decrease in power in the dynamic happy condition. Similarly a region in right fusiform gyrus showed decreased power in the dynamic happy condition relative to static happy during the 1200-1400 ms time window (see Figure 5.3.27). The virtual electrode constructed here revealed a very similar response to dynamic happy expressions, with a sustained power decrease in the 10-30 Hz range. Static happy expressions relative to baseline also showed a sustained decrease from 10-30 Hz again with a slightly later onset of 200 ms and a reduction in amplitude from ~1000 ms onwards. Slight increases in high frequency power (30-60 Hz) were also present, along with increases in low frequency power (2-6 Hz) from 500 ms onward. The direct contrast of dynamic and static happy expressions again showed an early power decrease within 200 ms in the 5-30 Hz range, followed by a power increase around 500 ms in the 10-25 Hz range which was then followed by a broad decrease in power (2-40 Hz) from 1000 ms as a result of the more sustained decrease in power to dynamic happy expressions and also the increases in high (30-60 Hz) and low (2-6 Hz) frequency power to static happy expressions.

The final virtual electrode was placed in a region in left STS where decreased power to dynamic happy relative to static happy expressions was found in the 2000-2200 ms time interval (see Figure 5.3.28). Dynamic happy expressions compared to baseline show scattered power decreases but note the broad power decrease from 2000 ms ranging from 5-60 Hz. Static happy faces compared to baseline also show scattered decreases in power (10-40 Hz) along with an increase in power around 2000 ms at 5 Hz and in the 20-60 Hz range. The direct comparison of dynamic and static happy expressions shows a power

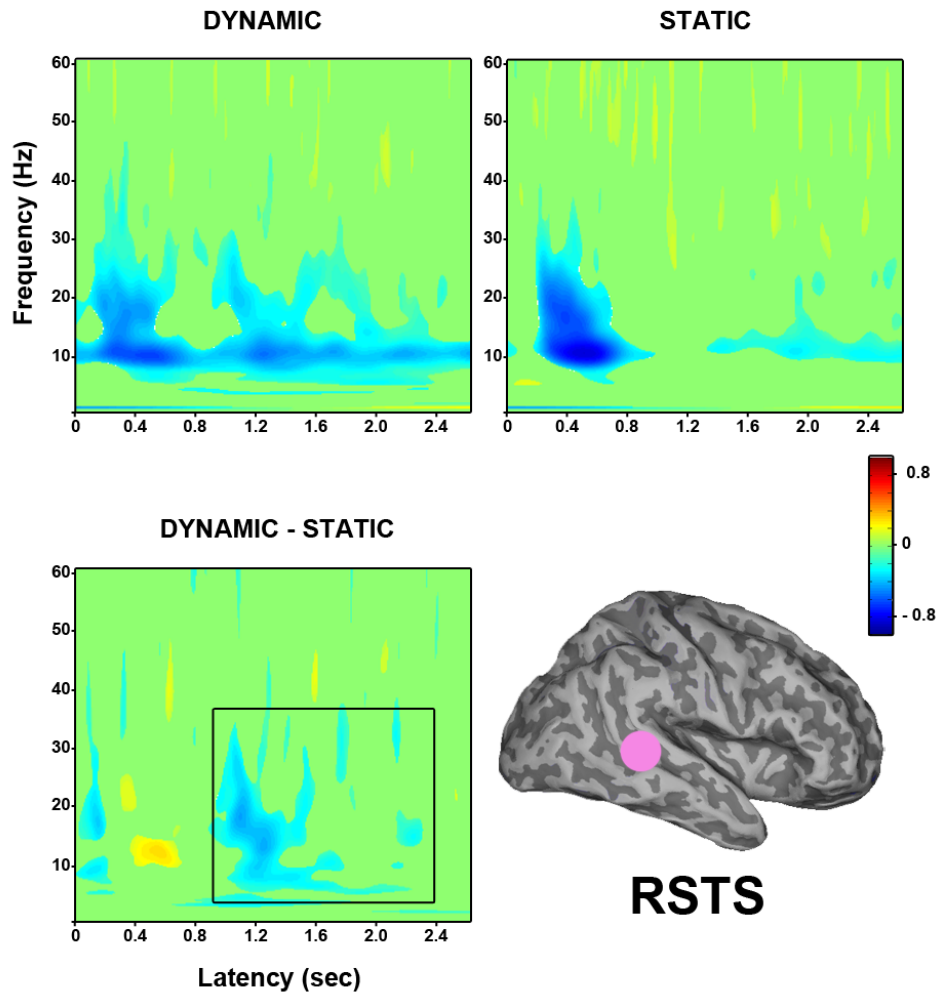


Figure 5.3.26: Group time frequency findings in right superior temporal sulcus (N=11), shows decreased power for dynamic happy relative to static happy expressions within 1000-1200 ms between 5-35 Hz. This is due to a greater and more sustained decrease in power (8-40 Hz) for dynamic happy faces from 800 ms onwards. Top left: Dynamic happy faces versus baseline fixation; Top right: Static happy faces versus baseline fixation; Bottom left: Dynamic versus static happy faces.

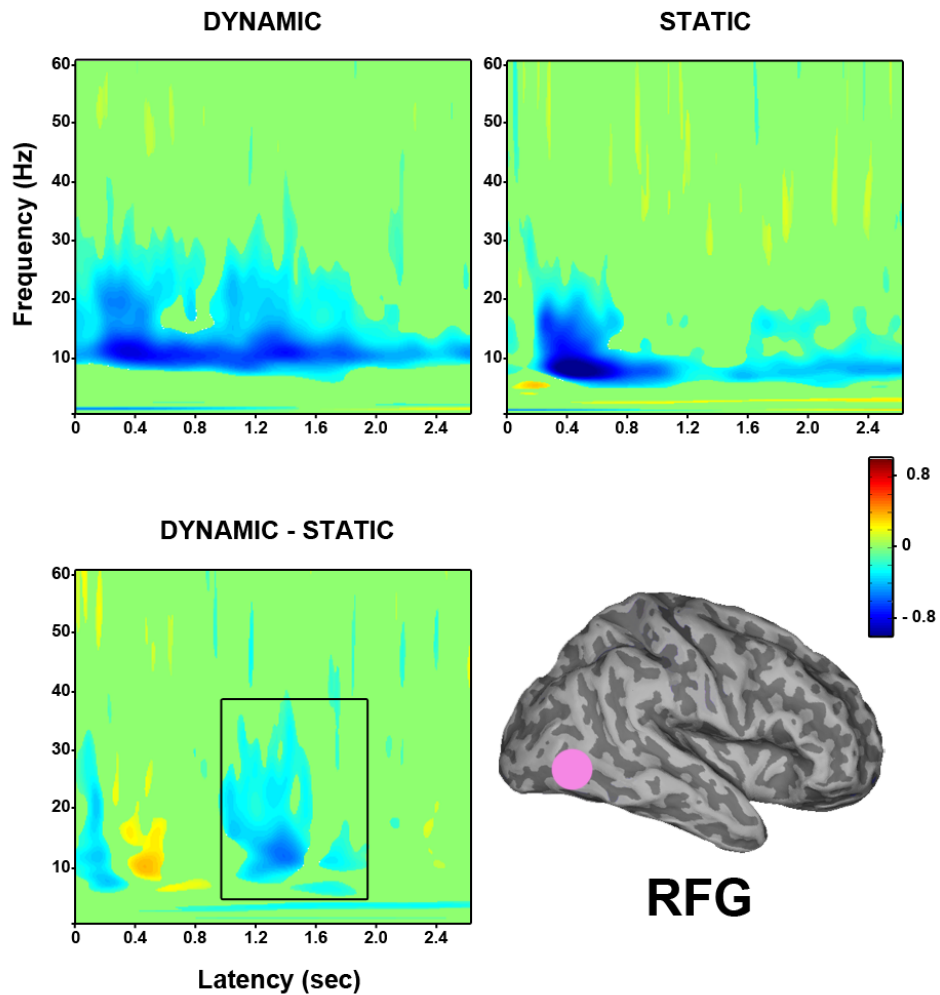


Figure 5.3.27: Group time frequency findings in right fusiform gyrus (N=12), shows decreased power for dynamic happy relative to static happy expressions within 1200-1400 ms between 2-40 Hz. This is due to a greater and more sustained decrease in power (10-30 Hz) for dynamic happy faces from 1000 ms onwards. Top left: Dynamic happy faces versus baseline fixation; Top right: Static happy faces versus baseline fixation; Bottom left: Dynamic versus static happy faces.

decrease around 2000 ms ranging from 8-35 Hz which is as a result of both the decrease in power in the dynamic happy condition as well as the slight power increase in the static happy condition.

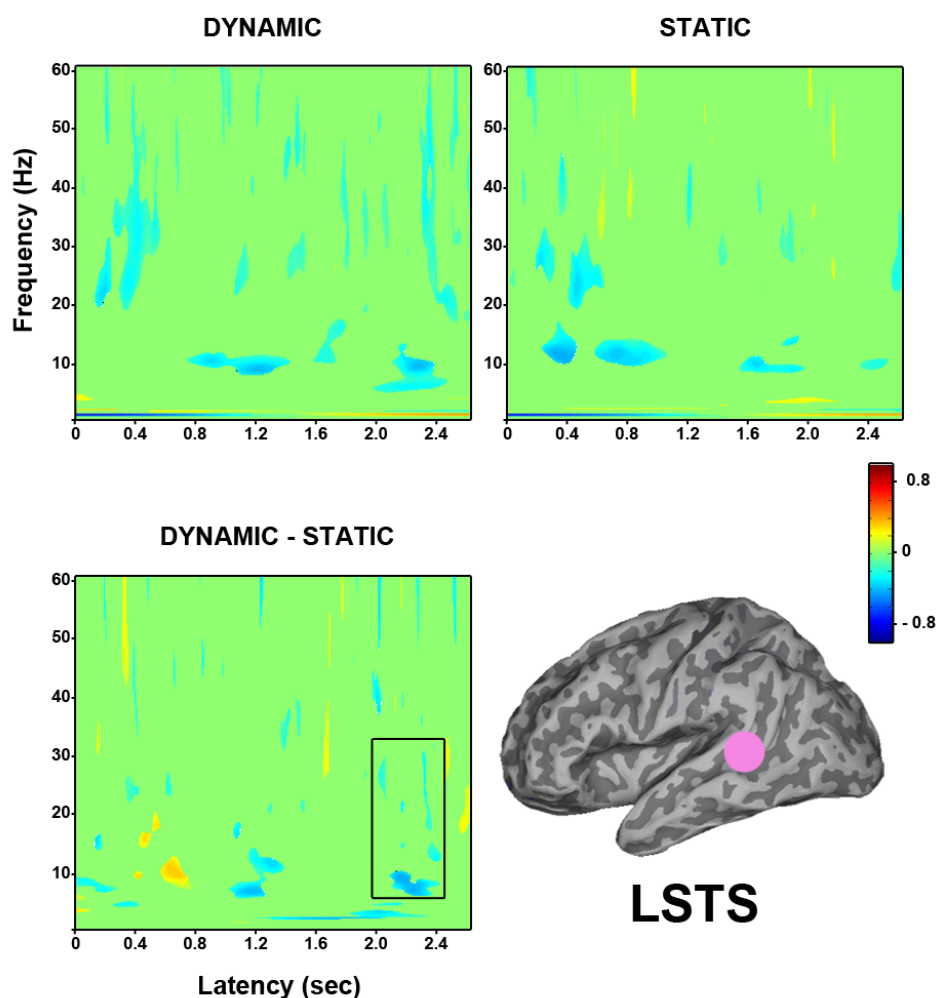


Figure 5.3.28: Group time frequency findings in left superior temporal sulcus (N=8), shows decreased power for dynamic happy relative to static happy expressions within 2000-2200 ms between 8-35 Hz. This is due to a decrease in power (5-60 Hz) for dynamic happy faces around 2000 ms. Top left: Dynamic happy faces versus baseline fixation; Top right: Static happy faces versus baseline fixation; Bottom left: Dynamic versus static happy faces.

Dynamic happy versus dynamic speech displays. Virtual electrodes were again constructed at the peak locations identified by SAM in order to map the time-frequency characteristics of these regions of interest. Virtual electrodes were only constructed for those participants who showed a peak at the selected location in the SAM volume. The first two virtual electrodes were constructed in bilateral IFG where early differences were found between dynamic happy and dynamic speech displays within 200 ms of stimulus onset. In left IFG this early difference was due to significantly greater increases in low

frequency power (2-6 Hz) for dynamic happy facial expressions within 200 ms of stimulus onset (see Figure 5.3.29). Similarly in right IFG the early difference was again due to

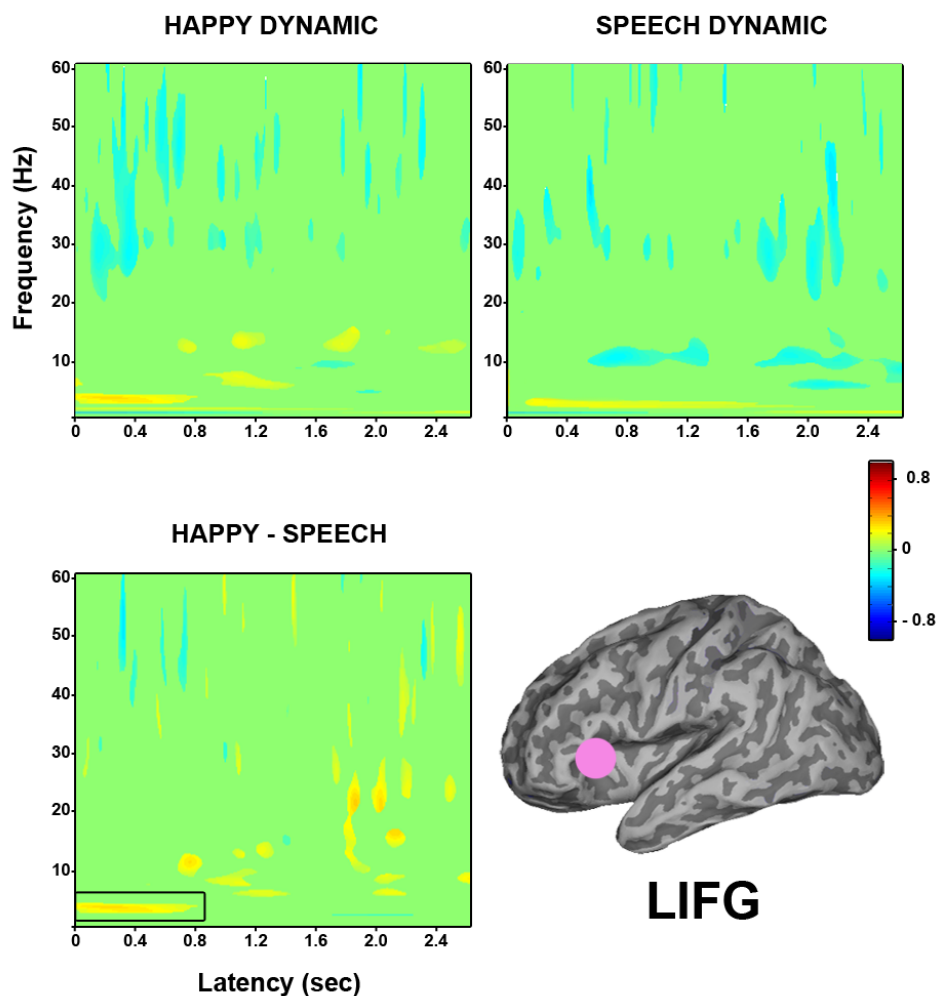


Figure 5.3.29: Group time frequency findings in left inferior frontal gyrus (N=8), shows significantly greater power (2-6 Hz) for dynamic happy relative to dynamic speech facial displays between 0-800 ms. This is due to a greater increase in low frequency power (2-6 Hz) for dynamic happy faces within 200 ms of stimulus onset. Top left: Dynamic happy faces versus baseline fixation; Top right: Dynamic speech faces versus baseline fixation; Bottom left: Dynamic happy versus dynamic speech faces.

significantly greater increases in low frequency power (2-6 Hz) for dynamic happy relative to dynamic speech facial expressions from 0-500 ms (see Figure 5.3.30).

A virtual electrode was then constructed in left middle occipital gyrus and revealed significantly greater decreases in power (8-22 Hz) for dynamic happy faces from 200-800 ms (see Figure 5.3.31). The final virtual electrode was constructed in the left fusiform gyrus and this also revealed significantly greater decreases in power (6-20 Hz) for dynamic happy facial expressions between 900-1600 ms (see Figure 5.3.32).

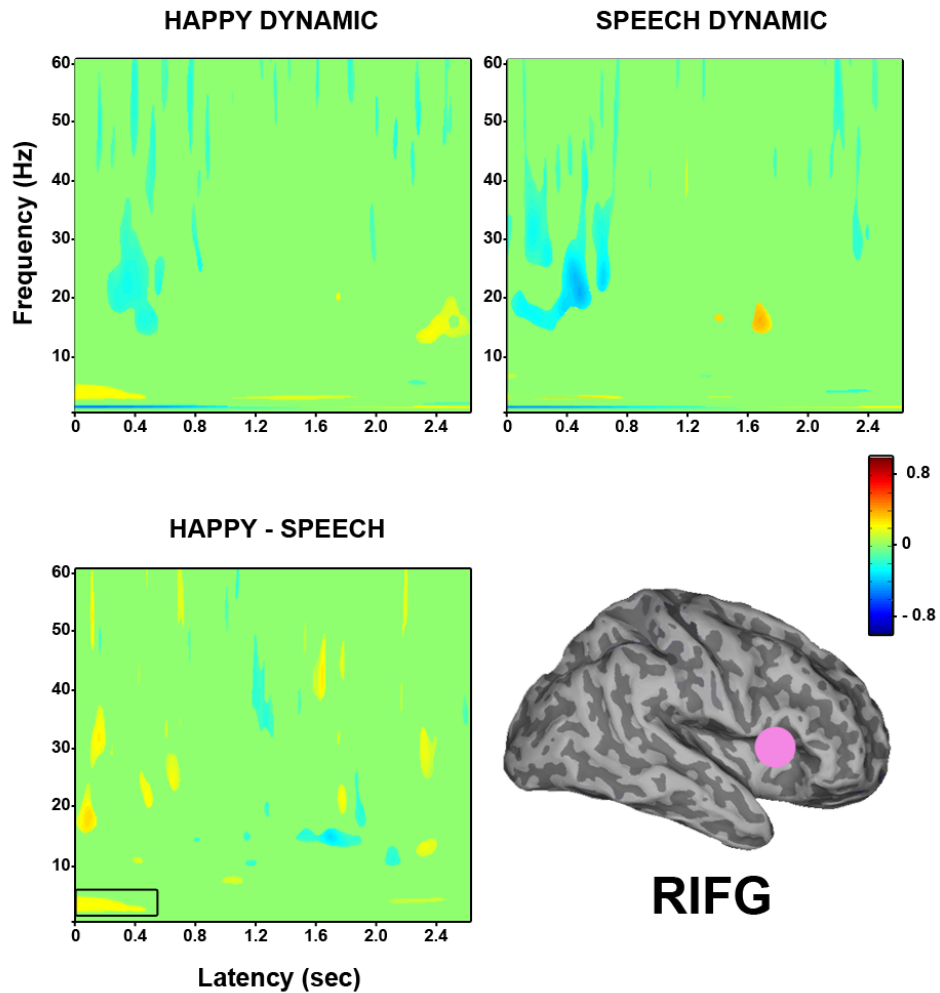


Figure 5.3.30: Group time frequency findings in right inferior frontal gyrus (N=9), shows significantly greater power (2-6 Hz) for dynamic happy relative to dynamic speech facial displays between 0-500 ms. This is due to a greater increase in low frequency power (2-6 Hz) for dynamic happy faces within 200 ms of stimulus onset. Top left: Dynamic happy faces versus baseline fixation; Top right: Dynamic speech faces versus baseline fixation; Bottom left: Dynamic happy versus dynamic speech faces.

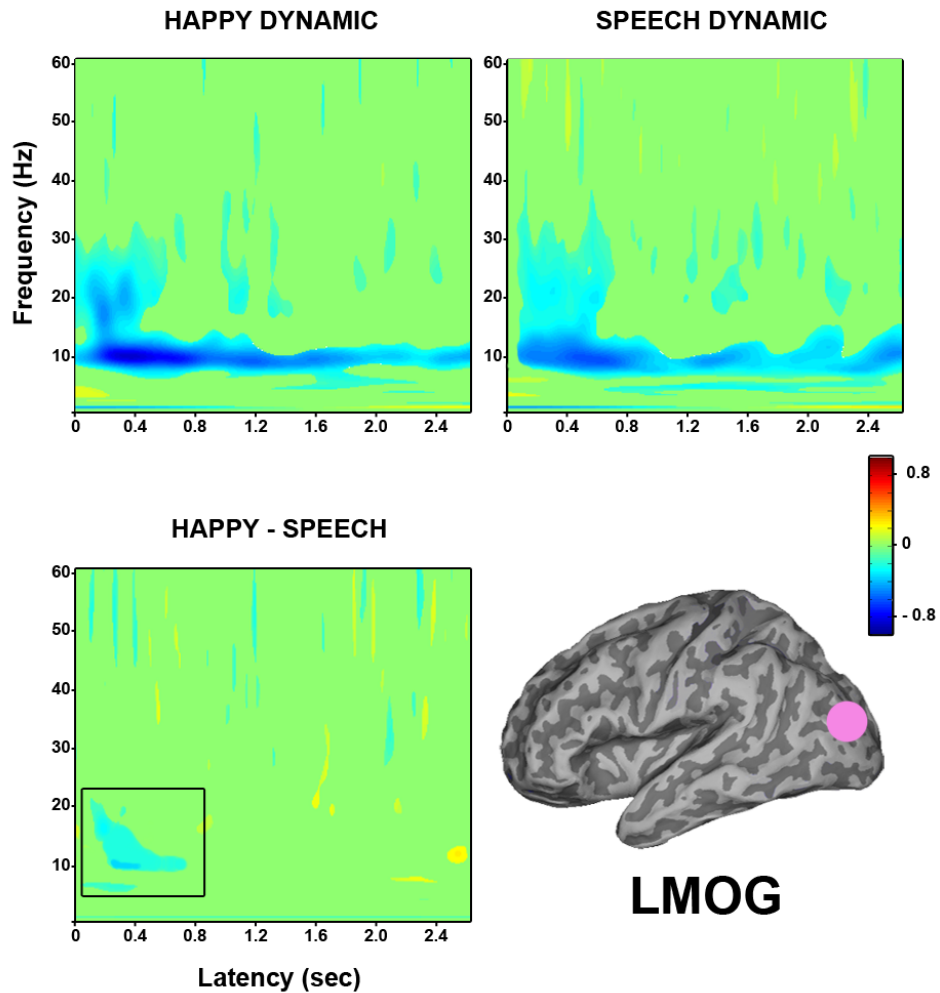


Figure 5.3.31: Group time frequency findings in left middle occipital gyrus (N=12), shows significantly less power (8-22 Hz) for dynamic happy relative to dynamic speech facial displays between 200-800 ms. This is due to a greater decrease in power (8-22 Hz) for dynamic happy faces around 200 ms. Top left: Dynamic happy faces versus baseline fixation; Top right: Dynamic speech faces versus baseline fixation; Bottom left: Dynamic happy versus dynamic speech faces.

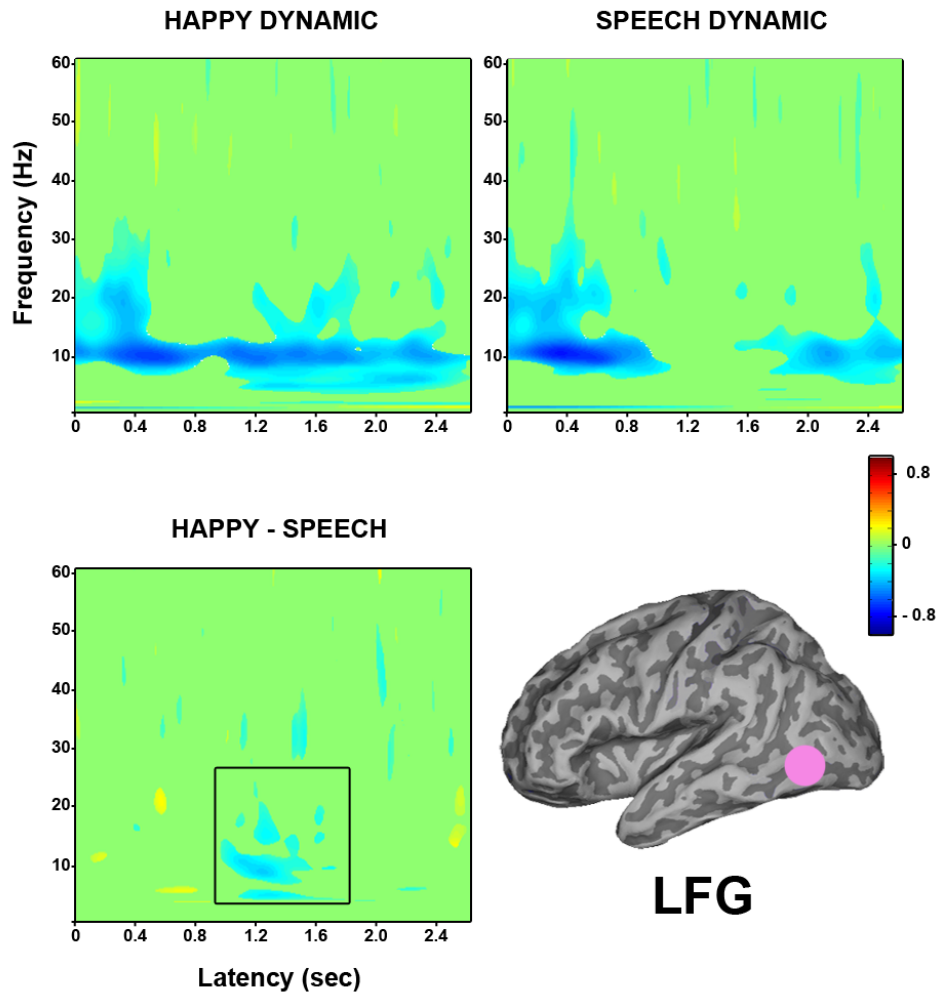


Figure 5.3.32: Group time frequency findings in left fusiform gyrus (N=12), shows significantly less power (6-20 Hz) for dynamic happy relative to dynamic speech facial displays between 900-1600 ms. This is due to a greater decrease in power (6-20 Hz) for dynamic happy faces from 900-1600 ms. Top left: Dynamic happy faces versus baseline fixation; Top right: Dynamic speech faces versus baseline fixation; Bottom left: Dynamic happy versus dynamic speech faces.

5.3.3 Dynamic speech versus static speech facial displays

5.3.3.1 Source analysis results

SAM was again computed across twelve different 200 ms time windows using a wide frequency band of 1-80 Hz, to identify sources of differential activity between dynamic speech and static speech facial displays, across the length of stimulus presentation. Group analysis was again performed using SnPm to identify significantly clustered peaks across the group of participants in response to dynamic speech versus static speech face stimuli. In the first time window from 0 to 200 ms peaks were identified in bilateral IFG that showed significantly greater oscillatory power in response to dynamic speech relative to static speech displays across the group, while regions in bilateral IOG showed significantly less power for dynamic speech compared to static speech displays. In the subsequent time window from 200-400 ms a peak was again identified in left IOG, this time showing significantly greater power for dynamic speech relative to static speech displays. A peak was identified in right STS in a later time window from 800-1000 ms, showing significantly less power for dynamic relative to static speech displays.

Three peaks were identified in the following time window from 1000-1200 ms, one in left postcentral gyrus showing significantly greater power for dynamic relative to static speech, along with a peak in left middle occipital gyrus and left IFG, both showing significantly less power for dynamic speech relative to static speech displays. In the next time window from 1200-1400 a peak was identified in left MTG as showing significantly less power for dynamic relative to static speech displays, and a peak in was also found in left middle frontal gyrus showing significantly less power for dynamic speech relative to static speech displays.

Two peaks were found in a later time window from 1800-2000 ms, in right IOG and right MTG, both showing significantly less power for dynamic compared to static speech displays. Another three peaks were found in the subsequent time window from 2000-2200 ms, in left MTG and bilateral STS, again all showing significantly less power for dynamic relative to static speech displays. Finally, two peaks were identified in the time window from 2200-2400 ms in right IOG and right STS, both showing significantly less power in response to dynamic compared to static speech displays.

Table 5.5: Brain regions showing significant differences in oscillatory power in response to dynamic speech versus static speech facial displays within the following time windows: (A) 0-200 ms (B) 800-1000 ms (C) 1000-1200 ms (D) 1200-1400 ms (E) 1800-2000 ms (F) 2000-2200 ms and (G) 2200-2400 ms. Co-ordinates indicate local maxima in Talairach space. Clusters are significant at $p < .05$. N = number of participants showing a peak in that region. L = Left; R = Right.

Region	N	Pseudo t	x	y	z
<i>(A) 0-200 ms</i>					
L Inferior frontal gyrus (BA 46)	8	+3.82	-42	42	6
R Inferior frontal gyrus (BA 47)	10	+4.54	57	33	-10
L Inferior occipital gyrus (BA 19)	12	- 5.51	-48	-80	-6
R Inferior occipital gyrus (BA 19)	12	- 6.09	48	-80	-6
<i>(B) 800-1000 ms</i>					
R Superior temporal sulcus (BA 22)	9	- 4.05	52	-48	8
<i>(C) 1000-1200 ms</i>					
L Postcentral gyrus (BA 3)	9	+ 4.48	-42	-24	60
L Middle occipital gyrus (BA 18)	10	- 3.68	-30	-81	-9
L Inferior frontal gyrus (BA 47)	8	- 4.76	-39	21	2
<i>(D) 1200-1400 ms</i>					
L Middle temporal gyrus (BA 21)	10	- 3.98	-51	6	-20
L Middle frontal gyrus (BA 6)	9	- 3.73	-30	6	52
<i>(E) 1800-2000 ms</i>					
R Inferior occipital gyrus (BA 18)	11	- 4.69	33	-87	-6
R Middle temporal gyrus (BA 21)	10	- 4.55	68	-15	-6
<i>(F) 2000-2200 ms</i>					
R Superior temporal sulcus (BA 13)	9	- 4 .44	51	-42	18
<i>(G) 2200-2400 ms</i>					
R Inferior occipital gyrus (BA 18)	12	- 4.63	36	-84	-12

5.3.3.2 Time frequency results

Virtual electrodes were again constructed at the peak locations identified by SAM in order to map the time-frequency characteristics of responses at these regions of interest. Once again virtual electrodes were only constructed for those participants who showed a peak at the selected location in the SAM volume. Firstly, virtual electrodes were constructed in bilateral IFG, where early differences between dynamic speech and static speech displays were found within 200 ms of stimulus onset, showing greater power for dynamic speech displays relative to static.

A virtual electrode constructed in the region in left IFG showed an increase in power from 5-10 Hz and 20-40 Hz within 200 ms of stimulus onset for dynamic speech relative to static speech displays (see Figure 5.3.33). This is driven by the slight increase in power from 3-10 Hz in response to dynamic speech relative to baseline, along with a decrease in power from 20-40 Hz for static speech relative to baseline. A virtual electrode constructed in the region in right IFG showed a similar power increase from 5-25 Hz and 40-60 Hz for dynamic relative to static speech displays within 200 ms (see Figure 5.3.34). This increase in power is driven by an increase in low frequency power from 3-10 Hz for dynamic speech relative to baseline, and also by a decrease in high frequency power between 20-60 Hz for static speech displays relative to baseline.

Early differences were also found in bilateral IOG, this time showing significantly less power for dynamic relative to static speech displays within 200 ms of stimulus onset. A virtual electrode constructed in left IOG revealed a strong power decrease between 5-22 Hz for dynamic relative to static speech displays within 200 ms of stimulus onset (see Figure 5.3.35). The time frequency map shows a strong sustained decrease in power in response to dynamic speech displays compared to baseline between 5-20 Hz for the duration of presentation. Static speech displays relative to baseline also show a sustained decrease in power between 5-20 Hz but at a later time from ~300 ms onwards.

A similar response pattern was found in the region in right IOG, where the direct contrast of dynamic and static speech displays revealed a decrease in power between 5-25 Hz within 200 ms.. This is again driven by a sustained decrease in power to dynamic speech displays between 5-25 Hz from stimulus onset. Static speech displays relative to baseline show an early increase in power between 15-60 Hz followed by a sustained decrease in power

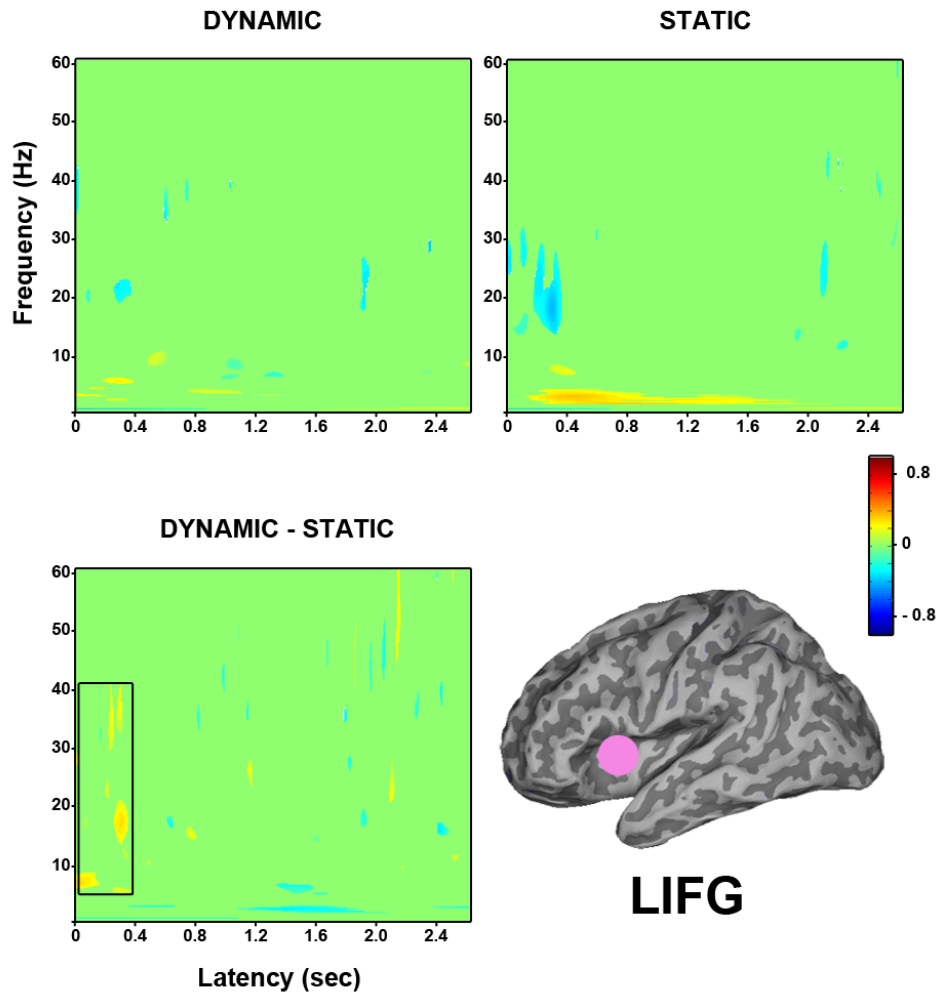


Figure 5.3.33: Group time frequency findings in left inferior frontal gyrus (N=8), shows early differences between dynamic speech and static speech displays around 200 ms, between 5-40 Hz. This is due to an increase in low frequency power (3-10 Hz) for dynamic speech faces and a decrease in power for static speech faces (20-40 Hz) within 0-200 ms. Top left: Dynamic speech faces versus baseline fixation; Top right: Static speech faces versus baseline fixation; Bottom left: Dynamic versus static speech faces.

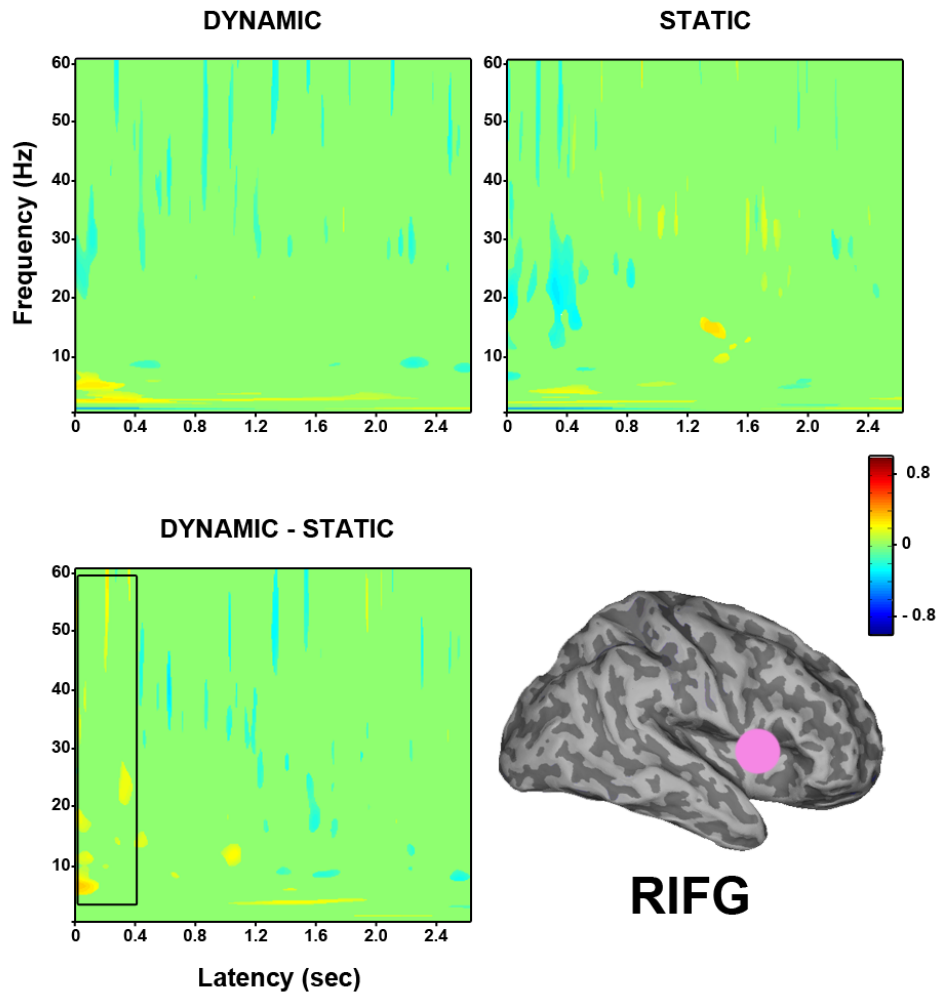


Figure 5.3.34: Group time frequency findings in right inferior frontal gyrus (N=10), shows early differences between dynamic speech and static speech displays around 200 ms, between 5-60 Hz. This is due to an increase in low frequency power for dynamic speech faces (3-10 Hz) and a decrease in high frequency power for static speech faces (20-60 Hz) within 0-200 ms. Top left: Dynamic speech faces versus baseline fixation; Top right: Static speech faces versus baseline fixation; Bottom left: Dynamic versus static speech faces.

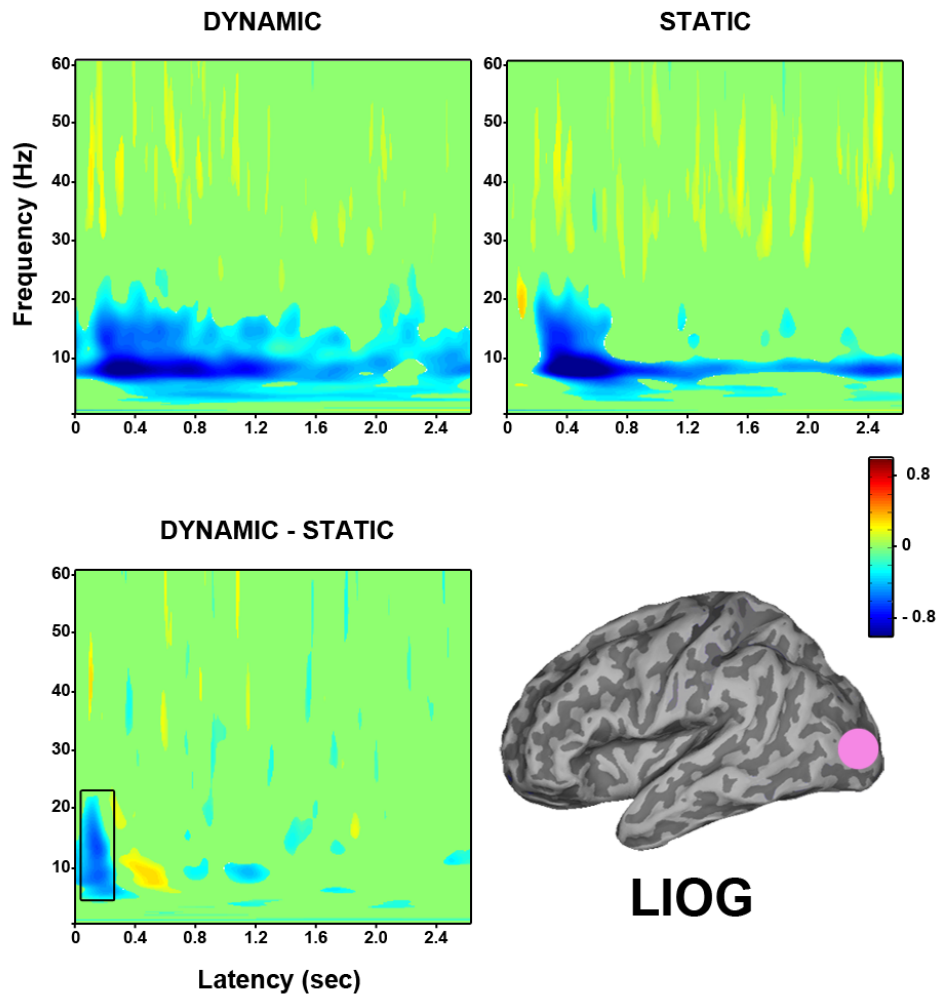


Figure 5.3.35: Group time frequency findings in left inferior occipital gyrus (N=12), shows early differences between dynamic speech and static speech displays around 200 ms, between 5-22 Hz. This is due to an early decrease in power (5-20 Hz) for dynamic speech faces within 0-200 ms. Top left: Dynamic speech faces versus baseline fixation; Top right: Static speech faces versus baseline fixation; Bottom left: Dynamic versus static speech faces.

between 10-20 Hz (see Figure 5.3.36). A virtual electrode constructed in the region in

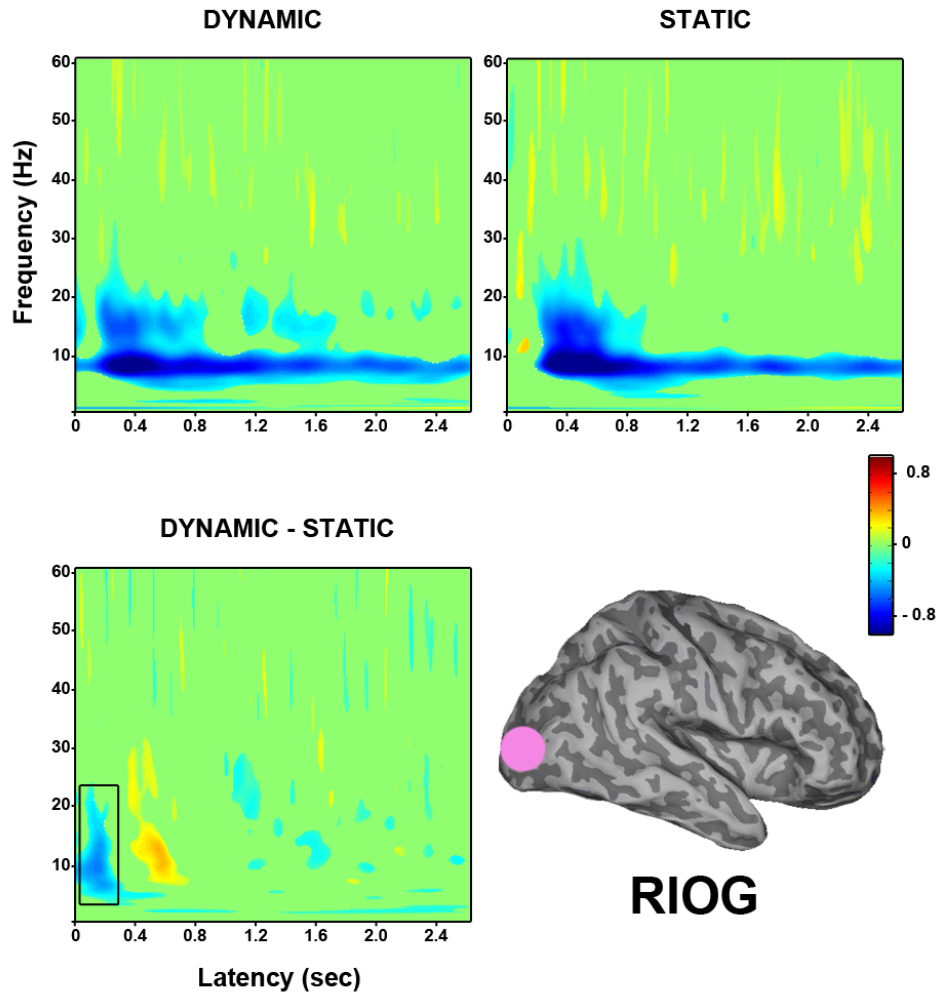


Figure 5.3.36: Group time frequency findings in right inferior occipital gyrus (N=12), shows early differences between dynamic speech and static speech displays around 200 ms between 5-22 Hz. This is due to an early decrease in power (5-20 Hz) for dynamic speech faces within 0-200 ms. Top left: Dynamic speech faces versus baseline fixation; Top right: Static speech faces versus baseline fixation; Bottom left: Dynamic versus static speech faces.

right STS revealed a decrease in power between 5-20 Hz and 40-60 Hz from 800-1000 ms for dynamic speech displays compared to static (see Figure 5.3.37). This appears to be driven by the sustained decrease in power from ~500 ms onwards between 5-30 Hz in the dynamic speech condition relative to baseline. Decreases in high frequency power between 40-80 Hz are also present in the dynamic speech condition, whereas static speech displays elicited an early and less sustained decrease in lower frequency power between 10-40 Hz.

The next virtual electrode was constructed in a region in left postcentral gyrus that showed significantly greater power for dynamic speech relative to static from 1000-1200 ms (see Figure 5.3.38). The direct contrast of dynamic versus static speech displays revealed an

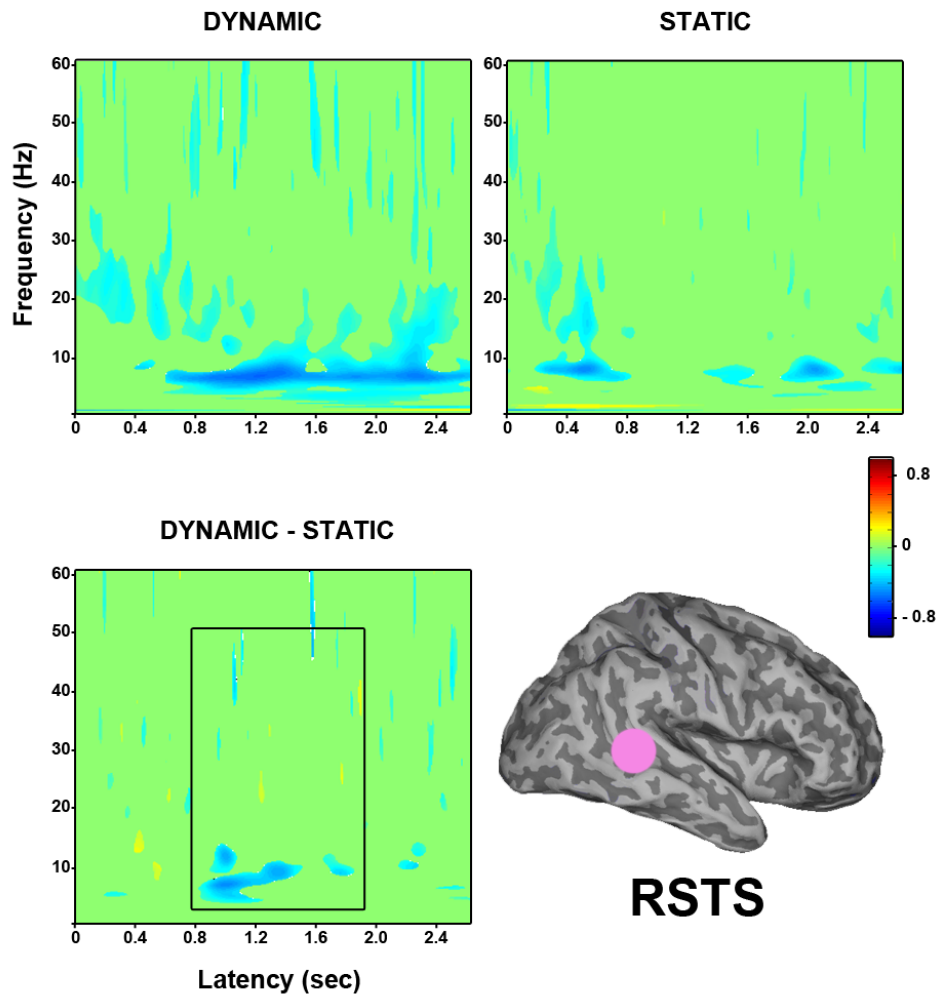


Figure 5.3.37: Group time frequency findings in right superior temporal sulcus (N=9), shows significantly less power for dynamic speech relative to static speech displays within 800-1000 ms, between 10-40 Hz. This is due to a sustained decrease in power (5-30 Hz) for dynamic speech faces from 500 ms onwards. Top left: Dynamic speech faces versus baseline fixation; Top right: Static speech faces versus baseline fixation; Bottom left: Dynamic versus static speech faces.

increase in power between 8-35 Hz centred around 1000 ms. This appears to be due to a power increase from 12-30 Hz in the dynamic speech condition and a decrease in power in the static speech condition from 10-20 Hz within this time period.

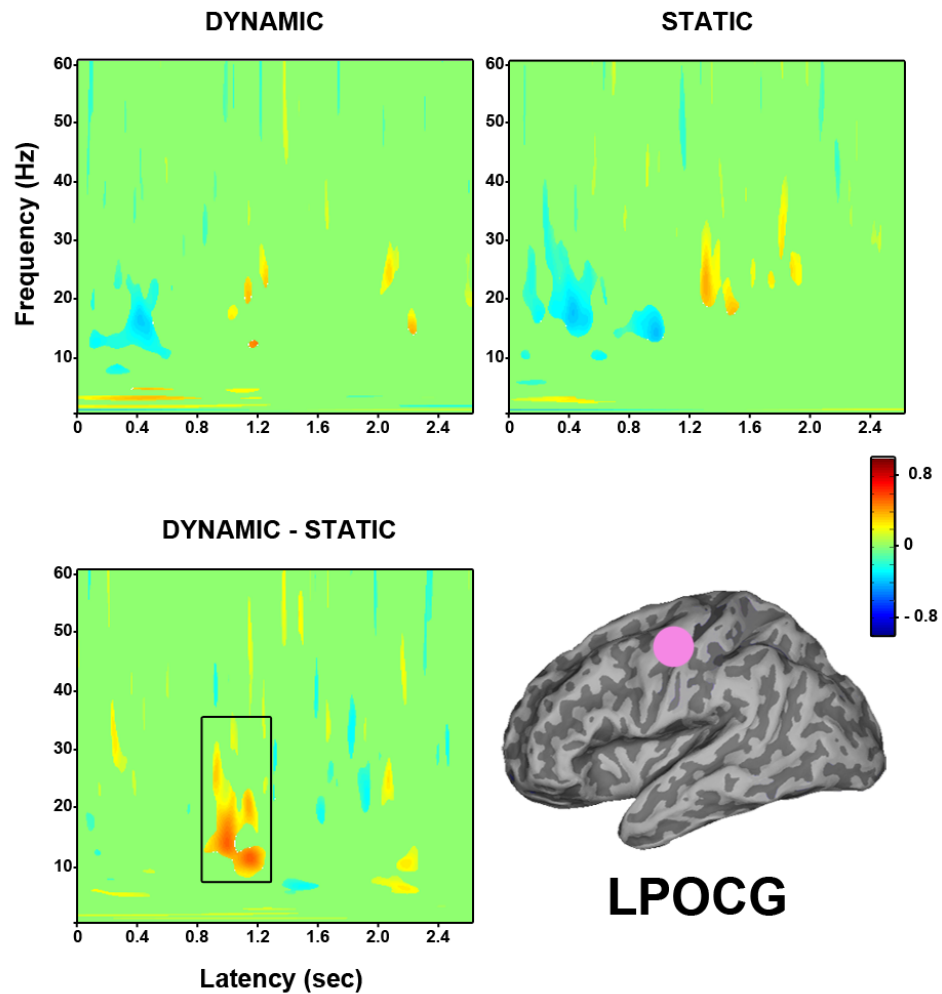


Figure 5.3.38: Group time frequency findings in left postcentral gyrus (N=9), shows significantly greater power for dynamic speech relative to static speech displays within 1000-1200 ms, between 8-35 Hz. This is due to an increase in power (12-30 Hz) for dynamic speech faces and a decrease in power (10-20 Hz) for static speech faces within 1000-1200 ms. Top left: Dynamic speech faces versus baseline fixation; Top right: Static speech faces versus baseline fixation; Bottom left: Dynamic versus static speech faces.

During this same time window from 1000-1200 ms a regions in left middle occipital gyrus was identified as showing significantly less power for dynamic speech displays relative to static. A virtual electrode constructed in this region showed a decrease in power between 5-30 Hz from 1000-1500 ms for dynamic relative to static speech displays. This appears to be driven by a sustained decrease in power between 5-20 Hz from 800 ms onwards in the dynamic speech condition. While the contrast of static faces with baseline, shows an early power decrease from 10-30 Hz within 500 ms of stimulus onset followed by a later

power decrease from approximately 1500 ms onwards (see Figure 5.3.39).

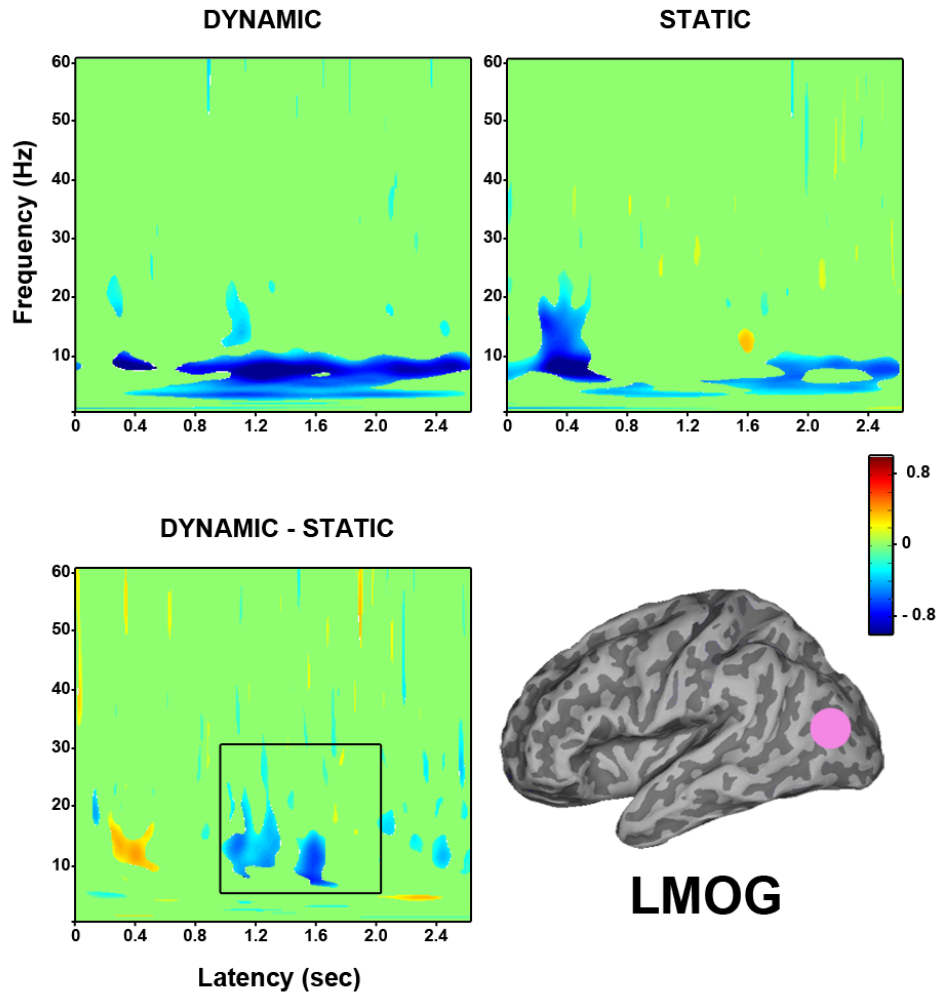


Figure 5.3.39: Group time frequency findings in left middle occipital gyrus (N=10), shows significantly less power for dynamic speech relative to static speech displays within 1000-1200 ms, between 5-30 Hz. This is due to a sustained decrease in power (5-20 Hz) for dynamic speech faces from 800 ms onwards. Top left: Dynamic speech faces versus baseline fixation; Top right: Static speech faces versus baseline fixation; Bottom left: Dynamic versus static speech faces.

A region in left IFG also showed significantly less power for dynamic relative to static speech displays during the 1000-1200 ms time window (see Figure 5.3.40). The time frequency map shows a decrease in power between 8-40 Hz at ~1000 ms for the direct contrast of dynamic versus static speech displays. This is due to both a decrease in power between 8-50 Hz in the dynamic speech condition, and an increase in power between 10-40 Hz in the static speech condition.

A virtual electrode was next constructed in a region in left MTG which was identified as showing significantly less power for dynamic compared to static speech displays in the time window from 1200-1400 ms. The direct contrast of dynamic versus static speech

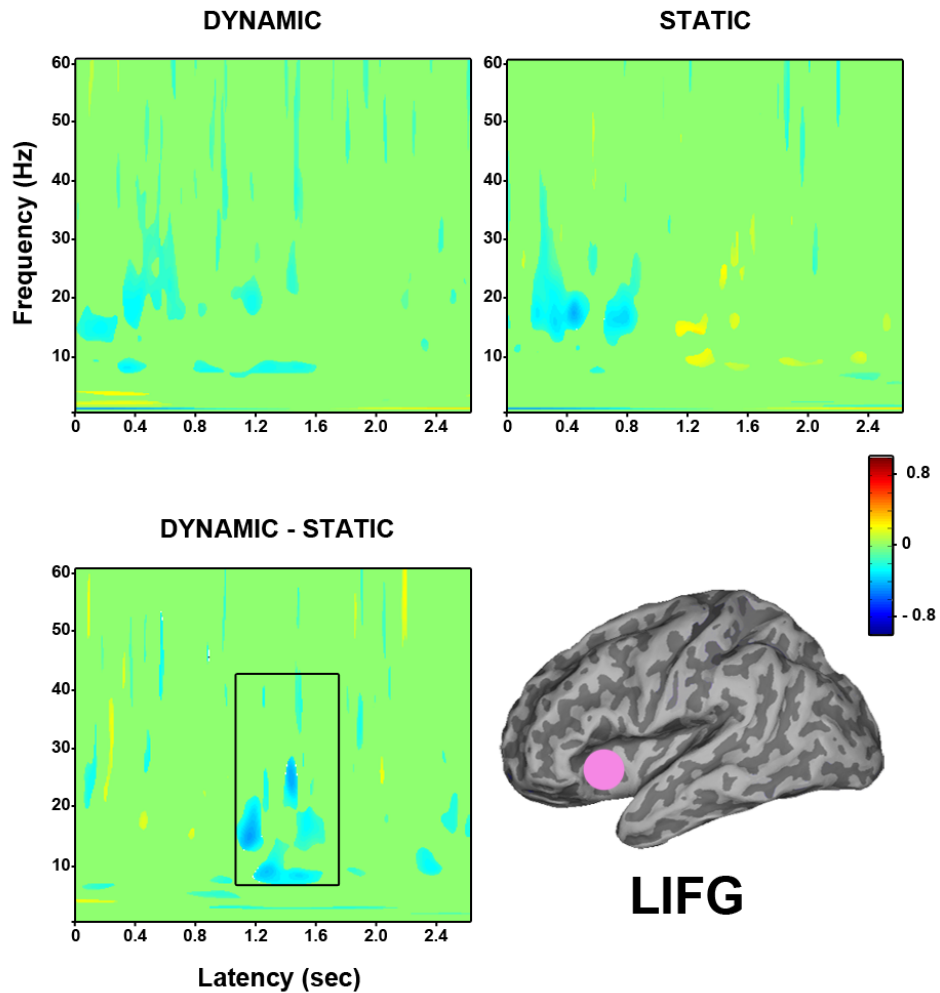


Figure 5.3.40: Group time frequency findings in left inferior frontal gyrus (N=8), shows significantly less power for dynamic speech relative to static speech displays within 1000-1200 ms, between 8-40 Hz. This is due to a decrease in power (8-50 Hz) for dynamic speech faces and an increase in power (10-40 Hz) for static speech faces around 1200 ms. Top left: Dynamic speech faces versus baseline fixation; Top right: Static speech faces versus baseline fixation; Bottom left: Dynamic versus static speech faces.

displays showed a sustained decrease in power between 5-20 Hz from ~1200 ms onwards, which is due to a sustained decrease in power in the dynamic speech condition between 5-30 Hz during this time and a slight increase in power around 15 Hz in the static speech condition (see Figure 5.3.41). During the same time window from 1200-1400 ms a region

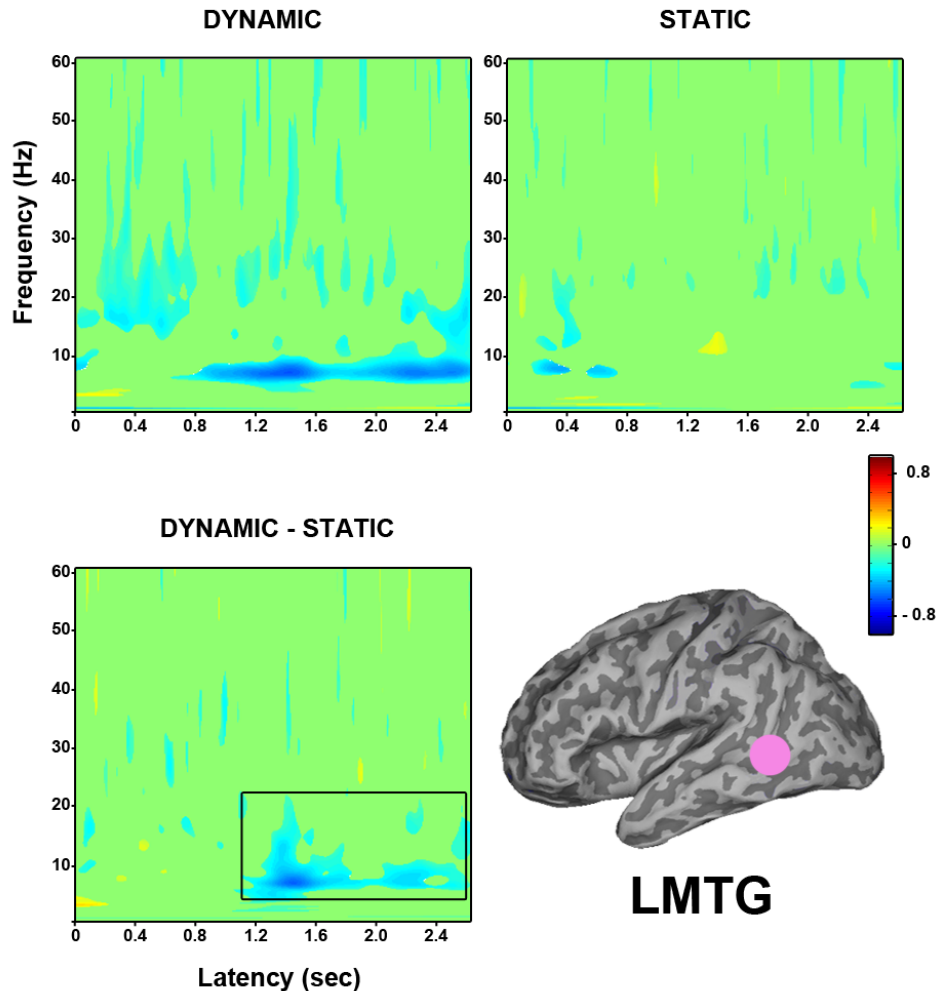


Figure 5.3.41: Group time frequency findings in left middle temporal gyrus (N=10), shows significantly less power for dynamic speech relative to static speech displays within 1200-1400 ms, between 5-20 Hz. This is due to a sustained decrease in power (5-30 Hz) for dynamic speech faces from 800 ms onwards. Top left: Dynamic speech faces versus baseline fixation; Top right: Static speech faces versus baseline fixation; Bottom left: Dynamic versus static speech faces.

in left middle frontal gyrus also showed significantly less power for dynamic relative to static speech displays (see Figure 5.3.42).. When a virtual electrode was constructed here the direct contrast of dynamic and static speech displays revealed a decrease in power between 3-30 Hz around 1300 ms. This appears to be driven by an increase in power in the static speech condition between 3-30 Hz from 1200-1500 ms. There is also a slight decrease in power in the dynamic speech condition between 5-10 Hz around 1200 ms.

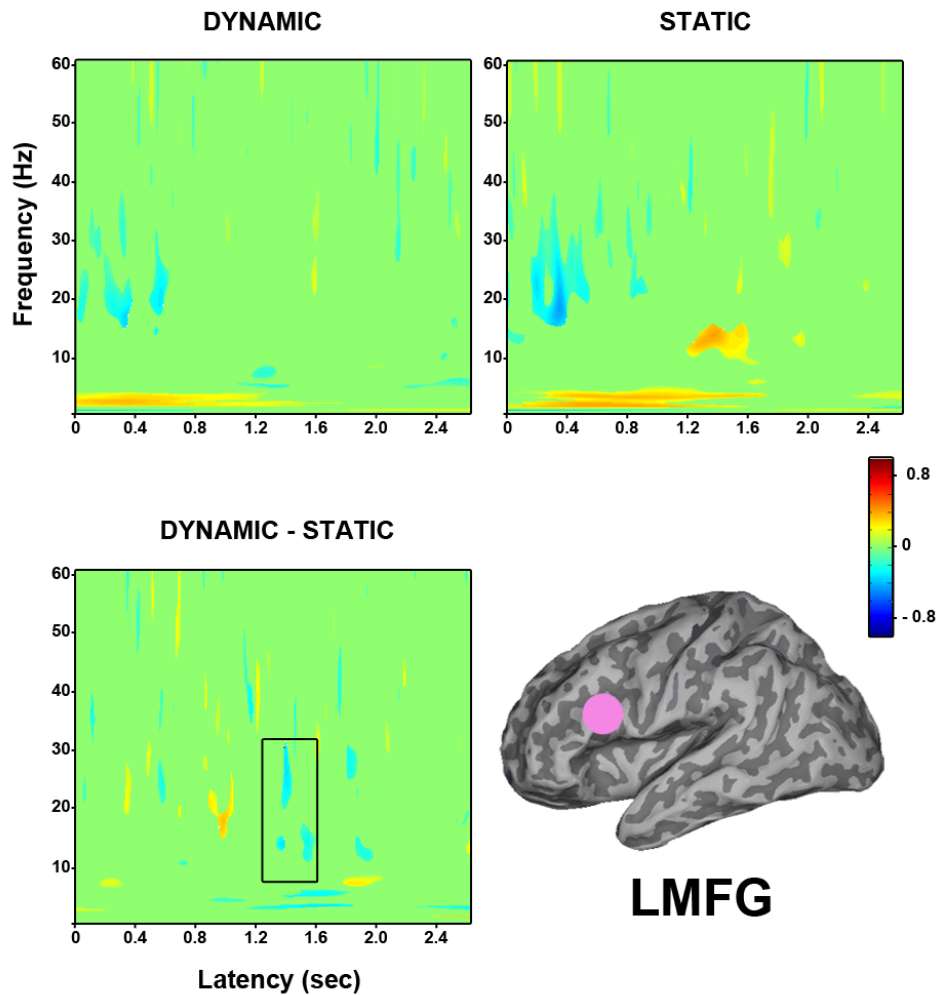


Figure 5.3.42: Group time frequency findings in left middle frontal gyrus (N=9), shows significantly less power for dynamic speech relative to static speech displays within 1200-1400 ms, between 3-30 Hz. This is due to an increase in power (3-30 Hz) for static speech faces around 1200 ms. Top left: Dynamic speech faces versus baseline fixation; Top right: Static speech faces versus baseline fixation; Bottom left: Dynamic versus static speech faces.

Another region in right IOG was identified in the later time window from 1800-2000 ms, showing significantly less power for dynamic relative to static speech displays (see Figure 5.3.43). A virtual electrode constructed here showed a decrease in power between 1-30 Hz around 2000 ms for the direct contrast of dynamic and static speech displays. This is due to the sustained decrease in power between 8-30 Hz in the dynamic speech condition. A sustained decrease in power is also shown in the static speech condition between 8-20 Hz but it is not as strong as in the dynamic speech condition. There is also a sustained increase in low frequency power between 2-8 Hz from stimulus onset in the static speech condition.

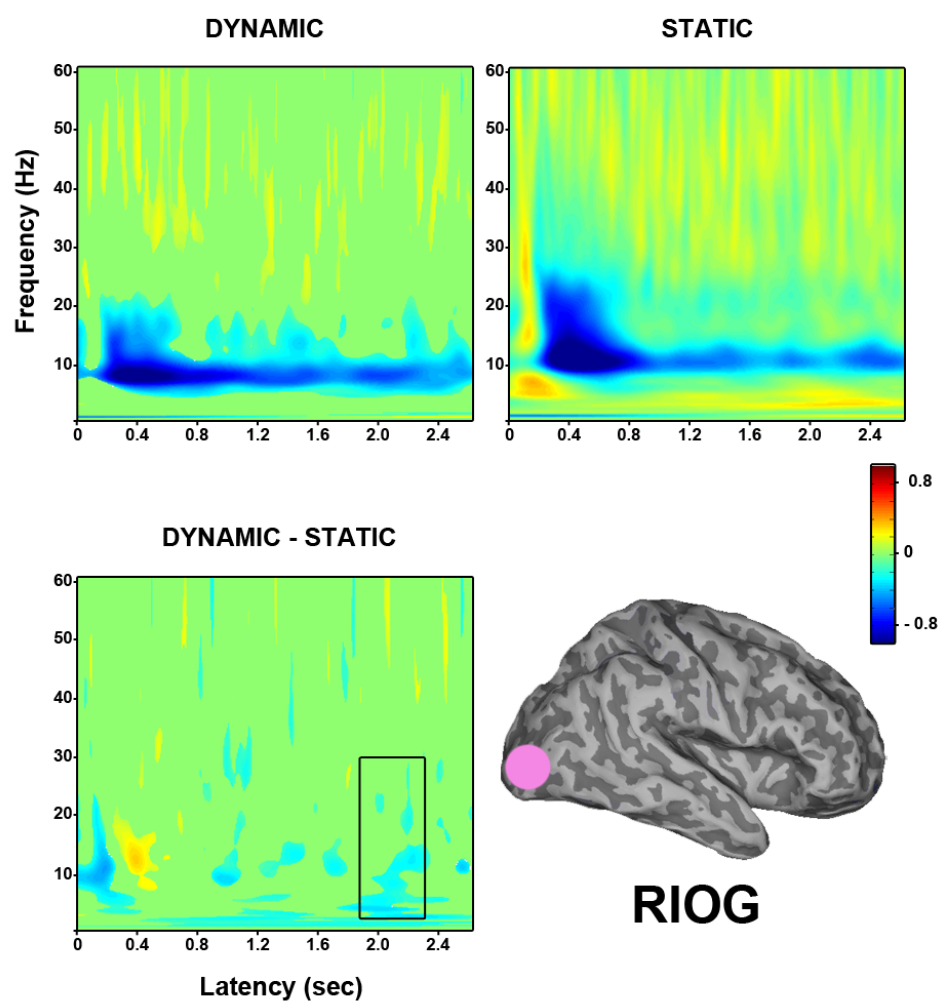


Figure 5.3.43: Group time frequency findings in left inferior occipital gyrus (N=11), shows significantly less power for dynamic speech relative to static speech displays within 1800-2000 ms, between 1-30 Hz. This is due to a greater sustained decrease in power (8-30 Hz) for dynamic speech faces from 800 ms onwards and an increase in low frequency power (2-8 Hz) for static speech faces. Top left: Dynamic speech faces versus baseline fixation; Top right: Static speech faces versus baseline fixation; Bottom left: Dynamic versus static speech faces.

A region in right MTG was also identified as showing significantly less power for dynamic

relative to static speech displays during this time window (1800-2000 ms). The time-frequency map shows a decrease in power between 5-30 Hz for the direct contrast of dynamic versus static speech displays, which is due to the sustained decrease in power between 5-30 Hz from 500 ms onwards in the dynamic speech condition (see Figure 5.3.44).

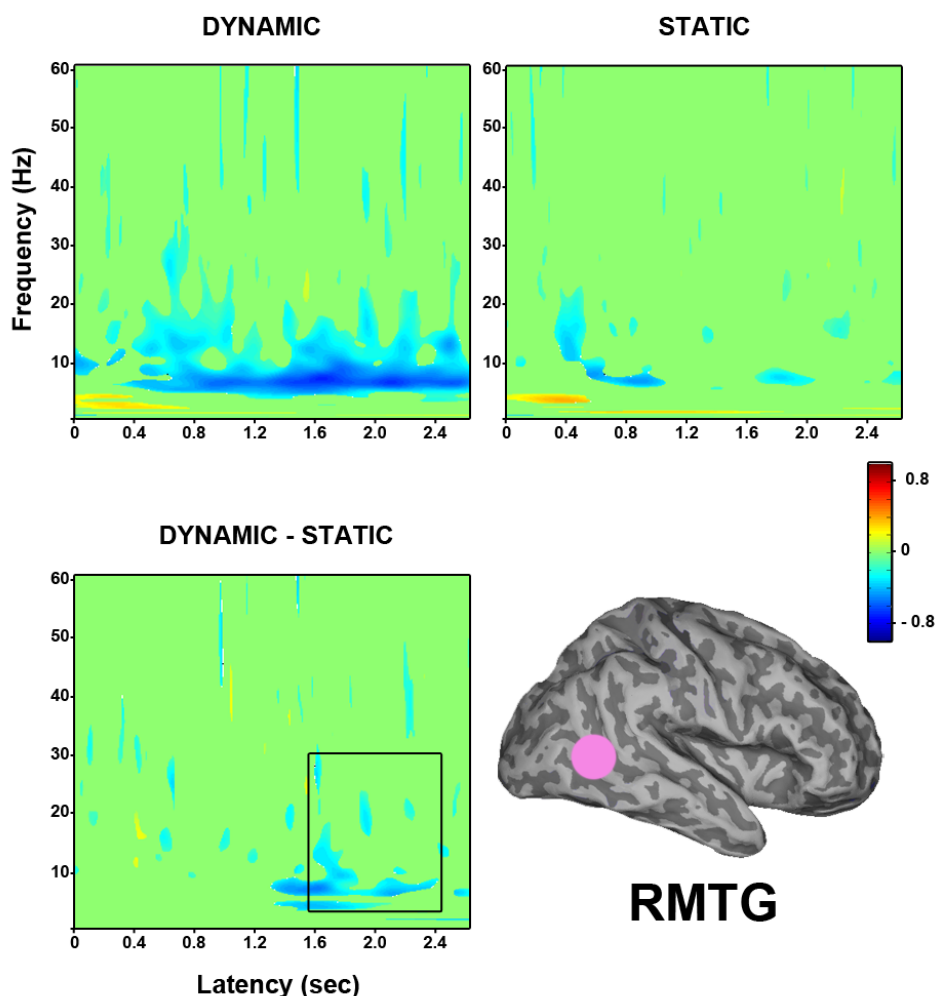


Figure 5.3.44: Group time frequency findings in right middle temporal gyrus (N=10), shows significantly less power for dynamic speech relative to static speech displays within 1800-2000 ms, between 5-30 Hz. This is due to a sustained decrease in power (5-30 Hz) for dynamic speech faces from 500 ms onwards. Top left: Dynamic speech faces versus baseline fixation; Top right: Static speech faces versus baseline fixation; Bottom left: Dynamic versus static speech faces.

In the subsequent time window from 2000-2200 ms a source was identified in right STS, again showing significantly less power for dynamic relative to static speech displays. A virtual electrode constructed in this region revealed a decrease in power between 5-40 Hz around 2000 ms when dynamic and static speech displays were directly contrasted. This is driven by the decrease in power between 5-40 Hz in the dynamic speech condition, com-

pared to only a slight increase in power in the static speech condition (see Figure 5.3.45).

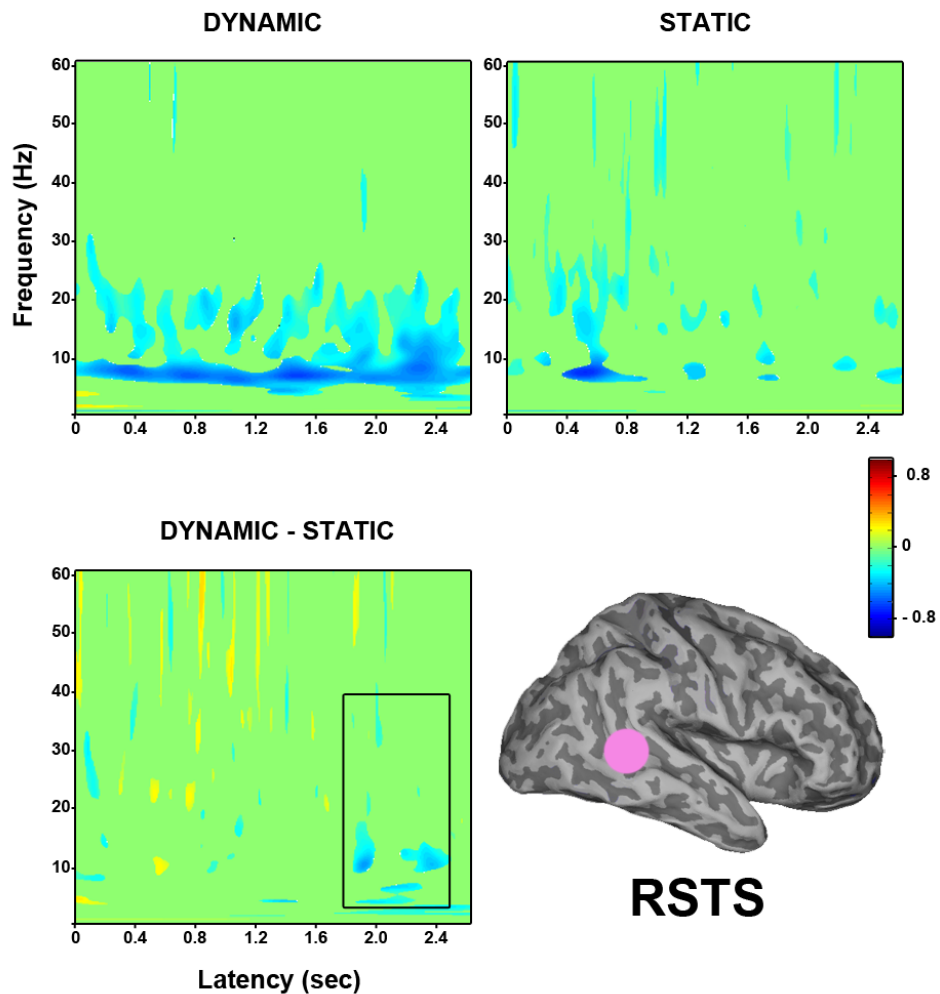


Figure 5.3.45: Group time frequency findings in right superior temporal sulcus (N=9), shows significantly less power for dynamic speech relative to static speech displays within 2000-2200 ms, between 5-40 Hz. This is due to a more sustained decrease in power (5-40 Hz) for dynamic speech faces from 1800 ms onwards. Top left: Dynamic speech faces versus baseline fixation; Top right: Static speech faces versus baseline fixation; Bottom left: Dynamic versus static speech faces.

In the final time window from 2200-2400 ms a region in right IOG was again identified as showing significantly less power for dynamic compared to static speech displays. A virtual electrode constructed here revealed a decrease in power between 5-30 Hz for the direct contrast of dynamic versus static speech displays, which is due to the stronger and more sustained decrease in power from 5-30 Hz in the dynamic speech condition (see Figure 5.3.46).

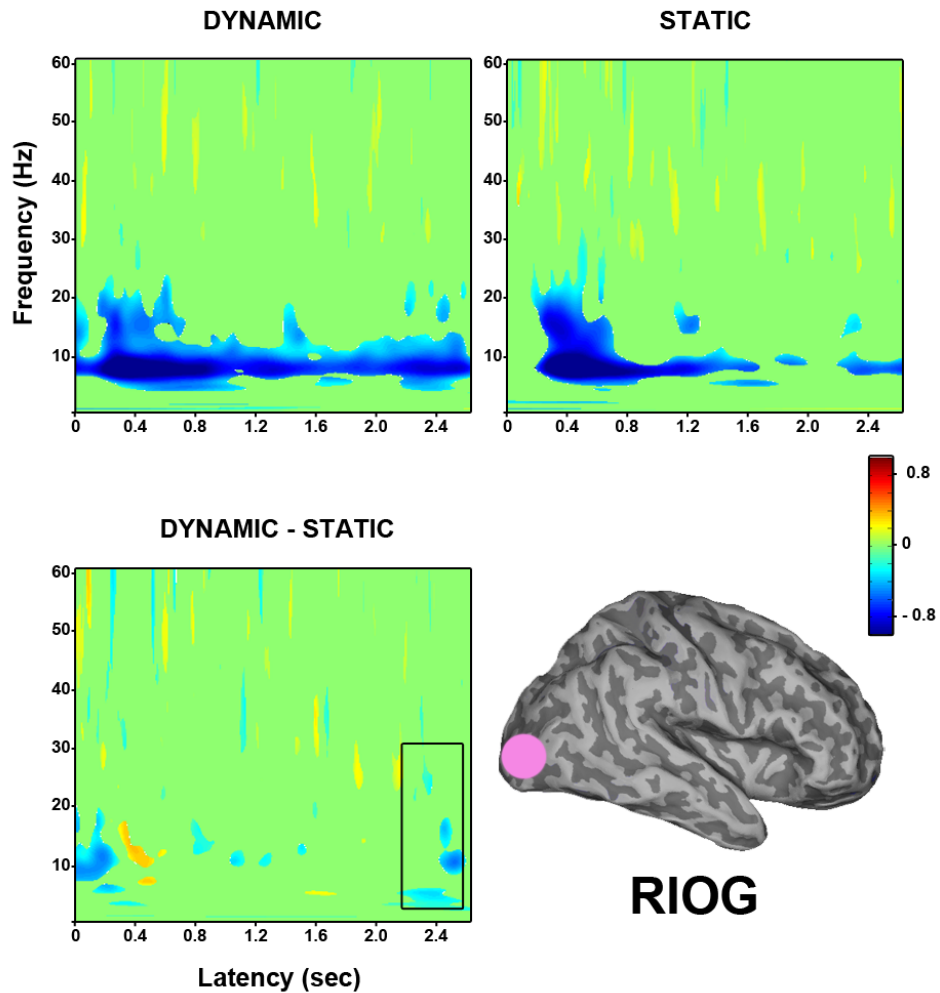


Figure 5.3.46: Group time frequency findings in right inferior occipital gyrus (N=12), shows significantly less power for dynamic speech relative to static speech displays within 2200-2400 ms, between 5-30 Hz. This is due to a more sustained decrease in power (5-30 Hz) for dynamic speech faces from 1800 ms onwards. Top left: Dynamic speech faces versus baseline fixation; Top right: Static speech faces versus baseline fixation; Bottom left: Dynamic versus static speech faces.

5.4 Discussion

The objective of this study was to investigate the neural processes involved in emotional face perception by examining the location, temporal structure and frequency information of the implicated neural regions, using more naturalistic dynamic facial stimuli. In addition, we aimed to assess the extent to which emotion-specific networks may be involved in processing different dynamic facial expressions, or if similar neural regions are involved but are activated at different time points. Due to the fact that emotional face processing can occur over both short and extended periods of time (Vuilleumier and Pourtois, 2007) and within multiple frequency bands (Güntekin and Basar, 2007), a wide frequency band (1–80 Hz) was used in this analysis over multiple short (200 ms) time windows in order to perform a thorough analysis of emotional face processing.

Consistent with the experimental hypotheses, dynamic angry, happy and speech facial displays elicited larger decreases in alpha and beta oscillatory power, relative to their static counterparts, particularly in regions of the core face perception network, in occipital and temporal cortices, due to enhanced neural processing for dynamic expressions (Singh et al., 2002; Jessen and Kotz, 2011). Furthermore, the regions that were identified in all of the different dynamic face contrasts closely matched the regions that were previously identified for the same contrasts using fMRI in chapter 2. In addition, regions of prefrontal cortex showed greater synchronisation in low frequency power (delta and theta) for the dynamic affective displays. Finally, little evidence was found for emotion-specific networks, rather it appears that common overlapping networks are involved in processing the different facial expressions at varying latencies and frequencies.

5.4.1 Occipito-temporal responses to dynamic facial expressions of emotion

In all three of the dynamic versus static contrasts (i.e. dynamic angry versus static angry, dynamic happy versus static happy and dynamic speech versus static speech) early differences were found in IOG within 200 ms of stimulus onset. Time frequency analyses revealed that these early differences were due to greater power decreases within 200 ms of stimulus onset, from approximately 8–30 Hz, for each of the different dynamic

facial expressions relative to their static counterparts (see Figure 5.3.1; Figure 5.3.16; Figure 5.3.17; Figure 5.3.35; Figure 5.3.36). This suggests that IOG are involved in processing the different dynamic and static facial expressions, but some additional processing was required for the dynamic stimuli, which is consistent with our findings from the whole group contrast (all dynamic versus static faces) in chapter 4. This early response in IOG may reflect the processing of low-level visual cues related to the emotional facial expressions (Vuilleumier and Pourtois, 2007; Morel et al., 2009), where dynamic expressions are processed earlier than their static counterparts.

Later differences were also found in inferior and middle occipital gyri for the three different dynamic versus static face contrasts, where each of the dynamic stimuli again elicited greater decreases in alpha and beta power relative to their static counterparts around 800 ms post stimulus onset. The responses in these regions were strikingly similar across the three different facial display categories, and were characterised by earlier and more sustained decreases in alpha and beta power for each of the different dynamic stimuli relative to their static counterparts. This may signify additional processing of the dynamic stimuli in these regions of occipital cortex, possibly due to increased attention (Jessen and Kotz, 2011).

Interestingly, regions of occipital cortex also showed differential responses to the affective dynamic facial expressions relative to the dynamic speech controls. Regions in bilateral IOG showed differential responses for dynamic angry relative to dynamic speech facial displays. These were characterised by greater decreases in alpha and beta power for dynamic angry facial expressions between 800-1000 ms (see Figure 5.3.12; Figure 5.3.13). This again supports the role of IOG in higher level face processing, where it appears to show a greater response to the affective information of the dynamic angry face stimuli, contrary to the notion that it is only involved in structural processing. Similarly, a region in left middle occipital gyrus showed significantly greater decreases in alpha and beta power for dynamic happy facial expressions relative to the dynamic speech controls between 1000-1600 ms (see Figure 5.3.31). These results therefore suggest that these regions of occipital cortex are more responsive to emotional facial expressions relative to non-emotional speech controls.

Previous studies have reported differential responses for emotional relative to neutral

expressions in occipital cortex. For example, Krolak-Salmon et al. (2001) reported differential activity related to emotional and neutral expressions between 250-550 ms in occipital areas, and between 550-750 ms in right occipito-temporal cortex, which may correspond to the responses reported here. Furthermore, Jessen and Kotz (2011) found that the contrast of both, angry and fearful visual displays to the neutral condition showed significant decreases in alpha power at bilateral posterior electrodes between 300-700 ms. In the beta band, the contrast of angry emotional displays to neutral displays revealed two significant clusters of decreased power in the right hemisphere, one between 250-500 ms and the other between 650-900 ms. In addition, Güntekin and Basar (2007) found significant differences in alpha oscillatory responses for angry and happy facial expressions relative to neutral displays in posterior cortical regions.

To summarise, regions of inferior and middle occipital cortices showed significantly greater decreases in alpha and beta power, which peaked earlier (within 200 ms) for each of the dynamic facial expressions relative to their static counterparts. Later differences were also found from around 800 ms where dynamic facial expressions of anger, happiness and speech elicited greater decreases in alpha and beta power compared to the static displays. Interestingly, differences between dynamic angry relative to dynamic speech and dynamic happy relative to dynamic speech were also identified in regions of inferior and middle occipital cortices around 800 ms. Both dynamic emotional facial expressions elicited greater decreases in alpha and beta power compared to dynamic speech displays at approximately 800 ms.

These findings of differential processing for the dynamic and static stimuli, and the affective versus speech displays in regions of occipital cortex are contrary to the notion that IOG is only involved in the structural encoding of the face (i.e. identity) as the structure of the face is not changing in these stimuli but the internal features are. These results are more consistent with Pitcher et al. (2011b) who propose a greater role for IOG in higher level face processing, and with previous studies that have found greater responses in visual cortical regions to emotional face stimuli, which is believed to be due to feedback from the amygdala and medial frontal cortices (Krolak-Salmon et al., 2001; Vuilleumier and Pourtois, 2007).

Like the responses described in occipital cortex, regions of middle and superior temporal

cortices also showed similar decreases in power for the three different dynamic facial displays relative to their static counterparts. Responses in these temporal regions were characterised by stronger and more sustained decreases in alpha and beta power (8-30 Hz) for each of the different dynamic facial expressions relative to the static controls, between around 200-2000 ms. Static expressions elicited decreases in the same range (8-30 Hz) but they were generally of much shorter duration, from around 200-500 ms. This greater suppression in the alpha and beta frequency ranges supports the notion of enhanced processing for the different dynamic facial stimuli in regions of temporal cortex (Singh et al., 2002; Muthukumaraswamy et al., 2006), which is consistent with the whole group results (all dynamic versus static) from chapter 4. These results also correspond well with the increases in BOLD identified in similar regions in chapter 2.

Furthermore, the similar response profiles described for the three different categories of facial display implies that these regions of temporal cortex are coding for motion specific properties of the stimuli but not affect in particular. This again is consistent with the results of the fMRI study in chapter 2, particularly the regions of interest analysis where STS showed a main effect of motion but not affect (see subsection 2.3.3). However, while the responses in these temporal regions were strikingly similar for the dynamic versus static angry and happy expressions, the responses for the dynamic versus static speech stimuli showed some differences in the alpha band compared to the two affective contrasts. The regions in right STS (see Figure 5.3.37) and left MTG (see Figure 5.3.41) displayed peak decreases in alpha power for dynamic compared to static speech stimuli that were later (~800 ms) than those shown for the angry and happy dynamic versus static contrasts in similar regions. This suggests that there may be some differences in the timing of responses for emotional relative to speech displays in regions of temporal cortex.

Consistent with this, a region was identified in right STS, which showed significantly less power for dynamic angry facial expressions relative to dynamic speech displays. Time-frequency analysis of this region revealed earlier and stronger peak decreases in power within 200 ms of stimulus onset in the 8-30 Hz frequency range for dynamic angry expressions relative to dynamic speech displays, and significant differences were also found again around 800 ms (see Figure 5.3.11). The early difference between dynamic angry and speech facial displays is consistent with Liu and Ioannides (2010) who found very

early responses in right STS to emotional facial displays well within 100 ms. It is also consistent with Batty and Taylor (2003) who reported a response in STS around 140 ms. Accordingly, Vuilleumier and Pourtois (2007) have suggested that there may be a rapid extraction of visual information related to emotion that occurs before more detailed perceptual processes are complete. The overall stronger decrease in alpha power in this region may reflect enhanced processing of the dynamic angry face stimuli relative to the neutral speech displays (Jessen and Kotz, 2011).

Notably, no significant differences were found in middle or superior temporal gyri for dynamic happy relative to dynamic speech displays. However, a region in left fusiform gyrus was identified as showing significantly less alpha and beta (8-30 Hz) power for dynamic happy relative to dynamic speech displays between 1000-1600 ms. The stronger suppression in alpha and beta frequency bands in this region may once again reflect enhanced processing of the dynamic happy stimuli relative to the speech controls. This is consistent with the results of the fMRI study in chapter 2 where it was shown that dynamic happy relative to dynamic speech facial displays elicited a significantly greater increase in BOLD response in left fusiform gyrus. This suggests that the left fusiform is differentially engaged in processing dynamic happy facial expressions relative to speech. Previous neuroimaging studies have also found increased activation in the fusiform gyrus in response to emotional face stimuli (Vuilleumier et al., 2001; Vuilleumier and Pourtois, 2007). The fact that these differences were found in the left hemisphere is also consistent with previous research that found a significant role of the left hemisphere in the processing of 'positive' affects (Breiter et al., 1996).

Taken together these findings reveal similar patterns of response in regions of the core face perception network for all three of the different dynamic facial expressions. In inferior occipital, middle occipital, middle temporal and superior temporal gyri, these responses were characterised by earlier and stronger peak decreases in alpha and beta power within 200 ms of stimulus onset, and relatively sustained responses throughout the duration of stimulus presentation. Whereas responses in the static conditions peaked later around 400 ms and were less sustained in these regions. However, differential responses were found in a region in right STS for dynamic angry relative to dynamic speech displays, and in left fusiform gyrus for dynamic happy compared to dynamic speech displays. These results

do not reliably support the theory of discrete networks involved in processing different facial expressions of emotion, but rather suggest that a common network of overlapping regions is involved and it is the variations in temporal and oscillatory dynamics within this network that facilitates different aspects of face processing.

5.4.2 Prefrontal and insular cortex responses to dynamic facial expressions of emotion

Regions of prefrontal cortex appeared to show more varied responses to the different dynamic and static face stimuli, however some regions, particularly inferior and middle frontal gyri, did show some similarities in their responses across the three different categories of dynamic facial displays relative to their static counterparts. These were mainly characterised by earlier increases in low frequency power (2-8 Hz) for the different dynamic compared to static facial displays, regardless of the specific expression displayed. In two separate studies Balconi and Lucchiari (2006) and Balconi and Pozzoli (2009) reported synchronisation in delta band for all faces which is consistent with the results reported here. The greater synchronisation in delta and theta power in the present study may signify increased processing of the dynamic facial displays in these regions of prefrontal cortex possibly due to the dynamic stimuli being more captivating and thus resulting in increased attention (Ambadar, 2002)

Two regions in prefrontal cortex, including left middle frontal gyrus and right superior frontal gyrus, showed significantly less power for dynamic angry relative to static angry facial expressions, around 1800 ms. In both regions this was due to greater decreases in alpha and beta power (10–30 Hz) for dynamic angry facial expressions. This greater suppression in alpha and beta power for dynamic angry expressions is consistent with Jessen and Kotz (2011) who also found decreased beta power for dynamic angry stimuli, and possibly reflects increased processing of dynamic angry stimuli in these regions. Additionally, both dynamic and static angry faces elicited increases in low frequency (1-6 Hz) power in these regions. These increases in low frequency power are consistent with Balconi and Lucchiari (2006) and Balconi and Pozzoli (2009) who reported increases in delta and theta power during emotional face processing. In left middle frontal gyrus the peak increase was earlier and more sustained in the dynamic angry condition relative to

the static, however in right superior frontal gyrus the increase in low frequency power was slightly stronger and more sustained in the static angry condition.

Two regions in bilateral IFG were identified as showing differential activation for dynamic happy relative to static happy facial expressions. The region in right IFG showed greater power for dynamic happy relative to static happy facial expressions within 200 ms. This was due to an early increase in low frequency power (3-12 Hz) for dynamic happy expressions, along with a decrease in higher frequency power (10-45 Hz) for static happy expressions. This increase in low frequency power is again in accordance with Balconi and Lucchiari (2006) and Balconi and Pozzoli (2009) who reported increases in delta and theta power during emotional face processing. Interestingly, the low frequency power increase peaked earlier in the dynamic happy condition relative to the static happy condition, which is similar to the response identified in left middle frontal gyrus for dynamic angry expressions described previously.

Conversely, the region in left IFG showed significantly less power for dynamic happy relative to static happy facial expressions. This was driven by a greater power decrease in the 16-28 Hz range in the dynamic happy condition, as well as a greater increase in low frequency power (2-10 Hz) in the static happy condition around 500 ms. The stronger decrease in beta power for dynamic happy faces is again consistent with Jessen and Kotz (2011) who reported greater decreases in beta power for dynamic emotional (fear and anger) stimuli, but extends their findings to dynamic happy stimuli. Notably, both regions in IFG did show an earlier increase in low frequency power for dynamic happy expressions, whereas static faces elicited a later and more sustained increase in low frequency power (~400 ms). However, the greater increase in low frequency power in right IFG for static happy faces is contrary to what was expected, as a greater increase in response to dynamic stimuli was predicted. This may be due to the fact that static faces were rated as more intense than dynamic stimuli (see subsection 2.2.1).

Differences were also found in bilateral IFG for the contrast of dynamic and static speech displays, where both regions showed significantly greater power for dynamic speech relative to static speech stimuli. The response profiles in both left and right IFG were similar for the dynamic versus static speech contrast. They were characterised by earlier and stronger peak increases in low frequency power (3-10 Hz) for dynamic speech stimuli,

along with greater decreases in power between 20-40 Hz for static speech stimuli, around 200 ms. The increases in low frequency power were earlier for the dynamic speech stimuli and there was a greater decrease in beta power for static speech stimuli here. This is contrary to the hypothesis that dynamic speech displays would be characterised by greater decreases in beta power relative to static speech displays.

A region in left middle frontal gyrus was identified as showing significantly less power for dynamic speech relative to static speech stimuli. This later difference was due to greater power for static speech stimuli from 10-20 Hz between 1200-1500 ms. However, the response to both dynamic and static speech displays again showed similar response patterns to those previously described. Dynamic speech displays were characterised by increases in low frequency power (3-7 Hz) from stimulus onset to around 1000 ms, as well as decreases in power from 20-50 Hz from 0 to 600 ms. Static speech stimuli showed a similar response but the increases in low frequency power started around 200 ms later until 1500 ms, with similar decreases in higher frequency power, followed by the previously mentioned increase in beta band power. A similar region was identified by Calvert and Campbell (2003).

Notably, regions of prefrontal cortex showed differential responses to both of the dynamic affective stimuli relative to the dynamic speech controls. Early differences were found in bilateral IFG for both dynamic angry and dynamic happy facial expressions relative to dynamic speech displays within 200 ms of stimulus onset. Furthermore both regions, in left and right IFG, showed extremely similar patterns of response for the two different contrasts. Both regions showed significantly greater increases in low frequency power (2-8 Hz) for each of the affective stimuli (dynamic angry and dynamic happy) relative to the dynamic speech displays. Low frequency oscillations in delta and theta ranges have been specifically linked with emotional processes (Güntekin and Basar, 2007; Knyazev, 2007). In line with this, Balconi and Lucchiari (2006) observed frontal theta synchronisation during emotional stimulus presentation.

The timing of the responses reported here also corresponds well with Balconi and Pozzoli (2009) who found greater synchronisation in delta and theta bands from 150-250 ms for emotional face stimuli relative to neutral. These early responses in bilateral IFG are also consistent with the findings of Eimer and Holmes (2002) who reported an early

effect arising around the same latency (~120 ms) from fronto-central ERP components in response to emotional facial expressions. Inferior frontal regions were also identified in chapter 2 as showing greater BOLD responses for both the dynamic angry and happy expressions relative to the dynamic speech displays (see Table 2.5 and Table 2.6). This provides converging evidence implicating regions of IFG in emotional face processing.

Finally, significant differences were found in the right insula for the contrast of dynamic angry with dynamic speech displays. This was characterised by greater increases in low frequency power (3-12 Hz) for dynamic angry facial expressions between 400-1200 ms, which is in line with previous research linking theta synchronisation with emotional face processing (Güntekin and Basar, 2007; Knyazev, 2007). Similarly the insula was identified in our fMRI study in chapters 2 and 3 as showing increased BOLD specifically in response to dynamic angry facial expressions.

Previous neuroimaging studies have reported insular activation to emotional facial expressions particularly aversive or threat-related emotions such as fear, anger and disgust (Phan et al., 2004; Fusar-Poli et al., 2009). The insula is therefore believed to be an important structure in emotion processing (Nagai et al., 2007), as it forms part of the interoceptive system that links external and internal information (Gobbini and Haxby, 2007). Notably, the timing of this response supports Adolphs (2002b) model of emotion recognition where he proposes that regions of the extended network, including insular cortex, are recruited from around 300 ms post stimulus onset, to link the perceptual representation of a face to conceptual knowledge of the emotional and social meaning of the perceived expression (see subsection 1.3.5).

Yet while the regions identified in the MEG and SAM analyses in this chapter were consistent with those identified in our previous fMRI and connectivity analyses, there were some noticeable differences. Differential activation was found in the amygdala for dynamic angry faces with fMRI, but sources were not found in this region in the present MEG analysis. This may possibly be due to the deep location of the amygdala which makes it more difficult for SAM to localise subcortical structures. However, previous MEG studies have localised amygdala activity with SAM (Luo et al., 2010). Another possibility is the difference in experimental design between the fMRI and MEG studies, as a block design was used in the fMRI but an event related design was used in the present

MEG study. The block design may provide more statistical power in smaller subcortical regions such as the amygdala making them easier to detect with fMRI.

5.4.3 Summary

Taken together these findings revealed enhanced processing for different dynamic facial displays in regions of the core face perception network. Moreover, similar patterns of response were found for all three of the different dynamic facial expressions in regions of the core face perception network, including, inferior occipital, middle occipital, middle temporal and superior temporal gyri. These responses were characterised by earlier and stronger peak decreases in alpha and beta power within 200 ms of stimulus onset, and showed relatively sustained responses throughout the duration of stimulus presentation. Whereas responses in the static conditions peaked later around 400 ms and were less sustained in these regions. However, differential responses were found in a region in right STS for dynamic angry relative to dynamic speech displays, and in left fusiform gyrus for dynamic happy compared to dynamic speech displays.

Regions of inferior and middle frontal gyri also showed enhanced processing for dynamic facial expressions. This was revealed in general, by earlier increases in low frequency power (2-8 Hz) for the different dynamic compared to static facial expressions, regardless of the specific expression displayed. Furthermore, dynamic affective displays were associated with greater synchronisation in delta and theta bands in regions of prefrontal cortex, which is in line with previous research linking synchronisation in these frequency bands with emotional face processing (Güntekin and Basar, 2007; Knyazev, 2007). Additionally, dynamic angry facial expressions were associated with greater increases in low frequency power in insular cortex between 400-1200 ms. These findings therefore suggest that regions of the face perception network, particularly the extended system, interact with varying temporal and oscillatory dynamics during the processing of different facial displays. In line with Adolphs (2002b) model of emotion recognition, these results show that processing dynamic facial expressions of emotion involves a network of overlapping regions that are differentially recruited over various periods of time and various different frequencies.

Chapter 6

Discussion

6.1 Introduction

Using a multi-modal approach the set of studies presented in this thesis aimed to explore the neural responses to dynamic faces across time, space and frequency. A major limitation of previous face perception research, as highlighted throughout the course of this thesis, is that it has largely focused on the neural responses to static face stimuli, which lack any temporal information, thereby compromising the ecological validity of such investigations (Carroll and Russell, 1997; Horstmann, 2002). Dynamic stimuli on the other hand, which display surface changes of facial musculature over time, are more realistic and therefore provide a better means of investigating the mechanisms of naturalistic face perception (Kilts et al., 2003; LaBar et al., 2003).

Furthermore, up until recently studies exploring the mechanisms of face and emotion perception have often adopted a modular approach by focusing on the selectivity of certain brain regions for processing specific categories of stimuli e.g. the fusiform gyrus as a face specific module (Kanwisher et al., 1997), or the amygdala as a fear processor (Calder et al., 2001). However, it is becoming increasingly more obvious that cognitive tasks, such as face processing, rely on distributed networks of regions (Haxby et al., 2000; Ishai, 2008) where information is continuously changing and integrated over time. Thus, a more integrated approach is needed in order to understand the full complexity of human face processing mechanisms in the brain. It is for this reason that a multi-modal approach employing a variety of different analysis techniques was adopted in the present thesis.

In the first instance fMRI was used to explore regions of significant activation in response to dynamic facial displays, as described in chapter 2. This analysis was then developed further by connectivity analysis in chapter 3, in order to assess interactions within the dynamic face perception network. In chapters 4 and 5, MEG was used along with SAM source analysis to assess the location, timing and frequency of differential responses to dynamic faces in general (chapter 4) and to specific dynamic facial expressions of anger, happiness and speech (chapter 5). This chapter summarises the key findings and their implications, addresses methodological issues, and provides suggestions for future research motivated by this work.

6.2 Key findings

6.2.1 Key findings from fMRI

Chapters 2 and 3 focused on the spatial domain, wherein fMRI was used as a tool to investigate the regions of activation in response to dynamic faces. The objective of the first study, described in chapter 2, was to use fMRI to identify regions of significant activation in response to dynamic facial expressions. In order to achieve this, firstly a set of dynamic and static face stimuli were purposely created. Exemplars of both dynamic and static happy, angry and speech facial displays were selected for this investigation, and were used in all further analyses presented in this thesis. The rationale for choosing angry and happy expressions was to contrast positive and negative emotion categories, whereas speech was chosen as a control for affective facial motion.

Based on previous research showing significant increases in activation to dynamic face stimuli, in regions along the dorsal pathway of the face perception network (MTG and STS), as well as regions in the extended system, such as the amygdala and IFG (Kilts et al., 2003; LaBar et al., 2003; Sato et al., 2004; Fox et al., 2009; Pitcher et al., 2011a), it was predicted that the dynamic facial expressions used in the present study would elicit activation in similar regions. In addition, the effects of emotion-specific facial dynamics were investigated by contrasting the dynamic facial expressions of anger and happiness with speech in order to assess the extent to which different structures in the distributed face perception system are involved in processing different dynamic facial expressions of

emotion.

As predicted, the direct contrast of all dynamic faces relative to static controls revealed a broad network of regions showing increased BOLD responses for dynamic faces, particularly in the dorsal pathway. This network comprised early visual regions, such as IOG, which were shown to be insensitive to motion or affect but sensitive to the visual stimulus. The STS, was shown to be specifically sensitive to motion, while the amygdala was recruited to process affect. Furthermore, a functional distinction was identified in the amygdala as it exhibited greater responses to the affective facial displays (angry and happy), relative to displays of speech. Regions of prefrontal cortex were recruited for additional face processing, including the IFG in the extended system, which was shown to be sensitive to affect but not motion in the right hemisphere. These findings are not only consistent with Haxby et al. (2000)'s distributed neural system for face perception, but also extend it to include dynamic facial information.

Analysis of the different dynamic facial expression categories revealed a common core system, including middle occipital gyri, MTG and STS, which was shown to be involved in processing all of the dynamic facial expressions. However, some differences in activation patterns for each of the different dynamic facial expressions were found in regions of the extended system. Dynamic angry facial expressions were associated with increased amygdala and insula activation, while dynamic happy expressions elicited greater fusiform activation, and dynamic speech displays were associated with increased activation in premotor and supplementary motor areas. This suggests that partly dissociable neural networks may be involved in processing different dynamic facial expressions of emotion (Hennenlotter and Schroeder, 2006), although additional information about the timing and frequency of responses must also be considered.

Having identified the network of regions involved in processing dynamic faces, the next stage then in chapter 3, was to assess the interactions between the regions of this network. Very few studies have assessed the connectivity within the face perception network, among the few studies that have, the emphasis has once again been on static faces. Thus very little is known about connectivity between regions mediating dynamic face perception. Therefore the objective of chapter 3 was to examine the associated functional relations between the neural regions mediating dynamic face perception i.e. to examine the effective

connectivity within Haxby et al.'s (2000) distributed face network with realistic dynamic facial expressions of emotion.

To this end two different forms of effective connectivity analysis, psychophysiological interaction (PPI) analysis and physiophysiological interaction (PYPI) analysis, were used to examine the covariance of changes in activity between different brain regions within the previously defined dynamic face perception network. PPI analysis was used to assess how activity in a particular brain region is modulated by the interaction between one brain region and an experimental condition, whereas PYPI analysis was used to measure how the activity in a particular brain region is modulated by the physiological interaction of two other brain regions.

It was hypothesised that PPI analysis would reveal correlations between early visual regions such as IOG and regions in the dorsal pathway, such as the STS, in response to dynamic face stimuli. It was also predicted that activation in the STS would be correlated with regions in the extended network when viewing dynamic facial expressions. Additionally, based on the results from chapter 2 showing some differential activation patterns for the different facial expressions, it was also predicted that distinct patterns of effective connectivity would be found within the dynamic face perception network for the different facial expressions.

As predicted, viewing dynamic facial stimuli in general was associated with increases in effective connectivity between IOG and STS, in the dorsal pathway. The STS was also coupled with MTG, as well as frontal regions, including superior frontal gyrus and pre-central gyrus. Thus, it was proposed that the STS facilitates processing of dynamic facial displays by acting as a relay centre between visual regions and frontal regions. Therefore, consistent with the results from chapter 2, regions of the core face perception system displayed similar patterns of effective connectivity across the different facial expression conditions. However, the coupling between regions of the core and the extended systems varied depending on the type of expression that was processed. These findings are in line with previous research by Fairhall and Ishai (2007), where they found that the effective connectivity between the core system and regions of the extended system, such as the amygdala and orbitofrontal cortex, were modulated by different types of static face stimuli.

Processing dynamic facial expressions of anger was associated with increases in effective connectivity between IOG and STS, and reciprocal connections between the STS and the amygdala, as well as reciprocal connections between the amygdala and the IFG. In addition, the IFG was effectively connected to the insula. Dynamic happy expressions, on the other hand, were associated with effective connectivity between IOG and IFG, and IFG and the fusiform gyrus, as well as between STS and fusiform gyri, and amygdala and fusiform gyri, among others. Both of these networks include regions involved in emotional processing. Furthermore both of these networks displayed effective connectivity between the IOG and IFG, which may also facilitate emotional processing (Dima et al., 2011). However, viewing dynamic speech stimuli, which lack any emotional content, was associated with increases in connectivity between IOG and precentral gyrus. The STS was again coupled with visual regions, lingual gyri and middle occipital gyri, and IFG was coupled with lingual gyri and MTG, regions involved in motion processing and motor movements.

With regards to the PYPI analysis it was predicted that IOG and STS activation would be correlated with fusiform activation based on findings from Turk-Browne et al. (2010) and Zhang et al. (2009) on resting state functional connectivity analysis of the face perception network. Also, based on our earlier fMRI results from chapter 2 showing STS and MTG activation to dynamic faces it was hypothesised that IOG and STS activation would correlate with activation in MTG. Furthermore, it was predicted that STS and amygdala activation would correlate with frontal regions in the extended system.

Consistent with these predictions and with Haxby's model, activation in IOG and STS did indeed predict activation in MTG in the core system, which is involved in processing biological motion. They also predicted activation in the amygdala, and IFG, which are recruited to process emotion. The interaction between the STS and the amygdala revealed significant correlations with visual regions, as well as regions in prefrontal cortex. Finally, the interaction between amygdala and IFG showed significant correlations again with regions of the core system in occipito-temporal cortex as well as with anterior and posterior cingulate.

Taken together, the findings from chapters 2 and 3 reveal a network of regions that are significantly more responsive to dynamic facial displays. Furthermore, differential

activation patterns were found for the different categories of facial expression. Therefore, while similar regions are involved in processing the different dynamic stimuli, the effective connectivity within these networks varies depending on the type of expression that is processed.

6.2.2 Key findings from MEG

Having established the spatial profile of the haemodynamic response to dynamic faces with fMRI in chapters 2 and 3, MEG was then employed in chapters 4 and 5 to directly measure the neural activity related to dynamic face processing in the temporal, spatial and frequency domains. A number of key issues were raised in chapters 4 and 5, which will be outlined here along with the key findings. Notably, it was shown that the majority of previous face perception studies using electrophysiological measures of brain activity (i.e. MEG/EEG) have again focused on static faces. Furthermore, many of these studies were primarily concerned with the temporal domain, with much fewer face perception studies exploring the frequency domain. In both chapters, the importance of induced oscillatory activity in brain function was stressed, and it was argued that induced oscillatory activity is an important feature of neural communication, which can provide additional information about the spatio-temporal dynamics of cognitive processes (Buzsáki and Draguhn, 2004). Therefore the aim of the analyses presented in chapters 4 and 5 was to thoroughly interrogate the dynamic face perception network by examining location, temporal structure and frequency information of the implicated neural regions i.e. to examine where, when and in what frequency band dynamic face processing takes place.

Firstly, the objective in chapter 4 was to use MEG and SAM source analysis to specifically assess the main effect of facial motion. This was achieved by identifying differential neural responses to dynamic relative to static face stimuli, and examining the timing, location, and frequency of oscillations contributing to them. In order to facilitate comparisons between the two studies a similar experimental design to that used in the fMRI study was adopted. Previous MEG studies have found decreased oscillatory power within the range of 5-25 Hz related to viewing general biological motion (Singh et al., 2002) and facial motion in particular (Muthukumaraswamy et al., 2006), which has been interpreted as representing increases in cortical activation. Furthermore, it has been shown that

decreases in cortical synchronisation within this frequency range are inversely related to increases in BOLD response.

It was therefore predicted that the processing of dynamic face stimuli would result in decreased beta power in regions of the dynamic face perception network, and that these regions would be spatially coincident with those identified previously with fMRI. In addition, based on previous research particularly by Ahlfors et al. (1999) and Jokisch et al. (2005), it was predicted that regions, such as IOG, would show earlier responses, followed by later responses in MTG and regions in STS.

Accordingly, sources of differential activation were indeed found in occipito-temporal and inferior frontal regions. Early differential responses were identified in bilateral IOG within 200 ms, followed by later responses in MTG and STS, within 800 ms of stimulus onset. These were all characterised by decreases in beta band oscillatory power. Additional regions including the insula, IFG and middle occipital gyri also showed decreases in beta band power to dynamic relative to static face stimuli from ~1000 ms post stimulus onset. Furthermore, despite the differences between MEG and fMRI imaging techniques, the regions localised by SAM corresponded closely with the regions of the dynamic face perception network that were identified with fMRI (this will be discussed in more detail in the following section). These findings again extend Haxby et al. (2000)'s model by demonstrating the temporal progression and frequency of responses that contribute to dynamic face perception.

Having assessed the main effect of facial motion with MEG in chapter 4, the next step in chapter 5 was to examine the effects of motion on the processing of different face stimuli and to explore the effects of emotion-specific facial dynamics with MEG. The dynamic and static stimuli for each of the different affects were directly contrasted, and both of the dynamic affects were contrasted with dynamic speech displays, then the resulting differential responses were examined in time, space and frequency.

As mentioned in subsection 6.2.1 some differences between activation patterns for each of the different dynamic facial expressions were found with fMRI, particularly in regions of the extended system. This could support the theory that partly dissociable neural networks are involved in processing different dynamic facial expressions of emotion (Hennelotter and Schroeder, 2006). However, it may also be the case that rather than separate

emotion-specific networks specialised in processing distinct emotions, there is a general network of neural regions interacting with varying dynamics. The latter hypothesis cannot be detected with fMRI due to its poor temporal resolution. By examining the spatio-temporal and frequency characteristics of responses, with MEG a better understanding of emotional face processing can be gained.

In chapter 5, it was once again highlighted that the majority of electrophysiological studies investigating the processing of emotional facial expressions have used static face stimuli. In fact, to date it appears no study has used dynamic angry, happy and speech stimuli in any MEG study. Also the majority of these studies have used conventional ERP methods with static faces, or in the case of MEG studies, have only examined the time course of neural responses to faces, neglecting the frequency domain (e.g. Liu et al., 2002; Itier et al., 2006; Sato et al., 2008). Hence very little is known about the frequency characteristics of the face perception network.

It was predicted that dynamic angry, happy and speech displays would elicit larger decreases in alpha and beta oscillatory power, relative to their static counterparts, due to enhanced neural processing for dynamic expressions (Singh et al., 2002; Jessen and Kotz, 2011). Based on findings from Balconi and Lucchiari (2006) and Balconi and Pozzoli (2009) showing greater synchronisation to emotional facial displays in delta and theta frequency bands, it was also hypothesised that these frequency bands would show emotional modulations for angry and happy facial expressions.

As expected, dynamic angry, happy and speech facial displays elicited larger decreases in alpha and beta oscillatory power, relative to their static counterparts, particularly in regions of the core face perception network, in occipital and temporal cortices, due to enhanced neural processing for dynamic expressions (Singh et al., 2002; Jessen and Kotz, 2011). Similar patterns of response were found for all three of the different dynamic facial expressions in regions of the core face perception network, including, inferior occipital, middle occipital, middle temporal and superior temporal gyri. These responses were characterised by earlier and stronger peak decreases in alpha and beta power within 200 ms of stimulus onset, and showed relatively sustained responses throughout the duration of stimulus presentation. Whereas responses in the static conditions peaked later around 400 ms and were less sustained in these regions. Furthermore, the regions that were

identified in all of the different dynamic face contrasts closely matched the regions that were previously identified for the same contrasts using fMRI in chapter 2.

Regions of inferior and middle frontal gyri showed enhanced processing for dynamic facial expressions. This was revealed in general, by earlier increases in low frequency power (2-8 Hz) for the different dynamic compared to static facial expressions, regardless of the specific expression displayed. Furthermore, dynamic affective displays were associated with greater synchronisation in delta and theta bands in regions of prefrontal cortex, which is in line with previous research linking synchronisation in these frequency bands with emotional face processing (Güntekin and Basar, 2007; Knyazev, 2007). Additionally, dynamic angry facial expressions were associated with greater increases in low frequency power in insular cortex between 400-1200 ms. These findings do not reliably support the theory of discrete networks involved in processing different facial expressions of emotion, but rather suggest that a common network of overlapping regions is involved and it is the variations in temporal and oscillatory dynamics within this network that facilitates face processing.

6.2.3 Integration of fMRI and MEG data

A goal of the present thesis was to investigate the spatio-temporal and frequency characteristics of dynamic face processing in the brain. In order to achieve this a multimodal approach was adopted, as different imaging techniques are better suited to measure different aspects of neural activity. fMRI and MEG were the techniques of choice for the present investigation, as these two techniques complement each other, with fMRI providing excellent spatial resolution and MEG providing the detailed temporal resolution not found with fMRI. However, while these techniques may complement each other, they do in fact measure very different signals. Thus, obtaining high-resolution images of brain activity across time, space, and frequency, requires the integration of information from multiple signal modalities, which can be challenging. Nevertheless, significant developments in integrating multiple neuroimaging modalities, particularly MEG/EEG and fMRI, have been made in recent years (Dale and Halgren, 2001).

Of particular relevance to the present thesis is the influential study by Singh et al. (2002) where they assessed the concordance between areas of activation recorded with fMRI and

sites of focal changes in cortical oscillatory activity recorded with MEG, during cognitive tasks. Interestingly, they found that decreases in alpha and beta power were inversely correlated with increases in the BOLD response during the performance of cognitive tasks. These findings therefore indicate an inverse relationship between neuronal synchrony and neuronal activation in alpha and beta bands. More recently, Stevenson et al. (2011) also found excellent spatial colocalisation between BOLD activation and beta desynchronisation in visual and sensorimotor areas. Similar results were obtained in the present thesis and these will be discussed in the following section.

6.2.3.1 A neural network for processing dynamic faces in time, space and frequency

In chapter 2, when dynamic faces were contrasted with static faces a network of regions was identified by fMRI as showing increased BOLD activation. When the same contrast was performed with MEG, in chapter 4, a similar network of regions was localised by SAM source analysis, showing decreases in beta power during different time periods. Figure 6.2.1 shows a very similar network of regions identified by both fMRI and MEG, including MTG, STS, middle occipital gyri, IFG and precentral gyri. This therefore demonstrates excellent spatial concordance between these two different techniques, whereby both converge on regions of the face perception network (Haxby et al., 2000; Ishai et al., 2005). Notably, the best spatial concordance between the two techniques was found around 1000 ms.

MEG was used to examine the detailed temporal progression within this network. The earliest response in this network was found in bilateral IOG, which responded within 200 ms of stimulus onset. This region in IOG forms part of the core system for visual analysis of faces in Haxby et al. (2000)'s model. Yet this region was not identified in the fMRI analysis of dynamic versus static faces. Time-frequency analysis of this region revealed a decrease in response to both the static and dynamic stimuli within 200 ms of stimulus onset, but overall a greater and more sustained decrease in power to the dynamic stimuli. This suggests that the IOG is involved in processing both static and dynamic face stimuli, but additional processing was required for the dynamic stimuli. This may explain why this region was not identified in the fMRI study, as the poor temporal resolution of fMRI

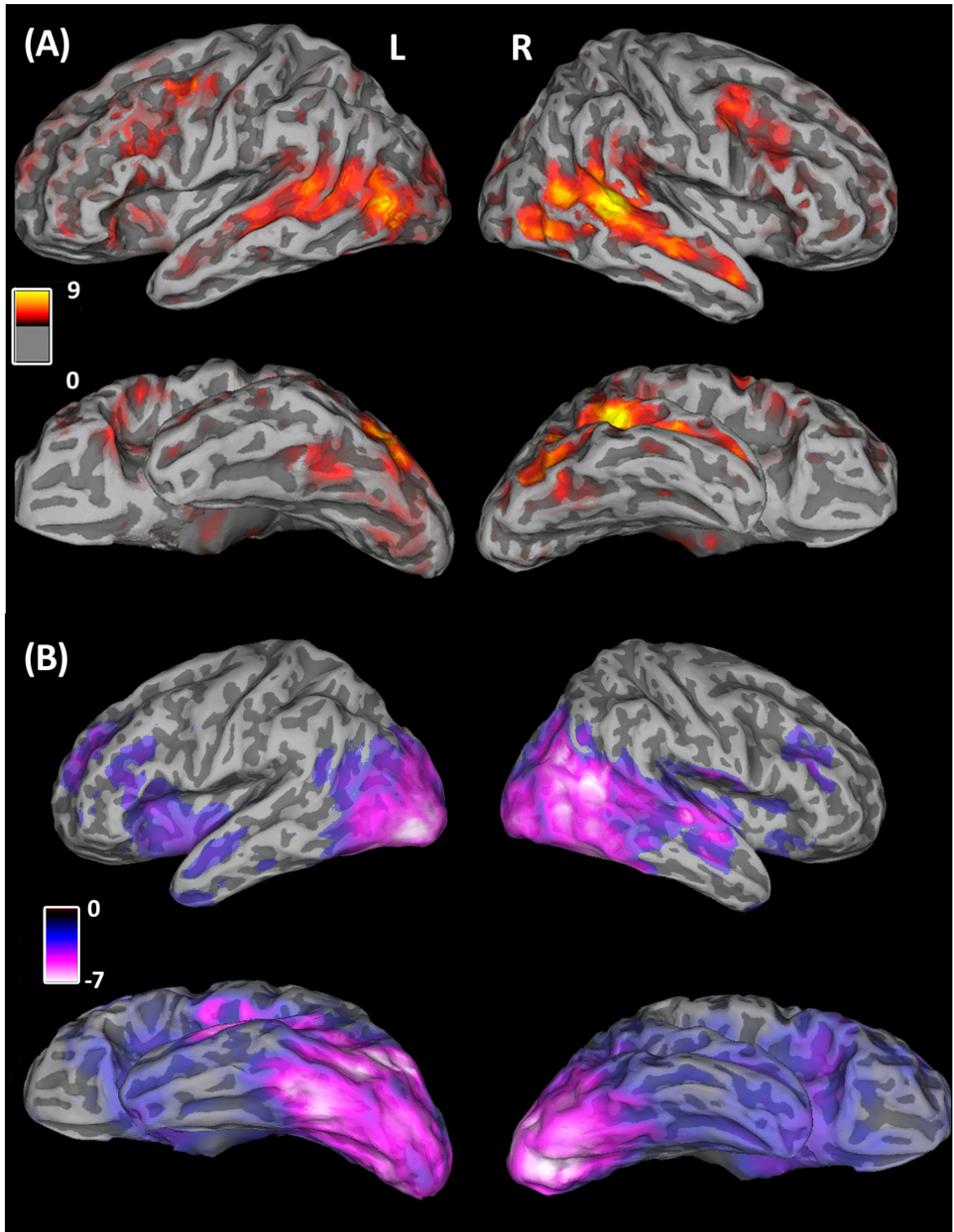


Figure 6.2.1: fMRI and MEG integration: (A) fMRI whole brain group results (N=14) for the dynamic versus static condition displayed on lateral and ventral views. Shows bilateral activation in MOG, MTG and extending along STS to frontal regions of the cortex, IFG and MFG, in both left (L) and right (R) hemispheres. Red-orange-yellow colour scale depicts increasing BOLD amplitude ($p < 0.05$). (B) Group SAM image (N=14) shows decrease in beta band power (12-30 Hz) for the contrast of dynamic versus static faces, between 1000-1500 ms post stimulus onset in bilateral IOG, MTG, STS and IFG, on lateral and ventral views. Blue-purple-white colour scale represents a decrease in signal power ($p < 0.05$).

may not have been sufficient to distinguish the difference in response between dynamic and static faces. This highlights the advantage of a multimodal approach.

Later responses were found in MTG and STS around 800 ms. The region in STS, in particular, showed a strong decrease in oscillatory power between 10-30 Hz from 800 ms onwards to dynamic faces, which is consistent with the significant increase in power found in this region in the fMRI study. Additional regions of the face perception network, including IFG and precentral gyri showed later differential activation around 1000 ms for dynamic relative to static faces. These findings therefore provide important information about the characteristics of the dynamic face perception network

A more complete view of the dynamic face perception network can then be gained by combining this information with the results from the connectivity analysis. Within this network firstly an early response occurred in IOG within 200 ms, where early visual processing takes place. The IOG was coupled with regions of MTG and STS, which all responded within 800 ms of stimulus onset. The regions in the STS maintain a sustained response, which feeds back into visual regions such as the IOG. Notably, the IOG also maintains a sustained response from 200 ms onwards for dynamic faces. This sustained response in IOG has important implications for hierarchical feed forward face perception models, as it suggests that IOG is not only involved in early visual analysis but may also play a role in higher level processing (Atkinson and Adolphs, 2011) such as facial expressions analysis (Pitcher et al., 2008), which may be due to the feedback connections from the STS.

The STS also feeds forward to frontal regions, including superior frontal and precentral gyri, and these regions responded differentially to dynamic relative to static faces around 1000 ms post stimulus onset. Regions in IFG responded around 1000 ms and feedback into the STS and occipito-temporal cortex. This suggests that the STS may act as a relay centre between regions involved in early visual perceptual processing, and regions of prefrontal cortex, which are involved in social processing. The sustained response in the STS provides converging evidence for this, as it may represent multiple activations, which facilitate the integration of information from multiple input areas (Hein and Knight, 2008). This provides valuable additional information towards a better understanding of how dynamic facial expressions are processed in time, space and frequency in an interacting

network of regions.

While the concordance between these fMRI and MEG analyses was extremely good there were a few regions that were activated in the fMRI study, but not visible in the group MEG data, and vice versa. As already stated bilateral IOG were localised with MEG but not with fMRI and the possible reason for this has already been explained. The amygdala was also identified with fMRI but not with MEG. These differences may have arisen from differences in sensitivities of the two methods. For example MEG is relatively insensitive to deep cortical sources such as the amygdala, whereas fMRI is insensitive to temporally short responses.

6.2.3.2 Differential activation of the dynamic face perception network

When the network of regions involved in processing dynamic angry facial expressions was investigated with both fMRI and MEG, again broadly similar regions of activation were found across the two modalities. Whereby decreases in alpha and beta power in the following regions, middle occipital gyri, MTG, and STS corresponded with increased BOLD responses in the same regions. The right amygdala and insula were identified as structures involved in processing dynamic angry faces with fMRI, but only the insula was localised with MEG. This may be because MEG is relatively insensitive to deep cortical sources. MEG, on the other hand, localised some additional sources in prefrontal cortex that were not identified with fMRI, this is possibly because the responses in these regions were more transient and also they were mainly characterised by changes in delta and theta bands. It is unclear how these frequency bands correlate with the BOLD response. However, regions in prefrontal cortex were identified with fMRI in the connectivity analysis.

Despite these discrepancies, a network of regions involved in processing dynamic angry facial expressions emerged. Within 200 ms early responses occurred in occipito-temporal regions, in IOG, followed by STS. Both of these regions are reciprocally connected and displayed similar response patterns, with an early peak decrease in alpha and beta frequency bands for dynamic angry expressions. These regions were also coupled with middle occipital gyrus, which responded around 200 ms, again showing decreased beta power for dynamic angry expressions. IOG was also coupled with regions in prefrontal cortex, where regions of IOG showed significantly greater increases in low frequency power (2-8 Hz) for

dynamic angry facial expressions within 200 ms of stimulus onset

This coupling between IOG and inferior frontal regions is again consistent with the view that the IOG is an important structure in the face perception network, which may be involved in multiple stages of face processing, rather than just the early structural encoding stage (Atkinson and Adolphs, 2011). It has also been suggested that the coupling between visual cortical and prefrontal regions may be important in facilitating facial affect processing (Dima et al., 2011). The amygdala is also effectively connected with frontal regions during the processing of dynamic angry expressions, and is reciprocally connected with IFG. Both are effectively connected to the right cingulate, hence these structures may work together to process the emotional content of the dynamic angry facial expressions, along with the insula which is also involved in processing dynamic angry facial expressions. This insular response was characterised by greater increases in low frequency power (3-12 Hz) for dynamic angry facial expressions between 400-1200 ms, which is in line with previous research linking theta synchronisation with emotional face processing (Güntekin and Basar, 2007; Knyazev, 2007).

This network corresponds with Adolphs (2002b) model of emotion recognition, where early structural processing occurs in occipital cortex and feeds forward into temporal regions, including MTG and STS. A perceptual representation of the facial expression is then generated from the combined information from regions of occipito-temporal cortex. . Additional structures including the amygdala, orbitofrontal cortex, somatosensory cortex and insular cortex, are then recruited from around 300 ms post stimulus onset, to link the perceptual representation to conceptual knowledge of the emotional and social meaning of the perceived expression. Importantly, information is then fed back to occipito-temporal regions to facilitate further processing of the facial expression.

When fMRI and MEG were used to investigate the network of regions involved in processing dynamic happy facial expressions, once again broadly similar regions of activation were found across the two modalities. Sources of decreased alpha and beta power were localised in middle occipital gyri, MTG, STS and fusiform gyri, which corresponded with increased BOLD responses in the same regions. The integration of the fMRI, MEG and connectivity analysis data reveals a neural network involved in processing dynamic happy facial expressions. Notably this network differs somewhat to that described for dynamic

angry facial expressions.

Once again IOG responded early within 200 ms of stimulus presentation, as characterised by a sustained decrease in power (8-30 Hz) with a strong peak around 200 ms. According to Adolphs (2002b) model this early response reflects the processing of low-level visual cues related to the emotional facial expression (Vuilleumier and Pourtois, 2007; Morel et al., 2009). Additionally, IOG was coupled with IFG, which also displayed an early response to dynamic happy expressions within 200 ms. This response was characterised by an early increase in low frequency power (2-8 Hz). Again, this coupling between IOG and IFG may facilitate processing of the emotional content from the dynamic face, in this case the happy expressions (Dima et al., 2011).

IFG was also effectively connected with the fusiform gyrus, which responded early, showing a sustained power decrease in the range of 8-28 Hz from 200 ms onwards. Interestingly, this coupling between IFG and fusiform gyrus appears to be specific to dynamic happy facial expressions, as these regions were not effectively connected during the processing of dynamic angry expressions. IOG was also coupled with the fusiform gyrus as well as with middle occipital gyrus. Accordingly, these regions all show broadly similar response profiles responding within 400 ms and maintaining a sustained decrease in power between ~8 to 30 Hz for the duration of the dynamic happy face displays.

The STS was also effectively connected with IOG as well as with MTG and both regions displayed greater and more sustained decreases in alpha and beta power from approximately 800 ms. The STS and postcentral gyrus were also effectively connected, and the postcentral gyrus response peaked around 400 ms again characterised by decreases in alpha and beta power. This again suggests that the STS acts as a relay centre between visual regions and regions that are involved in social perception. Where the postcentral gyrus, according to Adolphs (2002) theory of emotion recognition, is recruited to facilitate recognition of the happy emotional expressions i.e. the same neural mechanisms involved in generating the emotional experience.

Finally, converging results were once again obtained between fMRI and MEG during the investigation of the neural network involved in processing dynamic speech facial displays. Sources of decreased alpha and beta power were localised in middle occipital gyri, MTG, STS, IFG and middle frontal gyri, which corresponded with increased BOLD responses in

the same regions. However, there were two sources of difference, whereby fMRI identified a source in right precentral gyrus, which was not detected with MEG, while a source in left postcentral gyrus was localised with MEG but not with fMRI.

By integrating the information obtained from fMRI, MEG and connectivity analysis, the following neural network for processing dynamic speech facial displays can be described. IOG responded early, once again, within 200 ms of presentation of the dynamic speech stimuli. This response was characterised by a strong sustained decrease in power between 5-30 Hz, which reflects the processing of low-level visual cues related to the speech facial displays (Adolphs, 2002). Regions in IFG also responded within 200 ms, but showed an increase in power for dynamic speech displays, in a low frequency range from 3-10 Hz. Interestingly while both these regions responded early within 200 ms they were not effectively connected. IOG, was however effectively connected with STS, which responded later, around 800 ms again showing a sustained decrease in power in alpha and beta frequency bands.

STS was also effectively connected with middle occipital gyrus, which again responded around 800 ms showing decreased power, but this time in a slightly lower frequency range from 5-20 Hz. The STS was also coupled with frontal regions, again highlighting its role in linking early perceptual visual processing in inferior and middle occipital gyri, and higher level processing of the facial speech stimuli in inferior and middle frontal gyri. IFG were coupled with middle occipital and MTG, which showed similar response profiles that were characterised by sustained decreases in alpha and beta power from approximately 800 ms after presentation of dynamic speech stimuli. In contrast a region in postcentral gyrus responded differentially to dynamic speech displays around 1000 ms, but this response was characterised by an increase in power between 12-30 Hz for dynamic speech displays. In sum, it has been shown that a broad network of overlapping regions is involved in processing different dynamic facial stimuli where the effective connectivity within this network varies depending on the type of expression that is processed. Furthermore regions within this network were shown to interact with varying temporal and oscillatory dynamics during the processing of different facial displays.

6.3 Methodological considerations and limitations

As described in chapter 2, the stimuli used in the present thesis were purposely created in order to obtain examples of more naturalistic dynamic facial expressions. A number of measures were taken to evaluate these stimuli before they were used in the neuroimaging studies. The dynamic and static stimuli were evaluated psychometrically for recognition and intensity. Interestingly, happy faces were recognised better than angry faces, which could be a potential confound in the neuroimaging studies. However, Ekman and Friesen (1976) report that mean accuracy for recognition of the facial expression of happiness reached 100% making this the most easily recognised facial expression. Also, participants were not explicitly required to identify the type of facial expression in the fMRI and MEG studies, as they were attending to the identity of the face stimuli.

A possible confound could also arise from differences in the amount of motion contained in the different categories of facial stimuli. A motion capture technique was therefore used to estimate the amount of motion present in the different categories of facial expression. No significant differences were found across the different categories of facial display i.e., angry, happy and speech displays. However, a small sample size of four models was used, making it difficult to draw significant quantitative conclusions. A larger sample would provide a better approximation of the amount of motion across the different facial display categories. Furthermore, the models that were used in the motion capture experiment were not the same as those used to create the video clips. Thus, it is possible that there are additional forms of idiosyncratic motion in the video clips that were not identified with the motion capture technique. Ideally, therefore it would be best to perform the motion capture on the same models that are in the stimuli. Unfortunately this was not possible here.

A 1-back recognition task was used in both the fMRI and MEG studies in order to ensure that all participants were paying attention and engaging in the same processes while watching the stimuli. However, this task may have biased face processing due to cognitive influence from top-down processes, as previous studies have reported differences in neural activation patterns for passive versus active task instructions during emotion perception (see e.g., Costafreda et al., 2008). By focusing participants attention on the identity of the stimuli rather than the specific facial expression we tried to avoid additional

confounds from recognition of the facial expressions. This is particularly relevant to the connectivity analysis as it has been shown that the coupling between regions varies under different task conditions (Fairhall and Ishai, 2007). Therefore it would be interesting to see if the coupling identified between regions of the face perception network would change under different task conditions. In general there is a lot of variation in the face perception literature in experimental design, task, stimuli type, or button response, yet a robust network of regions is consistently identified but it is important to be aware of the effects of particular tasks.

Slightly different experimental designs were used in the fMRI and MEG studies which may have caused additional differences between the results obtained across the two modalities (see subsection 6.2.3). A block design was used in the fMRI study in order to maximise statistical power, however an event-related design was used in the MEG study to optimise results from the SAM analysis. However, identical stimuli, task and presentation time were used in the fMRI and MEG studies, in an attempt to reduce the effects of additional external confounding variables. Nevertheless, it would be beneficial to use the same event-related design in both experiments to facilitate better integration of the two modalities. Different participants were used in the fMRI and MEG studies. Ideally it would be advantageous to acquire data from the same participants in both the fMRI and MEG studies, again to facilitate better integration and comparison of the two modalities. However, because a limited number of face stimuli were shown in both the fMRI and MEG studies different participants were used to avoid participants becoming overly habituated to the faces. Possibly with a larger stimulus set, a counterbalanced and pseudo-random design could be used with the same participants in the fMRI and MEG. Age and gender have been shown to influence emotion processing (Fine et al., 2009; Fusar-Poli et al., 2009), hence these were matched where possible, although slightly more females were available in this opportunity sample.

6.4 Future directions

In relation to the current findings there are a number of potential avenues of research that could be explored. A multimodal approach was adopted here in order to combine the benefits of, excellent spatial resolution from fMRI, with the temporal and frequency

information from MEG, to gain a better understanding of face processing mechanisms in the brain. Furthermore, fMRI connectivity analysis was used to estimate connectivity within the face perception network. However, this connectivity analysis was based on the haemodynamic response signal, and consequently is an indirect measure of neural activity. Therefore, an important next step in this multimodal approach would be to measure connectivity within the face perception network at the neural or electrical level with MEG, to gain a better understanding of the electrical nature of connectivity within this network.

While standard methods of connectivity analysis are available for fMRI data, including the PPI analysis methods that were used in the present thesis, as well as DCM, with numerous publications on the different techniques (see chapter 3), connectivity analysis of MEG data has received less attention. MEG connectivity analysis is more challenging due to the multidimensional nature of the signal, which means that additional factors must be considered before connectivity analysis can be performed on MEG data. For example, connectivity analysis can be performed in source or sensor space. In sensor space there is poor spatial localisation, whereas in source space the ill-posed inverse problem has to be addressed. That is, multiple MEG sensors will be affected by a single current source, which means that the signals originating from spatially separate voxels in source space are not necessarily independent. This cross talk between voxels can therefore generate spurious connectivity results.

Yet despite these challenges, MEG connectivity analysis has been successfully implemented in a number of different MEG studies (Gross et al., 2001; Stam et al., 2007; Brookes et al., 2011), and it has recently become possible to use DCM on MEG data (Kiebel et al., 2009). Additionally, a compelling study by Brookes et al. (2011) compared measures of resting state functional connectivity using fMRI and MEG, and found good spatial agreement between the two modalities. These converging results are encouraging for the multimodal integration of fMRI and MEG connectivity data, and help to validate both methods. fMRI provides spatial information, which helps to reduce the uncertainties with MEG spatial localisation due to the inverse problem, while the addition of electrodynamic information verifies the neural basis of fMRI connectivity measures. It is therefore important to use complementary neuroimaging techniques to obtain converging connectivity

results, which will advance the field. Moreover, this will be particularly beneficial to clinical populations, such as patients with prosopagnosia (Thomas et al., 2009) and autism (Wicker et al., 2008), where it has been shown that connectivity measures are important in understanding neural dysfunction in these populations.

The direction of future research is multimodal in every sense of the word, both in relation to multimodal imaging and also in terms of multimodal perception. With the goal of achieving more naturalistic and ecologically valid stimuli researchers are now focusing on the multimodal nature of perception, where information from different modalities such as visual, auditory and tactile information is integrated over time (Jessen and Kotz, 2011). In the present thesis dynamic face stimuli were used as a more ecologically valid alternative to static faces, and consequently showed more widespread and differential patterns of neural activation. However, face and emotion perception are not solely dependent on visual information, auditory information is also important in social interaction and communication. Therefore an interesting avenue of future research would be to use dynamic audio-visual stimuli to explore the neural mechanisms of face and emotion perception, again with both fMRI and MEG.

In a recent EEG study, Jessen and Kotz (2011) found an interaction between visual and auditory information in emotion perception, where visual information influenced the processing of auditory emotional information within 100 ms. Schroeder et al. (2008) also found that visual information modulated auditory perception of audio-visual speech stimuli. Interestingly, they propose that this effect is related to the modulation of ongoing neuronal oscillatory activity, whereby non-auditory inputs to auditory cortex are proposed to modulate neuronal activity so that appropriately timed auditory inputs are amplified. This research is not only interesting from the perspective of audiovisual integration, but also because it sheds more light on the functional significance of neuronal oscillatory activity. It would be interesting to explore this hypothesis using audio-visual facial displays with MEG and SAM analysis.

6.5 Conclusion

In conclusion, this research employing two complementary neuroimaging techniques, uncovered a distributed network of overlapping regions that was shown to be involved in

processing different dynamic facial stimuli. Through the use of fMRI and connectivity analysis it was shown that the effective connectivity within this network varies depending on the type of expression processed. Furthermore, the regions within this network were shown to interact with varying temporal and oscillatory dynamics during the processing of different facial displays. This integrated multimodal approach offers a promising and useful way to examine the spatiotemporal and frequency dynamics of the neural processes involved in face perception.

References

- Adjamian, P., Barnes, G. R., Hillebrand, A., Holliday, I. E., Singh, K. D., Furlong, P. L., Harrington, E., Barclay, C. W., and Route, P. J. G. (2004). Co-registration of magnetoencephalography with magnetic resonance imaging using bite-bar-based fiducials and surface-matching. *Clinical Neurophysiology*, 115(3):691–698.
- Adolphs, R. (2002a). Neural systems for recognizing emotion. *Current Opinion in Neurobiology*, 12(2):169–177.
- Adolphs, R. (2002b). Recognizing emotion from facial expressions: psychological and neurological mechanisms. *Behavioral and Cognitive Neuroscience Reviews*, 1(1):21–62.
- Adolphs, R., Russell, J. A., and Tranel, D. (1999). A role for the human amygdala in recognizing emotional arousal from unpleasant stimuli. *Psychological Science*, 10:167–171.
- Adolphs, R., Tranel, D., Damasio, H., and Damasio, A. (1994). Impaired recognition of emotion in facial expressions following bilateral damage to the human amygdala. *Nature*, 372(6507):669–672.
- Ahlfors, S. P., Simpson, G. V., Dale, A. M., Belliveau, J. W., Liu, A. K., Korvenoja, A., Virtanen, J., Huotilainen, M., Tootell, R. B. H., Aronen, H. J., and Ilmoniemi, R. J. (1999). Spatiotemporal activity of a cortical network for processing visual motion revealed by MEG and fMRI. *Journal of Neurophysiology*, 82(5):2545–2555.
- Allison, T., Puce, A., and McCarthy, G. (2000). Social perception from visual cues: role of the STS region. *Trends in Cognitive Sciences*, 4(7):267–278.
- Allison, T., Puce, A., Spencer, D. D., and McCarthy, G. (1999). Electrophysiological

- studies of human face perception. I: Potentials generated in occipitotemporal cortex by face and non-face stimuli. *Cerebral Cortex*, 9(5):415–430.
- Ambadar, Z. (2002). *The effects of motion and orientation on perception of facial expressions and face recognition*. PhD thesis.
- Ambadar, Z., Schooler, J. W., and Cohn, J. F. (2005). Deciphering the enigmatic face: the importance of facial dynamics in interpreting subtle facial expressions. *Psychological Science*, 16(5):403–410.
- Ashley, V., Vuilleumier, C. A. P., and Swick, D. (2004). Time course and specificity of event-related potentials to emotional expressions. *Health Care*, 15(1):211–216.
- Atkinson, A. P. and Adolphs, R. (2011). The neuropsychology of face perception: beyond simple dissociations and functional selectivity. *Philosophical Transactions of the Royal Society of London. Series B, Biological sciences*, 366:1726–1738.
- Balconi, M. and Lucchiari, C. (2006). EEG correlates (event-related desynchronization) of emotional face elaboration: a temporal analysis. *Neuroscience Letters*, 392(1-2):118–123.
- Balconi, M. and Pozzoli, U. (2009). Arousal effect on emotional face comprehension: frequency band changes in different time intervals. *Physiology & Behavior*, 97(3-4):455–462.
- Barnes, G. R., Furlong, P. L., Singh, K. D., and Hillebrand, A. (2006). A verifiable solution to the MEG inverse problem. *NeuroImage*, 31(2):623–626.
- Barnes, G. R. and Hillebrand, A. (2003). Statistical flattening of MEG beamformer images. *Human Brain Mapping*, 18(1):1–12.
- Barrett, L. F. (2011). Was Darwin Wrong About Emotional Expressions? *Current Directions in Psychological Science*, 20(6):400–406.
- Basar, E., Basar-Eroglu, C., Karakas, S., and Schürmann, M. (2001). Gamma, alpha, delta, and theta oscillations govern cognitive processes. *International Journal of Psychophysiology*, 39(2-3):241–248.

- Bassili, J. N. (1978). Facial motion in the perception of faces and of emotional expression. *Journal of Experimental Psychology Human Perception and Performance*, 4(3):373–379.
- Batty, M. and Taylor, M. J. (2003). Early processing of the six basic facial emotional expressions. *Cognitive Brain Research*, 17(3):613–620.
- Bayle, D. J. and Taylor, M. J. (2010). Attention inhibition of early cortical activation to fearful faces. *Brain Research*, 1313:113–123.
- Beauchamp, M. S., Lee, K. E., Haxby, J. V., and Martin, A. (2002). Parallel Visual Motion Processing Streams for Manipulable Objects and Human Movements. *Neuron*, 34:149–159.
- Bentin, S., Allison, T., Puce, A., Perez, E., and McCarthy, G. (1996). Electrophysiological studies of face perception in humans. *Journal of Cognitive Neuroscience*, 8(6):551–565.
- Biswal, B., Yetkin, F. Z., Haughton, V. M., and Hyde, J. S. (1995). Functional connectivity in the motor cortex of resting human brain using echo-planar MRI. *Magnetic Resonance in Medicine*, 34(4):537–541.
- Blake, R. and Shiffrar, M. (2007). Perception of human motion. *Annual Review of Psychology*, 58:47–73.
- Bould, E. and Morris, N. (2008). Role of motion signals in recognizing subtle facial expressions of emotion. *British Journal of Psychology*, 99:167–189.
- Breiter, H. C., Etcoff, N. L., Whalen, P. J., Kennedy, W. a., Rauch, S. L., Buckner, R. L., Strauss, M. M., Hyman, S. E., and Rosen, B. R. (1996). Response and habituation of the human amygdala during visual processing of facial expression. *Neuron*, 17(5):875–87.
- Brookes, M. J., Gibson, A. M., Hall, S. D., Furlong, P. L., Barnes, G. R., Hillebrand, A., Singh, K. D., Holliday, I. E., Francis, S. T., and Morris, P. G. (2005). GLM-beamformer method demonstrates stationary field, alpha ERD and gamma ERS co-localisation with fMRI BOLD response in visual cortex. *NeuroImage*, 26(1):302–308.
- Brookes, M. J., Hale, J. R., Zumer, J. M., Stevenson, C. M., Francis, S. T., Barnes, G. R., Owen, J. P., Morris, P. G., and Nagarajan, S. S. (2011). Measuring functional connectivity using MEG: methodology and comparison with fcMRI. *NeuroImage*.

- Bruce, V. and Valentine, T. (1988). When a nod's as good as a wink: The role of dynamic information in facial recognition. In Gruneberg, M. M., Morris, P., and Sykes, R., editors, *Practical aspects of memory: Current research and issues*, pages 169–174. Wiley, Chichester, UK, volume 1 edition.
- Bruce, V. and Young, A. (1986). Understanding face recognition. *British Journal of Psychology*, 77:305–327.
- Buccino, G. (2004). The mirror neuron system and action recognition. *Brain and Language*, 89(2):370–376.
- Buzsáki, G. and Draguhn, A. (2004). Neuronal oscillations in cortical networks. *Science*, 304(5679):1926–9.
- Calder, A. J., Lawrence, A. D., and Young, A. W. (2001). Neuropsychology of fear and loathing. *Nature Reviews Neuroscience*, 2(5):352–363.
- Calder, A. J. and Young, A. W. (2005). Understanding the recognition of facial identity and facial expression. *Nature Reviews Neuroscience*, 6(8):641–651.
- Calder, A. J., Young, A. W., Rowland, D., Perrett, D. I., Hodges, J. R., and Etcoff, N. L. (1996). Facial emotion recognition after bilateral amygdala damage: Differentially severe impairment of fear. *Cognitive Neuropsychology*, 13(5):699–745.
- Campbell, R., MacSweeney, M., Surguladze, S., Calvert, G., McGuire, P., Suckling, J., Brammer, M. J., and David, a. S. (2001). Cortical substrates for the perception of face actions: an fMRI study of the specificity of activation for seen speech and for meaningless lower-face acts (gurning). *Cognitive Brain Research*, 12(2):233–243.
- Cantero, J. L. and Atienza, M. (2005). The role of neural synchronization in the emergence of cognition across the wake-sleep cycle. *Reviews in the Neurosciences*, 16(1):69–83.
- Carroll, J. M. and Russell, J. A. (1997). Facial expressions in hollywood's portrayal of emotion. *Journal of Personality and Social Psychology*, 72(1):164–176.
- Christie, F. and Bruce, V. (1998). The role of dynamic information in the recognition of unfamiliar faces. *Memory Cognition*, 26(4):780–790.

- Clark, V. P., Keil, K., Maisog, J. M., Courtney, S., Ungerleider, L. G., and Haxby, J. V. (1996). Functional magnetic resonance imaging of human visual cortex during face matching: a comparison with positron emission tomography. *NeuroImage*, 4(1):1–15.
- Corbetta, M., Patel, G., and Shulman, G. (2008). The reorienting system of the human brain: From environment to theory of mind. *Neuron*, 58(3):306–324.
- Costafreda, S. G., Brammer, M. J., David, A. S., and Fu, C. H. Y. (2008). Predictors of amygdala activation during the processing of emotional stimuli: a meta-analysis of 385 PET and fMRI studies. *Brain Research Reviews*, 58(1):57–70.
- Dale, A. M. and Halgren, E. (2001). Spatiotemporal mapping of brain activity by integration of multiple imaging modalities. *Current Opinion in Neurobiology*, 11(2):202–208.
- Damasio, A. R., Damasio, H., Rizzo, M., Varney, N., and Gersh, F. (1982). Aphasia with nonhemorrhagic lesions in the basal ganglia and internal capsule. *Archives of Neurology*, 39(1):15–24.
- Damasio, A. R., Tranel, D., and Damasio, H. (1990). Face agnosia and the neural substrates of memory. *Annual Review of Neuroscience*, 13:89–109.
- Darwin, C. (1872). *The expression of the emotions in man and animals*. London: John Murray.
- Das, P., Kemp, A. H., Liddell, B. J., Brown, K. J., Olivieri, G., Peduto, A., Gordon, E., and Williams, L. M. (2005). Pathways for fear perception: modulation of amygdala activity by thalamo-cortical systems. *NeuroImage*, 26(1):141–8.
- Decety, J. and Grèzes, J. (1999). Neural mechanisms subserving the perception of human actions. *Trends in Cognitive Sciences*, 3(5):172–178.
- Dima, D., Stephan, K. E., Roiser, J. P., Friston, K. J., and Frangou, S. (2011). Effective connectivity during processing of facial affect: evidence for multiple parallel pathways. *Journal of Neuroscience*, 31(40):14378–14385.
- Dougherty, R. F., Ben-Shachar, M., Bammer, R., Brewer, A. A., and Wandell, B. A. (2005). Functional organization of human occipital-callosal fiber tracts. *Proceedings of the National Academy of Sciences of the United States of America*, 102(20):7350–5.

- Downing, P. E., Jiang, Y., Shuman, M., and Kanwisher, N. (2001). A cortical area selective for visual processing of the human body. *Science*, 293(5539):2470–2473.
- Eger, E., Jedynak, A., Iwaki, T., and Skrandies, W. (2003). Rapid extraction of emotional expression: evidence from evoked potential fields during brief presentation of face stimuli. *Neuropsychologia*, 41(7):808–17.
- Eimer, M. and Holmes, A. (2002). An ERP study on the time course of emotional face processing. *Neuroreport*, 13(4):427–431.
- Eimer, M. and Holmes, A. (2007). Event-related brain potential correlates of emotional face processing. *Neuropsychologia*, 45(1):15–31.
- Eimer, M., Holmes, A., and McGlone, F. P. (2003). The role of spatial attention in the processing of facial expression: an ERP study of rapid brain responses to six basic emotions. *Cognitive Affective & Behavioral Neuroscience*, 3(2):97–110.
- Ekman, P. (1992). Symposium on Emotion New Findings , New Questions. *Society*, 3(1).
- Ekman, P. and Friesen, W. V. (1971). Constants across cultures in the face and emotion. *Journal of Personality and Social Psychology*, 17(2):124–129.
- Ekman, P. and Friesen, W. V. (1976). *Pictures of facial affect*. Consulting Psychologists Press, Palo Alto:CA.
- Ekman, P. and Friesen, W. V. (1982). Felt, false and miserable smiles. *Journal of Nonverbal Behavior*, 6:238–252.
- Ekman, P., Friesen, W. V., O’Sullivan, M., Chan, A., Diacoyanni-Tarlatzis, I., Heider, K., Krause, R., LeCompte, W. A., Pitcairn, T., and Ricci-Bitti, P. E. (1987). Universals and cultural differences in the judgments of facial expressions of emotion. *Journal of Personality and Social Psychology*, 53(4):712–717.
- Engel, A. K., Fries, P., and Singer, W. (2001). Dynamic predictions: oscillations and synchrony in top-down processing. *Nature Reviews Neuroscience*, 2(10):704–716.
- Engell, A. D. and Haxby, J. V. (2007). Facial expression and gaze-direction in human superior temporal sulcus. *Neuropsychologia*, 45(14):3234–41.

- Esslen, M., Pascual-Marqui, R. D., Hell, D., Kochi, K., and Lehmann, D. (2004). Brain areas and time course of emotional processing. *NeuroImage*, 21(4):1189–203.
- Fairhall, S. L. and Ishai, A. (2007). Effective connectivity within the distributed cortical network for face perception. *Cerebral Cortex*, 17(10):2400–2406.
- Fawcett, I. P., Barnes, G. R., Hillebrand, A., and Singh, K. D. (2004). The temporal frequency tuning of human visual cortex investigated using synthetic aperture magnetometry. *NeuroImage*, 21(4):1542–53.
- Felsen, G. and Dan, Y. (2005). A natural approach to studying vision. *Nature Neuroscience*, 8(12):1643–1646.
- Fine, J. G., Semrud-Clikeman, M., and Zhu, D. C. (2009). Gender differences in BOLD activation to face photographs and video vignettes. *Behavioural Brain Research*, 201(1):137–146.
- Foley, E., Rippon, G., Thai, N. J., Longe, O., and Senior, C. (2012). Dynamic facial expressions evoke distinct activation in the face perception network: a connectivity analysis study. *Journal of Cognitive Neuroscience*, 24(2):507–520.
- Fox, C. J., Iaria, G., and Barton, J. J. S. (2009). Defining the face processing network: optimization of the functional localizer in fMRI. *Human Brain Mapping*, 30(5):1637–1651.
- Fox, M. D., Corbetta, M., Snyder, A. Z., Vincent, J. L., and Raichle, M. E. (2006). Spontaneous neuronal activity distinguishes human dorsal and ventral attention systems. *Proceedings of the National Academy of Sciences*, 103(26):10046–10051.
- Fox, M. D., Snyder, A. Z., Vincent, J. L., Corbetta, M., Van Essen, D. C., and Raichle, M. E. (2005). The human brain is intrinsically organized into dynamic, anticorrelated functional networks. *Proceedings of the National Academy of Sciences*, 102(27):9673–9678.
- Fox, P. T. and Raichle, M. E. (1986). Focal physiological uncoupling of cerebral blood flow and oxidative metabolism during somatosensory stimulation in human subjects. *Proceedings of the National Academy of Sciences*, 83(4):1140–1144.

- Friston, K. J. (2009). Modalities, modes, and models in functional neuroimaging. *Science*, 326(5951):399–403.
- Friston, K. J., Buechel, C., Fink, G. R., Morris, J., Rolls, E., and Dolan, R. J. (1997). Psychophysiological and modulatory interactions in neuroimaging. *NeuroImage*, 6(3):218–29.
- Friston, K. J., Holmes, A. P., Worsley, K., Poline, J.-P., Frith, C., and Frackowiak, R. (1995). Statistical parametric maps in functional imaging : a general linear approach. *Human Brain Mapping*, 2:189 – 210.
- Furl, N., Van Rijsbergen, N. J., Kiebel, S. J., Friston, K. J., Treves, A., and Dolan, R. J. (2010). Modulation of perception and brain activity by predictable trajectories of facial expressions. *Cerebral Cortex*, 20(3):694–703.
- Fusar-Poli, P., Placentino, A., Carletti, F., Landi, P., Allen, P., Surguladze, S., Benedetti, F., Abbamonte, M., Gasparotti, R., Barale, F., Perez, J., McGuire, P., and Politi, P. (2009). Functional atlas of emotional faces processing: a voxel-based meta-analysis of 105 functional magnetic resonance imaging studies. *Journal of Psychiatry & Neuroscience*, 34(6):418–432.
- Gauthier, I., Behrmann, M., and Tarr, M. J. (1999). Can face recognition really be dissociated from object recognition? *Journal of Cognitive Neuroscience*, 11:349–370.
- Gitelman, D. R., Penny, W. D., Ashburner, J., and Friston, K. J. (2003). Modeling regional and psychophysiological interactions in fMRI: the importance of hemodynamic deconvolution. *NeuroImage*, 19(1):200–207.
- Gobbini, M. I. and Haxby, J. V. (2007). Neural systems for recognition of familiar faces. *Neuropsychologia*, 45(1):32–41.
- Greicius, M. D., Krasnow, B., Reiss, A. L., and Menon, V. (2003). Functional connectivity in the resting brain: a network analysis of the default mode hypothesis. *Proceedings of the National Academy of Sciences*, 100(1):253–258.
- Grosbras, M.-H., Beaton, S., and Eickhoff, S. B. (2012). Brain regions involved in human movement perception: A quantitative voxel-based meta-analysis. *Human Brain Mapping*, 33(2):431–454.

- Gross, J., Kujala, J., Hamalainen, M., Timmermann, L., Schnitzler, A., and Salmelin, R. (2001). Dynamic imaging of coherent sources: Studying neural interactions in the human brain. *Proceedings of the National Academy of Sciences*, 98(2):694–699.
- Grossberg, S. (2000). The complementary brain: unifying brain dynamics and modularity. *Trends in Cognitive Sciences*, 4(6):233–246.
- Grossman, E., Donnelly, M., Price, R., Pickens, D., Morgan, V., Neighbor, G., and Blake, R. (2000). Brain areas involved in perception of biological motion. *Journal of Cognitive Neuroscience*, 12(5):711–720.
- Grossman, E. D. and Blake, R. (2002). Brain areas active during visual perception of biological motion. *Neuron*, 35(6):1167–75.
- Grossman, E. D., Jardine, N. L., and Pyles, J. A. (2010). fMR-adaptation reveals invariant coding of biological motion on the human STS. *Frontiers in Human Neuroscience*, 4(15):1–18.
- Gschwind, M., Pourtois, G., Schwartz, S., Van De Ville, D., and Vuilleumier, P. (2012). White-matter connectivity between face-responsive regions in the human brain. *Cerebral Cortex*, 22(7):1564–1576.
- Güntekin, B. and Basar, E. (2007). Emotional face expressions are differentiated with brain oscillations. *International Journal of Psychophysiology*, 64(1):91–100.
- Güntekin, B. and Basar, E. (2009). Facial affect manifested by multiple oscillations. *International Journal of Psychophysiology*, 71(1):31–36.
- Hasselmo, M. E., Rolls, E. T., and Baylis, G. C. (1989). The role of expression and identity in the face-selective responses of neurons in the temporal visual cortex of the monkey. *Behavioural Brain Research*, 32(3):203–218.
- Hasson, U., Malach, R., and Heeger, D. J. (2010). Reliability of cortical activity during natural stimulation. *Trends in Cognitive Sciences*, 14(1):40–48.
- Haxby, J., Hoffman, E., and Gobbini, M. (2000). The distributed human neural system for face perception. *Trends in Cognitive Sciences*, 4(6):223–233.

- Haxby, J. V., Gobbini, M. I., Furey, M. L., Ishai, A., Schouten, J. L., and Pietrini, P. (2001). Distributed and overlapping representations of faces and objects in ventral temporal cortex. *Science*, 293(5539):2425–2430.
- Hein, G. and Knight, R. T. (2008). Superior temporal sulcus—It’s my area: or is it? *Journal of Cognitive Neuroscience*, 20(12):2125–2136.
- Hennenlotter, A. and Schroeder, U. (2006). Partly dissociable neural substrates for recognizing basic emotions: a critical review. *Progress in Brain Research*, 156:443–456.
- Hennenlotter, A., Schroeder, U., Erhard, P., Castrop, F., Haslinger, B., Stoecker, D., Lange, K. W., and Ceballos-Baumann, A. O. (2005). A common neural basis for receptive and expressive communication of pleasant facial affect. *NeuroImage*, 26(2):581–91.
- Henson, R. N., Ganel, T., and Otten, L. J. (2003). Electrophysiological and haemodynamic correlates of face perception, recognition and priming. *Cerebral Cortex*, 13:793–805.
- Hill, H., Jinno, Y., and Johnston, A. (2003). Comparing solid-body with point-light animations. *Perception*, 32(5):561–566.
- Hill, H. and Johnston, A. (2001). Categorizing sex and identity from the biological motion of faces. *Current Biology*, 11:880–885.
- Hillebrand, A., Singh, K. D., Holliday, I. E., Furlong, P. L., and Barnes, G. R. (2005). A new approach to neuroimaging with magnetoencephalography. *Human Brain Mapping*, 25(2):199–211.
- Hirai, M. (2003). An event-related potentials study of biological motion perception in humans. *Neuroscience Letters*, 344(1):41–44.
- Hoffman, E. A. and Haxby, J. V. (2000). Distinct representations of eye gaze and identity in the distributed human neural system for face perception. *Nature Neuroscience*, 3(1):80–84.
- Horovitz, S. G., Rossion, B., Skudlarski, P., and Gore, J. C. (2004). Parametric design and correlational analyses help integrating fMRI and electrophysiological data during face processing. *NeuroImage*, 22(4):1587–95.

- Horstmann, G. (2002). Facial expressions of emotion: does the prototype represent central tendency, frequency of instantiation, or an ideal? *Emotion*, 2(3):297–305.
- Horwitz, B. (2003). The elusive concept of brain connectivity. *NeuroImage*, 19(2):466–470.
- Howard, R. J., Brammer, M., Wright, I., Woodruff, P. W., Bullmore, E. T., and Zeki, S. (1996). A direct demonstration of functional specialization within motion-related visual and auditory cortex of the human brain. *Current Biology*, 6(8):1015–1019.
- Humphreys, G. W., Donnelly, N., and Riddoch, M. J. (1993). Expression is computed separately from facial identity, and it is computed separately for moving and static faces: neuropsychological evidence. *Neuropsychologia*, 31(2):173–81.
- Iacoboni, M., Woods, R. P., Brass, M., Bekkering, H., Mazziotta, J. C., and Rizzolatti, G. (1999). Cortical mechanisms of human imitation. *Science*, 286(5449):2526–2528.
- Ishai, A. (2008). Let's face it: it's a cortical network. *NeuroImage*, 40(2):415–9.
- Ishai, A., Schmidt, C. F., and Boesiger, P. (2005). Face perception is mediated by a distributed cortical network. *Brain Research Bulletin*, 67(1-2):87–93.
- Ishai, A., Ungerleider, L. G., Martin, A., Schouten, J. L., and Haxby, J. V. (1999). Distributed representation of objects in the human ventral visual pathway. *Neurobiology*, 96(16):9379–9384.
- Itier, R. J., Herdman, A. T., George, N., Cheyne, D., and Taylor, M. J. (2006). Inversion and contrast-reversal effects on face processing assessed by MEG. *Brain Research*, 1115(1):108–120.
- Itier, R. J. and Taylor, M. J. (2002). Inversion and contrast polarity reversal affect both encoding and recognition processes of unfamiliar faces: a repetition study using ERPs. *NeuroImage*, 15(2):353–72.
- Itier, R. J. and Taylor, M. J. (2004). N170 or N1? Spatiotemporal differences between object and face processing using ERPs. *Cerebral Cortex*, 14(2):132–142.
- Izard, C. (1971). *The face of emotion*. Appleton Century Crofts, New York.

- Jessen, S. and Kotz, S. a. (2011). The temporal dynamics of processing emotions from vocal, facial, and bodily expressions. *NeuroImage*, 58(2):665–674.
- Johansson, G. (1973). Visual perception of biological motion and a model for its analysis. *Perception & Psychophysics*, 14(2):201–211.
- Jokisch, D., Daum, I., Suchan, B., and Troje, N. F. (2005). Structural encoding and recognition of biological motion: evidence from event-related potentials and source analysis. *Behavioural Brain Research*, 157(2):195–204.
- Kaiser, J., Rahm, B., and Lutzenberger, W. (2008). Direct contrasts between experimental conditions may yield more focal oscillatory activations than comparing pre- versus post-stimulus responses. *Brain Research*, 1235:63–73.
- Kamachi, M., Bruce, V., Mukaida, S., Gyobaá, J., Yoshikawa, S., and Akamatsu, S. (2001). Dynamic properties influence the perception of facial expressions. *Perception*, 30:875–888.
- Kanwisher, N. (2000). Domain specificity in face perception. *Nature Neuroscience*, 3(8):759–763.
- Kanwisher, N., McDermott, J., and Chun, M. M. (1997). The fusiform face area: a module in human extrastriate cortex specialized for face perception. *The Journal of Neuroscience*, 17(11):4302–4311.
- Kanwisher, N. and Yovel, G. (2006). The fusiform face area: a cortical region specialized for the perception of faces. *Philosophical Transactions of the Royal Society of London. Series B, Biological Sciences*, 361(1476):2109–2128.
- Kawakami, O., Kaneoke, Y., Maruyama, K., Kakigi, R., Okada, T., Sadato, N., and Yonekura, Y. (2002). Visual detection of motion speed in humans: spatiotemporal analysis by fMRI and MEG. *Human Brain Mapping*, 16(2):104–118.
- Kiebel, S. J., Garrido, M. I., Moran, R., Chen, C.-C., and Friston, K. J. (2009). Dynamic causal modeling for EEG and MEG. *Human Brain Mapping*, 30(6):1866–1876.

- Kilts, C. D., Egan, G., Gideon, D. A., Ely, T. D., and Hoffman, J. M. (2003). Dissociable neural pathways are involved in the recognition of emotion in static and dynamic facial expressions. *NeuroImage*, 18(1):156–168.
- Kim, M., Ducros, M., Carlson, T., Ronen, I., He, S., Ugurbil, K., and Kim, D.-S. (2006). Anatomical correlates of the functional organization in the human occipitotemporal cortex. *Magnetic Resonance Imaging*, 24(5):583–590.
- Knight, B. and Johnston, A. (1997). The role of movement in face recognition. *Visual Cognition*, 4(3):265–273.
- Knyazev, G. G. (2007). Motivation, emotion, and their inhibitory control mirrored in brain oscillations. *Neuroscience and Biobehavioral Reviews*, 31(3):377–395.
- Knyazev, G. G., Bocharov, A. V., Levin, E. a., Savostyanov, A. N., and Slobodskoj-Plusnin, J. Y. (2008). Anxiety and oscillatory responses to emotional facial expressions. *Brain Research*, 1227:174–188.
- Krakowski, A. I., Ross, L. a., Snyder, A. C., Sehatpour, P., Kelly, S. P., and Foxe, J. J. (2011). The neurophysiology of human biological motion processing: A high-density electrical mapping study. *NeuroImage*, 56(1):373–383.
- Krolak-Salmon, P., Fischer, C., Vighetto, A., and Mauguière, F. (2001). Processing of facial emotional expression: spatio-temporal data as assessed by scalp event-related potentials. *The European Journal of Neuroscience*, 13(5):987–994.
- LaBar, K. S., Crupain, M. J., Voyvodic, J. T., and McCarthy, G. (2003). Dynamic perception of facial affect and identity in the human brain. *Cerebral Cortex*, 13(10):1023–1033.
- Le Bihan, D., Mangin, J. F., Poupon, C., Clark, C. a., Pappata, S., Molko, N., and Chabriat, H. (2001). Diffusion tensor imaging: concepts and applications. *Journal of magnetic resonance imaging*, 13(4):534–546.
- Lee, L. C., Andrews, T. J., Johnson, S. J., Woods, W., Gouws, A., Green, G. G. R., and Young, A. W. (2010). Neural responses to rigidly moving faces displaying shifts in social attention investigated with fMRI and MEG. *Neuropsychologia*, 48(2):477–90.

- Liu, J., Harris, A., and Kanwisher, N. (2002). Stages of processing in face perception: an MEG study. *Nature Neuroscience*, 5(9):910–916.
- Liu, J., Higuchi, M., Marantz, A., and Kanwisher, N. (2000). The selectivity of the occipitotemporal M170 for faces. *NeuroReport*, 11(2):337–341.
- Liu, L. and Ioannides, A. a. (2010). Emotion separation is completed early and it depends on visual field presentation. *PloS One*, 5(3):1–14.
- Logothetis, N. K. (2002). The neural basis of the blood-oxygen-level-dependent functional magnetic resonance imaging signal. *Philosophical transactions of the Royal Society of London. Series B, Biological sciences*, 357(1424):1003–37.
- Logothetis, N. K. (2008). What we can do and what we cannot do with fMRI. *Nature*, 453(7197):869–78.
- Luo, Q., Holroyd, T., Jones, M., Hendler, T., and Blair, J. (2007). Neural dynamics for facial threat processing as revealed by gamma band synchronization using MEG. *NeuroImage*, 34(2):839–47.
- Luo, Q., Holroyd, T., Majestic, C., Cheng, X., Schechter, J., and Blair, R. J. (2010). Emotional automaticity is a matter of timing. *The Journal of Neuroscience*, 30(17):5825–5829.
- Matsuzaki, N. and Sato, T. (2008). The perception of facial expressions from two-frame apparent motion. *Perception*, 37(10):1560–1568.
- Mechelli, A., Price, C. J., Friston, K. J., and Ishai, A. (2004). Where bottom-up meets top-down: neuronal interactions during perception and imagery. *Cerebral Cortex*, 14(11):1256–1265.
- Montgomery, K. J. and Haxby, J. V. (2008). Mirror neuron system differentially activated by facial expressions and social hand gestures: a functional magnetic resonance imaging study. *Journal of Cognitive Neuroscience*, 20(10):1866–1877.
- Morel, S., Ponz, A., Mercier, M., Vuilleumier, P., and George, N. (2009). EEG-MEG evidence for early differential repetition effects for fearful, happy and neutral faces. *Brain Research*, 1254:84–98.

- Morris, J. S., Frith, C. D., Perrett, D. I., Rowland, D., Young, A. W., Calder, A. J., and Dolan, R. J. (1996). A differential neural response in the human amygdala to fearful and happy facial expressions. *Nature*, 383(6603):812–815.
- Moscovitch, M., Winocur, G., and Behrmann, M. (1997). What is special about face recognition? Nineteen experiments on a person with visual object agnosia and dyslexia but normal face recognition. *Journal of Cognitive Neuroscience*, 9(5):555–604.
- Münte, T. F., Brack, M., Grootheer, O., Wieringa, B. M., Matzke, M., and Johannes, S. (1998). Brain potentials reveal the timing of face identity and expression judgments. *Neuroscience Research*, 30(1):25–34.
- Muthukumaraswamy, S. D., Johnson, B. W., Gaetz, W. C., and Cheyne, D. O. (2006). Neural processing of observed oro-facial movements reflects multiple action encoding strategies in the human brain. *Brain Research*, 1071(1):105–12.
- Muthukumaraswamy, S. D. and Singh, K. D. (2008). Spatiotemporal frequency tuning of BOLD and gamma band MEG responses compared in primary visual cortex. *NeuroImage*, 40(4):1552–60.
- Nagai, M., Kishi, K., and Kato, S. (2007). Insular cortex and neuropsychiatric disorders: a review of recent literature. *European Psychiatry*, 22(6):387–394.
- Nakashima, T., Kaneko, K., Goto, Y., Abe, T., Mitsudo, T., Ogata, K., Makinouchi, a., and Tobimatsu, S. (2008). Early ERP components differentially extract facial features: Evidence for spatial frequency-and-contrast detectors. *Neuroscience Research*, 62(4):225–235.
- Nichols, T. E. and Holmes, A. P. (2002). Nonparametric permutation tests for functional neuroimaging: a primer with examples. *Human Brain Mapping*, 15(1):1–25.
- Norman, K. a., Polyn, S. M., Detre, G. J., and Haxby, J. V. (2006). Beyond mind-reading: multi-voxel pattern analysis of fMRI data. *Trends in Cognitive Sciences*, 10(9):424–430.
- Nummenmaa, L., Passamonti, L., Rowe, J., Engell, A. D., and Calder, A. J. (2009). Connectivity analysis reveals a cortical network for eye gaze perception. *Cerebral Cortex*, 20(8):1780–1787.

- Ogawa, S., Lee, T. M., Kay, A. R., and Tank, D. W. (1990). Brain magnetic resonance imaging with contrast dependent on blood oxygenation. *Proceedings of the National Academy of Sciences*, 87(24):9868–9872.
- Ogawa, S., Menon, R. S., Tank, D. W., Kim, S. G., Merkle, H., Ellermann, J. M., and Ugurbil, K. (1993). Functional brain mapping by blood oxygenation level-dependent contrast magnetic resonance imaging. A comparison of signal characteristics with a biophysical model. *Biophysical Journal*, 64(3):803–812.
- Okada, Y. (1983). Neurogenesis of evoked magnetic fields. In Williamson, S., Romani, G. L., Kaufman, L., and Modena, I., editors, *Biomagnetism: An Interdisciplinary Approach*, pages 399–408. Plenum Press, New York.
- O’Toole, A. J., Roark, D. a., and Abdi, H. (2002). Recognizing moving faces: a psychological and neural synthesis. *Trends in Cognitive Sciences*, 6(6):261–266.
- Ozgoren, M., Basar-Eroglu, C., and Basar, E. (2005). Beta oscillations in face recognition. *International Journal of Psychophysiology*, 55(1):51–59.
- Palmer, H. S. (2010). Optogenetic fMRI sheds light on the neural basis of the BOLD signal. *Journal of neurophysiology*, 104(4):1838–40.
- Peelen, M. V., Atkinson, A. P., and Vuilleumier, P. (2010). Supramodal representations of perceived emotions in the human brain. *The Journal of Neuroscience*, 30(30):10127–10134.
- Penny, W. and Holmes, A. P. (2003). Random effect analysis. In Frackowiak, R., Frith, C., Dolan, R. J., Price, C. J., Zeki, S., and Penny, W., editors, *Human Brain Function*, pages 843–850. Academic, London.
- Perrett, D. I., Hietanen, J. K., Oram, M. W., and Benson, P. J. (1992). Organization and functions of cells responsive to faces in the temporal cortex. *Philosophical Transactions of the Royal Society of London. Series B, Biological Sciences*, 335(1273):23–30.
- Perrett, D. I., Smith, P. A., Potter, D. D., Mistlin, A. J., Head, A. S., Milner, A. D., and Jeeves, M. A. (1985). Visual cells in the temporal cortex sensitive to face view and gaze direction. *Proceedings of the Royal Society of London. Series B, Biological Sciences*, 223(1232):293–317.

- Pfurtscheller, G. (2001). Functional brain imaging based on ERD/ERS. *Vision Research*, 41(10-11):1257–1260.
- Pfurtscheller, G. and Lopes da Silva, F. H. (1999). Event-related EEG/MEG synchronization and desynchronization: basic principles. *Clinical Neurophysiology*, 110(11):1842–1857.
- Phan, K. L., Wager, T. D., Taylor, S. F., and Liberzon, I. (2004). Functional neuroimaging studies of human emotions. *CNS Spectrums*, 9(4):258–266.
- Phelps, E. A., O'Connor, K. J., Gatenby, J. C., Gore, J. C., Grillon, C., and Davis, M. (2001). Activation of the left amygdala to a cognitive representation of fear. *Nature Neuroscience*, 4(4):437–441.
- Phillips, M. L., Young, A. W., Senior, C., Brammer, M., Andrew, C., Calder, A. J., Bullmore, E. T., Perrett, D. I., Rowland, D., Williams, S. C., Gray, J. A., and David, A. S. (1997). A specific neural substrate for perceiving facial expressions of disgust. *Nature*, 389(6650):495–498.
- Pike, G., Kemp, R., Towell, N., and Phillips, K. (1997). Recognizing moving faces: the relative contribution of motion and perspective view information. *Visual Cognition*, 4(4):409–438.
- Pitcher, D., Dilks, D. D., Saxe, R. R., Triantafyllou, C., and Kanwisher, N. (2011a). Differential selectivity for dynamic versus static information in face-selective cortical regions. *NeuroImage*, 56(4):2356–2363.
- Pitcher, D., Garrido, L., Walsh, V., and Duchaine, B. C. (2008). Transcranial magnetic stimulation disrupts the perception and embodiment of facial expressions. *The Journal of Neuroscience*, 28(36):8929–8933.
- Pitcher, D., Walsh, V., and Duchaine, B. (2011b). The role of the occipital face area in the cortical face perception network. *Experimental Brain Research*, 209(4):481–493.
- Pizzagalli, D., Regard, M., and Lehmann, D. (1999). Rapid emotional face processing in the human right and left brain hemispheres: an ERP study. *NeuroReport*, 10(13):2691–2698.

- Puce, A., Allison, T., Bentin, S., Gore, J. C., and McCarthy, G. (1998). Temporal cortex activation in humans viewing eye and mouth movements. *The Journal of Neuroscience*, 18(6):2188–2199.
- Rizzolatti, G. and Craighero, L. (2004). The mirror-neuron system. *Annual Review of Neuroscience*, 27:169–192.
- Rizzolatti, G., Fadiga, L., Gallese, V., and Fogassi, L. (1996). Premotor cortex and the recognition of motor actions. *Cognitive Brain Research*, 3(2):131–141.
- Robinson, S. and Vrba, J. (1999). Functional neuroimaging by synthetic aperture magnetometry (SAM). In *Recent advances in biomagnetism*, pages 302–305. Tohoku University Press, Sendai.
- Rossion, B., Caldara, R., Seghier, M., Schuller, A.-M., Lazeyras, F., and Mayer, E. (2003). A network of occipito-temporal face-sensitive areas besides the right middle fusiform gyrus is necessary for normal face processing. *Brain*, 126:2381–2395.
- Rotshtein, P., Vuilleumier, P., Winston, J., Driver, J., and Dolan, R. (2007). Distinct and convergent visual processing of high and low spatial frequency information in faces. *Cerebral Cortex*, 17(11):2713–24.
- Rowe, J. B. (2010). Connectivity analysis is essential to understand neurological disorders. *Frontiers in Systems Neuroscience*, 4(144):1–13.
- Russell, J. A. (1994). Is there universal recognition of emotion from facial expression? A review of the cross-cultural studies. *Psychological Bulletin*, 115(1):102–141.
- Rykhlevskaia, E., Gratton, G., and Fabiani, M. (2008). Combining structural and functional neuroimaging data for studying brain connectivity: a review. *Psychophysiology*, 45(2):173–87.
- Said, C. P., Haxby, J. V., and Todorov, A. (2011). Brain systems for assessing the affective value of faces. *Philosophical Transactions of the Royal Society of London. Series B, Biological sciences*, 366(1571):1660–1670.

- Said, C. P., Moore, C. D., Engell, A. D., and Haxby, J. V. (2010). Distributed representations of dynamic facial expressions in the superior temporal sulcus. *Journal of Vision*, 10(5):1–12.
- Sato, W., Kochiyama, T., Uono, S., and Yoshikawa, S. (2008). Time course of superior temporal sulcus activity in response to eye gaze: a combined fMRI and MEG study. *Social Cognitive and Affective Neuroscience*, 3(3):224–32.
- Sato, W., Kochiyama, T., and Yoshikawa, S. (2010). Amygdala activity in response to forward versus backward dynamic facial expressions. *Brain Research*, 1315:92–9.
- Sato, W., Kochiyama, T., Yoshikawa, S., and Matsumura, M. (2001). Emotional expression boosts early visual processing of the face: ERP recording and its decomposition by independent component analysis. *Neuroreport*, 12(4):709–14.
- Sato, W., Kochiyama, T., Yoshikawa, S., Naito, E., and Matsumura, M. (2004). Enhanced neural activity in response to dynamic facial expressions of emotion: an fMRI study. *Brain Research*, 20(1):81–91.
- Saxe, R., Brett, M., and Kanwisher, N. (2006). Divide and conquer: a defense of functional localizers. *NeuroImage*, 30(4):1088–1096.
- Saygin, Z. M., Osher, D. E., Koldewyn, K., Reynolds, G., Gabrieli, J. D. E., and Saxe, R. R. (2011). Anatomical connectivity patterns predict face selectivity in the fusiform gyrus. *Nature Neuroscience*, 15(2):1–9.
- Schmolck, H. and Squire, L. R. (2001). Impaired perception of facial emotions following bilateral damage to the anterior temporal lobe. *Neuropsychology*, 15(1):30–38.
- Schroeder, C. E., Lakatos, P., Kajikawa, Y., Partan, S., and Puce, A. (2008). Neuronal oscillations and visual amplification of speech. *Trends in Cognitive Sciences*, 12(3):106–113.
- Schultz, J. and Pilz, K. S. (2009). Natural facial motion enhances cortical responses to faces. *Experimental Brain Research*, 194(3):465–475.

- Schweinberger, S. R. and Soukup, G. R. (1998). Asymmetric relationships among perceptions of facial identity, emotion, and facial speech. *Journal of Experimental Psychology Human Perception and Performance*, 24(6):1748–1765.
- Singh, K. D. (1995). Functional imaging of the brain using superconducting magneto-metry. *Endeavour*, 19(1):39–44.
- Singh, K. D., Barnes, G. R., and Hillebrand, A. (2003). Group imaging of task-related changes in cortical synchronisation using nonparametric permutation testing. *NeuroImage*, 19(4):1589–1601.
- Singh, K. D., Barnes, G. R., Hillebrand, A., Forde, E. M. E., and Williams, A. L. (2002). Task-related changes in cortical synchronization are spatially coincident with the hemodynamic response. *NeuroImage*, 16(1):103–114.
- Sprengelmeyer, R., Young, A. W., Schroeder, U., Grossenbacher, P. G., Federlein, J., Büttner, T., and Przuntek, H. (1999). Knowing no fear. *Proceedings Biological Sciences*, 266(1437):2451–2456.
- Sprengelmeyer, R., Young, A. W., Sprengelmeyer, A., Calder, A. J., Rowland, T., Perrett, D. I., Homberg, V., and Lange, H. (1997). Recognition of facial expressions: selective impairment of specific emotions in Huntington’s disease. *Cognitive Neuropsychology*, 14:839–879.
- Stam, C. J., Nolte, G., and Daffertshofer, A. (2007). Phase lag index: assessment of functional connectivity from multi channel EEG and MEG with diminished bias from common sources. *Human Brain Mapping*, 28(11):1178–1193.
- Stevenson, C. M., Brookes, M. J., and Morris, P. G. (2011). β -Band correlates of the fMRI BOLD response. *Human Brain Mapping*, 32(2):182–197.
- Streit, M. (1999). Neurophysiological correlates of the recognition of facial expressions of emotion as revealed by magnetoencephalography. *Cognitive Brain Research*, 7(4):481–491.
- Summerfield, C., Egner, T., Greene, M., Koechlin, E., Mangels, J., and Hirsch, J. (2006). Predictive codes for forthcoming perception in the frontal cortex. *Science*, 314(5803):1311–1314.

- Supek, S. and Aine, C. J. (1993). Simulation studies of multiple dipole neuromagnetic source localization: model order and limits of source resolution. *IEEE Transactions on Biomedical Engineering*, 40(6):529–540.
- Talairach, J. and Tournoux, P. (1988). *Co-planar stereotaxic atlas of the human brain: 3-dimensional proportional system - an approach to cerebral imaging*. Thieme Medical Publishers, New York.
- Thomas, C., Avidan, G., Humphreys, K., Jung, K.-j., Gao, F., and Behrmann, M. (2009). Reduced structural connectivity in ventral visual cortex in congenital prosopagnosia. *Nature Neuroscience*, 12(1):29–31.
- Thomas, C., Moya, L., Avidan, G., Humphreys, K., Jung, K. J., Peterson, M. a., and Behrmann, M. (2008). Reduction in white matter connectivity, revealed by diffusion tensor imaging, may account for age-related changes in face perception. *Journal of Cognitive Neuroscience*, 20(2):268–284.
- Tottenham, N., Tanaka, J. W., Leon, A. C., Mccarry, T., Nurse, M., Hare, T. A., Marcus, D. J., Westerlund, A., Casey, B. J., and Nelson, C. (2009). The NimStim set of facial expressions: judgments from untrained research participants. *Psychiatry Research*, 168(3):242–249.
- Tovée, M. J. (1998). Is face processing special? *Neuron*, 21(6):1239–42.
- Trautmann, S. A., Fehr, T., and Herrmann, M. (2009). Emotions in motion: dynamic compared to static facial expressions of disgust and happiness reveal more widespread emotion-specific activations. *Brain Research*, 1284:100–115.
- Tsao, D. Y., Freiwald, W. A., Tootell, R. B. H., and Livingstone, M. S. (2006). A cortical region consisting entirely of face-selective cells. *Science*, 311(5761):670–674.
- Turk-Browne, N. B., Norman-Haignere, S. V., and McCarthy, G. (2010). Face-Specific Resting Functional Connectivity between the Fusiform Gyrus and Posterior Superior Temporal Sulcus. *Frontiers in Human Neuroscience*, 4(176):1–15.
- Vaina, L. M., Solomon, J., Chowdhury, S., Sinha, P., and Belliveau, J. W. (2001). Functional neuroanatomy of biological motion perception in humans. *Proceedings of the National Academy of Sciences*, 98(20):11656–11661.

- Van Veen, B. D., van Drongelen, W., Yuchtman, M., and Suzuki, A. (1997). Localization of brain electrical activity via linearly constrained minimum variance spatial filtering. *IEEE Transactions on Biomedical Engineering*, 44(9):867–880.
- Vuilleumier, P., Armony, J. L., Driver, J., and Dolan, R. J. (2001). Effects of attention and emotion on face processing in the human brain: an event-related fMRI study. *Neuron*, 30(3):829–841.
- Vuilleumier, P. and Pourtois, G. (2007). Distributed and interactive brain mechanisms during emotion face perception: Evidence from functional neuroimaging. *Neuropsychologia*, 45(1):174–194.
- Watanabe, S., Kakigi, R., Koyama, S., and Kirino, E. (1999). Human face perception traced by magneto- and electro-encephalography. *Brain Research*, 8(2):125–142.
- Watanabe, S., Miki, K., and Kakigi, R. (2005). Mechanisms of face perception in humans: A magneto- and electro-encephalographic study. *Neuropathology*, 25(1):8–20.
- Wehrle, T., Kaiser, S., Schmidt, S., and Scherer, K. R. (2000). Studying the dynamics of emotional expression using synthesized facial muscle movements. *Journal of Personality and Social Psychology*, 78(1):105–119.
- Whalen, P. J., Rauch, S. L., Etcoff, N. L., McInerney, S. C., Lee, M. B., and Jenike, M. A. (1998). Masked presentations of emotional facial expressions modulate amygdala activity without explicit knowledge. *The Journal of Neuroscience*, 18(1):411–418.
- Wicker, B., Fonlupt, P., Hubert, B., Tardif, C., Gepner, B., and Deruelle, C. (2008). Abnormal cerebral effective connectivity during explicit emotional processing in adults with autism spectrum disorder. *Social Cognitive and Affective Neuroscience*, 3(2):135–143.
- Wicker, B., Keysers, C., Plailly, J., Royet, J. P., Gallese, V., and Rizzolatti, G. (2003). Both of us disgusted in my insula: the common neural basis of seeing and feeling disgust. *Neuron*, 40(3):655–664.
- Wiggett, A. and Downing, P. (2008). The face network: Overextended. *NeuroImage*, 40(2):420–422.

- Winston, J. S., O'Doherty, J., and Dolan, R. J. (2003). Common and distinct neural responses during direct and incidental processing of multiple facial emotions. *NeuroImage*, 20(1):84–97.
- Xu, Y., Liu, J., and Kanwisher, N. (2005). The M170 is selective for faces, not for expertise. *Neuropsychologia*, 43(4):588–97.
- Young, A. W., Aggleton, J. P., Hellawell, D. J., Johnson, M., Broks, P., and Hanley, J. R. (1995). Face processing impairments after amygdalotomy. *Brain*, 118:15–24.
- Young, A. W., Haan, E. H. F., and Bauer, R. M. (2008). Face perception: A very special issue. *Journal of Neuropsychology*, 2(1):1–14.
- Young, A. W., McWeeny, K. H., Hay, D. C., and Ellis, A. W. (1986). Matching familiar and unfamiliar faces on identity and expression. *Psychological Research*, 48(2):63–68.
- Young, M. P. and Yamane, S. (1992). Sparse population coding of faces in the inferotemporal cortex. *Science*, 256(5061):1327–1331.
- Zhang, H., Tian, J., Liu, J., Li, J., and Lee, K. (2009). Intrinsically organized network for face perception during the resting state. *Neuroscience Letters*, 454(1):1–5.

Appendix A

Foley, E., Rippon, G. and Senior, C. (2012). Dynamic facial expressions evoke distinct activation in the face perception network as revealed by parallel fMRI and MEG analysis. MEG UK. London, UK.

Foley, E., Rippon, G. and Senior, C. (2011). Dynamic facial expressions evoke distinct activation in the face perception network as revealed by parallel fMRI and MEG analysis. Cognitive Neuroscience Society Meeting. San Francisco, USA.

Foley, E., Rippon, G. and Senior, C. (2011). Dynamic facial expressions evoke distinct activation in the face perception network: Evidence from MEG. MEG UK. Glasgow, UK.

Foley, E., Rippon, G. and Senior, C. (2010). An investigation of the neural responses to dynamic faces using MEG. 17th International Conference on Biomagnetism (BIOMAG). Dubrovnik, Croatia.